Synthesis and Evaluation of Canola Oil Derived Biolubricants Using Heterogeneous Catalysts

A Thesis Submitted to the College of Graduate Studies and Research in Partial Fulfillment of the Requirements for the
Degree of Doctor of Philosophy (Ph.D.)
in the Department of Chemical and Biological Engineering,
University of Saskatchewan
Saskatoon, SK, Canada

By

Asish Kumar Reddy Somidi

PERMISSION TO USE

In presenting this thesis in partial fulfillment of the requirements for a Postgraduate degree from the University of Saskatchewan, I agree that the Libraries of this University may make it freely available for inspection. I further agree that permission for copying of this thesis in any manner, in whole or in part, for scholarly purposes may be granted by Dr. Ajay K. Dalai who supervised my thesis work, or in his absence, by the Head of the Department or Dean of the College of Engineering. It is understood that any copying or publication or use of this thesis thereof for financial gain shall not be allowed without my written permission. It is also understood that due recognition shall be given to me and to the University of Saskatchewan in any scholarly use which may be made of any material in my thesis.

Requests for permission to copy or to make other use of material in this thesis in whole or part should be addressed to:

Head of the Department
Department of Chemical and Biological Engineering
University of Saskatchewan
57 Campus Drive
Saskatoon, Saskatchewan
Canada S7N 5A9

ABSTRACT

The current research is focused on the preparation of a value-added product called biolubricant using canola oil and canola biodiesel as feedstocks. The presence of unsaturation among the selected feedstocks limits their application as a potential lubricant because unsaturation renders unfavourable oxidative and thermal stability, and poor lubricity when used as a lubricant. The two-step reaction pathway chosen to remove unsaturation in both the feedstocks and make potential lubricants are: (1) epoxidation of unsaturated fatty acids in the canola oil/canola biodiesel followed by epoxide ring opening and vicinal di-O-acetylation with acetic anhydride; and (2) epoxidation of unsaturated fatty acids in the canola oil/canola biodiesel followed by epoxide ring opening and O-alkylation with 1-propanol. This research work is primarily focused on the preparation and development of heterogeneous catalysts using metal oxides or metal supported catalysts for the above-mentioned two-step synthesis procedure.

The research work is divided into four phases. The first phase involved preparation of a heterogeneous catalyst for the epoxidation of unsaturated fatty acids in the canola oil. Sulfated tin oxide demonstrated promising activity with 100% conversion of canola oil to epoxidized canola oil (biolubricant base oil) at the optimum conditions such as: temperature (70^{o}C), ethylenic unsaturation in the canola oil to H_2O_2 molar ratio (1:3), ethylenic unsaturation in the canola oil to acetic acid molar ratio (1:2), catalyst loading of 10 wt% with respect to feed taken and reaction time of 6 h. Catalyst characterization was made to study the properties of sulfated-SnO_2 that promoted epoxidation reaction. Co-ordination of sulfate ions to the tin oxide surface after the calcination at 550^{o}C is found necessary because sulfate ions induce Lewis and Bronsted acidity to the catalyst surface. The epoxidation of canola oil reaction followed pseudo first-order reaction and the calculated activation energy was found to be 18 kcal/mol.

The second phase involved with the preparation of vicinal di-O-acetylated canola oil (biolubricant type 1) using heterogeneous catalyst by epoxide ring opening and vicinal di-O-acetylation of epoxidized canola oil. Catalyst screening tests showed that sulfated-ZrO_2 is highly selective in complete conversion of epoxidized canola oil to vicinal di-O-acetylated canola oil. The optimum conditions obtained from the Taguchi experimental design are: reaction temperature (130 ^{o}C), epoxy to acetic anhydride molar ratio (1: 1.25), 16 wt% of catalyst loading with respect

to the quantity of feed (epoxidized oil) taken, and a reaction time of 1 h 15 min. The reaction was found to follow the second-order and the calculated activation energy was 23 kcal/mol.

The third phase of the work is focused on the development of a single heterogeneous catalyst that is active for both epoxidation, epoxide ring opening and vicinal di-O-acetylation reactions in a single pot. 10 wt% MoO_3/Al_2O_3 was found to be highly active and selective in complete conversion of unsaturated canola oil to vicinal di-O-acetylated canola oil in a single pot in minimum reaction time. The optimum conditions obtained based on response surface methodology are: unsaturation in the canola oil to tert-butyl hydroperoxide molar ratio (1: 2.25), 10 wt% MoO_3/Al_2O_3 as catalyst for both steps, 12 wt% of catalyst loading with respect to amount of canola oil taken, epoxide to acetic anhydride molar ratio (1:2) and a reaction time of 5 h 30 min. These optimum conditions are also applied for the one-pot synthesis of vicinal di-O-acetylated canola biodiesel and complete conversion was found to happen in 4 h and 15 min. The developed one-pot synthesis procedure was found effective in minimizing work-up procedures for product extraction, minimized catalyst usage and reaction time. Further, evaluation and comparison of physicochemical properties of vicinal di-O-acetylated canola oil and vicinal di-O-acetylated canola biodiesel were also made to identify their application as a lubricant for various applications.

In the fourth phase O-propylated canola oil (biolubricant type 2) was synthesized from epoxidized canola oil by epoxide ring opening and O-propylation reaction. Al-SBA-15 catalyst with Si/Al ratio 10 showed promising activity with 100% conversion at the optimum conditions (based on response surface methodology). Catalyst characterization showed that impregnation of aluminum in the crystal lattice of SBA-15 promoted epoxide ring opening and O-propylation reaction. The optimum conditions are temperature (100 ^oC), epoxy to 1-propanol molar ratio (1:6), catalyst loading of 12 wt% with respect to epoxidized canola oil taken, and a reaction time of 6 h. The reaction kinetic showed that epoxide ring opening and O-propylation reaction followed second-order reaction, and the apparent activation energy was 12 kcal/mol. Al-SBA-15 was found to be an efficient catalyst for the preparation of O-propylated canola biodiesel. 100 % conversion was achieved in 6 h reaction time. Determination of physicochemical properties of O-propylated canola oil and canola biodiesel showed that they meet the specifications of transmission gear oil and anti-wear hydraulic oils.

ACKNOWLEDGEMENTS

I wholeheartedly take this opportunity to express my appreciation to all the individuals who helped me in the completion of this research work.

It gives me immense happiness and would like to convey my earnest gratitude to my supervisor Dr. Ajay K. Dalai, who gave me an opportunity to work in his research group, and provided complete support during the course of my Ph.D. program. His principles and attitude towards work highly motivated me and made me learn many things. I am very much thankful to him for his valuable inputs.

I wholeheartedly thank Dr. Catherine Niu, Dr. Jafar Soltan, Dr. Hui Wang, and Dr. Stephen Foley, for being my Ph.D. advisory committee members. I very much appreciate their valuable technical inputs during the committee meetings. Those comments have improved the quality of research.

I am grateful for the financial supporters of this research to Agriculture Development Fund (ADF), Saskatchewan Canola Development Commission (SaskCanola), and Natural Science and Engineering Council of Canada (NSERC), Canada.

I also acknowledge Dr. Sandeep Badoga, Ms. Heli Eunike, and Mr. Richard Blondin for their assistance with the analytical instruments during my program.

DEDICATION

This thesis is wholeheartedly dedicated to:

My loving God Shiridi Sai who gave me enough strength and courage with his warm blessings.

My parents, Madhusudhan Reddy Somidi and Rajitha Somidi, who always motivated me and made my life happy with their love and sacrifices.

My brother, Ajay Somidi, who is always there when I am in hard times.

My sweet wife, Santhoshima Challa, whose love and support is the biggest strength for me.

My best friend Praveen Roayapalley (kaka).

TABLE OF CONTENTS

LIST OF TABLES

LIST OF FIGURES

ABBREVIATIONS

$(Ac)_2O$	Acetic anhydride
AA	Acetic acid
Al-SBA-15 (10)	Al-SBA-15 catalyst with Si to Al ratio 10
AOCS	American Oil Chemists Society
ASTM	American Society for Testing and Materials
CCD	Central Composite Design
CO	Canola oil
DACO	Vicinal di-O-acetylated canola oil
DOE	Design of experiments
ECO	Epoxidized canola oil
EROP	Epoxide ring opening and O-propylation reaction
HP	Hydrogen peroxide
ICP-OES	Inductively Coupled Plasma Optical Emission Spectrometry
ISO	International Organization for Standardization
NMR	Nuclear Magnetic Resonance Spectrometry
OIT	Oxidative Induction Time
PAA	Peracetic acid
RPVOT	Rotating Pressure Vessel Oxidation Test
RBOT	Rotating Bomb Oxidation Test
RSM	Response Surface Methodology
SAE	Society of Automotive Engineers
TPD	Temperature Programmed Desorption
XANES	X-ray Absorption Near K-Edge Spectroscopy
XRD	X-ray diffraction

NOMENCLATURE

C_{PCO}	Concentration of epoxidized canola oil (mol/L)
$C_{PCO,0}$	Initial concentration of epoxidized canola oil (mol/L)
C_{POH}	Concentration of 1-propanol (mol/L)
$C_{POH,0}$	Initial concentration of 1-propanol (mol/L)
C_s	Vacant sites on the catalyst surface
C_t	Total active sites
C_t	Total number of active sites
D_{CO}	Diffusion coefficient CO in PAA (m^2/s)
$D_{ECO, (Ac)2O}$	Diffusivity of epoxy canola oil into acetic anhydride (m^2/s)
$D_{ECO, e}$	Effective diffusivity of epoxy canola oil (m^2/s)
D_p	Characteristic length (m)
K_1	Adsorption equilibrium constant for epoxy canola oil (L mol^{-1} min^{-1})
K_1	Equilibrium constant for peracetic acid formation (L/mol)
K_2	Adsorption equilibrium constant for acetic anhydride (L mol^{-1} min^{-1})
K_2	Equilibrium constant for the adsorption of CO on catalyst surface (L/mol)
K_3	Equilibrium constant for the adsorption of PAA on catalyst surface (L/mol)
K_3	Desorption equilibrium constant for vicinal di-O-acetylated canola oil (L mol^{-1} min^{-1})
k_c	Solid-liquid mass transfer coefficient (m/s)
kc_{CO}	Mass transfer co-efficient for canola oil (m/s)
K_{ECO}	Equilibrium constant for desorption of ECO on catalyst surface (mol/L)
K_s	Adsorption equilibrium constant for surface reaction (L mol^{-1} min^{-1})
K_{SR}	Equilibrium constant for surface reaction (L/mol)
$M_{(Ac)2O}$	Molecular weight of acetic anhydride (g/mol)
M_{PAA}	Molecular weight of peracetic acid (g/mol)
$-r^1_{obs}$	Observed initial reaction rate (mol/m^2. min)
r_{CO}	Rate of reaction (mol/g cat. h)
R_p	Radius of the catalyst particle (m)
t	Time (h)
V_{CO}	Molar volume of canola oil (m^3/mol)

V_{ECO}	Molar volume of epoxidized canola oil (m^3/mol)
W_{COr}	Mass transfer flux of canola oil (mol/m^2.s)
$W_{ECO,r}$	Mass transfer flux of epoxidized canola oil (mol/m^2.s)
X_{ECO} or X_{PCO}	Fractional conversion of epoxidized canola oil

GREEK NOMENCLATURE

Θ	Porosity of the catalyst
μ	Viscosity of the reaction mixture (cP)
ε	Porosity
ρ or ρ_{cat}	Density of catalyst particle (g/cm^3)
τ	Tortuosity

CHAPTER 1

INTRODUCTION

1.1 Introduction

Lubricants are commonly used to reduce wear and tear between contact surfaces, to promote the efficiency of the system, to prevent corrosion and also as heat resistant fluids (Bart et al. 2013). These are prepared from mineral oils and vegetable oils as feedstocks. Most of the lubricants available in the market are mineral oil derived lubricants and synthetic esters. Synthetic esters are specially formulated to meet government regulations, less hazardous and are biodegradable (Nagendramma et al. 2012). The global necessity for the lubricants was found more than 40 million metric tons by 2014 and is expected to increase by 2 % each year. More than 70 % of the lubricants produced are being consumed by automotive and industrial sectors. It was estimated that about 15 million tons of lubricant waste enter into biosphere each year leading to huge environmental pollution (Gawrilow et al. 2004). As per Schneider et al. (2006), about 50 % of the lubricants used end up as pollutants because of total-loss applications, volatility, spillage, and disposal. The environmental issues originated by the accretion of pollutants due to the extensive consumption of crude oil based lubricants lead renewed interest in exploring and using bio-based resources (Mobarak et al. 2014). Compared to crude oil derivatives bio-based oils are less toxic and eco-friendly. A lubricant formulated and prepared from plant or animal oils is known to be a biolubricant.

The chemical transformation of vegetable oils into biolubricants was considered to be a promising strategy to produce renewable and environmentally friendly fuel additives that can substitute mineral oil based lubricants. This strategy also helps in the development of sustainable green technology to produce wide varieties of value added chemicals and industrial products. Also, research on the synthesis of lubricants from vegetable oils has gained considerable interest because biolubricants showed superior thermal stability, lubricity, viscosity index, flash point, biodegradability and non-toxicity as compared to lubricants derived from mineral oils (Mobarak et al. 2014).

Vegetable oils comprise of triglycerides where the glycerol molecule is attached to different types of saturated and unsaturated fatty acids. The extent of unsaturation in a vegetable oil limits

its application as a potential substitute for mineral oil derived lubricant because unsaturation renders unfavourable physicochemical properties (Nagendramma et al. 2012). The promising reaction pathways by which unsaturation can be removed from fatty acids is by hydrogenation, epoxidation, epoxide ring opening with higher alcohols and carboxylic acids, and vicinal di-O-acetylation with carboxylic anhydrides. Among these, epoxidation followed by epoxide ring opening by alcohols, acids and anhydrides have drawn significant interest as the reactions can be promoted at moderate process conditions and the products found to exhibit promising lubricity properties (Adhvaryu et al. 2002; Lathi et al. 2007, Salimon et al. 2011; Sharma et al. 2013).

Vegetable oils containing a large amount of mono-unsaturation (oleic content) are considered to be potential feedstocks for the preparation of biolubricant (Lathi et al. 2007). High oleic containing vegetable oils are found to be promising feedstocks to produce stable biofuels such as biolubricant, biodiesel and biopolymers (Hwang et al. 2003). Thermally stable oleic compounds can be chemically modified to produce saturated fatty acid esters which have inherent lubrication properties (Wua et al. 2000). Canola oil is one among them with high oleic content (~65 %) in the form of glyceryl trioleate. Canola oil is comprised of 94 – 99 % triglyceride molecules. The triglyceride molecules have glycerol as back bone attached with the saturated and unsaturated fatty acids. The ester functionality (polarity) in the canola oil provides inherent lubricity, and the presence of long chain hydrocarbons promote thermal and hydrolytic stability. However, the presence of unsaturation limits its application for a potential lubricant, because olefinic sites are susceptible to oxidative and thermal degradation. Also, the extent of unsaturation in the oil also exhibits poor cold flow temperature behaviour (Nagendramma et al. 2012). Canola biodiesel (supplied by Miligan Biofuels Inc.,) is produced by transesterification of canola oil. It was found to contain unsaturated fatty acid methyl esters of oleic (~65%) and combined linoleic and linolenic acids (~32%).

The current research investigation is focused on the synthesis of biolubricants from canola oil and canola biodiesel as feedstocks. The reaction pathways chosen to remove unsaturation in both the feedstocks and make potential biolubricants are: (1) epoxidation of canola oil/canola biodiesel; (2) epoxidation of canola oil/canola biodiesel followed by epoxide ring opening and vicinal di-O-acetylation with acetic anhydride; and (3) epoxidation of canola oil/canola biodiesel followed by

epoxide ring opening and alcoholysis reaction with alcohol such as 1-propanol. Heterogeneous metal oxide catalysts are developed and used to catalyze the above-mentioned reaction pathways.

A systematic approach has been made to achieve the desired objectives. In each phase, based on the literature catalysts were selected, prepared and tested for the desired transformation. Also, the physicochemical characterization was made to study the properties resulted in effective catalysis. The active catalyst found was then used for the optimization of process parameters for maximizing conversion and yield. The design of experiments using statistical methods and statistical analysis was also made to build response model, to study the interactions between variables, analysis of variance and to understand the significance of selected parameters in promoting the selected reaction. Kinetic studies were also performed to build a kinetic model and to calculate the order and activation energy of the desired reactions, respectively. Also, measurement of physicochemical properties of the synthesized biolubricants such as oxidative stability in terms of oxidative induction time (OIT), lubricity in terms of wear scar diameter with respect to reference sample, kinematic viscosity, viscosity index, cloud and pour point, and flash point are made to compare the obtained properties with ISO and SAE specifications of gear oil lubricants.

CHAPTER 2

LITERATURE REVIEW

2.1 Introduction

Application of vegetable oils as potential lubricants in the raw material stage is found difficult because of the fatty acids profile, extent of degree of unsaturation among the fatty acids, and purity. All these factors tend to exhibit unfavourable tribological properties. In this regard, several modifications have been proposed and applied to improve the properties of the oils and make them suitable as lubricants. Some of the prominent modifications include esterification/transesterification of triglycerides to esters, partial selective hydrogenation at the unsaturation, epoxidation of triglycerides (unsaturated fatty acids attached), addition of alkyl functionality at the unsaturation through epoxide ring opening, genetic modifications by changing the fatty acid profiles through the addition of long chain fatty acids (polymerization), oligomerization or estolides formation, emulsification, and also by the addition of commercial viscosity promoters, cold flow temperature depressants and antioxidative additives (McNutt et al. 2016; Soni et al. 2014; Nagendramma et al. 2012).

Among these methods, chemical modification route (modification in fatty acid profile and unsaturation) is found more promising and efficient because it helps to synthesize various types of compounds desirable for various applications. Also, prominent physicochemical properties such as thermal stability, lubricity performance, and pour point can be modified by the addition or removal of necessary functionality. This method involves modification of double bonds by adding O-acetyl, O-alkyl, hydroxyl functionalities, and branching with long chain fatty acids. The prominent reasons in targeting unsaturation for chemical modification is because unsaturation is the major cause for an oil to show its susceptibility for unfavourable behaviour (Soni et al. 2014).

This literature review summarizes various modifications applied in the research articles for biolubricants preparation, their effect on the physicochemical properties, desired reaction conditions to promote selective reaction pathway, catalysts used and advancements in this field of study.

2.2 Esterification or transesterification of vegetable oils

Esterification or transesterification reaction involves reaction between triglycerides in the vegetable oils and short chain alcohols. This chemical pathway is applied to arrange acyl molecules to produce fatty acid alkyl esters. This multi-step process is used to prepare biolubricants because it reduces the bulkiness of the feedstock and produces alkyl esters which have inherent lubricity characteristics. Also, with the addition of different types of alkyl groups to the fatty acids, changes in the physicochemical properties can be observed. Figure 2.1 illustrates the reaction scheme involving esterification and transesterification of vegetable oil to methyl esters followed by the formation of triester. Trimethylolpropane is a common chemical used in the synthesis of triester. Several articles are found to be involved with the preparation of biolubricants using above mentioned pathway. Vegetable oils, epoxidized oils, waste cooking oils, biodiesel and functionalized fatty acids were found to be used as feedstocks.

Kamalakar et al. (2013) reported on the preparation of different types of biolubricants from non-edible grade rubber seed oil through esterification and transesterification reaction. This synthesis involved hydrolysis of rubber seed oil to produce fatty acids, followed by transesterification with 2-ethyl hexanol, neopetylglycol, trimethylol propane, and pentaerythritol. Four different type of biolubricants such 2-ethylhexyl esters, neopetylglycol esters, trimethylolpropane esters and pentaerythritol esters are prepared and characterized. Toluene sulfonic acid was used as a catalyst for transesterification and the favourable reaction temperature was reported to be between 135 to 140 ^{o}C. This study showed that prepared biolubricants exhibited high viscosity index and flash points along with the improvement in lubricity. Biolubricants were found to meet ISO 15380 specifications of hydraulic fluids. Also, this report confirms that physicochemical properties of polyesters are more promising that alkyl esters. Hence, esterification followed with polyesterification would be an efficient reaction pathway.

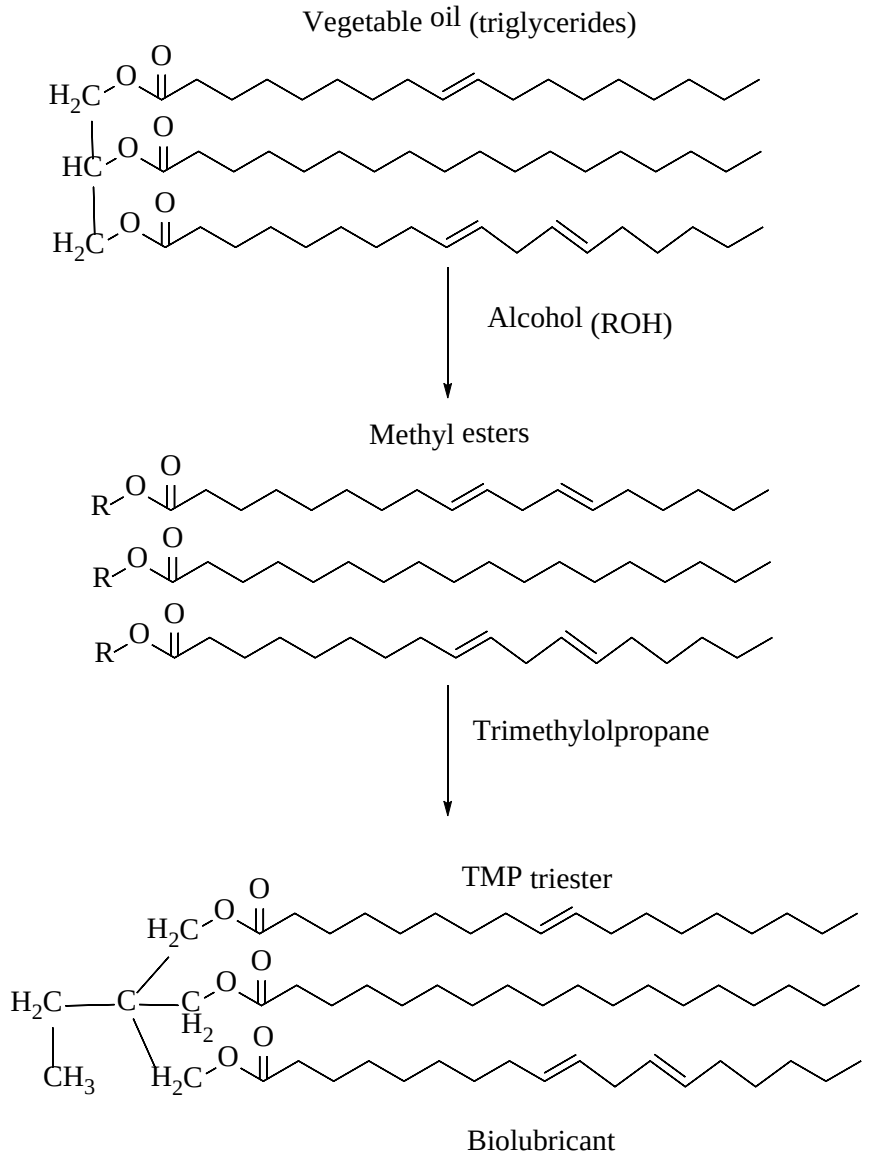

Figure 2.1 Reaction scheme for the preparation of biolubricants using esterification/transesterification step.

Muhammad et al. (2011) studied on the physicochemical properties of Jatropha oil based biolubricant prepared by the transesterification of its methyl esters with trimethylol propane. Sodium methoxide was reported as an active catalyst for this reaction. The reaction temperature of 150 ^{o}C and 10 mbar pressure are reported to desirable conditions to get maximum yield. Physicochemical properties of prepared biolubricant are pour point (-3 ^{o}C), viscosity index (183), kinematic viscosity at 40 ^{o}C (43 cSt) and kinematic viscosity at 100 ^{o}C (10 cSt). These properties were close to the ISO VG220 specifications of light gear oils. Kinetic studies showed that reaction

followed second-order with an apparent activation energy of 4 kJ/mol. Koh et al. (2014) also prepared biolubricant from palm oil by transesterification of methyl esters with trimethylol propane. This report also confirms that reaction temperature of 140 ^{o}C is most favourable and reaction followed the second order. Physicochemical properties of prepared palm oil derived biolubricant are pour point (-1 ^{o}C), viscosity index (187), kinematic viscosity at 40 ^{o}C (50 cSt) and kinematic viscosity at 100 ^{o}C (10 cSt).

Furthermore, Sripada et al. (2013) studied on the physicochemical properties of trimethylol propane based biolubricants prepared from canola oil and canola biodiesel. The optimum reaction conditions reported are reaction temperature 110 ^{o}C, trimethylol propane to methyl ester ratio of 4, 0.5 wt% of catalyst loading (sodium methoxide). More than 90 % formation of triester was happened in 5 h reaction time. Transesterification with trimethylol propane showed large improvement in the cold flow behaviour of biolubricant. The pour point of canola oil and methyl ester derived triester is found to be > -50 ^{o}C which is quite promising for extreme cold conditions. The oxidative stability of canola oil derived triester is found to be 2 h and is 0.8 h for biodiesel derived triester. The viscosity index of both the biolubricants was found to be between 190 – 200 cSt. Also, prepared biolubricants are found to be applicable as light gear oil lubricants.

Gryglewicz et al. (2013) studied on the application of enzymes as catalysts for the synthesis of rapeseed oil derived biolubricants. This synthesis involved transesterification of rapeseed oil methyl esters with higher alcohols such as neopentyl glycol, 2-ethylhexanol, and trimethylol propane. Enzymes such as Rhizomucor Miehei, Pseudomonas Cepacia, and Candida Antarctica are prepared and used for the transesterification reaction. In comparison to other enzymes, Candida Antarctica was found to be highly active and more than 97% conversion was achieved at the optimum conditions. The kinematic viscosities of prepared esters was found to be between 8 – 38 cSt at 40 ^{o}C and is between 3 – 8 cSt at 100 ^{o}C. The flash point of the biolubricants is observed between 200 – 225 ^{o}C and pour point (-31 - 18 ^{o}C). Silva et al. (2013) reported on the physicochemical properties of biolubricant derived from castor oil biodiesel. Amberlyst 15 ion exchange resin and sodium methoxide were found to be active catalysts for the transesterification of castor oil methyl esters using trilmethylol propane as a nucleophile. Jinho Oh et al. (2013) studied on the transesterification of soybean oil using long chain alcohols such as 1-ocatnol, dodecanol, tetradecanol, hexadecanol, 2-octanol, 3-octanol, trimethylol propane, and isooctanol.

Sulfated-ZrO_2 was found to be an active catalyst and high yield (> 80%) were found to be obtained at reaction conditions such as temperature (140 ^oC), free fatty acid to alcohol molar ratio (1:1), and reaction time of 4 h. The viscosity indices of biolubricants were found to be in between 45-195. Sreeprasanth et al. (2006) reported on the application of Fe-Zn complex as an efficient catalyst for the preparation of biolubricants from vegetable oils through a transesterification reaction. Zn^{+2} ions coordinated to the catalyst surface is found to promote transesterification of sunflower oil with octanol as a reactant.

In summary, the above review confirms that transesterification of vegetable oils could be a promising approach to synthesize biolubricants with improved physicochemical properties.

2.3 Epoxidation of vegetable oils

The epoxidation (oxygen transfer) reaction is one of the most prominent reaction in organic synthesis because many stable products can be produced and transformations can be investigated. Epoxidation reaction occurs by the transfer of oxygen from the peroxide to unsaturation (Saurabh et al. 2011). The mechanism involves electrophilic attack, with a transfer of a proton from epoxide oxygen to a carboxylic acid. Epoxidation reactions are carried out by using peracids, and formation of peracids is an in situ reaction between acid and peroxide (Ahulwalia et al. 2011; Saurabh et al. 2011). Uncatalyzed epoxidation of olefins is a slow reaction and hence requires a catalyst to enhance the rate of reaction. Epoxidation reaction can be promoted using mineral acids, ion exchange resins, enzymes and metal-supported catalysts (Tan et al. 2010). Catalyst containing Lewis acid sites (heterogeneous), proton donors (ion exchange resins and inorganic acids) usually promote epoxidation reaction. Active metal sites on the catalytic surface or proton source from the reaction form a partial co-ordinate bond with C=C of fatty acids and electrophilic oxygen between the carbonyl (CO) group and the acidic hydrogen atom. This helps in accomodating the substrate and reactant molecules over the catalyst surface and enhances the rate of epoxidation (Yin et al. 2005).

Following literature review provides information on the catalysts used to catalyze epoxidation of unsaturated vegetable oils, reaction conditions, and kinetics. Also, the effect on the physicochemical properties of the oils after the epoxidation was summarized based on the literature. Figure 2.2 shows the schematic representation of epoxidation of oleic, linoleic and linolenic acids in the triglycerides of a vegetable oil.

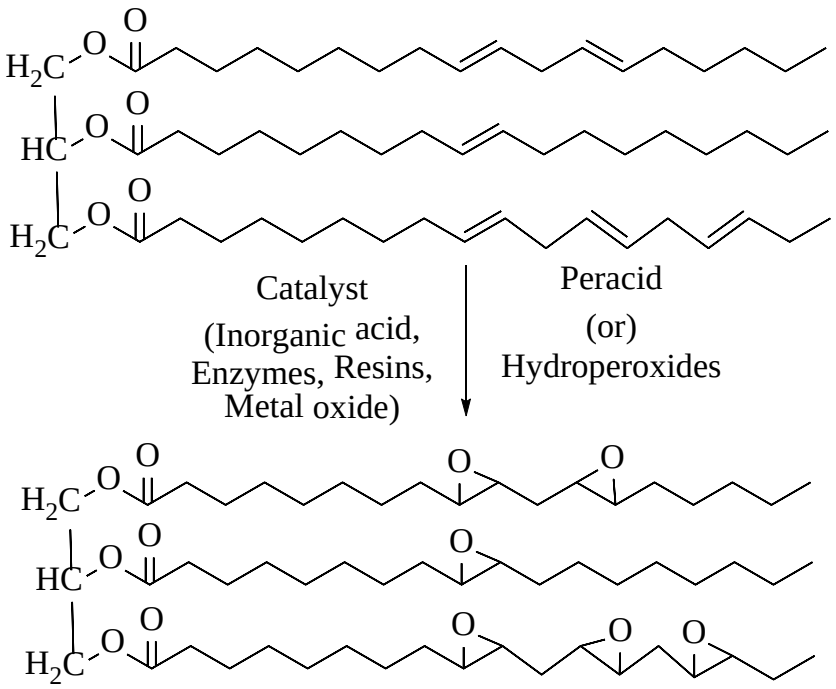

Figure 2.2 Epoxidation of unsaturated fatty acids in the triglycerides of vegetable oils

Dinda et al. (2008) reported on the epoxidation of unsaturated triglycerides in the cotton seed oil using hydrogen peroxide as oxidant. Inorganic acids such as sulphuric acid, formic acid, phosphoric acid, hydrochloric acid and nitric acids were found to be active in promoting epoxidation of cotton seed oil. Among these acids, sulfuric acid is reported to be most effective. More than 80 % conversion was observed. The reaction conditions reported to be favourable for epoxidation reaction catalyzed by inorganic acids are temperature (50 to 60 ^{o}C), molar ratio between peroxide to unsaturation in the oil (1.5 to 2.0) and about 2% of catalyst loading. Use of acetic acid promoted a faster rate of epoxidation reaction because of the formation of highly active peracetic acid. Kinetic studies showed epoxidation of cotton seed oil followed the pseudo first order and is endothermic in nature. Several reports also showed that sulfuric acid is the efficient catalyst for epoxidation of vegetable oils compared to other mineral acids, and also epoxidation reaction can be carried out at moderate process conditions (Meyer et al. 2008; Cai et al. 2008; Goud et al. 2006; Liankun et al. 2011). Following observations are made after the review of literature on the application of mineral acids for epoxidation reaction: (1) use of mineral acids as catalysts promoted side reactions such as estolides, epoxide ring opening, and hydroxylation resulting in lower yield and selectivity; (2) aqueous work-up procedures need to be employed to extract the product resulting in high usage of organic solvents and water; and (3) also used of acids is not found to be

attractive for industrial scale process because acids are corrosive and above mentioned challenges make the process more tedious and expensive.

Research has been focused on the application of enzymes as catalysts for epoxidation reaction to avoid side reactions, work-up procedures and to make process green. Novozym 435 (Candida Antarctica Lipase B) enzyme was reported to be highly active catalyst for the chemoenzymatic epoxidation of vegetable oils such as linseed, soybean, sunflower and rapeseed. The enzyme was found active using hydrogen peroxide and tert-butyl hydroperoxide as oxidizing agents. The unsaturation conversion to epoxide with anhydrous tert-butyl hydroperoxide was found higher because the use of hydrogen peroxide consequently deactivated the enzyme during the course of the reaction. Epoxidation reaction catalyzed using enzyme was found to be exothermic and reaction temperature of 50 ^{o}C is found favourable to carryout epoxidation reaction. Higher reaction temperatures resulted in lower conversions because of exothermicity and enzyme deactivation. The chemoenzymatic catalysis was found to be selective for epoxidation with no side reactions, and unsaturation to epoxide conversion of more than 90 % was obtained (Tornvall et al. 2007; Shangde et al. 2011; Vlcek et al. 2006). The prominent drawback found with chemoenzymatic catalysis is very slow rate of reaction.

There are several reports on the use of commercial ion exchange resins as catalysts which showed that Amberlite IR-120 H is highly active in epoxidizing unsaturated fatty acids of vegetable oils. Amberlite IR-120 H resin can catalyze epoxidation reactions only by using acetic acid as an oxygen carrier and hydrogen peroxide as oxidant. The ion exchange resin was reported to be an active catalyst for the epoxidation of vegetable oils such as canola oil, karanja oil, castor oil and soybean oil. The reaction conditions reported to be favourable for epoxidation reaction using Amberlite IR120 H catalyst are reaction temperature (50 to 70 ^{o}C), hydrogen peroxide to oil molar ratio (1 to 2), acetic acid to hydrogen peroxide molar ratio (1 to 2) and catalyst loading (10 to 20 wt%). 100 % conversion of unsaturation to epoxide was observed in reaction time of 6 to 15 h depending on the extent of unsaturation in the feedstock. The reaction was found to be exothermic and followed pseudo-first order reaction. Amberlite IR-120 H catalyst showed reusability up to three times (Petrovic et al. 2002; Mungroo et al. 2008; Sinadinovic-Fiser et al. 2008; Dinda et al. 2011).

Application of heterogeneous metal oxide and metal-supported catalysts for the catalytic epoxidation of vegetable oils would be a promising idea to overcome the challenges encountered

with the catalysts shown above. Solid acid catalysts with selective surface acidity helps to promote epoxidation reactions and could be considered as a substitute for inorganic acids, enzymes, and resins (Fan et al. 2003). Metals such as Ag, Ti, Mo, W and Au in the form of oxides were reported to be active for the epoxidation of alkenes. Koo et al. (2005) synthesized MCM-48-supported WO_3 particles to investigate their catalytic behaviour on the epoxidation of olefins. Nanoparticles with an average size of 3-10 nm were prepared and supported on mesoporous MCM-48. Their results indicated that 5.0 wt% of WO_3 particles supported on MCM-48 are capable of oxidizing more than 85% of reactant mixtures using hydrogen peroxide as oxidant. Using MCM-48 as support, the catalytic activity of WO_3 particles increased drastically. This was attributed to active metal distribution and close interaction between WO_3 particles and MCM-48 support.

Chimentao et al. (2006) documented on the application of silver in the form of nanowires as unique catalysts for the epoxidation of alkenes. Silver prepared from the reported method was found to have an average size of 150 nm and observed to be more selective for ethylene epoxidation. The redox property of the catalyst played an important role in adsorbing oxygen over the surface and accommodating it to the nucleophilic C=C bond. To increase the catalytic activity of silver for epoxidation of styrene, cesium is loaded as an active metal. Under optimum conditions 0.25 wt% of Cs over Ag gave a maximum conversion of 94.6%. The metal loading over silver surface lowered the reducibility of Ag, which in turn led to the enhancement of epoxidation on an oxygen-rich atmosphere.

Dellamorte et al. (2011) reported on the Pd-Ag bimetallic catalysts for ethylene epoxidation using oxygen as an oxidant. The conversion was reported to be more than 80% and enhancement in the activity and selectivity of silver was observed by the addition of palladium. Catalytic activities of silica-supported silver particles were investigated for the epoxidation of ethyl benzene at 120 ^{o}C using tert-butyl hydroperoxide (Raji et al. 2012). The increase in the reaction rates by using silver as a catalyst was correlated with the increase in the rate of decomposition of tert-butyl hydroperoxide and accommodation of electrophilic oxygen atom over the surface. Ozbek et al. 2011 studied the catalytic behaviour of copper oxide, silver oxide and aurum oxide for ethylene epoxidation. Results indicated that silver oxide served as the best catalyst for epoxidation of ethylene. It was reported that high surface area of silver oxide helped in attracting oxygen molecules to the active surface and enhanced epoxidation reaction. From the review collected, it

is understood that silver can act as a promising catalyst for epoxidation reactions in the form of metal oxide.

Oxides of titanium can act as a photocatalyst for epoxidation reactions under UV light. Titanium loaded on amorphous silica was reported to be an active catalyst for the epoxidation of C=C in fatty acids in several earlier works. Amorphous Ti-Si catalysts successfully resulted in high conversions only at high temperatures, high catalyst loadings and longer reaction times (Berlini et al., 2001). Novel Ti/SiO_2 nano-sized solid catalysts synthesized by Ali and Kumar et al. (2012) showed high activity for epoxidation of triglycerides under minimum optimum conditions. Ti/SiO_2 calcined at 750ºC was found to exist in nanoparticle form with high BET surface area of 278 m^2/g and pore diameter of 20-50 μm. Nano form showed enhancement in activity because of high surface redox sites in Ti/SiO_2. Under UV light, 100% epoxide yield was achieved at room temperature of 35ºC using 1.7 wt % of Ti on SiO_2. Reported methodology suggests that Ti/SiO_2 under UV radiation found to be highly active for the epoxidation of alkenes using hydrogen peroxide.

Polyoxometalates substituted with transition metals are found resistant to oxidation and hydrolysis. Hence, such polymetaloxolates are capable of introducing various kinds of catalytically active sites. These active sites were found to affect the catalyst in promoting the epoxidation reactions (Mizuno et al. 2005). Investigation on catalytic activities of $Na_5[PV_2MoO_{40}]$ polyoxometalates using TiO_2 nanomaterial support was carried out by Tangestaninejad et al. (2008). These polyoxometalates were active for the epoxidation of olefins in the presence of hydrogen peroxide. Their investigations resulted in 85% and 70% epoxidation of cyclo-octene and cyclo-hexene, respectively. From the above two studies, it can be inferred that polyoxoanions are capable of efficient epoxidation either by direct interaction with olefins or by depositing on metal oxide supports. Prepared TiO_2 nanomaterials exhibited high surface areas with octahedral interstitial sites that could accommodate these metal oxides.

Furthermore, epoxidation of vegetable oils showed improvement in the physicochemical properties of the oils. Wu et al. (2000) reported that the kinematic viscosity and oxidative stability of vegetable oils can be improved by epoxidation of unsaturated fatty acids. This was observed with rapeseed oil whose kinematic viscosity was found to increase from 35 to 87 cSt after epoxidation. The increase in the kinematic viscosity also exhibited improvement in lubricity

property. The oil exhibited > 95% biodegradability as well. However, the pour point of the epoxidized oil was found to decrease after epoxidation (-15 to -12 ^{o}C). A study by Silva et al. (2015) also concluded that epoxidation of unsaturated fatty acids in the vegetable showed improvement in the physicochemical properties.

The literature on the epoxidation of vegetable oils was found to focus on the use of commercial resins, enzymes, and acids as catalysts. Application of metal oxide catalysts for the epoxidation of vegetable oils still needs to be explored. The above-mentioned summary on the application of metal oxides for the epoxidation of short chain alkenes helps in the catalyst development for the epoxidation of vegetable oils.

In conclusion, based on the literature review on the epoxidation of vegetable oils, application of heterogeneous metal oxides as catalysts for the epoxidation of canola oil and canola biodiesel would benefit the process in minimizing work-up procedures to extract the product, could be reusable, eliminates side reactions and improves selectivity. Metal oxides such as TiO_2, WO_3, and MoO_3 can be considered for the development of catalysts for the epoxidation of unsaturated fatty acids in the canola oil or canola biodiesel. Supports such as mesoporous silica and aluminum oxide could be considered because the selected metal oxides showed promising metal-support interactions and promoted the epoxidation reaction. Physicochemical characterization of epoxidized canola oil and epoxidized canola biodiesel helps to evaluate the improvement in the properties after epoxidation and find the application of oil as a lubricant.

2.4 Partial Selective Hydrogenation

Selective hydrogenation of vegetable oils is also one of the prominent chemical modification widely used in oleochemical industries. This modification is employed to remove unsaturation in the triglycerides of vegetable oils and also to maintain desired saturated fatty acid content in the oil. Also, hydrogenation of vegetable oils is carried out to improve physicochemical properties such as thermal degradation and rancidity (Choo et al. 2001). The presence of poly (linoleic and linolenic) unsaturated fatty acids in the oil show more susceptibility towards thermal decomposition and also affect the storage and aging stability. In this regard, selective hydrogenation is employed to produce monounsaturated compounds which are comparatively more stable.

The abovementioned chemical modification was also applied to synthesize biolubricants because it is found to contribute necessary properties required for a lubricant (Kritchevsky et al. 1996). Preparation of biolubricants involving the conversion of polyunsaturated fatty acids to monoenic acids by selective hydrogenation should be selective because of the following reason. The process results in the formation of *cis* and *trans*-acids. *Cis*-isomeric acids are promising as lubricants compared to *trans*-isomers because they have better flow properties and do not freeze at ambient temperature. Oil with more than 80% cis-oleic acid content is preferred for industrial applications as biolubricant (Nohair et al. 2005). Figure 2.3 shows the schematic representation of hydrogenation of vegetable oils (Soni et al. 2014). Selective hydrogenation reactions proceed through the conversion of linolenic acids to linoleic and oleic acids, followed by the conversion of oleic acids to saturated (C18:0) fatty acids. The following review summarizes on the hydrogenation of vegetable oils, catalysts used and optimum reaction conditions for maximum conversion and selectivity.

Ni-SiO_2 is a prominent catalyst widely used for the hydrogenation reactions. For the hydrogenation of vegetable oils, Cu, Ru, Pd, Pt were also found to be promising metals as a catalyst. Jovanovica et al. (1998) studied on the hydrogenation of vegetable oils such as sunflower oil and soybean oil. Nickel supported on silicate is found to be active and selective in the conversion of unsaturated fatty acids in both the oils (C18:1, C18:2, C18:3) to stearic acid (C18:0). A study by Choo et al. (2001) shows that Pt is effective for the hydrogenation of oleic acids in the palm oil. Preparation of Pt colloids between 1 to 3 nm sizes was found important to show the activity and also particle size showed significant influence on the reaction rate and selectivity towards the *cis*-isomers formation (need to be high for a potential lubricant). Hydrogenation of oleic acid was found to be high compared to linoleic acid due to structure conjugation. The formation of *trans*-isomers was found significantly low indicating the importance of the catalyst for the preparation of biolubricants. Veldsink et al. (2001) studied the activity of Pd as active metal for the catalytic hydrogenation of sunflower seed oil. The report shows that Pd is effective for hydrogenating linoleic acids to stearic acid and is poor for hydrogenating oleic acid. Also, Pd is found highly selective for producing *trans*-isomeric fatty acids which are not desirable for lubricity applications due to poor flow behaviour.

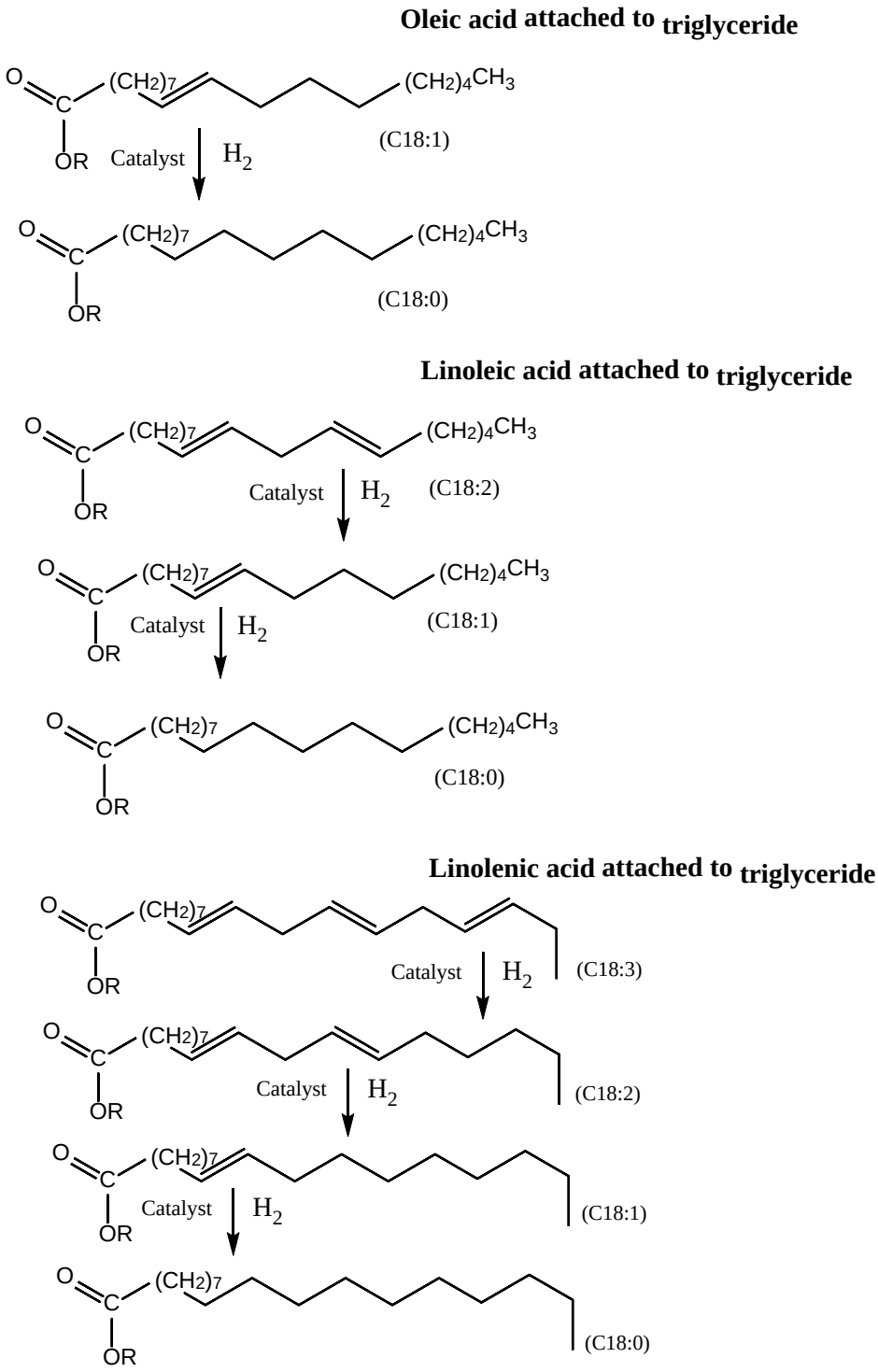

Figure 2.3 Reaction pathway for the selective hydrogenation of fatty acids in vegetable oils.

Ravasio et al. (2002) studied the activity of Cu supported on different supports such as SiO_2, TiO_2, Al_2O_3, ZnO, and sepiolite for the selective hydrogenation of rapeseed oil, sunflower oil, soybean oil, and soybean oil derived methyl esters. Reaction conditions reported for hydrogenation reaction are temperatures (180 and 270 ^oC), pressure 20 bar and reaction time between 3 to 20 h. 8 wt% Cu on SiO_2 support was found to be most effective for the hydrogenation of selected vegetable oils. The formation of C18:1 is more than 60 % at the selected conditions the and selectivity towards formation of *trans*-isomers is less than 20 %. The other important observation made in this report was an increase in C18:1 content remarkably enhanced the oxidative stability of the oils and the pour point was found to drop to -15 ^oC. There are several other reports studied on the hydrogenation of vegetable oils. Table 2.1 summarizes the available literature reports on the heterogeneous metal oxide catalysts used for the hydrogenation of vegetable oils.

Table 2.1 Literature on the metal oxide catalysts reported to be selective for hydrogenation of vegetable oils (Soni et al. 2014).

Feedstock	Metal Oxide Catalyst	Reaction conditions
1. Soybean oil (Jia et al. 2007)	Ruthenium nanoparticles	Temperature : 80 ^oC Pressure : 1.5MPa Reaction time : 12 h Particle size: 1 – 17 nm
2. Soybean oil (Choo et al. 2003)	Poly-Vinyl-Plastic stabilized Platinum and Palladium particles	Temperature : 35 ^oC Pressure : 0.1 MPa Reaction time : 1 h 30 min Particle size: 1.5 – 3 nm
3. Palm oil (Choo et al. 2001)	Platinum nanoparticles	Temperature : 35 ^oC Pressure : 0.1 MPa Reaction time : 1 h 30 min Particle size: 1.5 – 3 nm
4. Sunflower oil and Soybean oil (Jovanovica et al. 1998)	Nickel supported on silica	Temperature : 195-200 ^oC Pressure : 1.5 MPa Reaction time : 3 h

		Catalyst loading: 0.33 wt%
5. Sunflower oil derived ethyl esters (Nohair et al. 2005)	Palladium supported in silicon dioxide	Temperature : 40 ^{o}C Pressure : 1 MPa Catalyst loading : 0.3 -1.5 wt% Particle size: $10^5 – 4\times10^4$ nm
6. Rapeseed oil (Ravasio et al. 2002)	Copper supported on silicon dioxide	Pressure : 2 MPa Catalyst loading : 8 - 9 wt% Particle size: $10^5 – 4\times10^4$ nm
7. Sunflower seed oil (Veldsink et al. 2001)	Palladium nanoparticles	Temperature : 74 ^{o}C Pressure : 0.5 MPa of H_2 Particle size: 5 nm (pore size)

Wadumesthrige et al. (2009) reported on the changes in the physicochemical properties of oil after hydrogenation reaction, and also compared properties with epoxidized oils and ring opened oils. After hydrogenation, the oil exhibited improvement in oxidative stability and cetane number but showed poor cold flow behaviour. Cold flow properties were found to improve by adding hydroxyl and epoxy functionality at the unsaturation. Compared to epoxidized oils and hydroxylated oils, hydrogenated oils were found to show more oxidative stability, viscosity, and cetane number.

2.5 Estolides or Oligomerization of vegetable oils

Oligomerization or estolide formation reactions involve bonding between the double bonds of the unsaturated fatty acids to the long chain carboxylic acids (Soni et al. 2014). These reactions are carried out to change the fatty acid profile of the oils and results in the formation of oligomeric esters. The important reason behind carrying out oligomerization reactions is the attached secondary esters promote hydrolytic stability to the oil compared to it in its natural form. This is a very important property for a potential lubricant. Also, lubricants prepared from oligomerization reaction were found to show improvement in kinematic viscosity, oxidative stability, and lubricity. Hence, researchers have focused on the synthesis of biolubricants using oligomerization reaction.

Depending on the physical properties and extent of unsaturation in the feedstock, the addition of fatty acids (estolide number) will be done to obtain desired properties (Cermak et al. 2000; Isbell et al. 2011). Oligomerization of triglycerides results in highly viscous compounds that can be applicable as biolubricants for heavy duty operations and industrial machinery. Oligomerization of fatty acid alkyl esters would be promising for the preparation of different viscosity grade biolubricants. Oligomerization reactions are reported to occur at lower temperatures (between 40 to 100 ^{o}C) under vacuum. Acids such as perchloric acid, sulfuric acid, p-Toulenesulfonic acid are widely used in the literature to promote these reactions. Commercial Montmorillonite (K10) is also found active as a catalyst. The following literature review summarizes on the oligomerization of several vegetable oils, reaction conditions, catalysts used, and physicochemical properties of the prepared estolides. Figure 2.4 shown below shows the reaction schemes involving the formation of estolides by oligomerization reaction.

Different reactions steps involved for the preparation of several estolides are as follows.

Unsaturated trilgycerides + saturated carboxylic acid + catalyst = Bulky estolides

(Or)

Step 1: Unsaturated triglycerides ⟶ Unsaturated fatty acids

Step 2: Unsaturated fatty acids + saturated carboxylic acid + catalyst ⟶ Estolides

(Or)

Step 1: Unsaturated triglycerides ⟶ Alkyl esters

Step 2: Alkyl esters + saturated carboxylic acid + catalyst ⟶ Estolides

(i)

Triglyceride

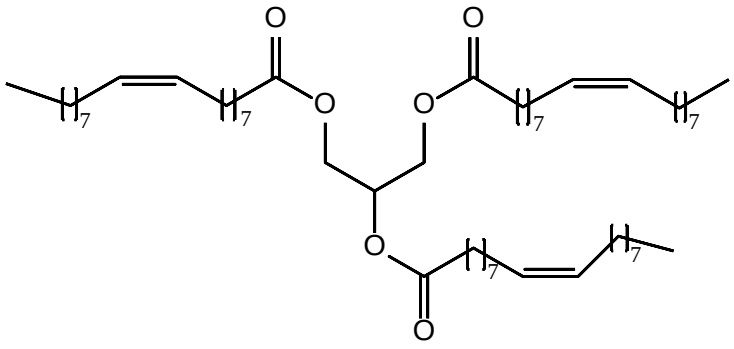

Catalyst

Epoxidation

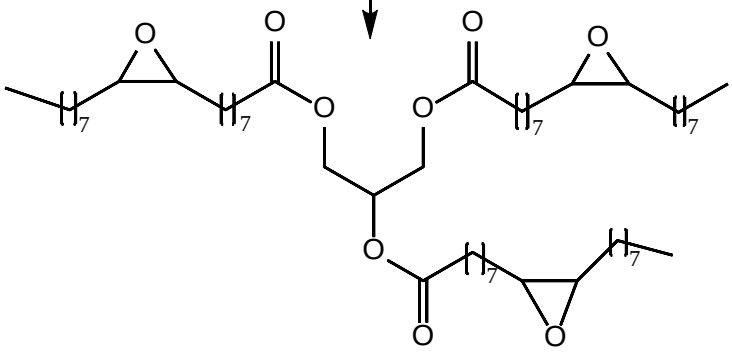

Catalyst

Epoxy ring opened with oleic acid

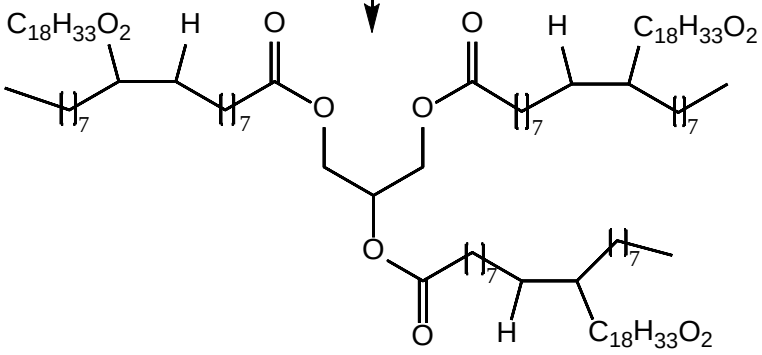

Estolide

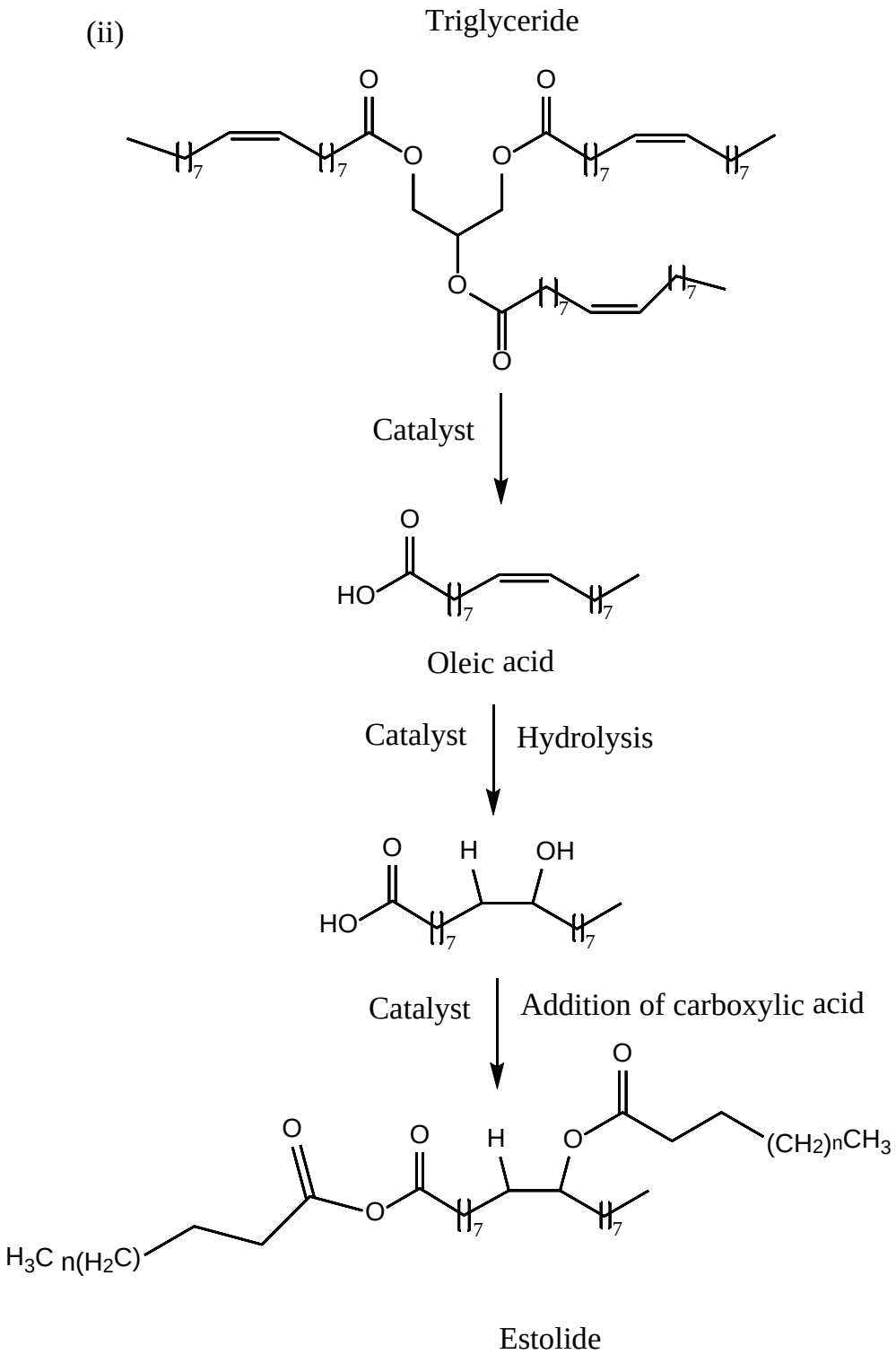

Figure 2.4 Reaction scheme for the estolide formation from (i) triglycerides, and (ii) carboxylic acids/fragments/alkyl esters.

Zapateiro et al. (2010) reported on the synthesis of several types of estolides from sunflower oil and investigated their application as a lubricant. Sulfuric acid was used as a catalyst for the oligomerization of olefins in the oil. The catalyst promoted the reaction by the formation of fatty acids followed by reaction with unsaturated sites. The reaction was found to be carried out at 50 ^{o}C and was monitored between 3 to 24 h. The molecular weight of the reaction mixture showed increment consecutively during the course of the reaction. The kinematic viscosities of the estolides formed at different reaction times were found between 279 to 431 cSt at 40 ^{o}C, 50 to 35 cSt at 100 ^{o}C. Monitoring the rate of oligomerization helps to control the kinematic viscosity of the oils and make them useful for several applications. The average viscosity index was found to be 179 which infers the ability of the estolides to resist the change against the temperature.

There are several other researchers who also worked on the oligomerization of several other oils and fatty acids and evaluated their physical properties. Table 2.2 summarizes the key findings on the articles of estolides derived from vegetable oils, alkyl esters and free fatty acids.

Table 2.2 Reaction conditions and properties of the estolides prepared from vegetable oils and fatty acids (McNutt et al. 2016).

Feedstock	Reaction conditions and key findings	Properties of estolides
Oleic and ricinoleic acids (Garcia-Zapaterio et al. 2013)	Temperature : 50 to 100 ^{o}C Catalysts screened : Sulfuric acid, perchloric acid, *p*-Toluensulphonic acid Sulfuric acid as a catalyst showed high degree of polymerization.	Kinematic viscosity at 40 ^{o}C : 582 to 6712 cSt Kinematic viscosity at 100 ^{o}C : 52 to 233 cSt Freezing temperatures: Oleic acid estolides (20 to -20 ^{o}C) Ricinoleic acid estolides (-20 ^{o}C below) Thermal stability: > 225 ^{o}C
Pennycress (Thlaspi arvenes L) based fatty acids (Cermak et al. 2015)	Temperature : 60 ^{o}C Pressure: 8 to 10 kPa Reaction time : 24 h	Kinematic viscosity at 40 ^{o}C : 494 to 498 cSt Kinematic viscosity

	Catalyst: Perchloric acid Physicochemical properties are effected by length of fatty acid chain and level of unsturation, and position of estolide attached.	at 100 ^{o}C : 42 to 75 cSt Viscosity index: 134-163 Pour point : -6 to 33 ^{o}C
Castor oil (Biresaw et al. 2011) (Estolides are prepared from the 2-ethyl hexanol castor oil derived esters reacted with lauric acid)	Temperature : 130 ^{o}C Pressure: 12 to 18 Pa Reaction time : 24 h Catalyst: Tin (II) 2-ethylhexanoate Yield : 73%	Kinematic viscosity at 40 ^{o}C : 51 cSt Kinematic viscosity at 100 ^{o}C : 10 cSt Viscosity index: 183 Pour point : < -54^{o}C RPVOT: 16 min
Lesquerella fatty acids and castor oil derived fatty acids (Cermak et al. 2006) Preparation of saturated and unsaturated fatty acid esters.	Temperature : 200 ^{o}C Pressure: 20 Pa Reaction time : 24 h	Kinematic viscosity at 40 ^{o}C : 30 to 70 cSt Kinematic viscosity at 100 ^{o}C : 6 to 12 cSt Viscosity index: 164 to 200 Pour point : -54 to 6 ^{o}C RBOT: 160 to 400 min
Oleic acid (Cermak et al. 2013) Preparation of estolides from oleic acid using linear alcohols	Temperature : 60 to 80 ^{o}C Reaction time: Proceeded until 99% complete formation of product is happened. Catalyst: Boron triflouride	Kinematic viscosity at 40 ^{o}C : 55 to 109 cSt Kinematic viscosity at 100 ^{o}C : 10 to 15 cSt Viscosity index: 163 to 184 Pour point : -9 to -33 ^{o}C
Oleic acid	Temperature : 60 to 80 ^{o}C	Kinematic viscosity

(Cermak et al. 2013) Preparation of estolides from oleic acid using various types of branched alcohols	Reaction time: Proceeded until 99% complete formation of product is happened. Catalyst: Boron triflouride	at 40 ^{o}C : 63 to 210 cSt Kinematic viscosity at 100 ^{o}C : 11 to 25 cSt Viscosity index: 149 to 192 Pour point : -39 to -24 ^{o}C
Coriander derived fatty acids and 2-ethyl hexanol fatty acid esters (Cermak et al. 2011) Estolides are prepared by capping with fatty acids.	Temperature : 60 ^{o}C Reaction time: 24 h, and more 4 h after the addition of 2-ethyl hexanol Pressure: 8 to 11 kPa Yield: up to 75%	Kinematic viscosity at 40 ^{o}C : 54 to 92 cSt Kinematic viscosity at 100 ^{o}C : 9 to 15 cSt Viscosity index: 151 to 165 Pour point : -33 to -12 ^{o}C
Castor oil (Biresaw et al. 2011) Estolides are prepared by reacting 2-ethyl hexanol esters with butanethiol	Reaction time : 3 h Photochemical reactor operated at low temperature < -28 ^{o}C.	Kinematic viscosity at 40 ^{o}C : 56 cSt Kinematic viscosity at 100 ^{o}C : 11 cSt Viscosity index: 144 Pour point : < -54 ^{o}C RPVOT: 224 min
Pennycress fatty acids (Cermak et al. 2015) Estolides prepared by preparing 2-ethyl hexanol ester followed by capping with fatty acids.	Temperature : 80 ^{o}C Pressure : 8 to 11 kPa Reaction time: 8 h Catalyst: Boron triflouride	Kinematic viscosity at 40 ^{o}C : 116 to 246 cSt Kinematic viscosity at 100 ^{o}C : 18 to 34 cSt Viscosity index: 169 to 183 Pour point : -24 to -12 ^{o}C

2.6 Epoxide ring opening and O-alkylation of epoxidized vegetable oils

The present section summarizes on the preparation of biolubricants by epoxide ring opening with alcohols, organic acids, and carboxylic anhydrides. Epoxidized vegetable oils are used as feedstocks for this chemical modification. The objective is to enhance the properties of the feedstock by adding stable functionality at the unsaturation. The addition of ester functionality using carboxylic acids and anhydrides not only promotes lubricity properties but also enhances cold flow temperature properties. This is because esters tend to resist crystallization of molecules at low temperatures (Sharma et al. 2015). The addition of alkoxy functionality at the unsaturation is reported to promote thermal and oxidative stability to the oil because alkoxy functionality is highly stable (Dinda et al. 2011). Following literature review provides insights on the application of various catalysts for the epoxide ring opening and O-alkylation of vegetable oils, and enhancement in the physicochemical properties of biolubricants compared to feedstocks.

Epoxide ring opening reactions are forwarded under the influence of a nucleophile. These reactions proceed through S_N1 or S_N2 type mechanisms depending on the nature of the catalyst and type of nucleophile used. Under acidic conditions, the reaction is found to proceed by the cleavage of C-O bonds followed by the attack of nucleophile at the most substituted carbon. For the preparation of biolubricants by epoxide ring opening reactions, special attention has been given for alcohols as nucleophiles (Sharma et al. 2013; Das et al. 2011; Fasi et al. 2005; Li et al. 2010).

Figure 2.5 shows the reaction schemes involving epoxidation of unsaturated triglycerides in the vegetable oils or alkyl esters, followed with epoxide ring opening with a nucleophile (alkoxylation, O-acetylation and di-O-acetylation). This could be two step (epoxidation, ring opening with alcohol or acid or anhydrides) or three step (epoxidation, ring opening with carboxylic acid and the addition of O-alkyl group to hydroxyl (OH) functionality).

Campanella et al. (2010) studied on the application of inorganic acids for the preparation of biolubricants from epoxidized sunflower oil. This study showed that sulfuric acid and fluoroboric acid could act as active catalysts for the epoxide ring opening and O-alkylation with methanol and ethanol as reactants. Sharma et al. (2006) reported on the synthesis of biolubricants from epoxidized soybean oil. Epoxide ring opening and hydroxylation reactions were carried out using octadanethiol, cyclohexyl mercaptan, butanethiol, and 1-decanethiol. The addition of

hydroxyl groups at the unsaturation exhibited improvement in the oxidative stability and lubricity property of the oil.

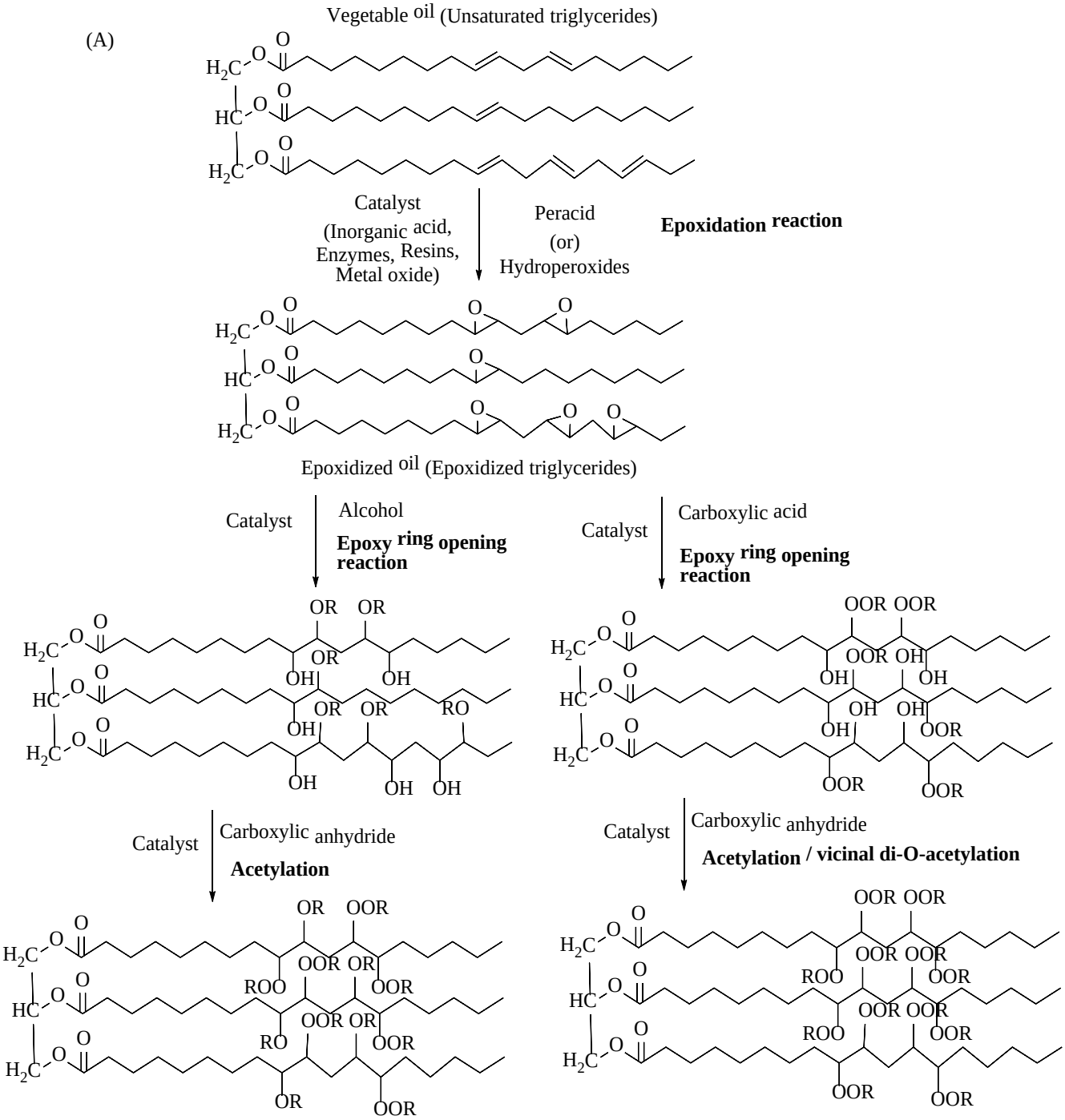

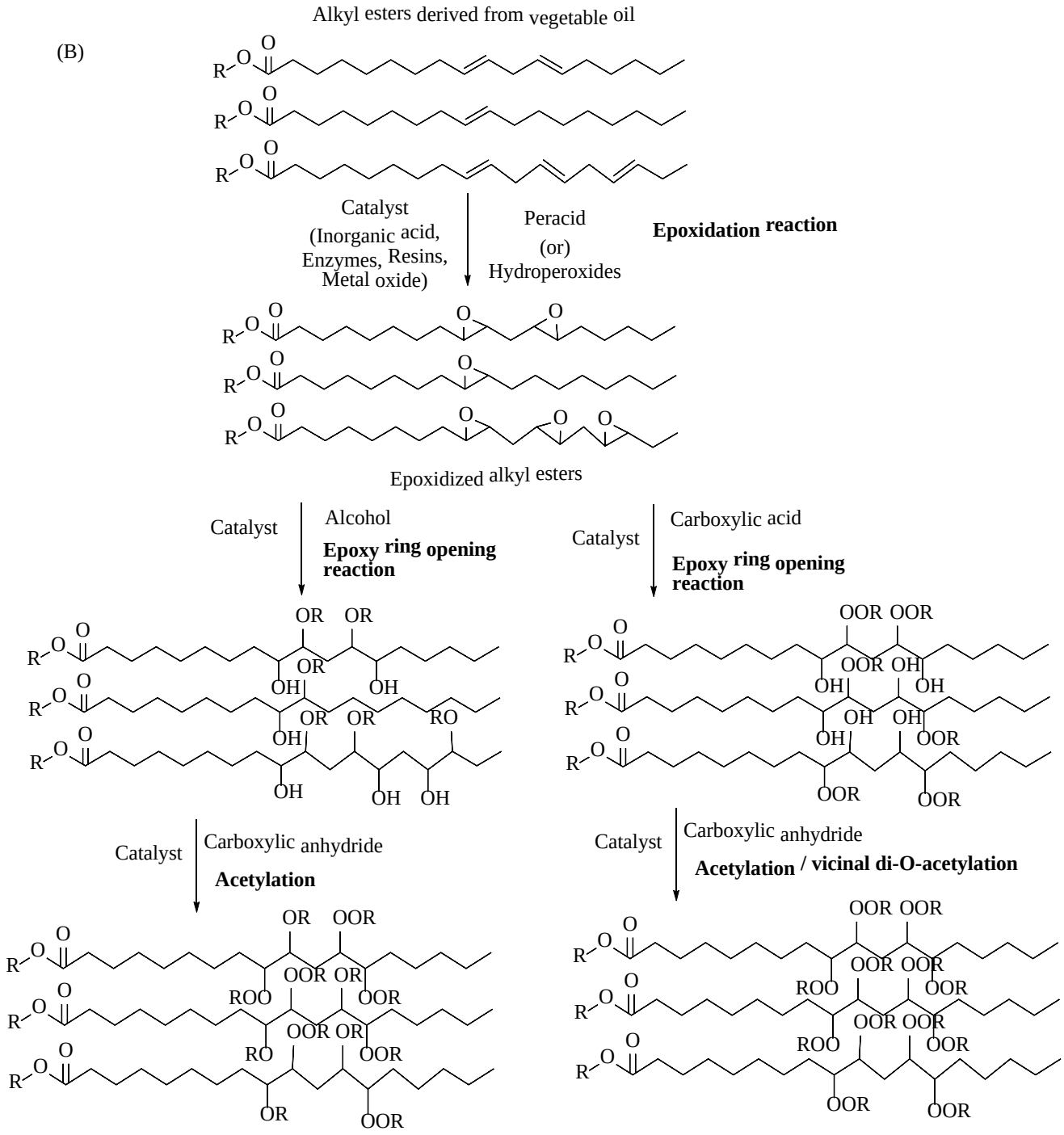

Figure 2.5 Reaction scheme for the preparation of biolubricants from (A) vegetable oil, and (B) alkyl esters through epoxidation and ring opening reaction.

Sharma et al. 2008 reported on the preparation of soyabean oil derived biolubricants. The biolubricants are prepared using several carboxylic anhydrides such as acetic anhydride, propionic anhydride, isobutyric anhydride, heptanoic anhydride and valeric anhydride. This report shows that BF_3 is a promising catalyst for the epoxide ring opening and O-acylation of epoxidized soyabean oil. Evaluation of tribological properties showed that addition of hexanoic anhydride at the epoxide centre enhanced lubricity properties of the oil. Patchara et al. 2011 studied on the improvement in the tribological properties of palm based methyl esters after the removal of unsaturation. Palm oil derived biolubricant was prepared by epoxidation followed by ring opening with 2-ethyl hexanol. The pour point of prepared biolubricant was found to be 9 ^{o}C. This report shows that pour point of epoxidized palm oil esters is increased after ring opening with alcohol.

Madankar et al. (2013) reported on the of synthesis of biolubricants from canola oil by epoxidation followed by oxirane ring opening with alcohols (2-ethyl hexanol, n-butanol, and amyl alcohol). Amberlyst 15 resin was found to be active in catalyzing ring opening reactions with above-mentioned alcohols. This report highlighted that increase in the branching at the unsaturation part promoted cold flow temperature behaviour, kinematic viscosity, flash point, and ability to reduce friction between surfaces (wear and tear). Among the prepared canola oil derivatives, a product which was ring opened with 2-ethyl hexanol exhibited superior pour point (-15 ^{o}C), and flash point of 405 ^{o}C. Epoxide ring opened and amylated canola oil was observed to have pour point of -8 ^{o}C, and flash point of 361 ^{o}C. Epoxide ring opened and n-butylated canola oil was observed to have pour point of -5 ^{o}C, and flash point of 361 ^{o}C. The reaction parameters favourable for ring opening reaction was found to be temperature (100 ^{o}C), alcohol loading of 2 wt% per gram of epoxidized oil taken, speed of agitation of 1000 rpm and reaction of 15 h for complete conversion. Amberlyst 15 catalyst showed reusability up to four times without considerable decrease in the conversion.

Furthermore, Hwang and Erhan (2001) also investigated on the preparation of soybean oil derived biolubricants in the presence of several alcohols. This study also concludes that substitution of higher alcohol chain molecules at the epoxy centre enhances the ability of biolubricant to resist freezing at low temperatures. The pour point of O-alkylated biolubricants were found to be between -3 to -9 ^{o}C. With the addition of 1% commercially available pour point

depressant the pour point of oils has drop down to great extent (up to -40 ^{o}C) making them suitable as a lubricant for extreme conditions.

Table 2.3 Additional literature on the preparation of biolubricants by epoxidation, epoxide ring opening and O-alkylation reaction (McNutt et al. 2016).

Feedstock and type of reaction	Reaction conditions	Physicochemical properties
Mustard oil (Kulkarni et al. 2013) Epoxidation of mustard oil followed by ring opening with 2-ethyl hexanol	Temperature : 120 ^{o}C Oil to alcohol molar ratio: 1: 1.6 Catalysts found to be active : Sulfuric acid, methanesulfonic acid, sulfamic acid Yield: 92 to 95 %	Viscosity index: 105 to 159 Pour point : -28 to -35 ^{o}C
Soybean oil (Hwang et al. 2006) Epoxidation, ring opening with Guerbet alcohols, and then transesterification reaction	Temperature : 120 ^{o}C Reaction time : 20 h Oil to alcohol molar ratio: 0.6 Catalysts found to be active : Sulfuric acid Conversion : 100 %	Kinematic viscosity at 40 ^{o}C : 60 to 75 cSt Kinematic viscosity at 100 ^{o}C : 8 to 10 cSt Viscosity index: 96 to 135 Pour point : -36 to -27 ^{o}C
Soybean oil (Hwang et al. 2006) Epoxidation, ring opening with Guerbet alcohols	Temperature : 110 ^{o}C Reaction time : 20 h Oil to alcohol molar ratio: 0.47 Catalysts found to be active : Sulfuric acid	Kinematic viscosity at 40 ^{o}C : 23 to 196 cSt Kinematic viscosity at 100 ^{o}C : 16 to 21 cSt Viscosity index: 86 to 113 Pour point : -18 ^{o}C
Epoxidized oleic acid (Salih et al. 2011)	Temperature : 70 to 100 ^{o}C Reaction time : 4.5 h Catalysts found to be active : p-Toulensulphonic acid	Viscosity index: 71 to 232 Pour point : -43 to -21 ^{o}C Flash point: 123 to 306 ^{o}C

Epoxy ring opening to form 9-Hydroxy-10-acyloxyoctadecanoic acid		
9-Hydroxy-10-acyloxyoctadecanoic acid (Salih et al. 2011) Feed reacted with octanol to form Octyl 9-hydroxy-10-acyloxyoctadecanoate	Temperature : 60 ^{o}C Reaction time : 10 h Catalysts found to be active : sulfuric acid	Viscosity index: 85 to 183 Pour point : -44 to -21 ^{o}C Flash point: 123 to 256 ^{o}C
Epoxidized oleic acid (Salih et al. 2011) Ring opening with alcohols to form alkyl 9-alkyloxy-10-hydroxyoctadecanoate	Temperature : 60 ^{o}C Reaction time : 20 to 22 h Catalysts found to be active : sulfuric acid	Viscosity index: 95 to 215 Pour point : -28 to -11 ^{o}C Flash point: 113 to 233 ^{o}C
Epoxidized castor oil, epoxidized linseed oil and epoxidized sunflower oil. (Hashem et al. 2013) Ring opening and esterification with oleic acid.	Temperature : 150 ^{o}C Reaction time : 4 to 5 h Catalysts found to be active : p-Toluensulphonic acid	Kinematic viscosity at 40 ^{o}C : 45 to 95 cSt Kinematic viscosity at 100 ^{o}C : 9 to 17 cSt Viscosity index: 180 to 189 Pour point : -9 to -15 ^{o}C Thermal stability: > 290 ^{o}C Oxidative induction time: 3 h to 5 h.
Waste cooking oil (Wang et al. 2015)	Temperature : 90 to 140 ^{o}C Reaction time : 4 to 5 h	Kinematic viscosity at 40 ^{o}C : 16 to 43 cSt Kinematic viscosity at 100 ^{o}C : 3 to 7 cSt

Epoxidation, transesterification with methanol, and ring opening with alcohols such as isooctanol, isotridecanol and isooctadecanol	Catalysts found to be active: Calcium oxide for ring opening reaction.	Viscosity index: 135 to 157 Pour point : -9 to -15 ^{o}C RPVOT: 70 to 127 min.
Karanja oil (Gorla et al. 2014) Epoxidation and ring opening with acetic anhydride.	Temperature : 140 to 150 ^{o}C Reaction time : 7 to 9 h Catalysts found to be active: Sulfuric acid	Viscosity index: 110 to 128 Flash point : 228 to 288 ^{o}C

From the above review, it can be understood that use of alcohols and anhydrides could be promising for the preparation of biolubricants through epoxide ring opening reaction, and also improve the physicochemical properties of the oil. Most of the literature available on the synthesis of biolubricants through epoxide ring opening and O-alkylation reactions used inorganic acids and commercial Amberlyst 15 resin as catalyst. There is a knowledge gap with respect to the application of metal oxides as catalysts for the preparation of biolubricants. Also, it will be promising because heterogeneous catalysts are widely acceptable for industrial process, simplifies the preparation process, and minimizes extraction procedures making the process environmentally friendly.

2.7 Ecofriendly and biodegradable characteristics of vegetable oil derived lubricants.

A lubricant is called to be eco-friendly and biodegradable if it demonstrates low particulate emissions, non-toxicity in its composition, and more than 70% degradability in four weeks at room temperature under the presence of microorganisms (Nagendramma et al. 2012). The characteristic properties of vegetable oil derived lubricants which make them eco-friendly are as follows. Strong inter molecular hydrogen bonding in the fatty acids of biolubricants exhibits higher boiling temperatures. Apparently, when biolubricants are used in engines they tend to produce low carbon emissions because of high flash points making them eco-friendly (Salimon et al. 2010). Also,

absence of aromatic, sulfur and nitrogen contents in the biolubricants makes them non-toxic (Levizzari et al. 1999; Krzan et al. 2004).

Fatty acids derived from natural sources such as plant or animal oils are found to be biodegradable (Hofland 2012). Since biolubricants are derived from plant oils by chemical modification of fatty acids they are also anticipated to be biodegradable. Biodegradability means ability of the oil to get easily breakdown into smaller fragments under the influence of microorganisms (esterases and lipases) at normal environmental conditions. This is determined in terms of time frame (Broekhuizen et al. 2003). Studies by Mecurio et al. 2003 showed that vegetable oil derived biolubricants are highly biodegradable. More than 70% biodegradation was observed in four weeks which is promising for their application as lubricants in industrial and automobile sectors. Also literature confirmed the biodegradability of vegetable oil derived biolubricants and methyl esters (Campo et al. 2007; Al-Darbi et al. 2005; Demirba et al. 2009).

This research investigation is also focused on the preparation of lubricants from vegetable oils. Since several studies confirmed that vegetable oil derived compounds are biodegradable, the biolubricants produced in this research are also anticipated to be biodegradable. Biolubricants prepared in this research are eco-friendly because, the qualitative analysis showed the absence of aromatics, sulfur and nitrogen compounds in the feedstocks. Also, the boiling points of biolubricants are found much higher when compared to mineral oil based lubricants. This could result in no emissions when used as lubricants in engines and gears.

2.8 Knowledge gaps

1. The potential of metal oxide catalysts for the synthesis of epoxidized canola oil and the physicochemical properties of epoxidized canola oil are not reported.
2. Synthesis of epoxide ring opened and vicinal di-O-acetylated canola oil (biolubricant type 1) using metal oxide catalysts and its kinetic studies are not investigated.
3. There is no research investigation on the application of heterogeneous catalyst for the one-pot synthesis of epoxide ring opened and vicinal di-O-acetylated canola oil/canola biodiesel.
4. Synthesis and physicochemical properties of epoxide ring opened and O-propylated canola oil/canola biodiesel (biolubricant type 2) are not studied. There is no metal oxide catalyst reported to be active for epoxide ring opening and O-propylation of canola oil/canola biodiesel.

2.9 Hypothesis

1. Metal oxide catalyst with selective Lewis acidity promotes epoxidation reaction. Sulfation of metal oxides helps in enhancing Lewis acidity of the catalyst surface and is anticipated to promote epoxidation reaction.
2. The solid acid catalyst promotes epoxide ring opening and vicinal di-O-acetylation reaction through protonation. Sulfation of metal oxides is a prominent approach for enhancing surface acidity to promote nucleophilic substitution reactions such as O-acetylation or di-O-acetylation.
3. Metal support interactions providing active surface acidity to promote both epoxidation and epoxide ring opening and vicinal di-O-acetylation reaction helps to synthesize biolubricants in one-pot using a single catalyst.
4. Epoxidation followed by epoxide ring opening with 1-propanol (nucleophile) reaction helps to synthesize O-propylated canola oil/canola biodiesel. Metal-metal or metal support interaction will generate Lewis acidity and helps to promote nucleophilic substitution reactions such as epoxide ring opening and O-propylation.

2.10 Research objectives

The overall objective of this Ph.D. research work is to develop metal oxide catalysts for the synthesis of biolubricants from canola oil and canola biodiesel, and evaluate their physicochemical properties as per ASTM and AOCS standard methods. Following are the sub-objectives involved to accomplish the overall objective.

1. Synthesis of epoxidized canola oil (biolubricant base oil) using metal oxide catalyst, process parameter optimization, kinetic studies, and evaluation of its physicochemical properties.
2. Synthesis of canola oil derived biolubricant by epoxide ring opening and vicinal di-O-acetylation of epoxidized canola oil, process parameter optimization and kinetic study.
3. One-pot synthesis of biolubricants such as vicinal di-O-acetylated canola oil and vicinal di-O-acetylated canola biodiesel, process parameter optimization, and comparison and evaluation of physicochemical properties.
4. Synthesis of canola oil/canola biodiesel derived biolubricant by epoxidation followed by epoxide ring opening and O-propylation reaction, process parameter optimization, kinetic study and evaluation of physicochemical properties.

2.11 Organization of the thesis

This thesis is divided into seven chapters, the work related to above-mentioned four objectives was included in chapter's three to six. In these chapter's, major emphasis was given to develop metal oxide catalysts for preparing desired biolubricants. A systematic approach was made in each phase of research work to accomplish the objectives and to fulfill the knowledge gaps.

The first chapter introduces the research work along with the research overview. The second chapter comprehensively summarizes the literature involved with the preparation of biolubricants through various chemical modifications, reaction conditions, catalysts found to be active and impact on the physicochemical properties after the chemical modification.

The third chapter focuses on the preparation of epoxidized canola oil. This phase involves catalyst preparation and characterization, optimization of process parameters, evaluation of inter and intra- particle mass transfer resistances, kinetic studies and development of the kinetic model, and evaluation of physicochemical properties of epoxidized canola oil.

In the fourth chapter, epoxidized canola oil was used as base oil for the preparation of biolubricant type 1 (vicinal di-O-acetylated canola oil). This phase involves catalyst preparation and characterization, process parameter optimization using Taguchi experimental design method, statistical analysis, evaluation of inter and intra- particle mass transfer resistances and kinetic studies and development of the kinetic model.

The fifth chapter of the work is emphasized on the preparation of catalyst that is active for both epoxidation, and epoxide ring opening and vicinal di-O-acetylation reactions. Also, one-pot synthesis procedure was developed to prepared biolubricants in less time, minimize work-up procedures and catalyst loading. This phase involves catalyst screening tests on model compounds, development of ^{1}H NMR methodology to predict conversion and side reactions, catalyst characterization, optimization of process parameters using central composite design scheme, statistical analysis using response surface methodology, and development of one-pot synthesis procedure for the preparation of canola oil and canola biodiesel derived biolubricants.

The sixth chapter of the work is focused on the preparation of canola oil and canola biodiesel derived biolubricants type 2 through epoxidation, epoxide ring opening, and O-propylation reaction. This phase also involves catalyst screening tests on model compounds, catalyst

characterization, optimization of process parameters using central composite design scheme, statistical analysis using response surface methodology, evaluation of inter and intra-particle mass transfer resistances, kinetic studies, development of the kinetic model, and measurement of physicochemical properties of the biolubricants.

The seventh chapter provides overall conclusions of this research work and recommendations for the future work.

CHAPTER 3

SYNTHESIS OF EPOXIDIZED CANOLA OIL (BIOLUBRICANT BASE OIL) AND EVALUATION OF PHYSICOCHEMICAL PROPERTIES

This part of the work has been published as research article and was presented at the following conferences:

1. Asish K. R. Somidi, Rajesh V. Sharma, Ajay K. Dalai, "Synthesis of Epoxidized Canola oil Using Sulfated-SnO_2 Catalyst," Industrial and Engineering Chemistry Research, 53 (49), 18668-18677 (2014).
2. Asish K. R. Somidi, Rajesh V. Sharma, Ajay K. Dalai, "Synthesis of Epoxidized Canola oil Using Sulfated-SnO_2 Catalyst," Oral presentation at 23rd Canadian Symposium on Catalysis, Edmonton, May 2014.
3. Asish K. R. Somidi, Rajesh V. Sharma, Ajay K. Dalai, "Surface properties of Sulfated-SnO_2 Catalyst for the synthesis of lubricant base oil from canola oil," Oral presentation at 26th Canadian Material Science Conference, Saskatoon, June 2014.

Contribution of the Ph.D. candidate

All the experimental and characterization work was conducted by Asish Somidi. Manuscript writing and revision work was done by Asish Somidi based on the suggestions from Dr. Ajay K. Dalai and Dr. Rajesh V. Sharma (postdoctoral fellow).

Contribution of this chapter to the overall Ph.D. work

This research work was focused on the synthesis of an intermediate product called epoxidized canola oil for the preparation of canola oil derived biolubricants.

3.1 Abstract

The main objective of this phase is to prepare a solid acid catalyst for the epoxidation of unsaturated fatty acids in the canola oil. Catalyst screening tests showed that SnO_2 exhibited promising activity (30% conversion) in reaction time of 6 h. The surface acidity of SnO_2 was enhanced to increase the catalytic activity by sulfate ions linkage after the calcination at 550 ^oC for 4 h. Sulfation treatment was selected because sulfation increases the surface acidity of the catalyst by three-fold times. A detailed catalyst characterization was done to measure the surface and bulk properties, and to understand the catalyst properties required for the effective catalysis. Process parameter optimization was undertaken to study the effect of each parameter on the unsaturation conversion to epoxide, and the optimum process conditions at which 100 % unsaturation conversion to epoxide obtained are: temperature (70 ^oC), catalyst loading of 10 wt % with respect to canola oil taken, ethylenic unsaturation to 30 wt % H_2O_2 molar ratio (1:3), ethylenic unsaturation to acetic acid molar ratio (1:2), and reaction time of 6 h. The formation of epoxidized canola oil was also identified by ^1H NMR, ^{13}C NMR, and FTIR. The reaction pathway of epoxidation of canola oil reaction was understood based on the kinetic studies. For the kinetic studies, reactions were carried out at different temperatures between 50 to 80 ^oC. Before testing the reaction mechanisms, theoretical calculations were made to prove the absence of inter and intra-particle mass transfer resistances. The epoxidation of canola oil reaction followed pseudo first-order reaction, and the calculated apparent energy of activation was 18 kcal/mol. Physicochemical characterization of epoxidized canola oil was made to understand and measure the properties of the oil after removing the unsaturation. The evaluated physicochemical properties of the epoxidized canola oil are: lubricity property in terms of wear scar length (189 μm), oxidative stability (60 h), cloud and pour point (15 and 9 ^oC), thermal stability (flash point, 319 ^oC), kinematic viscosities (114 cSt at 40 ^oC, 19 cSt at 100 ^oC) and viscosity index (188).

3.2 Introduction

This research work emphasizes on the synthesis of epoxidized canola oil, which is a base oil for the biolubricant synthesis. Commercially available epoxidized vegetable oils are produced by in-situ epoxidation process using peroxy acids as oxidizers catalyzed by mineral acids (Petrovic et al. 2002). Also, literature reports on the epoxidation of vegetable oils are mostly involved with the application of acids, enzymes, and ion exchange resins as catalysts. Though homogeneous

acid catalysts favour epoxidation reactions, there is possibility for side reactions such as oxirane ring opening to mono or diol, and hydroxyl ester formation (Lathi et al. 2006). In the case of enzymatic catalysis, deactivation of enzymes is observed because of the use of hydrogen peroxide. To avoid the limitations with mineral acids, enzymes, and resins, heterogeneous metal oxide catalysts are preferred. Also, use of heterogeneous catalysts would be more favourable with respect to ease of separation, reusability and environmental safety (Fadhel et al. 2010).

However, studies on the heterogeneous catalytic activity of metal oxides for epoxidation of vegetable oils are very limited. Campanella et al. (2004) used heterogeneous Ti-SiO_2 for the catalytic epoxidation of soybean oil and soybean methyl esters using hydrogen peroxide as oxidant. It is found that titanium on amorphous silica support is highly effective for epoxidation of unsaturated fatty acids using hydrogen peroxide as oxidant. Mohamed et al. (2007) reported on the catalytic activity of tungsten for the epoxidation of sunflower oil. Sulfated-SnO_2 is known to have strong surface acidity and comes under the class of super solid acid. It was used in most of the acid catalyzed reactions such as esterification and transesterification reactions (Khder et al. 2008). There was no literature report available on the use of sulfated-SnO_2 as a catalyst for the epoxidation of unsaturation in vegetable oils. Also, Sharma et al. (2013) reported that sulfated metal oxide surface can act as both solid acid and oxidative catalyst. Based on its acidic properties it was selected for epoxidation of unsaturated fatty acids in the canola oil.

The main objective of this research work is to synthesize epoxidized canola oil using sulfated tin oxide (sulfated-SnO_2) as a heterogeneous catalyst. This is a first report on the application of sulfated-SnO_2 for the epoxidation of unsaturation in the canola oil. Other objectives of this research work are: to determine the surface reaction mechanism, process parameter optimization, kinetic studies, development of a kinetic model, to identify order and activation energy of the reaction, and evaluation of tribological properties of epoxidized canola oil. This is done to measure and compare its properties with the ISO VG [viscosity grade] 46 specifications of gear oil lubricants.

3.3 Experimental

3.3.1 Chemicals and reagents

Canola oil was supplied by Loblaws Inc. (Montreal, Canada). The procurement of other chemicals includes glacial acetic acid (100%) from EMD Chemicals Inc. (Darmstadt, Germany), methylene chloride ACS grade, sulfuric acid, sodium thiosulphate, Tin (II) chloride dihydrate 98%

and Ammonium hydroxide ACS reagent from Sigma-Aldrich (St. Louis, MO, USA). Hydrogen peroxide GR grade (30 wt %) and ethyl acetate from EMD Chemicals Inc. (Darmstadt, Germany), and Wij's solution from VWR (San Diego, CA, USA).

3.3.2 Catalyst synthesis

Tin oxide (SnO_2) and sulfated-SnO_2 were prepared as per the following method (Khder et al. 2008). 100 g of tin (II) chloride dihydrate was dissolved in 2 L of distilled water with continuous stirring at 30 ^oC followed by the dropwise addition of 25 % (vol/vol) ammonium hydroxide solution until pH between 8-10. After the formation of a white precipitate, the solution was aged for 2 h at 30 ^oC. The precipitate was then filtered and washed with distilled water until pH 7 and dried at 120 ^oC for 12 h. 10 g of tin hydroxide powder is then treated with the 300 ml of 1M H_2SO_4 solution. Obtained gel was then dried at 120 ^oC for 12 h and calcined at 550 ^oC for 4 h to form sulfated-SnO_2. Also, synthesis of tin oxide was made by the calcination of tin hydroxide gel at same conditions.

3.3.3 Preparation procedures

The epoxidation of canola oil reaction scheme is shown in Figure 3.1. All experiments were performed in a 100 ml three-necked round bottom flask which contains magnetic stirrer and temperature controlled oil bath. The flask is connected to a condenser for reflux and a thermometer to measure the temperature of the reaction mixture. Calculated amounts of canola oil, acetic acid and catalyst were added initially and stirred at desired temperatures for 30 min. Then, required amount of 30 wt% hydrogen peroxide was added dropwise to the reaction mixture. Uniform stirring was maintained during the reaction time and samples were collected at regular intervals for measuring the oxirane content and iodine value analysis. Prior to the analysis, each sample is collected and extracted with ethyl acetate to separate oil and water mixture. Ethyl acetate in oil sample is degassed by using a rotary evaporator, and finally, anhydrous sodium sulfate is added to it to adsorb traces of water (Mungroo et al. 2011).

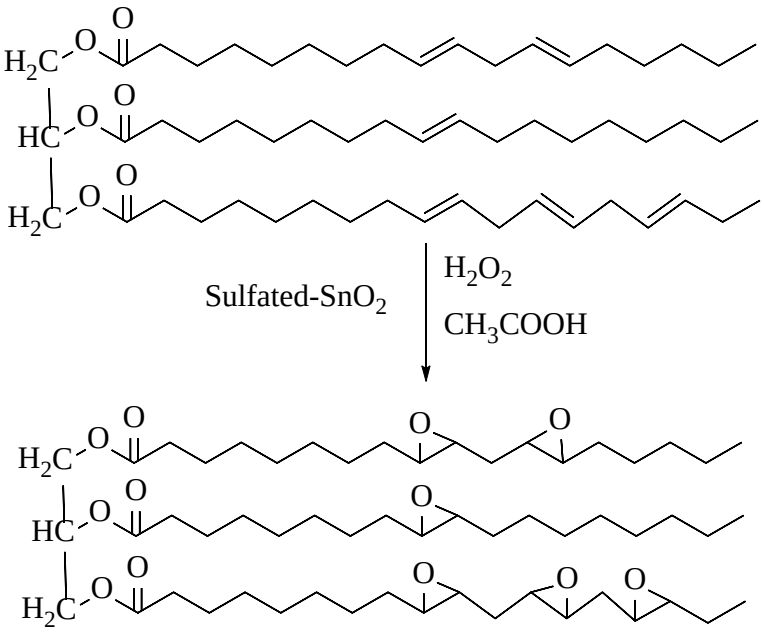

Figure 3.1 Epoxidation of canola oil reaction scheme

3.3.4 Method of analysis

The oxirane oxygen content of each sample was measured as per AOCS Cd 9-57 method by volumetric titration against 0.1 N HBr solution in glacial acetic acid, and iodine value which measures percentage unsaturation was determined using AOCS Cd 1-25 method. Also, product was confirmed with spectroscopic studies such as Infra-red spectroscopy, ^{13}C NMR, and ^{1}H NMR. Oxirane oxygen and percentage unsaturation conversion (mol %) are measured as follows:

$$\text{Oxirane oxygen} = \frac{\text{ml of HBr consumed x 0.1 x 1.60}}{\text{Quantity of sample taken, g}} \qquad (3.1)$$

$$\text{Iodine value (\%unsaturation)} = \frac{(B - S) \text{ x N x } 12.69}{\text{Quantity of sample taken, g}} \qquad (3.2)$$

Where B = volume of titrant, ml of blank, S = volume of titrant, ml of sample, and N = normality of $Na_2S_2O_3$.

3.3.5 Catalyst characterization methods

Both SnO_2 and sulfated-SnO_2 samples were characterized by following methods to determine and confirm the bulk and surface properties of the catalysts. For FT-IR analysis, a small amount of sample (5-10 mg) is mixed with KBr crystals (90-95 mg) and thoroughly grounded to form fine powder. The pellet was made from this powder using 6 mm dye under 10 ton of pressure. Further, IR analysis was carried out between frequency range 4000-400 cm^{-1} using Perkin Elmer spectrophotometer with 8 cm^{-1} resolution. Renishaw Raman InVia microscope (spectra-physics model 163) was used to obtain the Raman spectra of the samples. An argon ion laser beam with the wavelength 514 nm, the spot size of 1-2 µm and 3.6 mW power was used. The XRD patterns of the samples were determined on a Rigaku Diffractometer using CuKα radiation in the range $10\text{-}80^0$ with a scan rate of 2^o per minute. The specific surface area, pore volume, and pore size distributions were measured with a Micromeritics ASAP 2000 instrument using low temperature (77K) N_2 adsorption-desorption isotherms. Brunauer-Emmett-Teller (BET) method was used to measure the specific surface area, average pore diameter, and total pore volume were calculated using BJH adsorption and desorption isotherms. The thermal analysis of SnO_2 and sulfated-SnO_2 were investigated on TGA-Q500 series (TA instruments). Weighed samples were heated from 25 to 800^oC to study the weight loss attributed to the decomposition of these materials. Also, this study was made to investigate the decomposition of sulfate species at reaction and calcination temperatures. The NH_3-Temperature Programmed Desorption (NH_3-TPD) of both the samples were analyzed by TPD/TPR-2720 Micromeritics (USA) instrument to investigate acidic strengths of the samples. 0.1 g of sample was collected in a quartz tube and purged with helium at 200^oC for 2 h to remove impurities on the surface and then cooled down to room temperature by passing helium. About 3 wt% NH_3 in N_2 was passed through the sample at a flow rate of 30 mL/min for 3 h and physisorbed NH_3 was removed by passing helium at 100^oC for 1 h. The analysis was carried out between 100 to 800^oC with a 10^oC/min ramp rate.

3.3.6 Physicochemical properties evaluation of epoxidized canola oil

As per ASTM D97-11 and ASTM D2500 – 11 standards, cloud point and pour point of canola oil and epoxy canola oil are measured. The instrument used for this method was K46100 Cloud point and Pour point Apparatus [Koehler Instrument Company, Inc., USA]. The test sample was introduced into a test vessel and kept inside the cooling chamber. Observations were made for

every 3^{o}C drop in the temperature. Cloud point temperature was reported when there was any hazy appearance in the liquid and pour point temperature was recorded when the test sample was found to be immobile after a tilt.

Using DV-II+ viscometer [Brookfield, USA], dynamic viscosities of the canola oil and epoxy canola oil were measured at temperatures ranging from 26.5 ^{o}C -100^{o}C as per ASTM D2983-03 standard method. From the obtained dynamic viscosities, kinematic viscosities and viscosity index were calculated as per ASTM D2270 – 10 standard.

As per AOCS CD 12-57 – 1981 method on oxidative stability, induction time was calculated. Metrohm 743 Rancimat apparatus [Metrohm, Canada] was used to measure the oxidative property of the test samples. Test samples were heated to 112^{0}C in a test vessel and supplied with air at 12 l/h to get oxidized. Oxidized compounds were detected by a pulse in the collector vessel consisting of milli-pore water and electrodes. Induction time was measured at the point of time where there is a rapid increase in the oxidation. High Frequency Reciprocating Rig [HFRR] apparatus was used to measure the lubricity property of the oil samples. As per ASTM D6079, ASTM D7688 methods wear scar of the test samples were measured. 5% of the test sample was added to 2 ml standard diesel and moved against the metal surface at 50 Hz for 75 minutes. Using optical microscope wear scar diameter of test metal sample was measured.

3.4 Results and discussion

3.4.1 Catalyst characterization

The FT-IR spectra of SnO_2 and sulfated-SnO_2 samples shown in Figure 3.2 are interpreted as follows. The absorption broad band centered at 627 cm^{-1} indicates O-Sn-O stretching and the band at 3430 cm^{-1} is due the presence of hydroxyl groups on the surface of the samples. The bands at 1209, 1151, and 1010 cm^{-1} of sulfated-SnO_2 are due to the asymmetric and symmetric stretching frequencies of sulfate ions (Khalaf et al. 2011; Krishnakumar et al. 2008). Figure 3.3 illustrates the Raman spectra of SnO_2 and sulfated-SnO_2 molecules. Raman shifts obtained at 634, 704 and 478 cm^{-1} correspond to the rotational and vibrational modes of O-Sn-O molecules. Raman intensities of sulfated-SnO_2 were observed to be less compared to the SnO_2 spectra because of the decrease in the polarizability and crystalline size of sulfated-SnO_2 due to strong interactions between SO_4^{-2} and SnO_2 molecules (Zhao et al. 2009). FT-IR and Raman spectroscopic analysis confirmed the

presence of sulfate linkage (acidity) on the catalyst which is important for promoting the oxidation reactions.

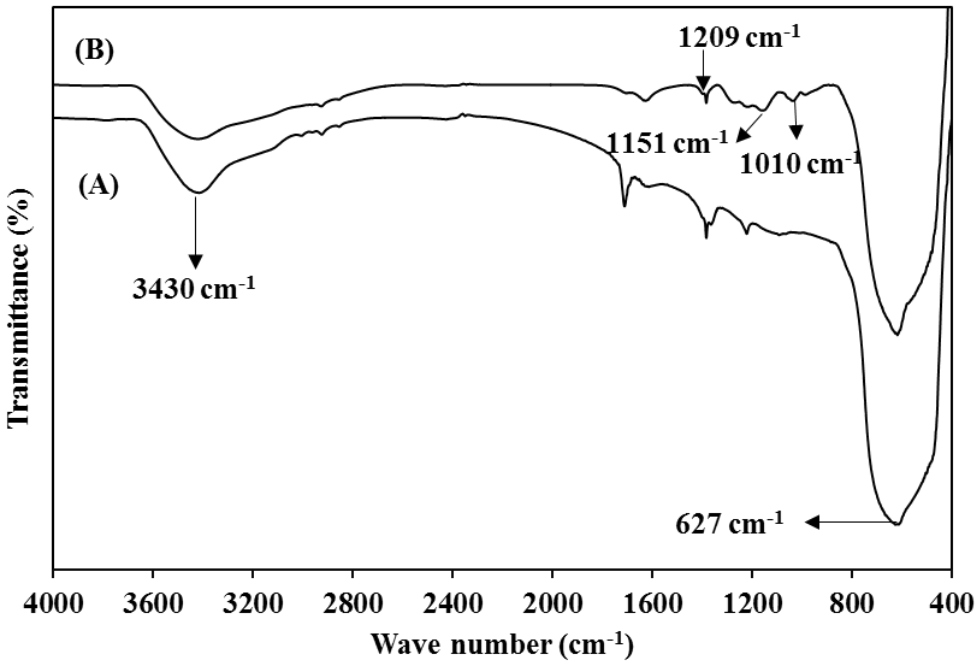

Figure 3.2 FT-IR spectra of (A) SnO_2, and (B) Sulfated -SnO_2

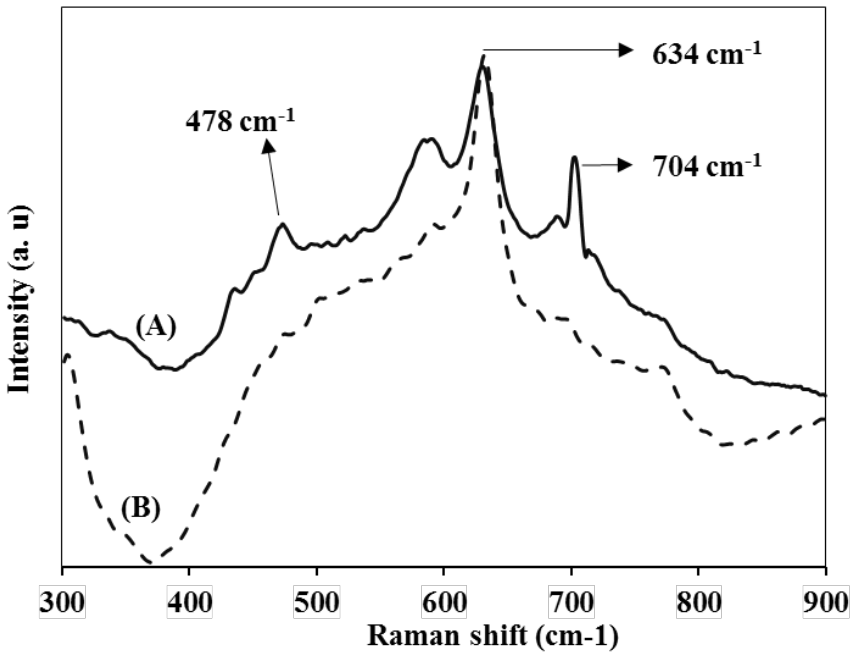

Figure 3.3 Raman spectra of (A) SnO_2, and (B) Sulfated -SnO_2

BET surface area measurement of both the samples exhibited type IV isotherm with hysteresis loop. Specific surface areas of SnO_2 and sulfated-SnO_2 were found to be 16 m^2/g and 38 m^2/g, respectively. An increase in the BET surface area of sulfated-SnO_2 is due to the formation of sulfate ions (SO_4^{-2}) linkage. BJH pore size distributions also elucidate that accumulation of sulfates on the oxide surface increased its pore volume from 0.1 to 0.2 cm^3/g and resulted in the decrease of average pore diameter to 17 nm. Table 3.1 summarizes the BET surface area and BJH pore size results. As anticipated, for bulky molecular transformation the porous catalyst is needed and hence sulfation improves the pore volume and is expected to increase the conversion.

Table 3.1 BET and BJH results of SnO_2 and Sulfated-SnO_2

Catalyst	BET surface area (m^2/g)	Pore volume (cm^3/g)	Average pore diameter (nm)
SnO_2	16	0.1	23
Sulfated-SnO_2	38	0.2	17

The obtained XRD patterns of SnO_2 and sulfated-SnO_2 are represented in Figure 3.4. The peaks corresponding to $2\theta = 26.5^o, 33.8^o, 37.9^o, 51.8^o, 64.9^o, 71.5^o$ represent the diffractions from planes (110), (101), (200), (211), (112), (202) of SnO_2 molecules which confirms the tetragonal crystal phase (Krishnakumar et al. 2008). The addition of sulfates did not result in any crystalline phase change. The approximate crystalline sizes of SnO_2 and sulfated-SnO_2 were calculated using Scherrer's equation, $d_{avg} = (0.8 \times \lambda)/ (\beta \times \text{Cos}\theta)$, where d_{avg} is the average crystal size, β is the FWHM (full width half max) of the reflection peak and θ is the Bragg's angle. The calculated average crystalline size of sulfated-SnO_2 was found to be 19 nm and 25 nm for SnO_2. The addition of sulfate ions resulted in the decrement of crystalline size because bulky sulfate groups prevent the agglomeration of SnO_2 particles during the calcination (Krishnakumar et al. 2008). The crystalline spacing in sulfated-SnO_2 was measured using Bragg's equation ($d_{spacing} = (\lambda)/ (2 \times \text{Sin}\theta)$ and was found to be 0.5 nm. This data is in agreement with the report by Jogalekar et al. (1998).

The thermal analysis is shown in Figure 3.5 elucidates the percentage weight loss of SnO_2 and sulfated-SnO_2 samples between the temperature range 25-800^{o}C. SnO_2 was found to be very stable at applied temperatures and percentage change in the weight was observed to be negligible (< 0.3 wt %). Sulfated-SnO_2 was also found to be very stable up to 600 ^{o}C with negligible weight loss (<

1 wt %), but the increment in the weight loss after 600 ^{o}C is because of the evolution of sulfate ions from the catalyst surface (Khder et al. 2008). The TGA analysis confirmed the stability of sulfated-SnO_2 at calcination and reaction temperatures.

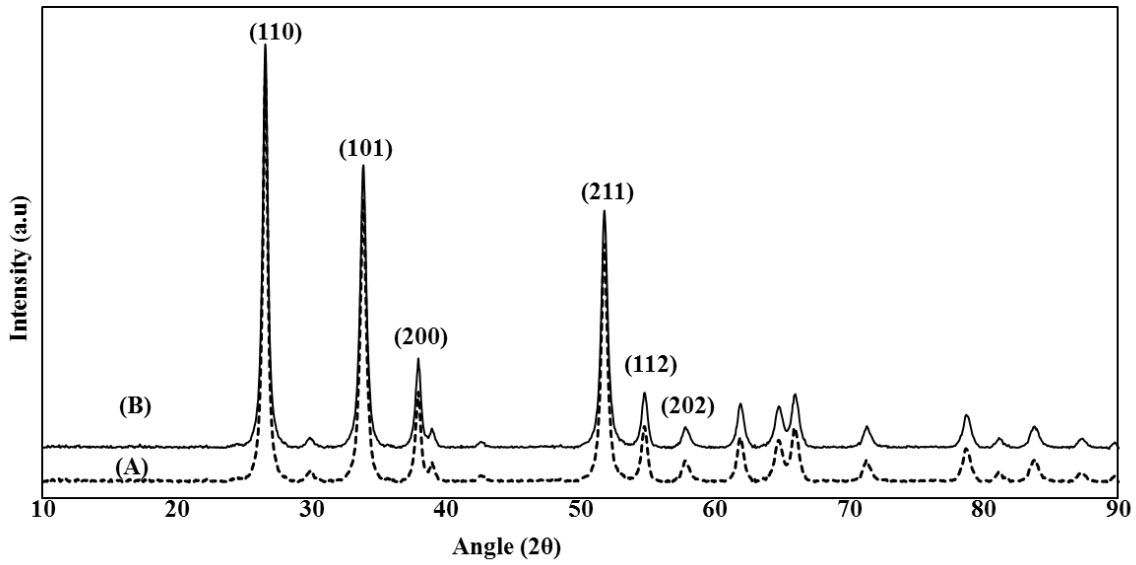

Figure 3.4 XRD peak pattern of (A) SnO_2, and (B) Sulfated-SnO_2

Figure 3.6 shows the NH_3-temperature programmed desorption behaviour of both the test samples. The sulfated-SnO_2 showed high temperature desorption of ammonia between 400-600^{o}C which corresponds to the strong acidity region. This could be because of the coordination of sulfate ions to tin oxide surface. In comparison to SnO_2 acidic strength, it can be confirmed that sulfated-SnO_2 is more acidic. Sharma et al. (2013) reported that sulfation of metal oxide surface increases the catalytic oxidative activity by three-fold and hence, it can be concluded that sulfation is the key to increase the conversion of canola oil to epoxidized canola oil.

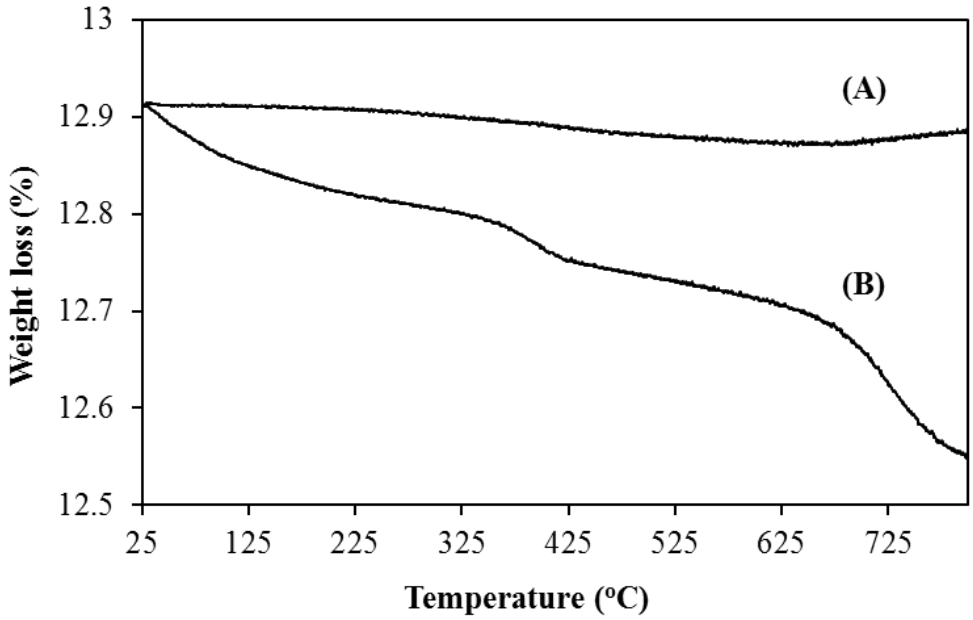

Figure 3.5 TGA analysis of (A) SnO_2, and (B) Sulfated-SnO_2

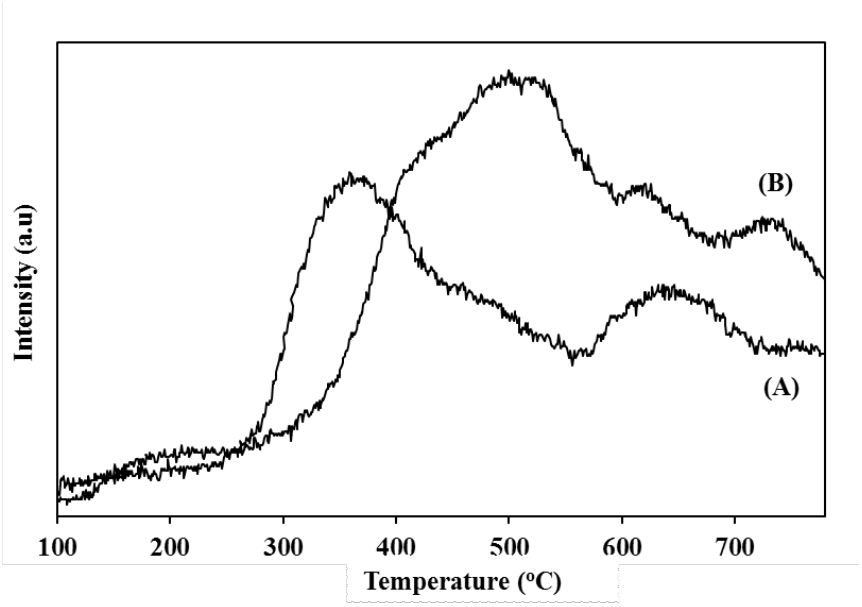

Figure 3.6 NH_3-TPD profiles of (A) SnO_2, and (B) Sulfated-SnO_2

3.4.2 Process parameter optimization study

3.4.2.1 Effect of inter-particle and intra-particle mass transfer resistances

In any heterogeneous catalytic reactions, the overall rate of reaction proceeds through rate of mass transfer of the reactants from bulk phase to the surface of the catalyst, rate of surface reaction and rate of desorption of products from the active sites. Since canola oil molecules are complex, viscous and bulky, a liquid film interphase may form between the catalyst surface and bulk fluid phase resulting in external mass transfer resistance. This film can also hinder diffusion of other canola oil molecules to access into the pores of the catalyst leading to internal mass transfer resistance (Fogler et al. 2002). Influence of external mass transfer resistance on sulfated-SnO_2 was investigated by changing the rate of mixing at different speeds ranging from 600-1000 rpm. Table 3.2 illustrates the effect of agitation speed on percentage conversion of canola oil to epoxidized canola oil based on the iodine value measurement. All the reactions were carried out at 70 ^oC for 6 h with 5 g of canola oil, 6.5 g of 30 wt% hydrogen peroxide and 4 g of acetic acid. The influence of speed of agitation on the conversion beyond 1000 rpm showed no effect. Hence, 1000 rpm is considered as optimum. Also, theoretical calculations were performed to confirm the absence of inter-particle and intra-particle mass transfer resistances.

Table 3.2 Effect of the agitation speed on percentage conversion of canola oil to epoxidized canola oil using a sulfated-SnO_2 catalyst. Reaction conditions: Canola oil (5.0 g), 30 wt% hydrogen peroxide (5.0 g), acetic acid (3 g), 10 wt% sulfated-SnO_2 catalyst, temperature (70 ^oC) and reaction time (8 h).

Speed of agitation (rpm)	% unsaturation conversion (mol%)
400	50
600	81
800	93
1000	100
1200	100

Sherwood number and Wilke-chang equations were used to calculate the mass transfer coefficients and investigate the inter-particle mass transfer resistances. Considering canola oil molecules as limiting reactants, the value of diffusivity of canola oil (D_{CO}) was evaluated from the Wilke-chang equation $D_{CO} = 117 \times 10^{-18} \times (\Psi \times M_{PAA})^{0.5} \times T / (\mu \times V_{CO}^{0.6})$ (Yadav et al. 2012), and was found to be 2×10^{-10} m^2/s. Where Ψ=1 (association factor of peracetic acid), M_{PAA} is the molecular weight of peracetic acid, T is reaction temperature in K (343 K), μ is the viscosity of reaction mixture (4.4 cP), and V_{CO} represent molar volume of canola oil (900 cm^3/mol). The mass transfer coefficient of canola oil (k_{cCO}) was calculated by equation $Sh = k_{cCO} \times (D_p/D_{CO})$, where D_p is the diameter of the catalyst particle (647 µm). Assuming Sherwood number value as 2 in extreme cases (Sharma et al. 2013; Yadav et al. 2012), the calculated value of k_{cCO} was found to be 5×10^{-7} m/s. The mass transfer flux of canola oil was calculated by $W_{COr} = k_{cCO} \times C_{Cos}$ (Yadav et al. 2012) where C_{Cos} is the concentration of canola oil and is taken as 384 mol/m^3 (assuming concentration at surface equal to bulk concentration), which was found to be 2×10^{-4} mol/ m^2s. Since measured initial reaction rate of 3×10^{-8} mol/m^2.s at standard reaction conditions is much lower than mass transfer rates, it is clear that the reaction is not controlled by the external mass transfer resistances.

The influence of intra-particle pore diffusion resistance is estimated by dimensionless parameter Weisz-Prater criterion $C_{WP} = r_{obs} \times \rho_c \times R_p^2 / D_{eCO} [C_{COS}]$ (Fogler et al. 2002), where r_{obs} is evaluated from observed rate of reaction, C_{COS} corresponds to concentration of canola oil at the external surface (384 mol/m^3), R_p is particle radius (324 µm), ρ_c is the density of catalyst (1.5 g/cm^3) and D_e is the effective diffusivity calculated from bulk diffusivity, constriction factor, porosity (θ) and tortuosity (τ). The typical values of constriction factor, porosity (θ) and tortuosity (τ) were taken as 0.8, 0.4 and 3.0 as a conservative estimate (Fogler et al. 2002). Calculated C_{WP} was found to be 0.004 which is much less than 1. Hence, it can be confirmed that there is no intra-particle diffusion resistance present in the reaction system at the reaction conditions used for the epoxidation reaction.

3.4.2.2 Effect of catalyst loading

Catalyst loading screening tests were carried out on experimental conditions such as reaction temperature of 70 °C, ethylene unsaturation of canola oil to 30 wt% hydrogen peroxide in 1: 3 molar ratio, ethylene unsaturation of canola oil to acetic acid in 1:2 molar ratio and speed of

agitation between 1000-1200 rpm. The effect of sulfated-SnO_2 loading on the epoxidation reaction was studied from 2.5 to 12.5 wt% with respect to the amount of canola oil taken (grams of catalyst taken per gram of oil). It was noticed that the percentage conversion of unsaturation in the canola oil to epoxidized canola oil was found to increase until 10 wt% sulfated-SnO_2 loading due to increase in the active site concentration. After 6h reaction time, sulfated-SnO_2 with 10 wt% loading showed 100 % unsaturation conversion in the canola oil with maximum oxirane content of 6.5. Further increase in the catalyst loading showed similar conversion after 6 h. Hence, 10 wt% loading was considered as an optimum loading to carry out further studies. Figure 3.7.A shows percentage unsaturation conversion in the canola oil based on iodine value measurement (equation 3.2) and oxirane content (equation 3.1) at different catalyst loadings.

3.4.2.3 Effect of hydrogen peroxide

Ethylenic unsaturation of canola oil to hydrogen peroxide molar ratio was varied in the range 1: X where X= 0, 0.8, 1.6, 2.4, 3 and 4. From Figure 3.7.B it can be observed that, an increase in hydrogen peroxide molar ratio enhanced the rate of oxirane (epoxidized canola oil) formation with the corresponding increase in percentage unsaturation conversion. Oxirane levels for lower hydrogen peroxide molar ratio from 0 to 2.4 were observed to be less and there was no effect beyond 3 molar ratio loading. Hence, the ethylenic unsaturation of canola oil to hydrogen peroxide molar ratio 1:3 was considered as optimum loading with maximum oxirane content.

3.4.2.4 Effect of acetic acid

Acetic acid acts as an oxygen carrier in the epoxidation reactions. It should be considered that use of excess acetic acid could result in the hydrolysis of the oxirane ring formed (Mungroo et al. 2011). Effect of acetic acid on the epoxidation of canola oil reaction was investigated at six different ethylenic unsaturation of canola oil to acetic acid molar ratios ranging from 1: Y (Y = 0, 0.5, 1, 1.5, 2, 2.5). Figure 3.7.C explains the effect of acetic acid loading with respect to oxirane content and percentage unsaturation conversion. It can be observed that the increase in acetic acid loading enhanced the rate of epoxidation conversion, but excess loading resulted in epoxy ring opening. After 6 h of reaction time with ethylenic unsaturation to acetic acid molar ratio of 1:2, 100% unsaturation conversion was achieved with maximum oxirane content. Hence, this amount of loading was taken as optimum loading for the temperature effect studies.

(A)

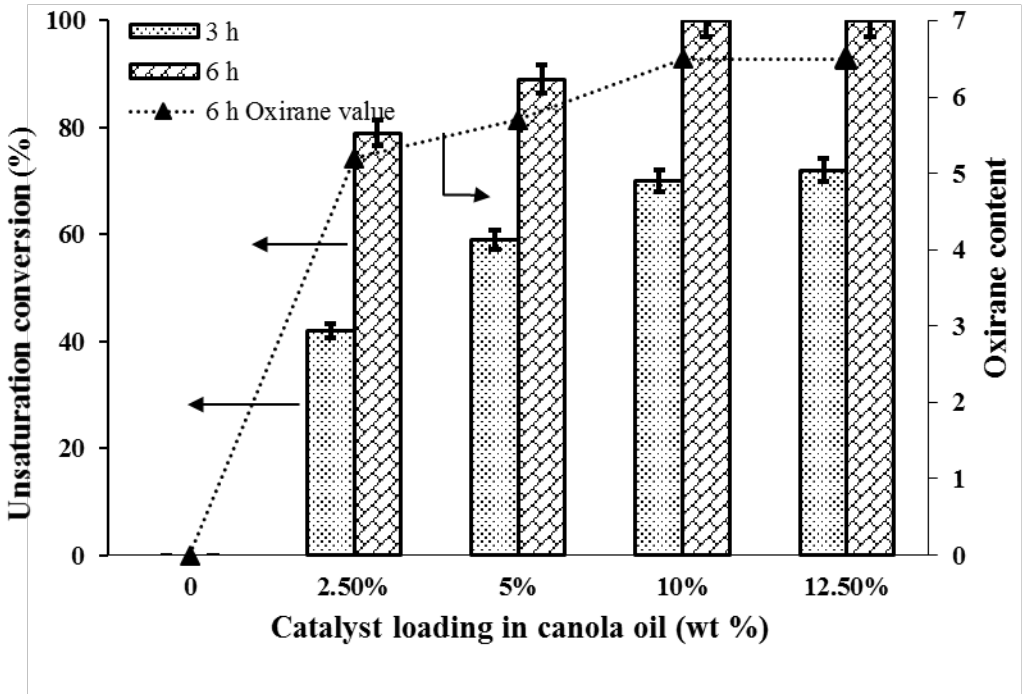
3 h
6 h
6 h Oxirane value
Unsaturation conversion (%)
Oxirane content
0
2.50%
5%
10%
12.50%
Catalyst loading in canola oil (wt %)

(B)

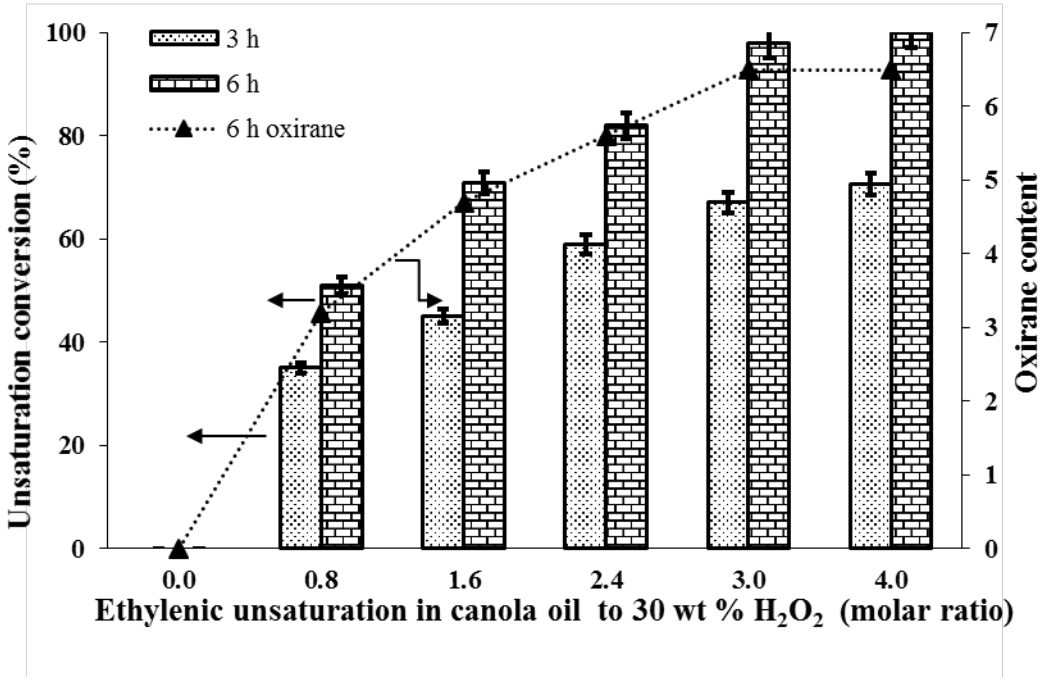
3 h
6 h
6 h oxirane
Unsaturation conversion (%)
Oxirane content
0.0
0.8
1.6
2.4
3.0
4.0
Ethylenic unsaturation in canola oil to 30 wt % H_2O_2 (molar ratio)

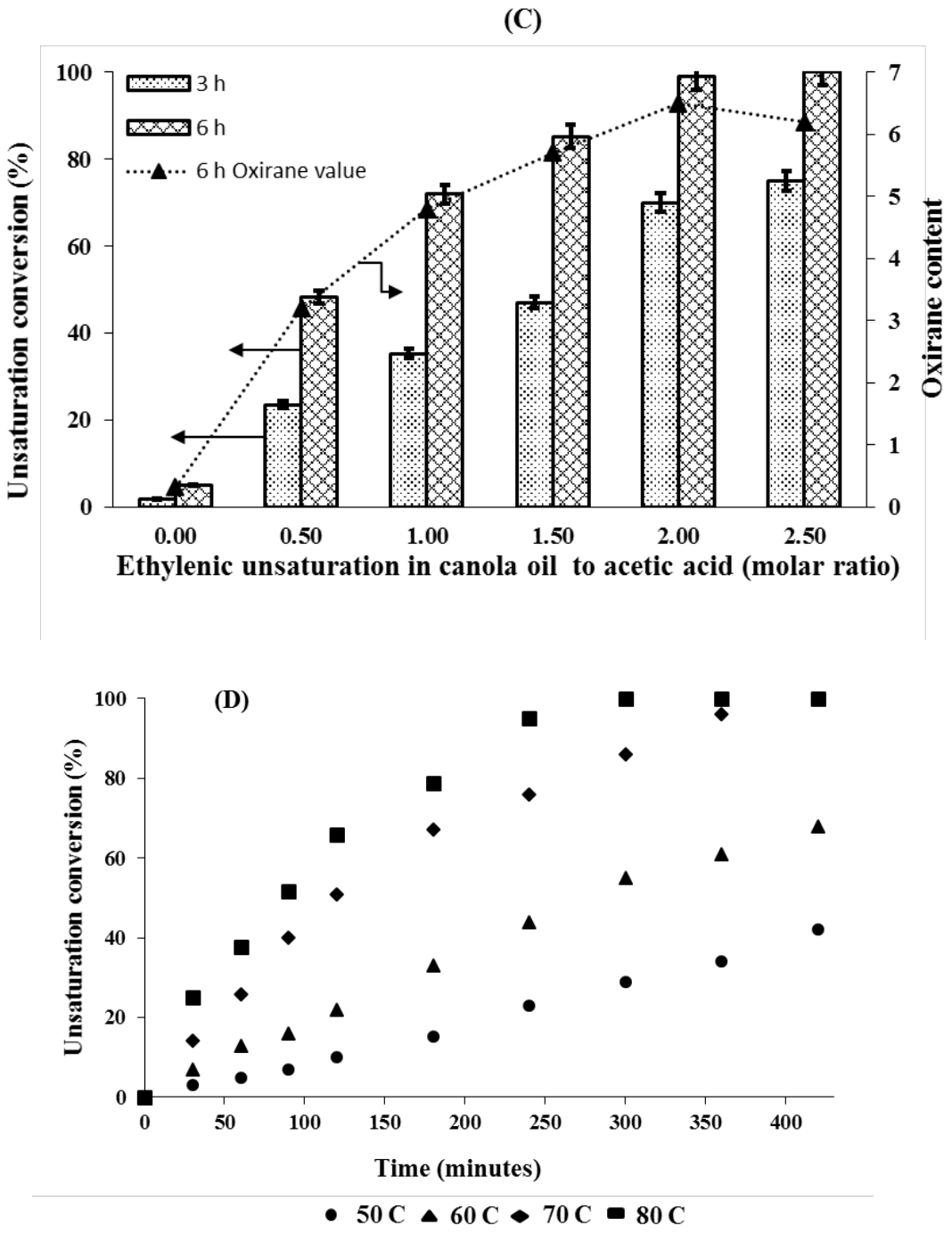

Figure 3.7 Process parameter optimization study for the epoxidation of canola oil. Reaction conditions: catalyst loading (0 – 12.5 wt %) w.r.t canola oil, ethylenic unsaturation in canola oil to 30 wt% H_2O_2 molar ratio loading (0 – 4.0), ethylenic unsaturation in canola oil to acetic acid loading (0 – 2.5), Temperature (50-80 ^oC), reaction time (7 h) and agitation speed (1000 rpm). (A)

Effect of catalyst loading, (B) effect of H_2O_2 loading, (C) effect of acetic acid loading, and (D) effect of reaction temperature.

3.4.2.5 Effect of temperature

Temperature effect studies were carried out between 50 – 80 ^oC to investigate the rate of epoxy formation and unsaturation conversion with respect to optimized conditions such as 10 wt% catalyst loading, ethylenic unsaturation to hydrogen peroxide molar ratio 1:3, and acetic acid to ethylenic unsaturation of canola oil molar ratio 2:1. Figure 3.7.D illustrates the effect of temperature on the epoxidation reaction of canola oil. As expected, higher temperatures favoured maximum rate of epoxy formation (Saurabh et al. 2011). Though the rate of unsaturation conversion was found to be high at 80 ^oC, epoxy ring opening was observed after 6 h. Considering stability of the product, 70 ^oC was taken as an optimum condition with 100 % unsaturation conversion at 6 h reaction time.

3.4.2.6 Catalyst reusability study

Catalyst reusability of sulfated-SnO_2 was tested up to 4 runs. After each run, the catalyst was separated and washed with 50 ml of ethyl acetate to extract the oil accumulated in the catalyst pores during the course of the reaction. Ethyl acetate helps in the separation of aqueous phase (hydrogen peroxide and acetic acid) and an oil phase. The catalyst was the dried in oven at 100 ^oC for 12 h. There was a loss of 5 % in the catalytic activity after each run which was made up with fresh catalyst. FTIR spectra of reused catalyst after each recycle show low intensity peaks of canola oil which may be due to the presence of traces of oil inside the pores. It was found difficult to eliminate the traces of oil in the pores after repeated washing with ethyl acetate. The blockage of pores with oil may be the reason for the decrease in catalytic activity by 5% after each run. Table 3.3 shows the reusability of sulfated-SnO_2 at the optimum conditions in 6 h of reaction time.

Table 3.3 Catalyst reusability studies of the sulfated-SnO_2 catalyst. Reaction conditions: Canola oil (5.0 g), 30 wt% hydrogen peroxide (6.5 g), acetic acid (4.0 g), 10 wt% sulfated-SnO_2 catalyst with respect to canola oil, temperature (70 ^oC) and reaction time (6 h).

Catalyst run	Unsaturation conversion (mol %)
1	100
2	95
3	90
4	86

3.4.3 Development of kinetic model and reaction mechanism for the epoxidation reaction of canola oil

The reaction pathway of epoxidation of unsaturated fatty acids in the canola oil can be understood by the development of the kinetic model. For the kinetic study, reactions were carried out at temperatures 50, 60, 70 and 80 ^oC. Samples were collected and analyzed periodically to fit a kinetic model of the mechanism shown in Figure 3.8. As per Fieser and Fieser's reagents for organic synthesis (Tse-Lok et al. 2006), the reaction between 30 wt% hydrogen peroxide and acetic acid to form peracetic acid can be accelerated by maintaining the temperature of the reaction mixture at 70 ^oC. Considering this report, formation of peracetic acid in the mixture was assumed to be fast and simultaneous. Since acetic acid molar ratio with respect to hydrogen peroxide is taken in excess, it was assumed that remaining acetic acid can thrive the peracetic acid formation at equilibrium. Both Eley-Rideal and Langmuir-Hinshelwood-Hougen-Watson (LHHW) mechanisms were tested, and it was found that LHHW mechanism holds good for this reaction. Considering LHHW dual site mechanism, the rate of reaction on the active sites of the catalyst is mainly controlled by three steps namely: (1) adsorption, (2) surface reaction and (3) desorption. Figure 3.8 shows the plausible reaction mechanism of the epoxidation of canola oil reaction involving above mentioned three steps on sulfated-SnO_2. The steps for the development of kinetic model are made based on Figure 3.8.

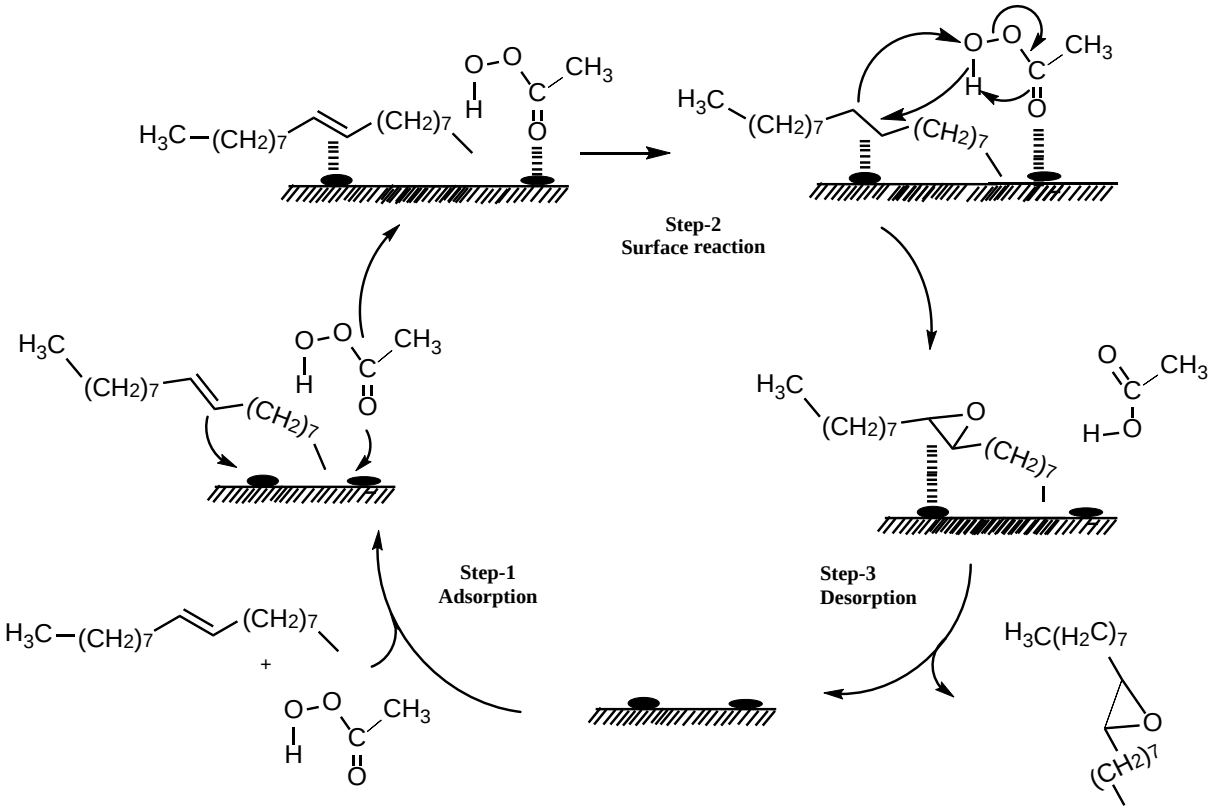

Figure 3.8 Proposed LHHW type of reaction mechanism for the epoxidation of unsaturation in the canola oil.

The reaction between hydrogen peroxide *(HP)* and acetic acid *(AA)* to form peracetic acid *(PAA)* can be written as,

$$HP + AA \overset{K_1}{\rightarrow} PAA + H_2O \tag{3.3}$$

Assuming weak adsorption of canola oil and peracetic acid on the active sites of the catalyst, adsorption of canola oil (*CO*) and *PAA* on vacant site is given by,

$$CO + S \overset{K_2}{\leftrightarrow} CO.S \tag{3.4}$$

$$PAA + S \overset{K_3}{\leftrightarrow} PAA.S \tag{3.5}$$

Surface reaction of *CO* and *PAA* leading to formation of *ECO* is written as,

$$CO.S + PAA.S \overset{K_{SR}}{\longleftrightarrow} ECO.S + S \tag{3.6}$$

Desorption of *ECO* is given by,

$$ECO.S \overset{K'_{ECO}}{\longleftrightarrow} ECO + S \tag{3.7}$$

If C_t is the total concentration of active sites, it can be expressed as

$$C_t = C_{CO} + C_{PAA} + C_{ECO} + C_S \tag{3.8}$$

Which can also be written as,

$$C_t = K_2 C_{CO} C_S + K_3 C_{PAA} C_S + K_{SR} C_{ECO} + C_S \tag{3.9}$$

From equation 3.9, the concentration of vacant sites can be written as,

$$C_S = \frac{C_t}{K_2 C_{CO} + K_3 C_{PAA} + K_{SR} C_{ECO} + 1} \tag{3.10}$$

If surface reaction is controlling, then the rate of reaction of *CO* is given as,

$$-r'_{CO} = -\frac{d_{CO}}{dt} = K_{SR} C_{CO.S}\, C_{PAA.S} - K'_{SR} C_{ECO.S}\, C_S \tag{3.11}$$

If the value of C_S is replaced from equation 3.9, then

$$-\frac{dC_{CO}}{dt} = \frac{K_{SR}\, C_t^2 \{ K_2 K_3\, C_{CO} C_{PAA} - (K'_{SR} K'_{ECO} C_{ECO.S}/K_{SR})\}}{(K_2 C_{CO} + K_3 C_{PAA} + K_{SR} C_{ECO} + 1)^2} \tag{3.12}$$

Since the reaction is far away from equilibrium,

$$-\frac{dC_{CO}}{dt} = \frac{K_{SR}\, C_t^2\, K_2 K_3\, C_{CO} C_{PAA}}{(K_2 C_{CO} + K_3 C_{PAA} + K_{SR} C_{ECO} + 1)^2} \tag{3.13}$$

At time t = 0, concentration of product $C_{ECO} = 0$,

$$-\frac{dC_{CO}}{dt} = \frac{k_r\, w\, C_{CO} C_{PAA}}{(K_2 C_{CO} + K_3 C_{PAA} + K_{SR} C_{ECO} + 1)^2} \tag{3.14}$$

Where $k_r w = K_{SR}\, K_2\, K_3\, C_t^2$; w = catalyst weight (g cat/L of liquid phase). When adsorption constants values are not significant, equation 3.14 can be reduced as

$$-\frac{dC_{CO}}{dt} = k_r\, w\, C_{CO} C_{PAA} \tag{3.15}$$

Since the excess amount of peracetic acid was used in the reaction, it can be assumed that $C_{PAA} = C_{PAA,0}$. Then the above equation in terms of fractional conversion can be written as,

$$-\frac{dX_{CO}}{dt} = k' \ (1 - X_{CO}) \quad (3.16)$$

Where

$$k' = k_r \, w \, C_{PAA,0} \quad (3.17)$$

Integrating the equation (3.16), the final equation is given as,

$$-\ln(1 - X_{CO}) = k' \, t \quad (3.18)$$

A plot of -ln (1- X_{CO}) vs. time (t) was made to calculate the reaction rate constants (Table 3.4) at different temperatures. It was noticed that the values of rate constant found to increase along with the reaction temperatures, and the reaction is found to follow pseudo first order with respect to canola oil. The apparent activation energy of canola oil to epoxidized canola oil was calculated by Arrhenius plot -ln k vs. 1/T (Figure 3.9) and was found to be 18 kcal/mol. Based on the developed kinetic model, and surface structure of sulfated-SnO_2 reported by Khder et al. 2008, a possibly true LHHW dual site reaction mechanism was proposed and is shown in Figure 3.8. The first step involves the adsorption of canola oil and peracetic acid on to the catalyst surface. The second step relates to surface reaction, where electrophilic peracetic acid oxidizes unsaturation by withdrawing electrons from the double bonds of canola oil resulting in an ether formation. In the final step, epoxidized canola oil is desorbed from the active surface.

Table 3.4 Rate constant (*k*) for epoxidation reaction of canola oil between 50 to 80 ^{o}C.

Sr.no	Temperature (^{o}C)	Temperature, T (^{o}K)	Rate constant, k (min^{-1})	1/T	-ln k
1	50	323	0.0893	0.003096	2.415
2	60	333	0.2157	0.003003	1.533
3	70	343	0.5959	0.002915	0.517
4	80	353	0.8603	0.002833	0.1504

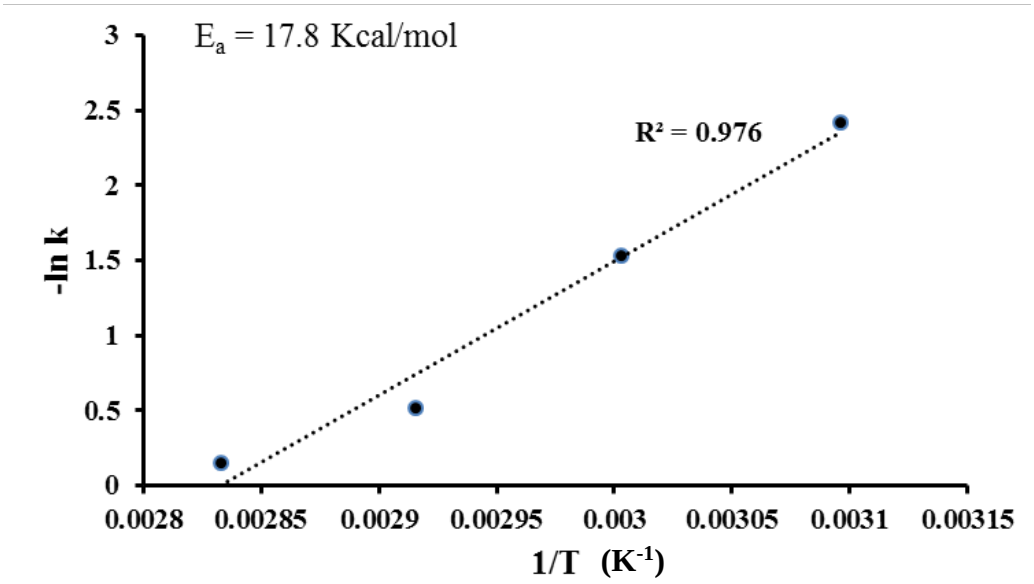

Figure 3.9 Arrhenius plot –ln k vs 1/T for the epoxidation reaction of canola oil.

3.4.4 Confirmation of products

3.4.4.1 Product isolation

Unsaturated fatty acids in the canola oil underwent epoxidation reaction in the presence peracetic acid by sulfated-SnO_2 as catalyst (Scheme 3.1). After complete formation of the product, following procedure has been followed to extract the product. Reaction mixture at the end consists of epoxidized canola oil, peracetic acid, acetic acid, catalyst, hydrogen peroxide and water. Initially, 100 ml of ethyl acetate is added to the mixture to separate aqueous and organic (oil) layer. Oil layer is collected and added with 150 ml of ethyl acetate and water. The addition of water helps in dissolving acids. Further, extracted oil is added with sodium bicarbonate solution to dissolve traces of acids. Finally, oil collected in the supernatant phase is added to sodium sulfate to adsorb traces of water molecules and then filtered. Ethyl acetate in the oil phase is then degassed using rotary evaporator at 40 ^{o}C.

3.4.4.2 FT-IR, ^{1}H and ^{13}C NMR spectroscopic confirmation of canola oil and epoxidized canola oil

Figure 3.10 shows the FT-IR spectra of canola oil and epoxidized canola oil. The characteristic peaks at 3007 cm^{-1} and 721 cm^{-1} correspond to bending and vibrational stretching of C-H in C=C-H of unsaturated fatty acids in the canola oil. Disappearance of these bands in the IR spectra of

epoxidized canola oil indicates complete conversion of C=C in the canola oil. The new peak at 828 cm^{-1} is due to the formation of cyclic ether (epoxy) at C=C. The ^{1}H NMR and ^{13}C NMR spectra also confirmed the absence of unsaturation among the triglyceride molecules of the canola oil after epoxidation. Chemical shift at 5.3 ppm in ^{1}H NMR spectra and at 130 ppm in ^{13}C NMR are observed due to the presence of olefinic (-C=C-) carbon atoms. Both of the spectra in epoxidized canola oil showed no chemical shifts at 5.3 ppm and 130 ppm respectively after complete reaction indicating the disappearance of double bonds. ^{1}H NMR spectra of epoxidized canola oil showed a new peak between 2.9 – 3.1 ppm region, this characteristic peak is because of C-H protons attached to the epoxy group (Sharma et al. 2013; Mungroo et al. 2011).

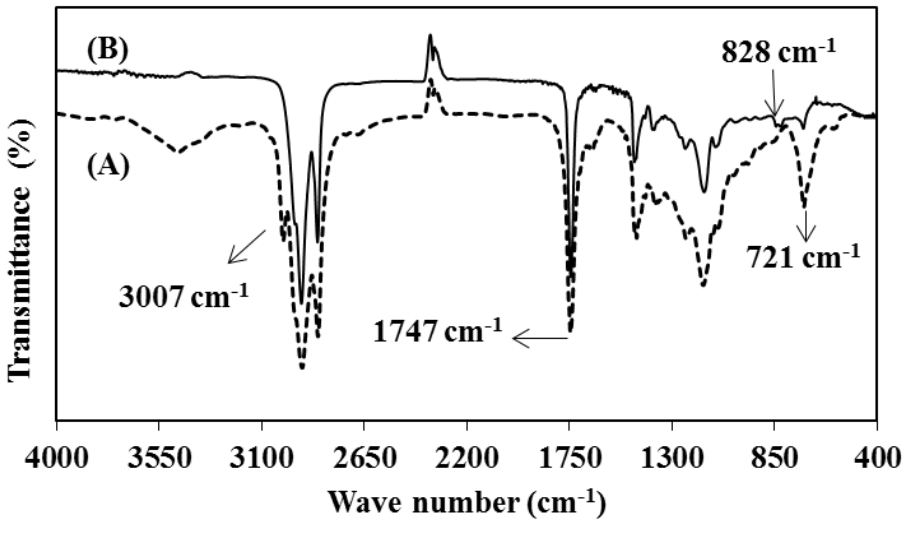

Figure 3.10 FT-IR spectra of (A) Canola oil, and (B) Epoxidized canola oil.

3.4.4.3 Comparative property evaluation of canola oil and epoxidized canola oil

Epoxidized canola oil is a saturated fatty acid ester and could be a promising source for the synthesis of many value added products such as lubricants, polymers, additives, etc. Ester linkage in organic compounds renders inherent lubricity properties (Sripada et al. 2013). Hence, evaluation of tribological properties of canola oil and epoxidized canola are made to measure the improvement in the properties after the removal of unsaturation. The viscosity of the fluids tends to decrease with increase in temperature, a factor called viscosity index which was used to quantify this change. Higher the value of viscosity index lesser is the change in its viscous nature with respect to temperature. The viscosity of canola oil and epoxidized canola oil were measured at

different temperatures ranging from 25 – 100 °C. Kinematic viscosities of both the samples were found to decrease with increase in temperature. Also, due to the removal of unsaturation, viscosity of canola oil was found to increase more than 3.5 times. The viscosity index of epoxidized canola at 40 °C with kinematic viscosity 114 mm^2/s was calculated to be 141 which is more than ISO VG 46 standard specification for light gear oil lubricant.

A measure of the cloud point and pour point of oil samples helps to determine the cold flow properties. Cloud point temperature was reported when there is any haziness appeared in the sample and pour point was reported at the temperature where liquid mobility is stopped. Canola oil has a cloud point of -5 °C and it was found to increase to 15 °C after epoxidation of unsaturation. The pour point of canola oil was observed to be -15 °C and 9 °C for epoxidized canola oil. Epoxidized canola showed undesired cold flow properties and limits its application as an additive for diesel-type engines especially in winter. It was reported that the presence of excess long chain saturated fatty acids leads to poor cold flow temperature behaviour (Nagendramma et al. 2012). This might be the reason for high cloud and pour point temperatures of epoxidized canola oil. The undesired cold flow properties have been overcome by epoxy ring opening and esterification with acetic anhydride (Sharma et al. 2013). After esterification step, canola oil derived biolubricant showed pour point of -9 (±2) °C which meets ISO VG 46 light gear oil lubricant specifications. Since epoxidized canola oil has ether and ester functionality, it can be used as additive for high temperature diesel fuel type engines (Laubli et al. 1986), and lubricant base oil for canola oil biolubricant synthesis (epoxy ring opened and esterified product).

The friction wear scar resulted by the addition of canola oil and epoxidized canola separately to a reference diesel sample was measured using HFRR (High Frequency Reciprocating Rig) apparatus. For measuring wear scar diameter of the test sample, a pure diesel sample was used as a reference. 5% vol/vol solution of canola oil in standard diesel sample and 5% vol/vol solution of epoxidized canola oil in standard diesel sample respectively, were used as contacting fluids for lubrication. Table 3.5, shows the obtained wear scar diameters of canola oil and epoxidized canola. It is evident from the table that highest wear scar diameter of 380 µm which was resulted with the standard diesel sample was reduced to 252 and 189 µm, respectively, by minimum dilution of 5% vol/vol of canola oil and epoxidized canola oil. From Table 3.5, it can be observed that kinematic viscosities of epoxidized canola oil are high which meet the ISO VG46 specifications of light gear

oil lubricant. It shows that the removal of unsaturation improved the viscosity properties of canola oil and reflects its effect on lubricity between surfaces. By the addition of 5% vol/vol epoxidized canola oil to standard diesel sample the wear scar length was reduced confirming the importance of treated canola oil in reducing friction between the surfaces. Hence, this study proves that epoxidized canola oil has good lubricity properties and can be used as an additive to diesel fuel type engines to reduce friction, wear, and tear.

Oxidative stability of oil samples are measured by Rancimat method (Laubli et al. 1986). This method determines a parameter known as oxidative induction time, which is the elapsed time between the start of the test and the moment at which sudden increase in the conductivity is detected due to the onset of decomposition under isothermal condition. The oxidative induction time of canola oil was found to be 3.8 h and 60 h for the epoxidized canola oil. From the report (Sharma et al. 2013), saturated canola triglyceride esters formed by epoxide ring opening and esterification with acetic anhydride showed oxidative induction time of 56 h. The high oxidative induction time of epoxidized canola oil confirms that the removal of unsaturation in the canola oil improved its oxidative stability which is important for a potential lubricant.

Table 3.5 Tribological properties of epoxidized canola oil

Sr. no	Tribological property	Canola oil	Epoxidized canola oil	ISO VG 46 specifications
1	Kinematic viscosity at 40 ^{o}C (cSt)	28	114	>41.4
2	Kinematic viscosity at 100 ^{o}C (cSt)	0.1	19	>4.1
3	Viscosity index	--	141	>90
4	Cloud point (^{o}C)	-5	15	-
5	Pour point (^{o}C)	-15	9	-10
6	Oxidative induction time (h)	3.8	60	-
7	Wear scar diameter (μm)	252	189	-

3.5 Conclusions

Sulfated-SnO_2 was found to be the active and selective catalyst for the epoxidation of unsaturation in the canola oil. 100 % unsaturation conversion to epoxide was obtained in 6 h at the optimum conditions: temperature (70 ^oC), catalyst loading of 10 wt% with respect to amount of canola oil taken, ethylenic unsaturation to 30 wt% H_2O_2 molar ratio (1:3), and ethylenic unsaturation to acetic acid molar ratio (1:2). The final product formation was also confirmed with ^1H NMR, ^{13}C NMR and FTIR. A kinetic model was developed for this reaction and it follows LHHW type mechanism. The reaction followed pseudo first order and the calculated energy of activation was found to be 18 kcal/mol. Evaluation of physicochemical properties of epoxidized canola oil showed that removal of unsaturation in the canola oil enhanced its physicochemical properties. Compared to canola oil, epoxidized canola oil demonstrated excellent lubricity properties with improved oxidative stability, viscosity, and lubricity. Since the product is derived from natural vegetable oil, it is renewable, biodegradable and eco-friendly. Therefore, it can be considered as a potential source for lubricity applications.

CHAPTER 4

SYNTHESIS OF VICINAL DI-O-ACETYLATED CANOLA OIL (BIOLUBRICANT TYPE 1) USING SULFATED-ZrO_2 CATALYST

This part of the work has been published as research article and was presented at the following conference:

1. Asish K. R. Somidi, Rajesh V. Sharma, and Ajay K. Dalai, "Catalytic Vicinal Diacylation of Epoxidized triglycerides in Canola oil," Journal of American Oil Chemists Society, 92, 1365-1378 (2015).
2. Asish K. R. Somidi, Rajesh V. Sharma, Ajay K. Dalai, "Catalytic Vicinal Diacylation of Epoxidized Triglycerides in Canola oil." Poster presentation at the 65th Canadian Chemical Engineering Conference, Calgary, AB, October 2015.

Contribution of the Ph.D. candidate

All the experimental and characterization work was conducted by Asish Somidi. Manuscript writing and revision work was done by Asish Somidi based on the suggestions from Dr. Ajay K. Dalai and Dr. Rajesh V. Sharma.

The contribution of this chapter to the overall Ph. D. work

This research work was focused on the synthesis of one of the types of biolubricant called vicinal di-O-acetylated canola oil using epoxidized canola oil as feedstock.

4.1 Abstract

The epoxide ring opening and vicinal di-O-acetylation of fatty acids in the vegetable oils was found to be a promising reaction to synthesize stable biolubricants and bioplasticizers. The current research investigation is emphasized on the synthesis of a value added product vicinal di-O-acetylated canola oil by sulfated-ZrO_2. The two-step research approach employed includes (i) epoxidation, and (ii) epoxide ring opening and vicinal di-O-acetylation of epoxidized triglycerides in the canola oil. Sulfated-ZrO_2 was prepared and characterized to measure the physicochemical properties required for the effective catalysis. Taguchi (L16 orthogonal array) statistical design method was employed to optimize the process conditions for the maximum formation of vicinal di-O-acetylated canola oil. Sulfated-ZrO_2 demonstrated promising activity for the epoxide ring opening and vicinal di-O-acetylation of canola oil, and 99 % conversion was achieved at the optimum process conditions of reaction temperature 130 ^oC, epoxy to acetic anhydride molar ratio (1: 1.25), 16 wt% of catalyst loading and reaction time of 1 h which was inferred from the Taguchi analyses. The products were characterized and confirmed by IR, ^1H NMR, and sodium spray mass spectroscopy. The spectroscopic analysis also confirmed the absence of intermediate products. The statistical analyses were undertaken to determine the order, rank, and interactions among the process variables. The reaction followed Langmuir-Hinshelwood-Hougen-Watson (LHHW) type mechanism and the kinetic data was fitted in overall second order equation. The calculated apparent activation energy was 23 kcal/mol. The evaluated physicochemical properties of the di-O-acetylated canola oil (biolubricant type 1) are: lubricity in terms of wear scar diameter (120 µm), oxidative stability (56 h), cloud and pour point (-3 and -9 ^oC), thermal stability (flash point, 309 ^oC), kinematic viscosities (200 cSt at 40 ^oC, 84 cSt at 100 ^oC) and viscosity index (433).

4.2 Introduction

Epoxidation of unsaturated fatty acids followed by epoxide ring opening with alcohols, carboxylic anhydrides and acids are found to be a promising route to synthesize biolubricants from vegetable oils. The addition of alkyl branch at the unsaturation improved tribological properties of the oils such as rancidity, lubricity, kinematic viscosity, pour and cloud point, boiling point and phase transition temperatures. Also, fatty acids with ester functionality at the unsaturation are found to have superior lubricity properties when compared to alcohol or ether functionality (Lathi et al. 2007; Sharma (a) et al. 2006; Sharma et al. 2013). This work focusses on the synthesis of

unsaturation free canola oil with vicinal di-O-acetylated fatty acids by oxirane ring opening reaction with the acetic anhydride. The product obtained from this process is a saturated triglyceride ester. Since esters are prominently used in manufacturing lubricants, fuel additives, plasticizers, cosmetics, flavors, paints etc. (Gryglewicz et al. 2006), the aforementioned canola oil derived compound could be a value added product for many industrial applications.

Furthermore, most of the literature on the preparation of vicinal di-O-acetylated vegetable oils involves three-step reaction, and the use of inorganic acids and commercial resins as catalysts. Considering the limitations associated with these catalysts, this research investigation has given importance in developing an active heterogeneous catalyst for the synthesis of vicinal di-O-acetylated canola oil from epoxidized canola oil in a single step. The rate of epoxy ring opening in fatty acids and the addition of nucleophilic or electrophilic carboxyl group at the epoxy centre depends on the strength of the solid acid catalyst used. Also, solid acid catalysts promote epoxy ring opening reactions by protonation (Sharma et al. 2013; Salimon et al. 2011). Sulfated-ZrO_2 is considered as super solid acid catalysts and is reported to be an active catalyst for mono-acylation of alcohols, amines, phenols, aromatics and anthracenes using carboxylic anhydrides as acylating agents under solvent free conditions (Ratnam et al. 2007; Deutsch et al. 2005; Deutsch et al. 2000). Sulfation of metal oxides enhances the surface acidity (Lewis and Bronsted acidic sites) and helps in promoting the rate of reaction.

From the reported knowledge, heterogeneous sulfated-ZrO_2 was synthesized and used for the vicinal di-O-acetylation of epoxidized canola oil. This may be the first report on the application of sulfated-ZrO_2 as a catalyst for the synthesis of vicinal di-O-acetylated esters from epoxidized canola triglyceride molecules using acetic anhydride. Also, this research work includes physicochemical characterization of sulfated-ZrO_2, process parameter optimization studies using Taguchi's orthogonal array design, inter and intra-particle mass transfer resistance calculations, kinetic model development and spectroscopic characterization of the product.

4.3 Experimental

4.3.1 Chemicals and reagents

Acetic anhydride was procured from Alfa Aesar (USA), ammonium hydroxide ACS reagent, commercial Amberlite IR-120 resin from Sigma–Aldrich (St. Louis, MO, USA). Glacial

acetic acid, sulfuric acid, methylene chloride, ethyl acetate and hydrogen peroxide (30% wt/wt) from EMD Chemicals Inc. (Darmstadt, Germany), and catalyst precursor zirconyl (IV) nitrate hydrate from ACROS ORGANICS (Canada).

4.3.2 Catalyst synthesis

The catalyst was prepared as per the following procedure. The precursor zirconyl (IV) nitrate powder was completely dissolved in the distilled water until a clear solution is formed and then 25 % vol/vol aqueous ammonium hydroxide was added until the solution pH is 10 to precipitate zirconium hydroxide. The collected precipitate was washed with distilled water to dissolve excess ammonium hydroxide. Zirconium hydroxide precipitate is then dried at 100 ^{o}C for 24 h to remove excess moisture. 1M H_2SO_4 solution was used for the sulfation of zirconium hydroxide. A molar ratio of 2: 1 ($Zr(OH)_4$: H_2SO_4) was maintained and the treated zirconium hydroxide was then dried at 100 ^{o}C for 12 h, and then calcined at 550 ^{o}C for 3 h to form sulfated-ZrO_2. Zirconium hydroxide was calcined at similar conditions to obtain ZrO_2 (Deutsch et al. 2000).

4.3.3 Synthesis of epoxidized canola oil

Epoxidized canola oil was prepared at the optimum conditions as follows. For 100 g of canola oil, 30 wt% hydrogen peroxide and glacial acetic acid were added to maintain the molar ratio of ethylenic unsaturation in canola oil to acetic acid 2:1, ethylenic unsaturation in the canola oil to hydrogen peroxide molar ratio of 2:3. About 22 wt % catalyst (Amberlite IR-120 H) was added to the reaction mass and was uniformly stirred in 1000 ml three necked round bottom flask at 70 ^{o}C for 8 h. The complete conversion of the reaction was assessed by the volumetric titration methods; iodine value and oxirane oxygen content (equations 4.1 and 4.2 shown below). Epoxidized canola oil was extracted from the reaction mixture using ethyl acetate as a solvent, and the final product formation was confirmed by ^{1}H NMR, FTIR, and sodium spray mass spectrometer.

4.3.4 Synthesis of epoxide ring opened and vicinal di-O-acetylated canola oil

All the catalytic experiments were performed in a 50 ml three necked round bottom flask. Figure 4.1 shows the reaction scheme for the preparation of vicinal di-O-acetylated canola oil. The flask was connected with a reflux condenser, thermometer, and stirrer. The uniform reaction temperature was maintained by using a temperature controlled oil bath. For the synthesis of epoxide ring opened and vicinal di-O-acetylated canola oil, epoxidized canola oil and acetic anhydride are

taken in 1:1.25 (epoxy : acetic anhydride) molar ratio with 16 wt% catalyst loading based on the quantity of epoxidized canola oil, and the mixture was uniformly stirred at 1000 rpm for 1 h and 15 min at 130 ^{o}C. Initial epoxy content at 0 h and the rate of epoxy conversion during the course of the reaction was measured using equations 4.2 and 4.3, respectively. Also, FT-IR, ^{1}H NMR, and sodium spray mass spectroscopy spectroscopic techniques were used to identify any side reactions, and also to confirm the product.

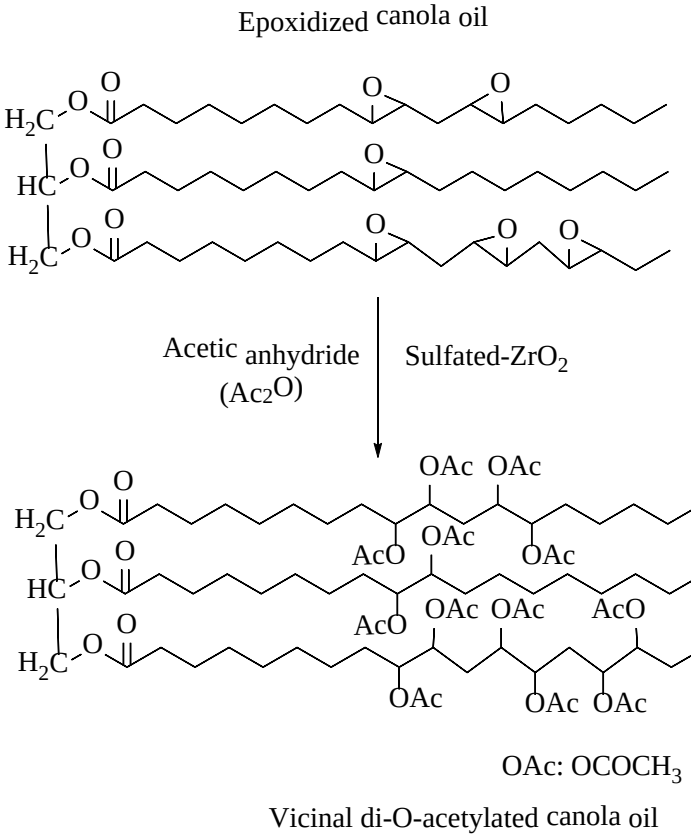

Figure 4.1 Reaction scheme for the preparation of vicinal di-O-acetylated canola oil (biolubricant type 1).

4.3.5 Method of analysis

The amount of unsaturation present in the fatty acids of the canola oil during the course of the reaction was determined by the iodine value as per the AOCS Cd 1-25 standard method. The conversion of unsaturation to epoxide was assessed by AOCS Cd 9-57 volumetric titration method. The equations are shown in Chapter 3. Equation 4.1 was used to measure the rate of epoxy conversion for the epoxide ring opening and di-O-acetylation reaction. Also, spectroscopic

techniques such as FT-IR, ^{1}H NMR, and electron spray mass spectroscopy were employed to identify and confirm the products.

Epoxy conversion (%)

$$= \frac{\text{Oxirane value at O h (t0)} - \text{Oxirane value at time (t)}}{\text{Oxirane value at O h (t0)}} \times 100 \qquad (4.1)$$

4.3.6 Purification of biolubricant

The purification process of the end product vicinal di-O-acetylated canola oil involves following steps: (1) ethyl acetate was used to extract the organic phase (oil and acetic anhydride), (2) the organic phase was then washed with sufficient aqueous saturated sodium bicarbonate solution to dissolve and neutralize the acids until it's pH was 7, (3) extracted organic phase (ethyl acetate and oil) was then dried on the anhydrous sodium sulfate, and (4) ethyl acetate was then removed by rotary evaporation.

4.3.7 Catalyst Characterization Techniques

FTIR and pyridine adsorbed FTIR analyses were carried out on a Perkin-Elmer spectrophotometer with 8 cm^{-1} resolution and frequency range between 4000 – 400 cm^{-1}. Prior to the analysis 0.1 g of sample was treated with 50 µl pyridine and heated at 150^{o}C for 30 min. The thermal analysis of the catalyst was investigated on SDT Q600 series simultaneous TGA/DSC (TA instruments). About 38 mg of sample is weighed and heated from 17 – 135 ^{o}C (ramp rate of 5 ^{o}C/min) to investigate the percentage weight loss distributions due to the decomposition of sample and sulfate ions at the reaction temperatures. The average particle size distributions in the catalyst sample was determined using Zetasizer Nano range Dynamic Light Scattering instrument (Malvern Instruments Ltd.). The amount of sulfur content (wt/wt) in the sulfated-ZrO_2 catalyst was determined with the Vario EL III CHNS elemental analyzer (Elementar Americas Inc.). The other characterization techniques are already mentioned in the Chapter 3.

4.3.8 Spectroscopic Characterization Techniques

The ^{1}H NMR spectra were obtained on a Bruker AM500 NMR spectrometer (BBO probe) operated at a frequency of 500.29 MHz for ^{1}H. ^{2}H field-frequency lock unit was arranged to monitor the magnetic field stability. Deuterated chloroform ($CDCl_3$) was used as a reference solvent for the NMR. The mass distributions in the end product were analyzed by MDS SCIEX mass

spectrophotometer (QSTAR XL MS/MS system). About 10 mg of the product was diluted with 1 ml methanol and about 1 mg sodium chloride crystals were added to it. The solution was then fused into the system at 5µl/min. The FTIR spectrum of the epoxidized canola oil and the product were obtained using Perkin Elmer spectrophotometer, operated with 8 cm^{-1} resolution and the frequency range between 4000 – 400 cm^{-1}.

4.3.9 Taguchi optimization by L_{16} orthogonal array design

The execution of Taguchi L16 (4^3) design method was made to investigate the effect of process parameters such as reactant loading, temperature, and catalyst loading on the epoxy conversion to vicinal di-O-acetylated canola oil product, and also to optimize the above process conditions for the maximal product formation. The important feature of this particular method is the use of special orthogonal arrays which minimizes the number of experiments and gives information on all the factors that affect the epoxy conversion (response) (Tilay et al. 2010). This method includes three steps: (1) designing the matrix of experiments based on the number of factors and their levels, (2) conducting the experiments and data analysis (S/N ratio, response plot and ANOVA), and (3) determination of optimum levels for factors, confirmation and validation of the obtained data (Chowdhury et al. 2014). Based on the preliminary experimental results, three independent process parameters and their corresponding levels are chosen (Table 4.1). MINITAB (Minitab Inc. USA for Windows 7) software was used to design the orthogonal array matrix, to plot the main effects for signal to noise (S/N) ratios and means, and also to enlist the response table for signal to noise ratios (S/N) and means for determining the delta and rank of the corresponding process parameters. The signal to noise ratios (S/N) for each parameter and their corresponding levels were calculated based on 'larger is better' characteristic because the main objective of this process parameter optimization study is to obtain the maximum epoxy conversion to the vicinal di-O-acetylated product (Tilay et al. 2010). The S/N ratio was calculated as per the following equation 4.4 (Roy et al. 2001):

$$\frac{S}{N} = -10\ Log\ \left\{\frac{1}{n}\sum_{i=1}^{n}\frac{1}{{y_i}^2}\right\} \qquad (4.2)$$

Where y is the epoxy conversion for a corresponding trial, n represents the number of experimental trials in the particular parametric combinations and i is the replicate number.

Table 4.1 Process conditions and their levels for the synthesis of vicinal di-O-acetylated canola oil. Epoxy to acetic anhydride molar ratio was taken based on the molecular weight of epoxy canola oil (~932.75 g/mol). Catalyst loading (%wt) which is g of catalyst used per 100 g of epoxy canola oil.

Process parameter	Temperature (^oC)	*Epoxy to Acetic anhydride molar ratio(1:X)	Catalyst loading(%wt)
Level 1(L_1)	100	1.25	4
Level 2(L_2)	110	2.5	8
Level 3(L_3)	120	3.25	12
Level 4(L_4)	130	5	16

*Epoxy to acetic anhydride molar ratio is represented as 1 : X, where X=1.25, 2.5, 3.25, 5

4.4 Results and discussion

4.4.1 Catalyst characterization

Table 4.2 illustrates the BET specific surface area, pore size distributions of ZrO_2 and sulfated-ZrO_2 samples after the calcination at 550 ^oC. The N_2 adsorption of sulfated-ZrO_2 at -196 ^oC exhibited type (IV) isotherm with a hysteresis loop indicating the characteristics of a mesoporous solid. The BET specific surface area of sulfated-ZrO_2 was found to be 127 m^2/g with a pore volume of 0.2 cm^3/g and 4.4 nm average pore diameter. In comparison to ZrO_2, the enhancement in the surface area and pore volume of sulfated-ZrO_2 was observed due to the accumulation of sulfate ions on the ZrO_2 surface (Ratnam et al. 2007). For bulky molecules like epoxidized canola triglycerides, the porous catalyst is favourable to minimize mass transfer limitations and is anticipated to increase the epoxy conversion. Enhancement in the surface area by sulfation also provides more surface acidity to promote the reaction (Sharma et al. 2013).

The XRD diffractograms of ZrO_2 and sulfated-ZrO_2 are shown in Figure 4.2. The intensities of the bands corresponding to $2\Theta = 30^o$, 35.4^o, 50.5^o, and 60.3^o represent the diffractions from tetragonal crystal phases of the sample. The average crystalline size of ZrO_2 and sulfated-ZrO_2 (d_{avg}) was measured by Scherrer's equation (Heshmatpour et al. 2012), $d_{avg} = (K \times \lambda) / (\beta \times Cos\theta)$ and was found to be 15 nm and 10 nm, respectively, where K is the shape factor, β represents the half

width of the diffraction peak (FWHM), λ is the wavelength of Cu Kα radiation, θ is the Bragg's angle. The crystalline spacing in sulfated-ZrO_2 was measured using Bragg's equation at 2θ with maximum intensity, $d_{spacing} = \lambda / (2 \times \sin\theta)$ and was found to be 0.3 nm. From XRD analysis it can be confirmed that sulfation treatment did not perturb the tetragonal crystal phase of ZrO_2 and applied calcination temperature was sufficient to retain its crystallinity. The presence of sulfate ions hinder the crystal growth during the calcination and this may be the reason for the decrease in the crystal size of sulfated-ZrO_2.

Table 4.2 BET specific surface area and BJH pore size distributions of ZrO_2 and Sulfated-ZrO_2

Catalyst	BET surface area (m^2/g)	Pore volume (cm^3/g)	Avg. pore diameter (nm)
ZrO_2	9	0.1	30
Sulfated-ZrO_2	127	0.2	4.4

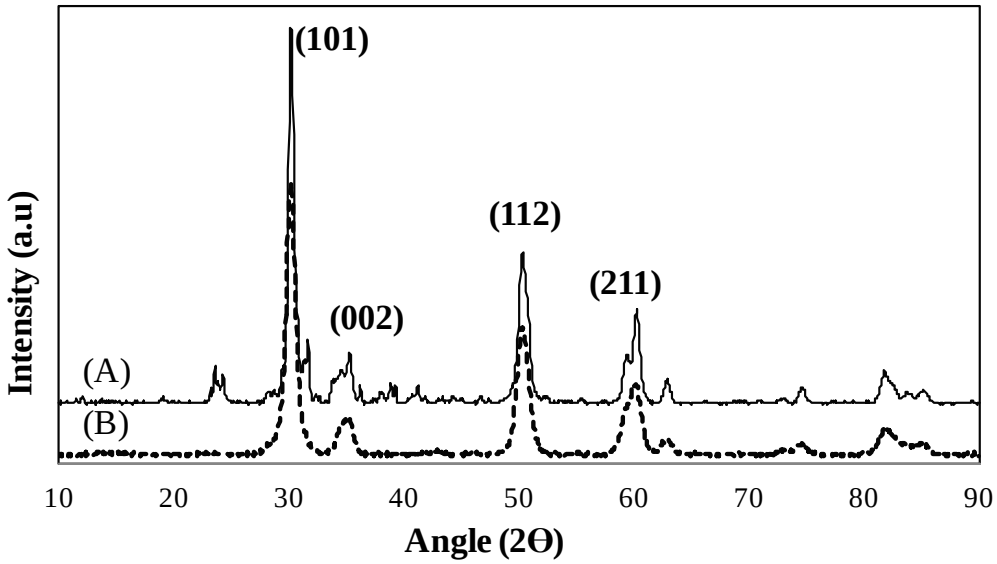

Figure 4.2 X-ray diffraction patterns of (A) ZrO_2, and (B) sulfated-ZrO_2

The FTIR study on sulfated-ZrO_2 confirmed the presence of sulfate anions coordinated to the ZrO_2 surface (Figure 4.3.A). The IR band at 610 cm^{-1} represents the characteristic crystalline zirconia and corresponds to Zr-O stretching and Zr-O_2-Zr asymmetric modes. The bands 1419,

1010 and 830 cm^{-1} are due to the symmetric (S=O) and asymmetric (O-S-O) stretching of retained sulfate ions on the surface of ZrO_2 after the calcination. The broad bands at 3000 and 1655 cm^{-1} were observed due to the bending modes of hydroxyl molecules associated with the sulfate ions (Gawade et al. 2013; Deshmane et al. 2013; Chen et al. 2005). Furthermore, pyridine adsorbed FTIR analysis was undertaken to identify the type of acidic sites present on the sulfated-ZrO_2 catalyst (Figure 4.3.B). The IR transmittance of sulfated-ZrO_2 at 1535 cm^{-1} infers the presence of Bronsted acid type, 1445 cm^{-1} is because of the existence of Lewis acid sites, and 1490 cm^{-1} is attributed to both Bronsted and Lewis sites (Sun et al. 2005). The CHNS data also demonstrates that 3.5 wt% of sulfur content exists in the catalyst. From the above characterization, the existence of sulfate ions on the ZrO_2 was confirmed which is important to induce acidity to the catalyst surface.

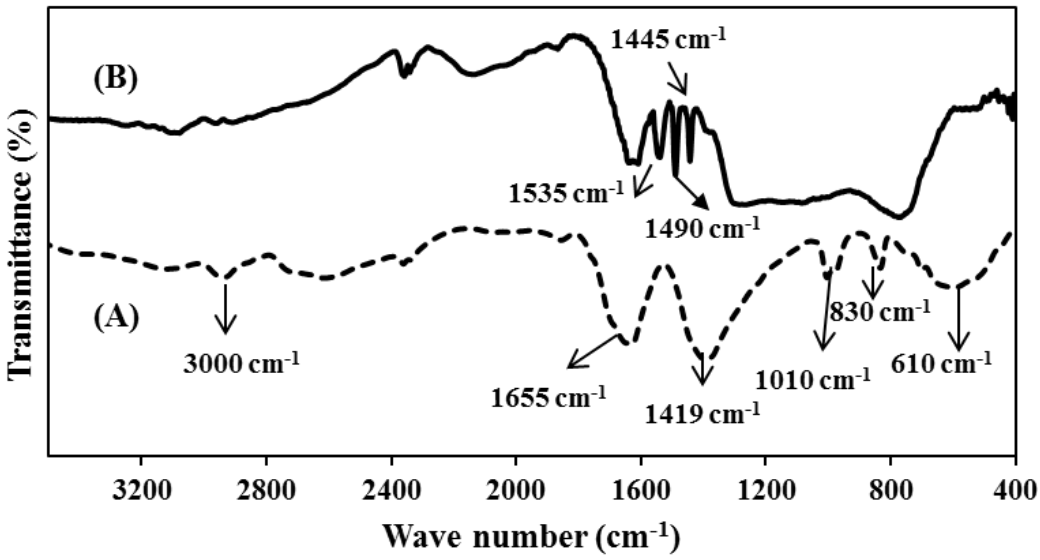

Figure 4.3 (A) Infrared (IR) spectra of sulfated-ZrO_2, and (B) pyridine adsorbed-IR spectra of sulfated-ZrO_2

The acid site distribution on the prepared catalyst was investigated by NH_3-Temperature Programmed Desorption curves (Figure 4.4). The low intensity desorption peak observed between 150 - 380 ^oC corresponds to physisorption/chemisorption of ammonia molecules on the weak and strong acidic sites of the sulfated-ZrO_2 catalyst surface, and the high intensity desorption region between temperatures 540 to 680 ^oC is due to super acidic sites of sulfated-ZrO_2 (Gawade et al. 2013). The super acidic sites of sulfated-ZrO_2 are obtained because of sulfate linkage on the surface

which is important to promote epoxide ring opening and vicinal di-O-acetylation reactions (Sharma et al. 2013). From the above analysis, it is evident that sulfated-ZrO_2 has required acidity on its surface to catalyze the desired transformation.

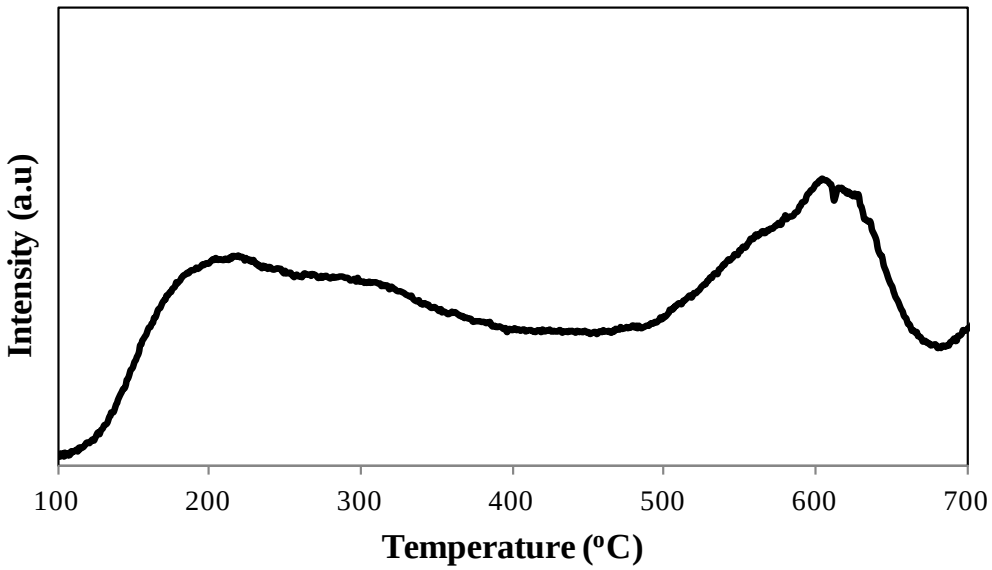

Figure 4.4 NH_3 –Temperature programmed desorption behaviour of sulfated-ZrO_2

Figure 4.5 shows the Thermogravimetric Analysis and Differential Thermogram (TGA/DTG) behaviour of the sulfated-ZrO_2 operated between 17 to 135 ºC (reaction temperatures). The weight loss observed between 17 to 135 ºC was found to be ~ 3 %. This weight loss could be due to the desorption of the physisorbed water on the surface of the catalyst. The DTG curve of the sulfated- ZrO_2 exhibited exothermic nature ($\Delta T > 0$) at the reaction temperatures (100 to 130 ºC) which might be due to evaporation of moisture from the catalyst surface. The absence of exothermic or endothermic crystallization peaks between aforementioned temperatures indicates that sulfated-ZrO_2 didn't undergo any phase transformation. It also elucidates that catalyst is stable at the reaction temperatures (Deshmane et al. 2013). From TGA analysis, it can be confirmed that catalyst did not exhibit any sulfate decomposition at the reaction temperatures.

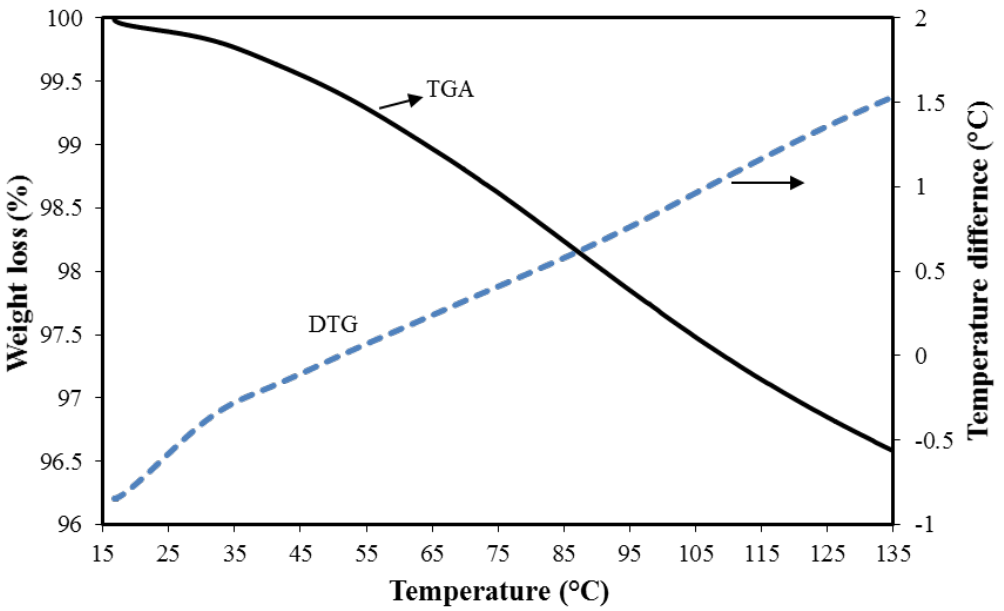

Figure 4.5 Thermogravimetric and differential thermogram analysis (TGA/DTG) of Sulfated-ZrO_2

4.4.2 Prediction of optimal conditions by L_{16} (4^3) – orthogonal array method

Table 4.3 illustrates the ANOVA results obtained for the L16 orthogonal array design. Among three process parameters studied, the F value of the temperature was found to be maximum, indicating its highest influence on the epoxy conversion followed by the catalyst loading and epoxy to acetic anhydride molar ratio. Also, the obtained P values for temperature and catalyst loading are found to be less than 0.05 elucidating the significant effect on the epoxy conversion. Considering the criterion ″larger is better″, the response of means and S/N ratio for the L16 orthogonal array was calculated to maximize the epoxy conversion.

Table 4.4 shows the response values for means and S/N ratios with corresponding delta values and ranks of the system. The significance of the delta is it quantifies the size of the effect of process variables (temperature, catalyst loading and epoxy to acetic anhydride molar ratio), and rank indicates the degree of their effect on the epoxy conversion. A higher delta value of a factor indicates its higher effect on the response (epoxy conversion). From the obtained delta values and ranks enlisted in Table 4.4, it can be concluded that the temperature effect on epoxy conversion to vicinal di-O-acetylated canola oil is maximum followed by the effect of catalyst loading and epoxy to acetic anhydride molar ratio.

Table 4.3 Analysis of variance results (ANOVA) for the selected factors

Factor	DF	Sum of squares	Mean square	*F*-value	*P*-value
Temperature	3	5665.8	1888.6	21.4	0.0013
Molar ratio	3	723.3	241.1	2.7	0.1358
Catalyst loading	3	2731.3	910.4	10.3	0.0087
Residual	6	528.4	88.1		
Total	15	9648.8			

Table 4.4 Response table for signal to noise (S/N) ratios and means

Level	Temperature		Catalyst loading		Molar ratio*	
	S/N	mean	S/N	mean	S/N	mean
1	32.3	44.5	34.3	56.9	34.7	61.9
2	36.3	68.5	35.3	63.9	36.3	71.6
3	37.8	78.8	37.3	76.1	36.9	73.9
4	39.7	96.3	39.1	91.1	38.1	80.6
Delta	7.4	51.8	4.8	34.2	3.4	18.6
Rank	1		2		3	

*Epoxy to acetic anhydride molar ratio

Further, to understand the effect of each factor on the overall response characteristic, and to estimate optimum levels of each factor, the main effect plots for means were created using MINITAB software. These plots are generated by plotting response (epoxy conversion) to the corresponding level in each factor. Figure 4.6 shows the main effect plots for means. The line that connects different factor levels represents the main effect of a factor at corresponding level for the epoxy conversion. The high mean of a level in the factor suggests the appropriate level to be selected for the optimal condition to get high epoxy conversions. From Figure 4.6 it can be observed that for each of the three variables at four levels, the highest mean corresponding to the maximum epoxy conversion suggests that temperature at level 4 and catalyst loading at level 4 showed a main effect, and these levels are the best levels for each of the significant factors.

Although acetic anhydride loading has an insignificant effect on the epoxy conversion (from ANOVA analysis), its molar ratio at level 1 was considered as an optimized condition because, with the above selected optimized conditions maximum epoxy conversion of 98.9% was achieved after 1 h (Table 4.5, Experiment no. 16). In order to confirm and validate the optimum conditions, the experiment was carried out for thrice and the average conversion obtained was 99.1%. Deviation in the epoxy conversion for every reproducibility run is ±0.5%.

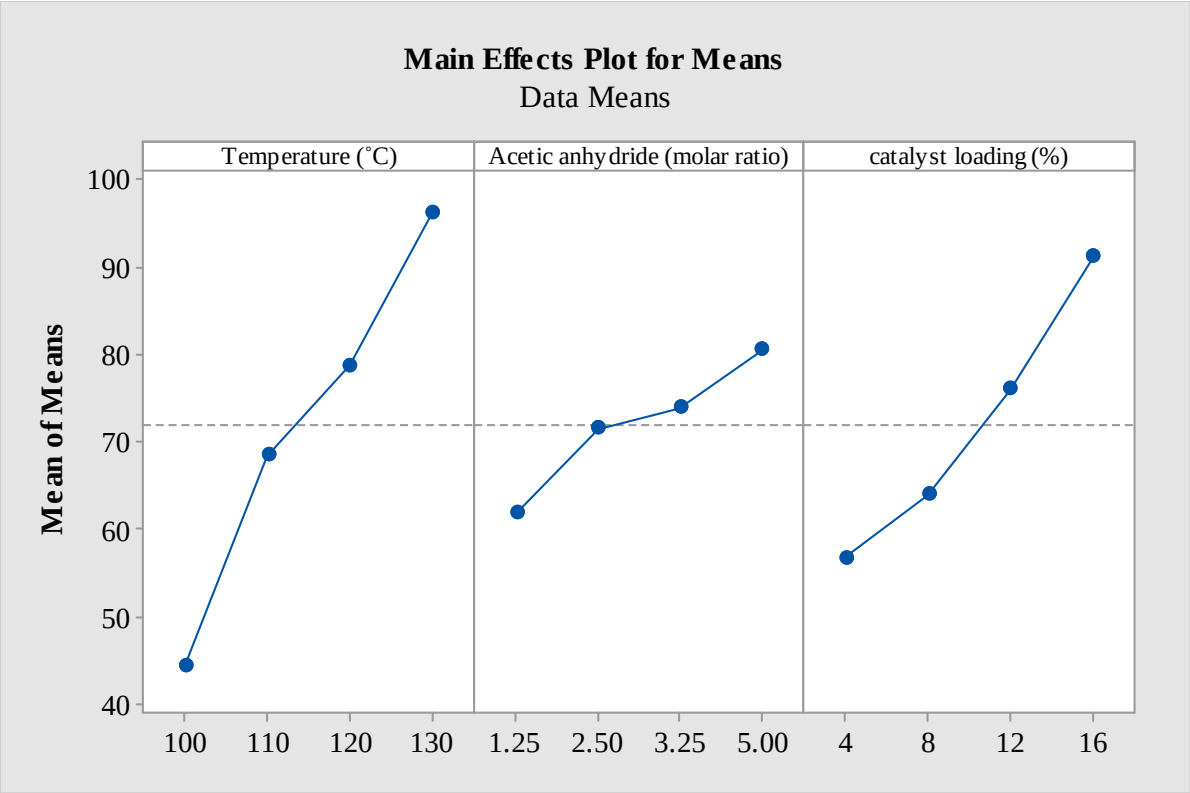

Figure 4.6 Main effect plots for means (A) temperature, (B) catalyst loading, and (C) acetic anhydride molar ratio.

Table 4.5 L16 orthogonal array project design and epoxy conversion.

Run no.	Epoxy canola oil (g)	Temperature (^oC)	Epoxy to acetic anhydride molar ratio(1:X)	Catalyst loading (% wt)	Epoxy conversion (%) after 1 h	S/N ratio calculated
1	2	100	1.25	4	25	27.9
2	2	100	2.5	8	33	30.3
3	2	100	3.25	12	47	33.5
4	2	100	5	16	72	37.1
5	2	110	2.5	4	58	35.2
6	2	110	1.25	8	42	32.4
7	2	110	5	12	77	37.7
8	2	110	3.25	16	97	39.7
9	2	120	3.25	4	54	34.6
10	2	120	5	8	83	38.4
11	2	120	1.25	12	81	38.1
12	2	120	2.5	16	97	39.7
13	2	130	5	4	90	39.0
14	2	130	3.25	8	97	39.7
15	2	130	2.5	12	99	39.9
16	2	130	1.25	16	99	39.9
17	2	130	1.25	16	99	-
18	2	130	1.25	16	98.9	-
19	2	130	125	16	99.4	-

*Per epoxy to acetic anhydride molar ratio is represented as 1 : X, where X=1.25, 2.5, 3.25, 5

Process conditions (Table 4.5: Epoxy canola oil (2 g), temperature 100 -130 ^oC, stirring speed of 1000 rpm , catalyst loading (4-12 wt%) on the basis of epoxy canola oil taken and reaction time of 1 h). Catalyst loading (% wt) represents the g of catalyst used per 100g of epoxidized canola oil. Experiment no. 17, 18 and19 represent the reproducibility studies at the optimal process conditions obtained from Taguchi design.

4.4.3 Interaction between process variables

The interactions between the process variables such as temperature, catalyst loading and epoxy to acetic anhydride molar ratio effect on the epoxy conversion were deduced from Table 4.5 and Figure 4.7. It was observed that at every temperature level, an increase in the sulfated-ZrO_2 loading showed enhancement in the epoxy conversion to vicinal di-O-acetylated canola oil, which is because of the availability of more number of active sites on the catalyst surface present in the form of sulfate linkage. Also, the increment in the reaction temperature decreases the viscosity of the oil which would help to increase the flow of the oil in the mesoporous catalyst and hence increases the rate of the reaction. However, reaction temperature beyond 130 ^oC is not suggested because, epoxidized oil tends to polymerize at high temperatures, and also the reaction can be carried out below the boiling point of acetic anhydride (Park et al. 2005). Among four different levels of temperature, it is significant to note that the rate of epoxy conversion at level 4 (130 ^oC) is very high (> 90% in 1 h) at all the catalyst loadings. The interactions between acetic anhydride and temperature also showed the similar (increasing) effect on the epoxy conversion. For the epoxy to acetic anhydride molar ratios of 1:1.25 and 1:2.5, there was a monotonic increment in the epoxy conversion with the increase in the temperature. But, with 1: 3.25 molar ratio loading, the conversion at 120 ^oC is found to be low because of the minimum amount of catalyst loading (Table 4.5). The change in the epoxy conversion with 1: 5 molar ratio is not significant at four different temperatures (Figure 4.7); however, the rate of epoxy conversion is found to be high. The interactions between the catalyst loading and acetic anhydride is described as follows. With the minimum amount of acetic anhydride loading (1:1.25), an increase in the amount of catalyst loading showed a significant increase in the epoxy conversion. But, with higher acetic anhydride loading, the conversion was found to decrease because of the high accumulation of acetic anhydride molecules on the sulfated-ZrO_2 catalyst surface (Dejaegere et al. 2011). Also, a high concentration of acetic anhydride leads to the accumulation of molecules inside the catalyst pores which would hinder epoxidized canola oil molecules to participate in the reaction.

Based on the observed interactions among the process variables, it is significant to note that high epoxy conversions can be obtained by increasing the reaction temperature and the amount of catalyst loading i.e. increase in the catalyst active sites. The minimum amount of acetic anhydride loading not only promotes higher epoxy conversions but also helps in minimizing (i)

work up procedures to extract the product, (ii) catalyst deactivation and (iii) side reactions at higher temperatures.

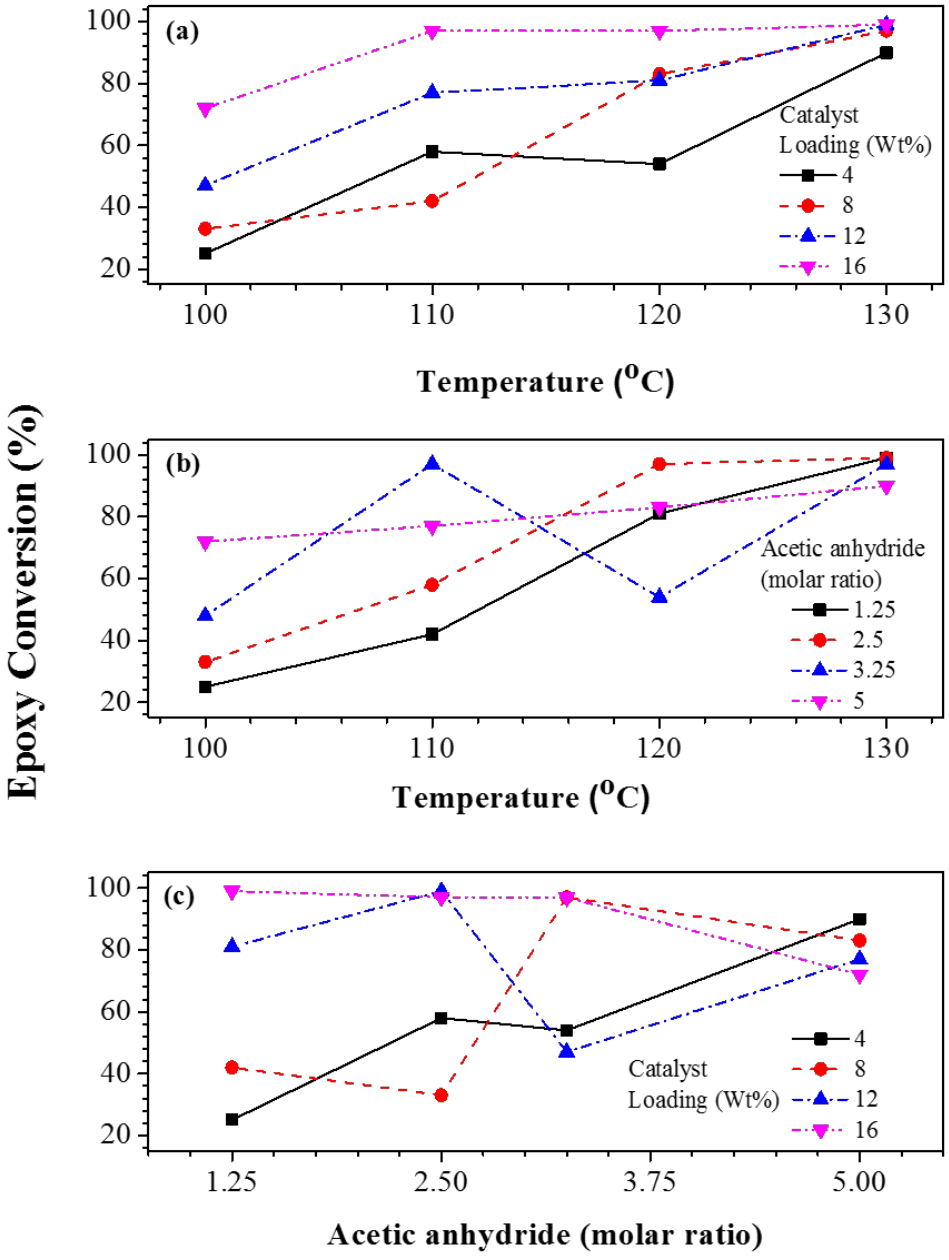

Figure 4.7 Interaction plots between variables for epoxide ring opening to di-O-acetylation. (a) temperature vs. catalyst loading, (b) temperature vs. acetic anhydride molar ratio, (c) acetic anhydride molar ratio vs. catalyst loading.

4.4.4 Spectroscopic characterization and product confirmation

The FTIR analysis of the epoxidized canola oil and vicinal di-O-acetylated canola oil was undertaken to characterize and identify the functional groups present in the molecules (Figures 4.8.A and 4.8.B). The distinct adsorption bands which were found in epoxidized canola oil and vicinal di-O-acetylated canola oil at 2855 cm^{-1} and 2930 cm^{-1} correspond to C-H symmetric and asymmetric stretching vibrations of the long chain fatty acids. The band at 722 cm^{-1} is because of the C-H bending vibrations of the saturated fatty acids present in the oils (Akintayo et al. 2006). It is important to observe that the intensity of adsorption band at 722 cm^{-1} in vicinal di-O-acetylated canola oil is significantly higher compared to epoxidized canola oil indicating the higher extent of saturation. The adsorption bands at 1230, 1155, 1098 cm^{-1} attribute to triglyceride ester triplet caused by –COO molecular vibrations which is in accordance with the literature reports (Dejaegere et al. 2011; Akintayo et al. 2006). The -COC- (epoxy) doublet adsorption band at 823 cm^{-1} in epoxidized canola oil was found to be absent in vicinal di-O-acetylated canola oil indicating the complete conversion (Mungroo et al. 2008). The symmetric stretching vibrations of carbonyl functionality (C=O) present in the carboxylic acids of the fatty acids show a distinct adsorption band at 1740 cm^{-1}. The intensity (% area) of the adsorption broad band at 1740 cm^{-1} in vicinal di-O-acetylated canola oil is found to be higher than epoxidized canola oil. This is because of the addition of acyl group (R-C=O) to the epoxy group. Also, di-O-acetylation at the epoxy group was also confirmed by the high intensity adsorption bands at 1371 cm^{-1} and 1460 cm^{-1} which attribute to the symmetric and asymmetric vibrations of methyl (-CH_3)groups (Akintayo et al. 2006; Guo-dong et al. 2014).

The structure of the vicinal di-O-acetylated canola oil was also confirmed by ^1H NMR spectroscopy. Figure 4.9.a illustrates the distinctive changes that occurred in the molecular structure of epoxidized canola oil after the complete reaction. Based on the chemical shifts and literature reports by Satyarthi et al. (2011), Sharma et al. (2013) and Akintayo et al. (2006), the ^1H NMR molecular characterization of both the oils are shown in Figures 4.9.a and 4.9.b. The proton chemical shift between 0.85 – 1.0 ppm is due to the terminal methylene group (-CH_3) of fatty acids attached to the glycerol. The protons of aliphatic –CH_2 groups of the fatty acids were found to exhibit at 1.2 – 1.4 ppm. The characteristic proton signals of –CH_2 groups of the glycerol are obtained at 4.10 – 4.40 ppm, and –CH protons of glycerol at 5.25 ppm in both the oils.

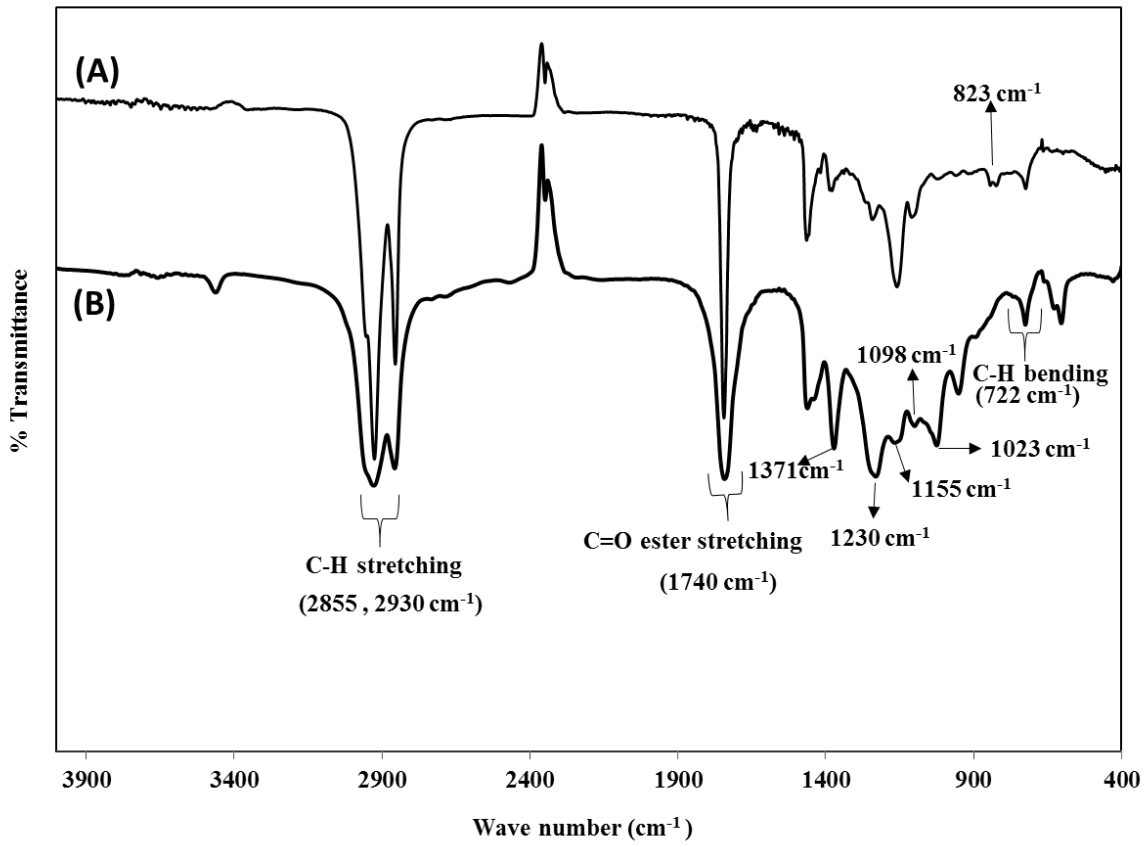

Figure 4.8 Infrared (IR) spectra of (A) epoxidized canola oil, and (B) vicinal di-O-acetylated canola oil.

The chemical shift at 2.85 – 3.15 ppm is due to the protons attached to an epoxy group of the fatty acids. The ratio of protons at this signal interprets that epoxy protons of oleic acid show a chemical shift at 2.90 ppm, linoleic acid at 2.97 ppm and linolenic acid between 3.05 – 3.15 ppm. There is no chemical shift observed at this range in ^{1}H NMR of vicinal di-O-acetylated canola oil elucidating the complete conversion of epoxy protons of oleic, linoleic and linolenic acid. After epoxide ring opening and di-O-aceylation reaction, the product vicinal di-O-acetylated canola oil exhibited additional chemical shifts at 5 ppm and 2.1 ppm which are interpreted as follows (Figure 4.9.b). The chemical shift obtained at 5.0 ppm attributes to –C**H** protons attached to –OAc groups of vicinal di-O-acetylated canola oil after epoxy ring opening and vicinal di-O-acetylation. The high intensity chemical shift at 2.1 ppm is attributed to the methyl group protons of the ester groups (-OOC-C**H$_3$**) formed after the epoxy ring opening and vicinal di-O-acetylation. ^{1}H NMR

spectroscopic analysis also confirmed the formation of vicinal di-O-acetylated canola oil with 100 % epoxy conversion.

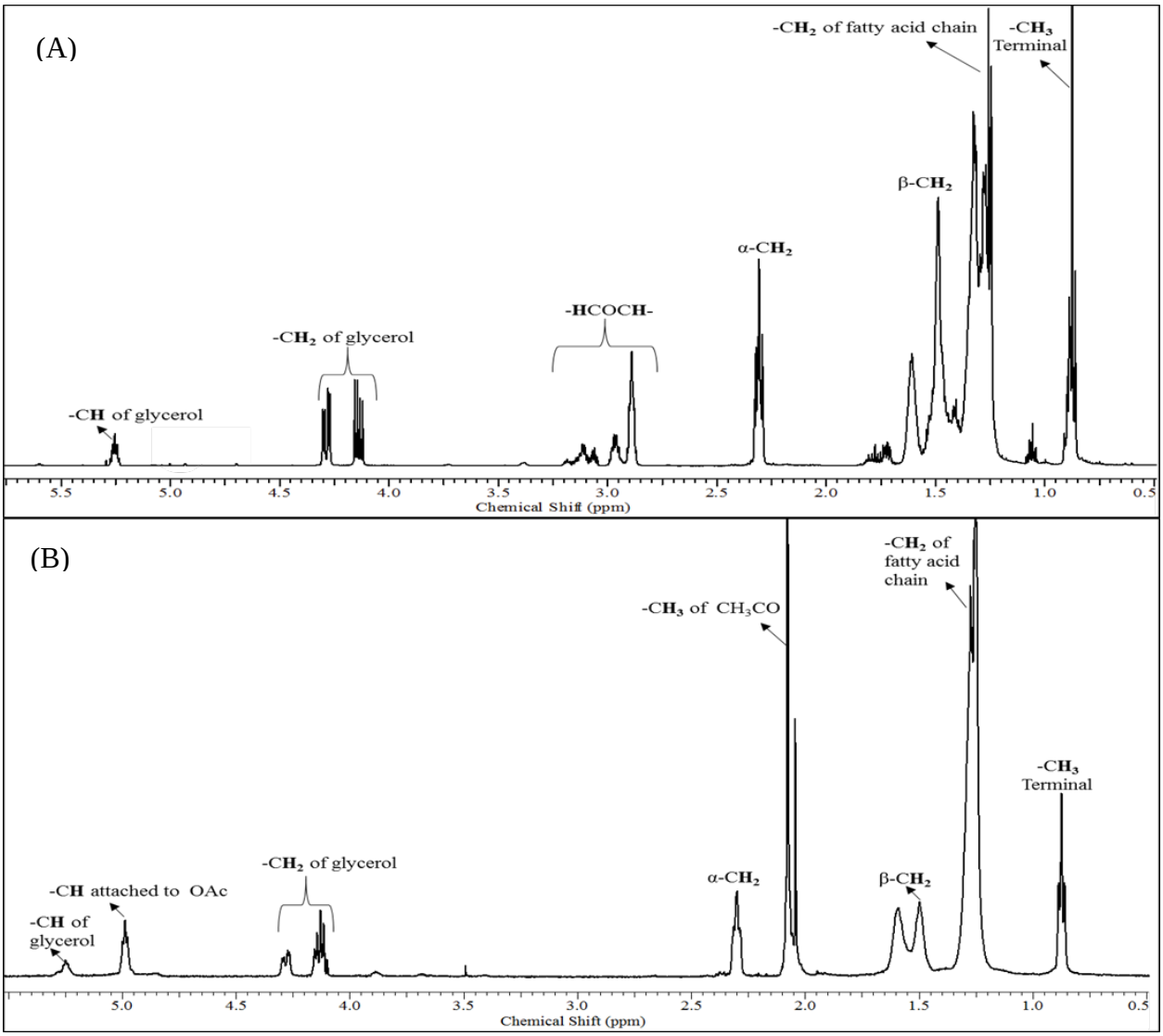

Figure 4.9 ^{1}H NMR spectra of (A) epoxidized canola oil, and (B) di-O-acetylated canola oil.

Epoxidized canola oil is a mixture of different types of epoxidized triglycerides. The triglycerides are attached with fatty acids ranging from C_{16} to C_{22}. Since the feedstock is not unimolecular, to identify following aspects such as: (i) mass range of the feedstocks, (ii) maximum mass percentage compound, (iii) mass range and molecular weight of the product and (iv) confirmation of the product by exact mass values, sodium spray mass spectroscopic analysis was undertaken. The mass range values of the compounds present in the epoxidized canola oil were found to be 932, 946, and 960. The mass value of the major composition compound was found to

be epoxidized glyceryl trioleate (932). This is because canola oil consists of oleic acid as major compound (> 65%). After the di-O-acetylation reaction, the obtained mass value range of the compounds were 1238, 1252, and 1266. These are the expected exact mass values, and also these mass values confirm that epoxy ring opened and di-O-acetylation reaction was happened without any possible side reactions such as mono-acylation and diol formation.

4.4.5 Catalyst reusability test

The change in the catalytic activity of sulfated-ZrO_2 for the synthesis of vicinal di-O-acetylated fatty acids of canola oil was tested up to three runs. Table 4.6 shows the percentage epoxy conversion to vicinal di-O-acetylated canola oil obtained after each run. The catalyst reusability tests were carried out at the optimum conditions: epoxy to acetic anhydride molar ratio of 1:1.25, catalyst loading of 16 wt% based on the amount of epoxy canola oil, temperature of 130 ^oC, reaction time of 1h and 15 min, and speed of agitation of 1000 rpm. Prior to each run, the used catalyst was refluxed with 25 ml of ethyl acetate to dissolve the organic phase adsorbed in the catalyst pores during the course of the reaction. The catalyst was regenerated by drying at 120 ^0C for 4. There was no fresh catalyst added to makeup during the reusability study. Sulfated-ZrO_2 showed reusability up to three times with marginal decrease in the epoxy conversion after the second run. The nature of the product obtained after each run was found to be same. The marginal decrease in the catalytic activity might be due to the deactivation of sulfate sites by the adsorption of acetic anhydride during the course of the reaction.

Table 4.6 Recyclability study of sulfated-ZrO_2 for the conversion of epoxidized canola oil to di-O-acetylated canola oil.

Catalyst run	% Conversion (mol %)
1	100
2	100
3	95

4.4.6 Identification of the absence of inter and intra-particle mass transfer resistances

In order to develop a true intrinsic kinetic equation for the epoxide ring opening and vicinal di-O-acetylation reaction of canola oil, it is important to ascertain the absence of inter and intra-particle diffusion resistance. Since the substrate epoxidized canola oil is bulky and viscous, there is a likelihood of formation of liquid film interface over the catalyst surface during the reaction. Hence, theoretical analysis was done to ensure the absence of mass transfer resistances (inter and intra-particle). This heterogeneous catalytic reaction may have involved following steps: (i) bulk diffusion of epoxidized canola oil (ECO) and acetic anhydride ($(Ac)_2O$) on to the catalyst surface, (ii) intra-particle diffusion of ECO and $(Ac)_2O$ through the pores of sulfated-ZrO_2, (iii) surface reaction between ECO and $(Ac)_2O$ and (iv) desorption of epoxy ring opened and vicinal di-O-acetylated canola oil. To prove the absence of inter-particle mass transfer resistance, the inequality that has been employed is rate of mass transfer (mass transfer flux (W_{ECO})) of ECO and $(Ac)_2O$ should be far greater than the observed initial reaction rate within the catalyst particle ($W_{ECO,r} >> r_{obs}$) (Asthana et al. 2003). The diffusivity of ECO through $(Ac)_2O$ was determined using Wilke-Chang equation (equation 4.3). The calculated value was found to be 8×10^{-11} m^2/s. To determine the mass transfer flux $W_{ECO,r} = k_c \times C_{ECO,S}$, the solid-liquid mass transfer coefficient (k_c) was found from Sherwood number $Sh = k_c \times (d_p / D_{ECO,(Ac)2O})$ (28) , where d_p is the average diameter of the catalyst particles. As a conservative estimate, the value of Sh was taken as 2, and the concentration of the ECO at the surface was considered to be equal to bulk concentration. The obtained value of mass transfer flux is 0.08 $mol/m^2.s$, which is found to be much higher than observed initial reaction rate 7×10^{-11} $mol/m^2.s$. Hence, the theoretical analysis elucidates the absence of external mass transfer resistance.

$$D_{ECO,(Ac)_2O} = \frac{117.3 \times 10^{-18} \times (\Psi \times M_{(Ac)_2O})^{0.5} \times T}{(\mu \times V_{ECO}{}^{0.6})} \qquad (4.3)$$

To investigate the internal pore mass transfer diffusion effect on the reaction rate, the dimensionless parameter Weisz-Prater criterion C_{wp} (equation 4.4) which is the "ratio of the intrinsic reaction rate to the intra-particle diffusion rate" (Baroi et al. 2013) was considered.

$$C_{wp} = \frac{-r_{obs} \times R_P^2 \times \rho_{Cat}}{(D_e \times C_{ECO,S})} \qquad (4.4)$$

Where D_e is the effective diffusivity of ECO (limiting reactant) calculated from the equation $D_{ECO,e} = D_{ECO,(Ac)2O} \times$ porosity (ε) / tortuosity (τ). As a conservative estimate, the value of ε is taken as 0.4 and τ as 3.0 (Fogler et al. 2002). The calculated value of $D_{ECO,e}$ is found to be 1.0×10^{-11} m^2/s. By substituting the values of $C_{ECO,S}$ (7×10^{-11} m^2/s), the concentration of ECO at the catalyst surface, R_p radius of the catalyst particle (653.5 nm) and density of the catalyst (1.5 g/cc) , the , value of C_{wp} was obtained as 0.081 ($C_{wp} << 1$). Hence, it confirms the absence of inter-particle diffusion resistance at the reaction conditions for the epoxide ring opening and vicinal di-O-acetylation of canola oil reaction.

4.4.7 Kinetic model development

Langmuir-Hinshelwood-Hougen-Watson (LHHW) dual site (similar in nature) model was tested to generate the rate expression for the epoxide ring opening and vicinal di-O-acetylation reaction of canola oil. In the absence of inter and intra particle mass transfer resistances, the reaction could be primarily controlled by (i) adsorption of ECO and $(Ac)_2O$ on to the active sites of sulfated-ZrO_2 catalyst, (ii) surface reaction between ECO and $(Ac)_2O$, (iii) desorption of vicinal di-O-acetylated canola oil (DACO). This model is represented by the following steps.

(a) The physisorption of the reactants on the vacant sites of the catalyst is given as

$$ECO + S \underset{k_{-1}}{\overset{k_1}{\rightleftharpoons}} ECO.S \qquad (4.5)$$

$$(Ac)_2O + S \underset{k_{-2}}{\overset{k_2}{\rightleftharpoons}} (Ac)_2O.S \qquad (4.6)$$

(b) Surface reaction between the ECO and $(Ac)_2O$ to form the product

$$ECO.S + (Ac)_2O.S \underset{k_{-s}}{\overset{k_s}{\rightleftharpoons}} DACO.S + S \qquad (4.7)$$

(c) Desorption of DACO from the active sites of the catalyst

$$DACO.S \underset{k_{-3}}{\overset{k_3}{\rightleftharpoons}} DACO + S \qquad (4.8)$$

The rate rption of ECO and $(Ac)_2O$ is written as

$$-r'_{ECO} = r_{AD} = k_1 \left(C_{ECO} C_s - \frac{C_{ECO.S}}{K_1}\right) \qquad (4.9)$$

$$-r'_{(Ac)_2O} = r_{AD} = k_2 \left(C_{(Ac)_2O} C_s - \frac{C_{(Ac)_2O.S}}{K_2}\right) \quad (4.10)$$

$$Where\ K_1 = \frac{k_1}{k_{-1}}, K_2 = \frac{k_2}{k_{-2}}$$

The rate of surface reaction between ECO and $(Ac)_2O$ is given as

$$-r'_{ECO,S} = r_s = k_s \left(C_{ECO.S}\, C_{(Ac)_2O.S} - \frac{C_{DACO.S}\, C_S}{K_S}\right) \quad (4.11)$$

$$Where\ K_S = \frac{k_S}{k_{-S}}$$

Similarly, the rate of desorption of the product is written as

$$-r'_{DACO.S} = r_D = k_3 \left(C_{DACO.S} - \frac{C_{DACO}\, C_S}{K_3}\right) \quad (4.12)$$

$$Where\ K_3 = \frac{k_3}{k_{-3}}$$

Adsorption and desorption steps were used to eliminate $C_{ECO.S}$, $C_{(Ac)2O.S}$ and $C_{DACO.S}$ in equation 4.11, because it is difficult to readily measure the concentrations of both adsorbed and desorbed species on the catalyst surface. When the surface reaction rate is limiting, and by the condition that adsorption and desorption constants k_1, k_2 and k_3 are large when compared to surface reaction (i.e., $-r'_{ECO}/k_1 \approx 0$, $-r'_{(Ac)2O}/k_2 \approx 0$ & $-r'_{DACO}/k_3 \approx 0$) (Fogler et al. 2002) . The surface reaction rate is written as;

$$-r'_{ECO,S} = r_s = k_s\, K_1 K_2\, C_S^2 \left(C_{ECO}\, C_{(Ac)_2O} - \frac{C_{DACO}}{K_1 K_2 K_S}\right) \quad (4.13)$$

If C_t is the total number of active sites of the catalyst, it was written in terms of C_S as;

$$C_S = \frac{C_t}{1 + K_1 C_{ECO} + K_2 C_{(Ac)_2O.S} + K_S C_{DACO}} \quad (4.14)$$

Substituting C_s in equation 4.13,

$$-r'_{ECO,S} = r_s = \frac{k_s\, K_1 K_2\, C_t^2 \left(C_{ECO}\, C_{(Ac)_2O} - \frac{C_{DACO}}{K_1 K_2 K_S}\right)}{(1 + K_1 C_{ECO} + K_2 C_{(Ac)_2O} + K_S C_{DACO})^2} \quad (4.15)$$

At time t=0, the molar ratio of $(Ac)_2O$ and ECO is taken as M (i.e., $C_{(Ac)_2O,0}$ / $C_{ECO,0}$ = M), and C_{DACO} = 0. Then equation 4.15 is reduced to equation 4.16,

$$r_s = -\frac{d_{ECO}}{dt} = \frac{k_s\, K_1 K_2\, C_t^2\, \left(C_{ECO}\, C_{(Ac)_2O}\right)}{\left(1 + K_1 C_{ECO} + K_2 C_{(Ac)_2O}\right)^2} \qquad (4.16)$$

According to Fogler et al. (2002) if the reaction rate is temperature dependent and irreversible surface reaction limited, increase in the temperatures results in the decrease of adsorption equilibrium constants due to less surface occupancy by the adsorbed species, and hence denominator of the catalytic rate law approaches to unity, based on this knowledge equation 4.16 can be written as;

$$r_s = -\frac{d_{ECO}}{dt} = k_s\, K_1 K_2\, C_t^2\, \left(C_{ECO}\, C_{(Ac)_2O}\right) \qquad (4.17)$$

In terms of fractional conversion, the equation 4.17 is written as

$$\frac{dX_{ECO}}{dt} = k\, C_{ECO,O}^2 (1 - X_{ECO})(M - X_{ECO}) \qquad (4.18)$$

$$Where\ k = k_s\, K_1 K_2\, C_t^2$$

The final equation obtained after integration is

$$\ln\left(\frac{(M - X_{ECO})}{M * (1 - X_{ECO})}\right) = k\, C_{ECO,O}^2 (M - 1)\, t \qquad (4.19)$$

The value of M is 5.13.

A plot of ln ((5.13-X_{ECO})/5.13× (1- X_{ECO}) vs time (Figure 4.10) was made at different temperatures (100 – 130^{o}C), and the plots were found to give excellent fit indicating that the reaction is an overall second order and the reaction validates the Langmuir-Hinshelwood-Hougen-Watson model. With the rate constants obtained at different temperatures, an Arrhenius plot (–ln k vs 1/T) (Figure 4.11) was made, and the calculated apparent activation energy of the reaction is 23 kcal/mol. This value indicates that the epoxide ring opening and di-O-acetylation of canola oil reaction is an intrinsic kinetically controlled reaction.

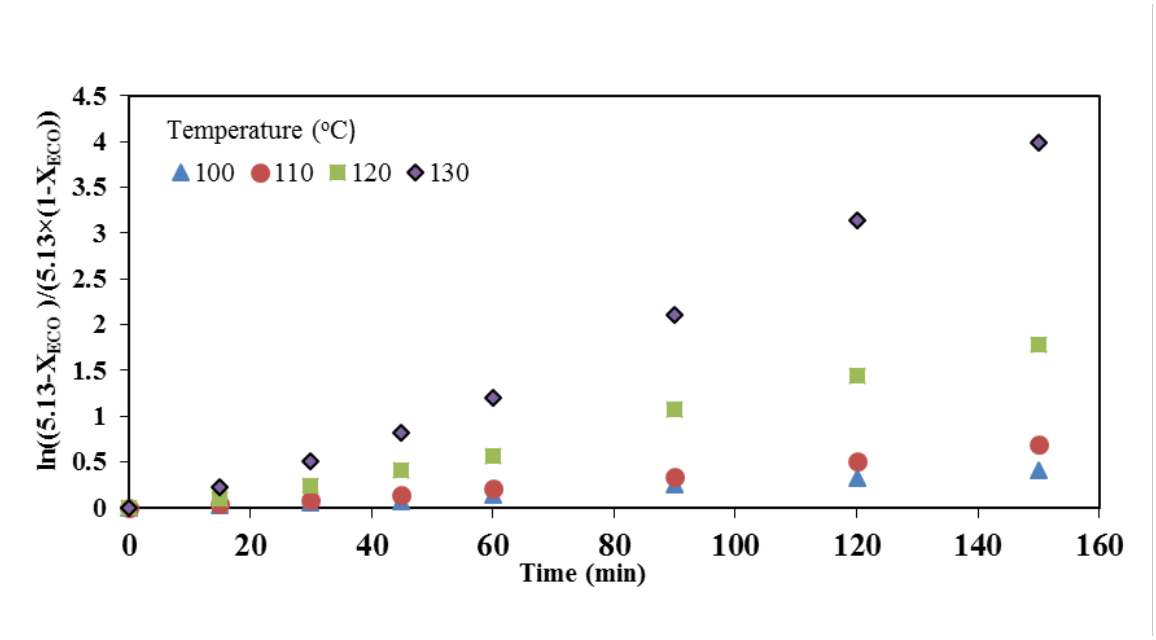

Figure 4.10 Plot of ln((5.13-X_{ECO})/5.13× (1- X_{ECO})) vs time between 100 - 130 °C.

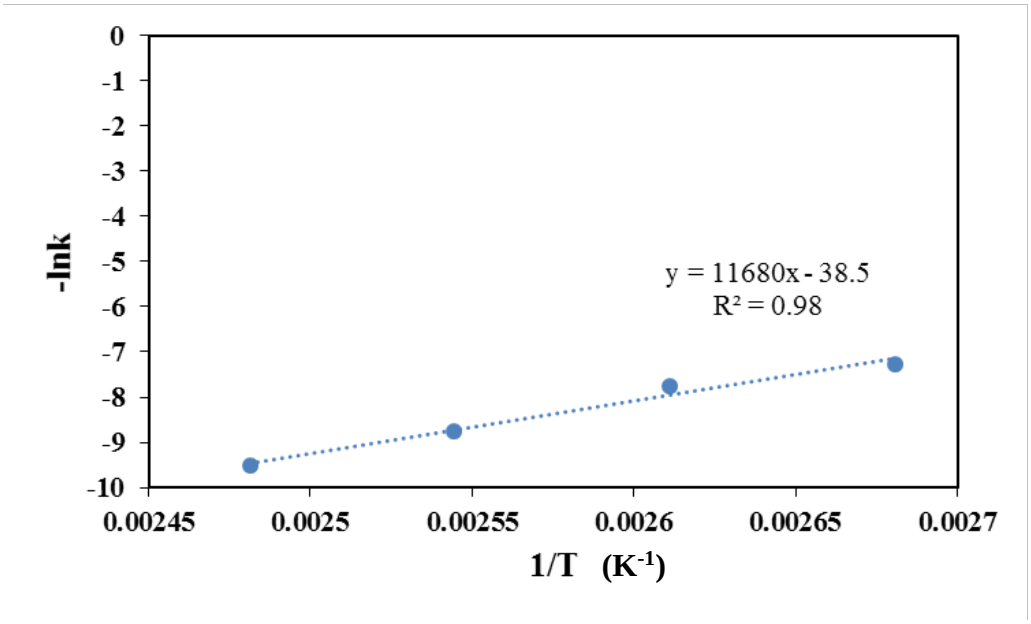

Figure 4.11 Arrhenius plot (–ln k vs 1/T) of epoxide ring opening and vicinal di-O-acetylation reaction measured at temperatures between 100 to 130 °C.

4.5 Conclusions

Heterogeneous sulfated-ZrO_2 was found to be an active catalyst for the synthesis of vicinal di-O-acetylated canola oil. The optimized process parameters for 100 % epoxy conversion are temperature of 130 ^oC, epoxy to acetic anhydride molar ratio of 1:1.25, 16 wt% catalyst loading based on the amount of epoxidized canola oil taken, stirring speed of 1000 rpm and reaction time of 1 h 15 min. Epoxide ring opening and vicinal di-O-acetylation of canola oil was found to follow overall second order reaction and the proposed Langmuir-Hinshelwood-Hougen-Watson model was validated.

CHAPTER 5

ONE-POT SYNTHESIS OF CANOLA OIL BASED BIOLUBRICANTS CATALYZED BY MoO_3/Al_2O_3 AND EVALUATION OF PHYSICOCHEMICAL PROPERTIES

A part of this work has been published as research article and was presented at the following conferences:

1. Asish K. R. Somidi, Umashankar Das, and Ajay K. Dalai, "One-pot synthesis of canola oil based biolubricants catalyzed by MoO_3/Al_2O_3 and process optimization study," Chemical Engineering Journal, 293, 259-272 (2016).
2. Rajesh V. Sharma, Asish K. R. Somidi, Ajay K. Dalai, "Preparation and properties evaluation of biolubricants derived from canola oil and canola biodiesel," Journal of Agricultural and Food Chemistry, 63 (12), 3235-3242 (2015).
3. Asish K. R. Somidi, Umashankar Das, Ajay K. Dalai, "One-pot synthesis of canola oil based biolubricants using MoO_3/Al_2O_3 catalyst." Oral presentation at the 24th Canadian Symposium on Catalysis, Ottawa, Ontario, May 2016.
4. Asish K. R. Somidi, Rajesh V. Sharma, Ajay K. Dalai, "Preparation and properties evaluation of biolubricants derived from canola oil and canola biodiesel," Oral presentation at the 65th Canadian Chemical Engineering Conference, Calgary, AB, October 2015.

Contribution of the Ph.D. candidate

All the experimental and characterization work was conducted by Asish Somidi. Manuscript writing and revision work of this chapter was done by Asish Somidi based on the suggestions from Dr. Ajay K. Dalai and Dr. Umashankar Das (Manuscript 1).

The physicochemical characterization of prepared biolubricants was done by Asish Somidi. Dr. Rajesh V. Sharma (postdoctoral fellow) has written the manuscript. Revision and rebuttal work was done by Asish Somidi and Dr. Ajay K. Dalai (Manuscript 2).

The contribution of this chapter to the overall Ph. D. work

In Chapters 3 and 4, synthesis of epoxidized canola oil and di-O-acetylated canola oil, respectively, were prepared separately using different catalysts. The current work shows preparation and development of a single heterogeneous catalyst for the one-pot synthesis of epoxidized canola

oil/canola biodiesel and di-O-acetylated canola oil/canola biodiesel. Also, This chapter demonstrates the evaluation and comparison of the lubricity properties of the biolubricants prepared from the canola oil and canola biodiesel.

5.1 Abstract

Research on the formulations of vegetable oils into biolubricants has gained significant interest due to their promising lubricity and eco-friendly properties. The epoxidation of unsaturated groups in vegetable oil followed by epoxide ring opening by acetic anhydride provides vicinal di-O-acetylated glyceryl fatty acid esters as a stable and potential biolubricant. The present study is emphasized on the development of a single and novel heterogeneous catalyst for both the reaction steps (epoxidation and di-O-acetylation) to produce biolubricants from canola oil and canola biodiesel (methyl fatty acid esters). Group VI metal oxides (Cr, W and Mo) impregnated on aluminum oxide were prepared and screened for their catalytic activity on the epoxidation and vicinal di-O-acetylation steps. MoO_3/Al_2O_3 was found to be the most effective catalyst for the epoxidation of canola oil and canola biodiesel and its further conversion to corresponding vicinal di-O-acetylated derivatives (biolubricants). The response surface methodology (RSM) was employed for optimizing the process conditions and statistical analysis for both the reaction steps separately. Based on the process optimization study, 10 wt% MoO_3/Al_2O_3 was found to be the efficient catalyst for 100% conversion of unsaturated groups to the epoxide and its further conversion to vicinal di-O-acetylated products in a one-pot synthesis. All the products were confirmed by ^1H NMR and mass spectrometry. The physicochemical characterization of MoO_3/Al_2O_3 was carried out to evaluate and understand the properties required for effective catalysis. This study discloses MoO_3/Al_2O_3 as a promising catalyst for the synthesis of biolubricants from vegetable oils. The present study also involves evaluation and comparison of physicochemical properties of vicinal di-O-acetylated canola oil and vicinal di-O-acetylated canola biodiesel. The properties of these biolubricants were compared for low temperature characteristics such as cloud point and pour point, kinematic viscosity, viscosity index, lubricity by using high frequency reciprocating rig apparatus, thermal stability by thermogravimetric analysis, and oxidative stability. Biolubricant from canola biodiesel has a low cloud point and pour point properties, better friction, and anti-wear properties, is less viscous and has the potential to substitute petroleum based automotive lubricants. Biolubricant from canola oil has high thermal

stability, is more viscous and more effective at higher temperature conditions. This study shows that both the biolubricants are attractive, renewable, and ecofriendly substitutes for the mineral oil based lubricants.

5.2 Introduction

Growing research on the transformation of biomass into bio-fuels and new value added chemicals helps in the advancement of green technology to produce sustainable and environmentally friendly materials (Bella et al. 2015). Bio-based materials such as vegetable oils, forestry, and agricultural wastes are considered to be potential renewable and alternative energy sources. Some of the promising alternative industrial products derived from aforementioned feedstocks are biolubricants, biodiesel, biopolymer based batteries, cellulosic components for solar cells fabrication, alternative chemicals extracted from biomass sources, functionalized glycerol derivatives and polyols (Xie et al. 2015; Bella et al. 2014; Issariyakul et al. 2008; Pagliaro et al. 2007).

Investigation of the literature reports on the preparation of vicinal di-O-acetylated glyceryl fatty acid esters from vegetable oil feedstocks reveal that: (1) the synthesis of the final product involves a multi-step reaction process which includes epoxidation, epoxide ring opening, mono acetylation and its conversion to di-O-acetylated products, (2) different catalysts are used for each reaction step, and the products formed in each step were isolated through extraction procedures and used for the next reaction steps, (3) most of the studies used commercial resins as catalysts for the epoxide ring opening and vicinal di-O-acetylation of fatty acids which cannot be reused in multi-batch processes due to loss of catalytic activity. The novelty of this research work is emphasized on the development of a single heterogeneous catalyst that can be used for both epoxidation and epoxide ring opening to produce vicinal di-O-acetylated products from canola oil and canola biodiesel in a single step with high conversion and yield.

Group VI transition metals such as chromium, tungsten, and molybdenum are found to be active for the epoxidation of unsaturated methyl esters and triglycerides (Satyarthi et al. 2011; Poli et al. 2009). In the present work, these metal oxides supported on aluminum oxide were investigated for their activity on the epoxidation of canola oil and canola biodiesel, and epoxide ring opening to produce vicinal di-O-acetylated products. Initially, the catalysts were prepared and

screened on the model compounds such as methyl oleate and glyceryl trioleate which are major components in the canola biodiesel and canola oil, respectively. The optimized catalyst was characterized to determine the textural properties, surface acidity, and functional groups present on the catalyst surface. ^{1}H NMR was used to monitor the reaction progress and to confirm the structure of the products. Electron ionization mass spectrometry analysis was also undertaken to confirm the product formation and mass distributions in the biolubricants.

Central composite design (CCD) methodology was used to find out the optimum process conditions for the epoxidation of canola oil, epoxide ring opening and vicinal di-O-acetylation of canola oil and canola biodiesel using MoO_3/Al_2O_3 catalyst. A response surface model was developed for both the reaction steps separately. Statistical analysis was also carried out to study the effects of the chosen process parameters on the response (unsaturation and epoxide conversion) and the analysis of variance (ANOVA). Based on the optimum conditions obtained from the response surface methodology, one-pot synthesis of canola oil and canola biodiesel biolubricants was performed. The optimized catalyst was also tested for its reusability in one-pot synthesis.

5.3 Experimental

5.3.1 Chemicals and reagents

Canola biodiesel was supplied by Miligan Biofuels Inc. (Saskatoon, Canada). Ammonium molybdate, toluene (ACS grade), and sodium bicarbonate (ACS grade) were procured from Fisher Chemicals (Edmonton, Canada). *Tert*-butyl hydroperoxide (70 wt% in water), acetic anhydride (ACS grade), and aluminum nitrate nonahydrate (ACS grade, 98-102% pure) were purchased from Alfa-Aesar (Massachusetts, USA). Sodium sulfate anhydrous (ACS grade) and ethyl acetate (ACS grade) were purchased from VWR international (Edmonton, Canada). Ammonium hydroxide (ACS grade), glyceryl trioleate (> 99%) and methyl oleate (>99%) were procured from Sigma-Aldrich (St. Louis, USA).

5.3.2 Catalyst preparation

Ammonium heptamolybdate tetrahydrate [$(NH_4)_6Mo_7O_{27}\cdot 4H_2O$] was used as a precursor for the impregnation of molybdenum on the aluminum hydroxide [$Al(OH)_3$] support. The preparation of MoO_3/Al_2O_3 with 5, 10 and 15 wt % of molybdenum loading was carried out as follows. 100 g of aluminum nitrate nonahydrate was dissolved in the distilled water (1L). The

solution was heated to 80 ^{o}C with continuous stirring for 2 h. 25% v/v aqueous NH_4OH solution was then added to the stirred solution to maintain the pH between 8.5-9.5 for precipitating $Al(OH)_3$. The collected precipitate was filtered and repeatedly washed with distilled water until the filtrate showed pH 7. The precipitate was then dried at 120 ^{o}C for 24 h. $Al(OH)_3$ crystals thus obtained were ground to fine powder. The wet impregnation (sequential pore filling) technique was employed in the preparation of MoO_3/Al_2O_3 with the metal loadings as indicated above. About 0.73 g of $[(NH_4)_6Mo_7O_{27}\cdot 4H_2O]$ was added to 8.4 g of $Al(OH)_3$ to obtain 5 wt% MoO_3/Al_2O_3. For the preparation of 10 wt% MoO_3/Al_2O_3 and 15 wt% MoO_3/Al_2O_3, 1.47 g and 2.20 g of $[(NH_4)_6Mo_7O_{27}\cdot 4H_2O]$ were added separately to each 8.4 g of $Al(OH)_3$ support, respectively. After impregnation, the samples were dried at 120 ^{o}C for 3 h and calcined in the calcination oven at 550 ^{o}C for 6 h to obtain 5 wt% MoO_3/Al_2O_3, 10 wt% MoO_3/Al_2O_3 and 15 wt% MoO_3/Al_2O_3. $Al(OH)_3$ was calcined at the similar conditions to obtain Al_2O_3. Similar procedure was used to prepare 5 wt% Cr_2O_3/Al_2O_3 and 5 wt% WO_3/Al_2O_3 for catalyst screening tests. For 1.5 g of $Al(OH)_3$, about 0.58 g of chromium nitrate, and 0.1 g of ammonium metatungstate were used for impregnation, and then samples are dried and calcined at 550 ^{o}C for 6 h to obtain 5 wt% Cr_2O_3/Al_2O_3 and 5 wt% WO_3/Al_2O_3, respectively.

5.3.3 Catalyst characterization methodology

Inductively Coupled Plasma Optical Emission Spectrometry (ICP-OES) (iCAP 700 series) was used to identify the amount of molybdenum present in the catalyst samples after calcination. About 0.1 g of sample was digested in 5 ml aqua regia and the volume was adjusted to 5% v/v aqueous solution for analysis after complete digestion. The other catalyst characterization techniques are explained in Chapters 3 and 4.

5.3.4 Preparation of anhydrous tert-butyl hydroperoxide in toluene

Anhydrous *tert*-butyl hydroperoxide in toluene as a solvent was prepared for the epoxidation of unsaturated fatty acids in the feedstocks canola oil and canola biodiesel. Anhydrous condition was maintained in order to avoid aggregation of MoO_3/Al_2O_3 catalyst particles in the presence of moisture (experimental observations). About 125 ml of 70 wt % *tert*-butyl hydroperoxide in water was added to 90 ml toluene (reagent grade). The solution was then aged for an hour to separate the aqueous layer (~30 ml). The remaining organic layer was collected in a 500 ml single neck round bottom flask which is equipped with a Dean-Stark apparatus. The

solution was then refluxed at 107 ^{o}C to remove residual water (~7.5 ml) from the organic phase. The organic phase was then washed with anhydrous sodium sulfate to remove excess moisture and then transferred into a 500 ml amber glass bottle. The prepared solution was stored in a desiccator at room temperature for use in the reaction. ^{1}H NMR was used to determine the molarity of the prepared solution using equation 5.1 as follows (Hill et al. 1983):

$$Molarity = \frac{A}{(0.1\,A + 0.32\,B)} \quad (5.1)$$

Where A is the integration value of –C**H$_3$** protons (δ = 1.3 ppm) of *tert*-butyl hydroperoxide and B is the integration value of -C**H$_3$** protons (δ = 2.40 ppm) of toluene. The molarity of the prepared solution was determined around 4.4 M.

5.3.5 Experimental design and statistical analysis

Central Composite Design (CCD) scheme was used for the optimization of process variables for both the reaction steps (epoxidation of canola oil and vicinal di-O-acetylation of epoxidized canola oil) using minimum number of experiments. Minitab software was used for the experimental design and statistical analysis. The four process parameters such as temperature (^{o}C), wt% of metal loading on the support, feedstock to reactant molar ratio, and catalyst loading (wt%) per gram of feedstock were chosen for process optimization. Each parameter has three levels which were represented as low (-1), medium (0), and high (+1) range. The process parameters and their respective levels chosen for the epoxidation reaction are shown in Tables 5.1 and 5.2 for the vicinal di-O-acetylation of epoxidized canola oil. In both the reactions, temperature range was varied between 60 to 120 ^{o}C, substrate to reactant molar ratio between 1 to 3 mol, molybdenum loading between 5 to 15 wt%, catalyst loading between 4 to 12 wt% per gram of feedstock, speed of agitation 450 rpm and the reaction time 4 h. A total of 27 runs were performed for each reaction step initially based on the CCD scheme shown in equation 5.2 (Kang et al. 2015). This equation is a combination of three categories: factorial (2^{p}), axial (2×p) and centre (3) runs, and p denote the number of process parameters.

$$Number\ of\ runs = 2^{p} + (2 \times p) + center\ runs = 2^{4} + (2 \times 4) + 3 = 27 \quad (5.2)$$

Table 5.1 Selected process parameters and their levels chosen for the epoxidation of canola oil

Parameters	Symbols	Coded levels		
		-1	0	+1
Temperature (°C)	X_1	60	90	120
Metal loading (wt %)	X_2	5	10	15
tert-butyl hydroperoxide (molar ratio)	X_3	1	2	3
Catalyst loading (wt %)	X_4	4	8	12

Table 5.2 Selected process parameters and their levels chosen for the preparation of canola oil biolubricant (vicinal di-O-acetylation reaction)

Parameters	Symbols	Coded levels		
		-1	0	+1
Temperature (°C)	Y_1	60	90	120
Metal loading (wt %)	Y_2	5	10	15
Acetic anhydride molar ratio	Y_3	1	2	3
Catalyst loading (wt %)	Y_4	4	8	12

Based on the responses (% unsaturation or epoxide conversion) obtained in each experimental run, main effect plots were plotted to investigate the effect of individual parameter on the overall response characteristic, as well as counter plots for determining the optimum conditions for maximum conversion. Also, a response surface quadratic model was developed for each reaction step which includes process parameters in individual, squared and cross effect forms. ANOVA analysis was performed for the proposed models to identify the importance of process variables in all the forms based on the F-test statistic and P-values, and the regression coefficient of the model (Borugadda et al. 2015).

5.3.6 ^{1}H NMR methodology

The progress of the epoxidation of canola oil followed by epoxide ring opening and vicinal di-O-acetylation reaction was monitored by ^{1}H NMR. The percentage of unsaturation conversion in the canola oil was calculated by the equation 5.3, and the percentage of epoxide conversion to corresponding di-O-acetylated product was calculated as per equation 5.4:

$$\text{Unsaturation conversion (\%)} = \frac{U_x - U_y}{U_x} \times 100 \qquad (5.3)$$

$$\text{Epoxide conversion (\%)} = \frac{E_x - E_y}{E_x} \times 100 \qquad (5.4)$$

U_x = Area of unsaturation in the canola oil (δ = 5.29 – 5.43 ppm) with respect to –CH_2 protons of glycerol at δ = 4.25 – 4.32 ppm.

U_y = Area of unsaturation in the product (epoxide canola oil) (δ = 5.29 – 5.43 ppm) with respect to –CH_2 protons of glycerol at δ = 4.25 – 4.32 ppm.

E_x = Area of epoxide protons in the epoxide canola oil (δ = 2.85 – 3.15 ppm) with respect to –CH_2 protons of glycerol at δ = 4.25 – 4.32 ppm.

E_y = Area of epoxide protons in the product vicinal di-O-acetylated canola oil (δ = 2.85 – 3.15 ppm) with respect to –CH_2 protons of glycerol at δ = 4.25 – 4.32 ppm.

5.3.7 Reaction set-up and experimental procedure

5.3.7.1 Reaction schemes

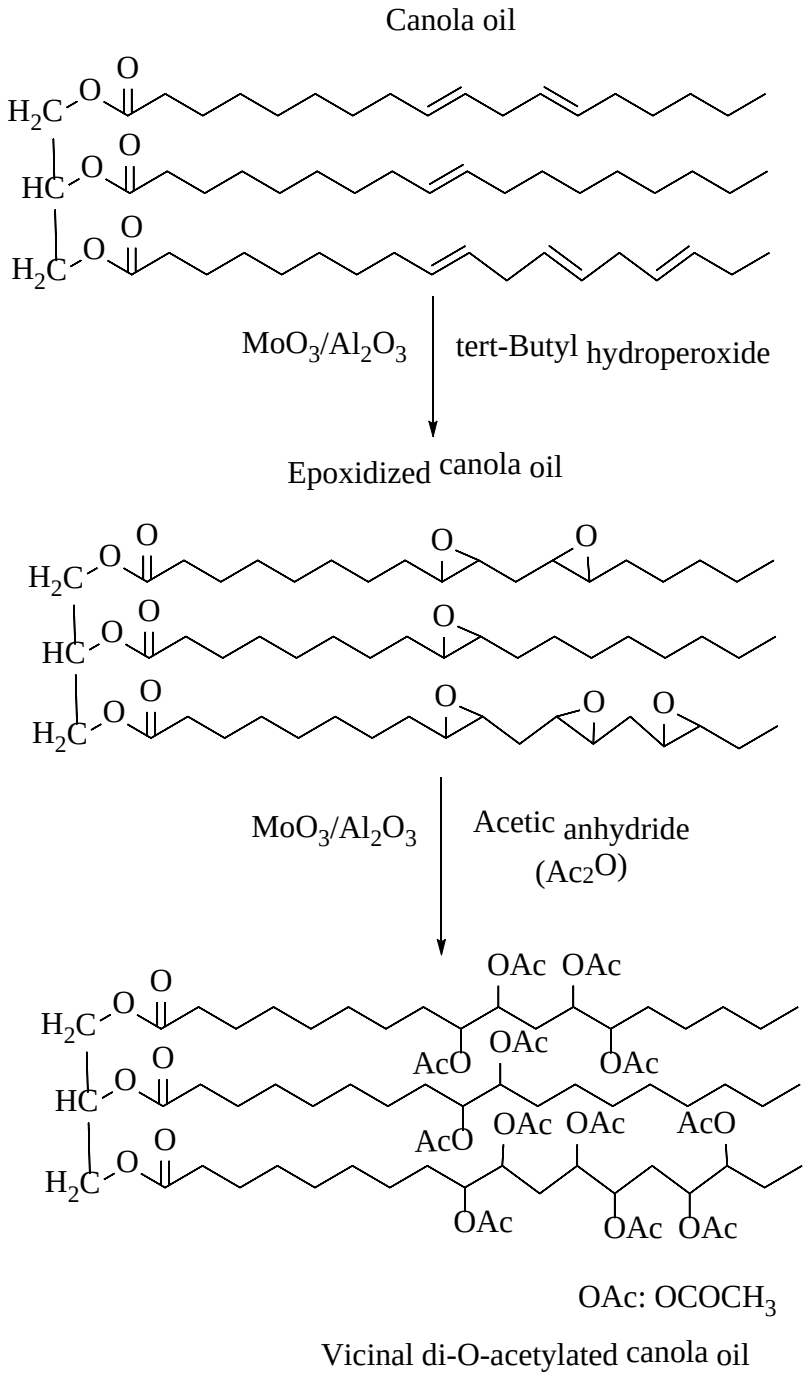

Figure 5.1 Reaction scheme for the synthesis of di-O-acetylated canola oil using MoO_3/Al_2O_3

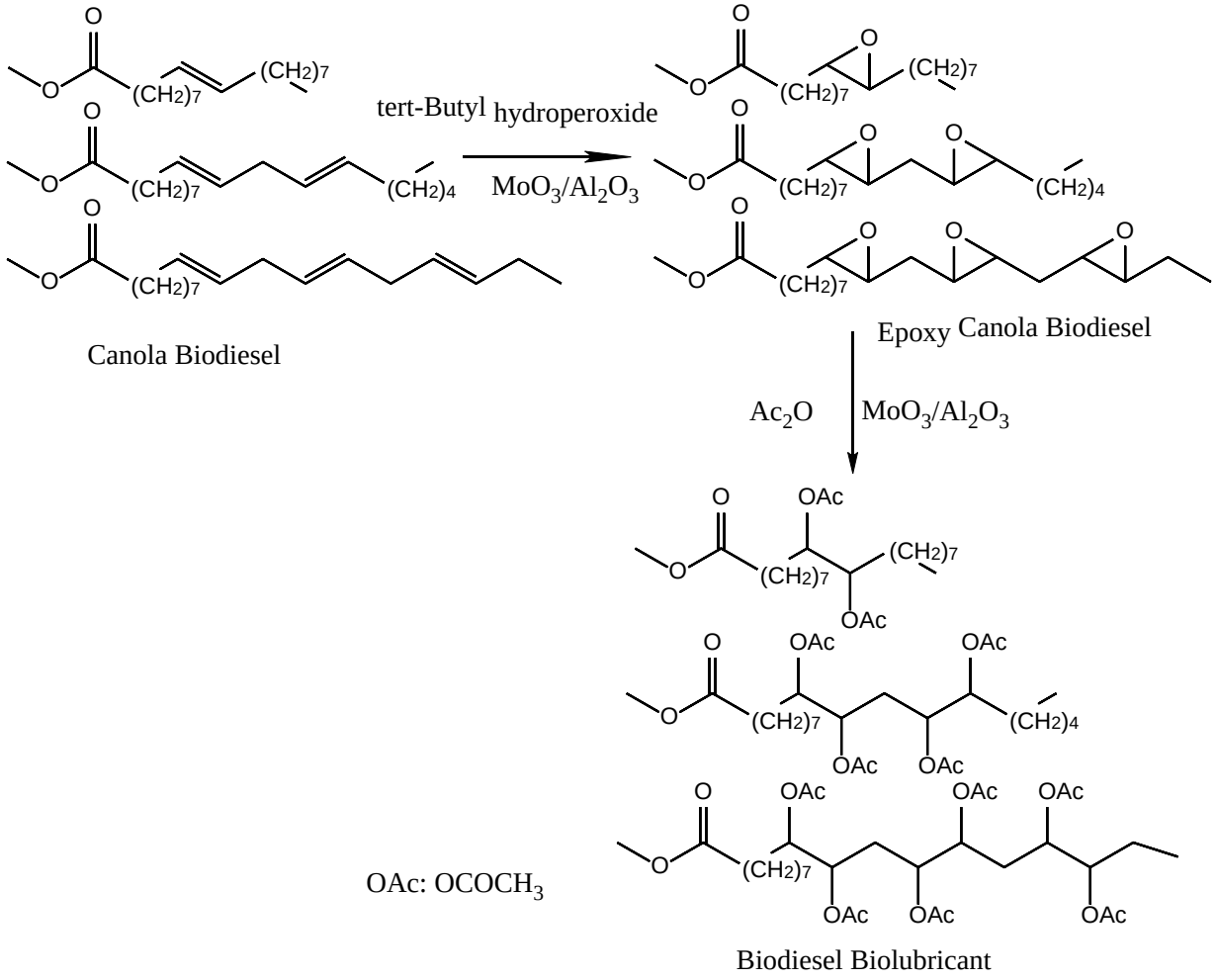

Figure 5.2 Reaction scheme for the synthesis of di-O-acetylated canola biodiesel using MoO_3/Al_2O_3

5.3.7.2 Preparation of epoxidized feedstocks

Epoxidation of canola oil and canola biodiesel was carried out at the optimum reaction conditions obtained from the Response Surface Methodology (RSM) which is discussed in the later part of this manuscript. Figures 5.1 and 5.2 show the reaction scheme for the epoxidation of unsaturated fatty acids in the feedstocks, respectively. The catalytic epoxidation of canola oil and canola biodiesel was performed in a 10 ml single neck round bottom flask connected to a reflux condenser. The reflux condenser was attached to a drying tube filled with drierite crystals to maintain anhydrous conditions. Uniform heating and stirring were supplied to the reaction mixture using temperature controlled oil bath equipped with a magnetic stirrer. In the epoxidation reaction, 15 wt% MoO_3/Al_2O_3 was used as a catalyst. Typically, for 0.5 g of feedstock, 1:2.25 molar ratio

of anhydrous tert-butyl hydroperoxide (TBHP) in toluene was used. These molar ratios were considered based on the unsaturation in the feedstock. About 5 wt% of catalyst (wt% is based on per gram of feedstock taken) was added to the reaction mixture and the reaction mass was uniformly stirred for 10 min at an optimized temperature of 120 ^{o}C and optimum stirring speed of 450 rpm. The reaction time was about 1 h for 100 % epoxidation of canola oil and is 30 min for the 100 % conversion of canola biodiesel to epoxidized canola biodiesel. After the complete epoxidation reaction, the products were extracted using ethyl acetate, and the organic phase was washed with brine solution, and the solvent was evaporated under reduced pressure using a rotatory evaporator. ^{1}H NMR was used to confirm the product formation.

5.3.7.3 Preparation of vicinal di-O-acetylated products (biolubricants)

The conversion of epoxidized canola oil and epoxidized canola biodiesel to its corresponding vicinal di-O-acetylated derivatives (Figures 4.1 and 4.2) was performed using the optimum process conditions as follows: epoxide to acetic anhydride molar ratio 1:2, reaction temperature 120 ^{o}C, stirring speed 450 rpm, 10% MoO_3/Al_2O_3 as catalyst, and a catalyst loading of 12 wt% per gram of feedstock. For complete conversion of epoxide to vicinal di-O-acetylated product it took around 5 h for epoxidized canola oil, and 4 h for epoxidized biodiesel. The products were extracted using ethyl acetate and then treated with saturated aqueous sodium bicarbonate solution to neutralize the acids in the reaction mixture. Finally, ethyl acetate was removed under reduced pressure using a rotatory evaporator. The ^{1}H NMR spectra confirm a complete conversion of epoxidized canola oil and epoxidized canola biodiesel into their corresponding vicinal di-O-acetylated derivatives.

5.3.8 Physicochemical characterization of canola oil based biolubricants

The ASTM and AOCS standard test methods applied to characterize the prepared biolubricants were already discussed in Chapter 2, Section 2.3.6.

5.4 Results and discussion

5.4.1 Catalyst screening on the model compounds

Since glyceryl trioleate is a major component (~65%) in the canola oil, it was considered as a model compound for the catalyst screening tests (Przybylski et al. 2011). Group VI metal

oxides supported on the aluminum oxide such as 5 wt% Cr_2O_3/Al_2O_3, 5 wt% MoO_3/Al_2O_3, and 5 wt% WO_3/Al_2O_3 were tested for their activity on the epoxidation of glyceryl trioleate, and epoxide ring opening to produce vicinal di-O-acetylated glyceryl trioleate. MoO_3/Al_2O_3 showed higher activity for the epoxidation reaction compared to Cr_2O_3/Al_2O_3 and WO_3/Al_2O_3. 100% conversion of glyceryl trioleate to epoxidized glyceryl trioleate was achieved at the following reaction conditions: unsaturation in the glyceryl trioleate to tert-butyl hydroperoxide molar ratio (1:2), 5 wt% MoO_3/Al_2O_3 as catalyst, reaction temperature 100 ^oC, stirring speed 450 rpm, catalyst loading of 10 wt% per gram of glyceryl trioleate, and reaction time for 5 h. Using the similar reaction conditions, epoxidation was carried out without the catalyst and only Al_2O_3, but no epoxidized products were formed. Also, from ^1H NMR it was observed that the percentage decomposition of tert-butyl hydroperoxide is high over MoO_3/Al_2O_3 followed by Cr_2O_3/Al_2O_3 and WO_3/Al_2O_3. Hence, Mo was found to be most suitable and active catalyst for the epoxidation of glyceryl trioleate. The role of Mo in catalyzing epoxidation reactions is also documented in the literature (Lathi et al. 2007). The product was extracted using ethyl acetate and the solvent was removed under a reduced pressure using a rotatory evaporator to obtain epoxidized glyceryl trioleate.

The conversion of epoxidized glyceryl trioleate to its corresponding vicinal di-O-acetylated product was carried out at the following process conditions: epoxide to acetic anhydride molar ratio (1:3), 10 wt% catalyst loading per gram of epoxidized canola oil, stirring speed 450 rpm, reaction temperature 120 ^oC, and reaction time 5 h. At these reaction conditions, 11.1% epoxide conversion was observed with no catalyst, 29.4% conversion with Al_2O_3 as a catalyst, 28.5% with 5 wt% Cr_2O_3/Al_2O_3, 46.9% with 5 wt% WO_3/Al_2O_3, and 76% with 5 wt% MoO_3/Al_2O_3 catalyst (Figure 5.3). MoO_3/Al_2O_3 and WO_3/Al_2O_3 promoted high epoxide conversion to vicinal di-O-acetylation at the above reaction conditions. Since MoO_3/Al_2O_3 was found more active compared to other metal oxides, it was considered for the optimization of process parameters to synthesize biolubricants from the canola oil and canola biodiesel. The formation of epoxidized glyceryl trioleate and vicinal di-O-acetylated glyceryl trioleate was confirmed by ^1H NMR and mass spectrometry. A mass value of 932.76 for epoxidized glyceryl trioleate and 1238.84 for vicinal di-O-acetylated glyceryl trioleate confirmed the desired product formation. MoO_3/Al_2O_3 also catalyzed 100% conversion of epoxidized methyl oleate to vicinal di-O-acetylated product at the same reaction conditions.

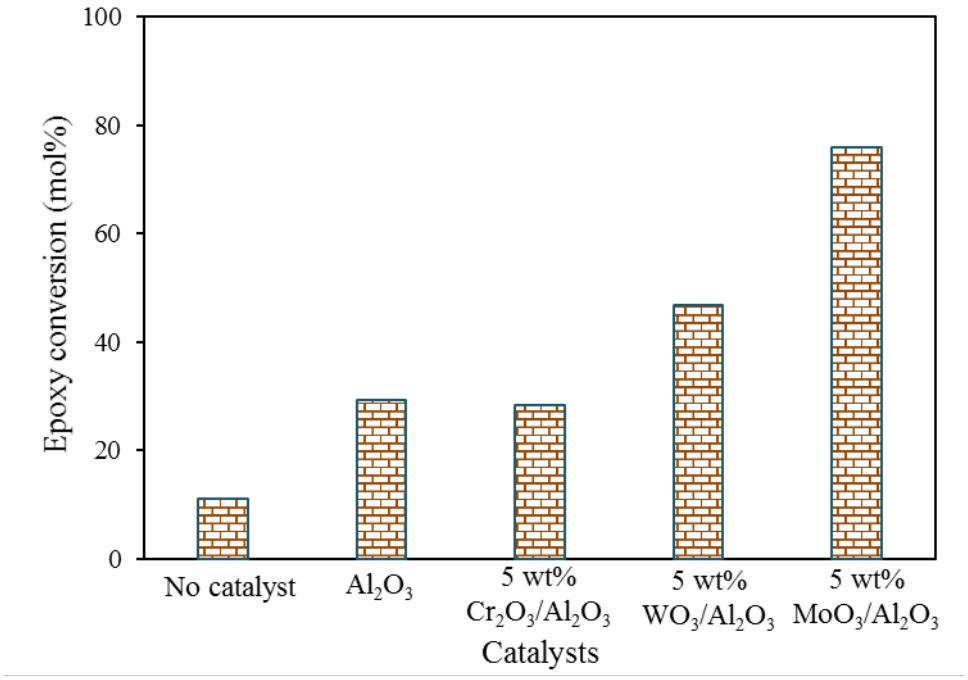

Figure 5.3 Catalyst screening tests for the conversion of epoxidized glyceryl trioleate to vicinal di-O-acetylated glyceryl trioleate.

5.4.2 Characterization of MoO_3/Al_2O_3 catalyst

The specific surface area and the pore size distributions of the support and the catalysts are shown in Table 5.3. The BET surface area of the support was found to decrease with an increase in the loading of molybdenum oxide. The nitrogen adsorption/desorption isotherms of the prepared catalysts showed type IV characteristic with H1 type hysteresis loop indicating that catalyst samples are mesoporous in nature (Figure 5.4) (Badoga et al. 2014). There is no considerable change observed in the pore volume and pore diameter of the catalysts after calcining at 550 ^{o}C. This indicates that the prepared support $Al(OH)_3$ is stable, and the applied calcination temperature is sufficient to retain the pore size distributions of the catalysts. This is one of the important reasons for using prepared $Al(OH)_3$ as a support than commercially available γ-Al_2O_3. It was anticipated that the hydroxyl groups in the $Al(OH)_3$ will provide an adequate surface for the metal-support interactions thus minimizing the pore blockage as compared to commercial γ-Al_2O_3 which is already calcined at a higher temperature.

Table 5.3 Textural properties of the support and catalysts, and CO chemisorption analysis of MoO_3/Al_2O_3 with different metal loadings

Sample	Surface area (m^2/g)	Pore volume (cm^3/g)	Pore diameter (nm)	Metal dispersion (%)
$Al(OH)_3$	418	0.3	3.6	-
5% MoO_3/ Al_2O_3	366	0.4	3.7	5.2
10% MoO_3/ Al_2O_3	340	0.4	3.7	6.3
15% MoO_3/ Al_2O_3	296	0.3	3.7	6.4

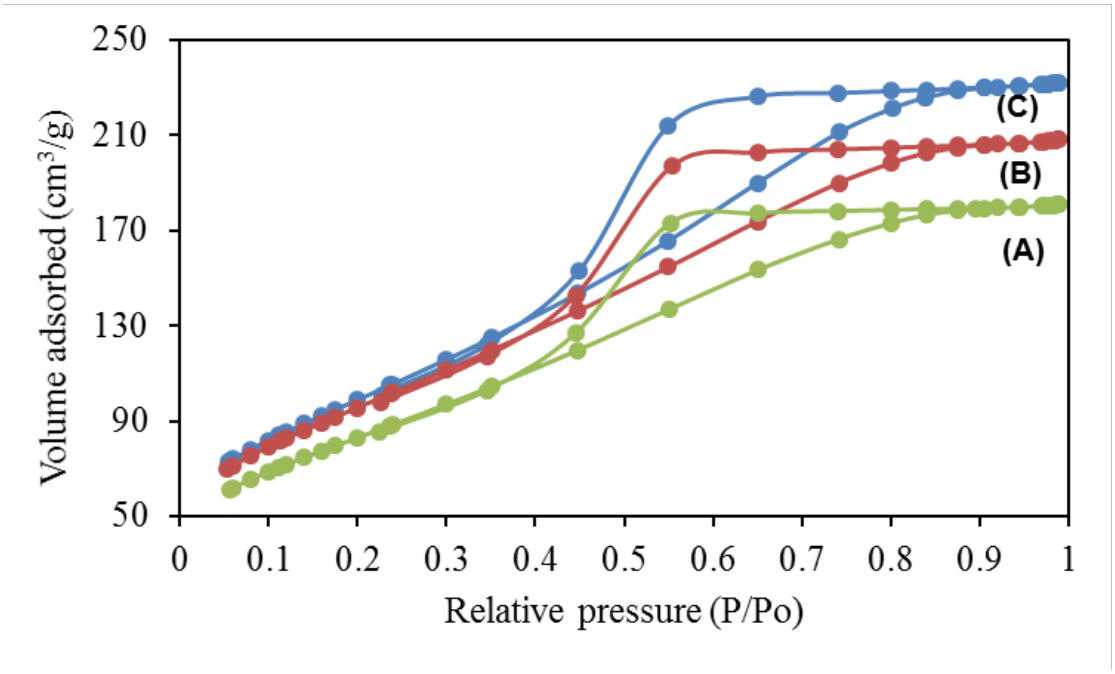

Figure 5.4 Nitrogen adsorption-desorption isotherms (A) 5 wt% MoO_3/Al_2O_3, (B) 10 wt% MoO_3/Al_2O_3, and (C) 15 wt% MoO_3/Al_2O_3.

The CO chemisorption analysis (Table 5.3) showed 5.2, 6.3 and 6.4% molybdenum dispersion in 5, 10 and 15 wt% MoO_3/Al_2O_3, respectively. The crystallite size was found 24.5 nm for 5 wt% MoO_3/Al_2O_3, 20.4 nm for 10 wt% MoO_3/Al_2O_3 and 19.9 nm for 15 wt% MoO_3/Al_2O_3. The increase in the molybdenum loading showed a decrease in the crystallite size.

The ICP quantitative analysis showed 5% of molybdenum in 5 wt% MoO_3/Al_2O_3, 11% in 10 wt% MoO_3/Al_2O_3, and 15% in 15 wt% MoO_3/Al_2O_3 catalyst samples. These values indicate that the required amount of $(NH_4)_6Mo_7O_{27}\cdot 4H_2O$ precursor was treated with the $Al(OH)_3$ support to obtain the desired catalysts as mentioned above. The X-ray diffraction (XRD) patterns of the prepared catalysts are shown in Figure 5.5. The diffractions from the crystal planes (311), (222), (400) and (440) in all the catalyst samples at 2Θ = 37.5, 40, 46, and 67°, respectively, were attributed to γ-Al_2O_3 (Castro et al. 2012). This indicates that the support $Al(OH)_3$ was changed to γ-Al_2O_3 at the applied calcination temperature. The XRD patterns of 5 wt% MoO_3/Al_2O_3 were found similar to the patterns of γ-Al_2O_3 indicating that molybdenum oxide is well dispersed. In the case of 10 wt% and 15 wt% molybdenum loading, low intensity peaks between 2Θ = 20 – 30° were observed due to the diffractions from $Al_2MoO_3O_{12}$ crystals present in the samples (Kitano et al. 2013).

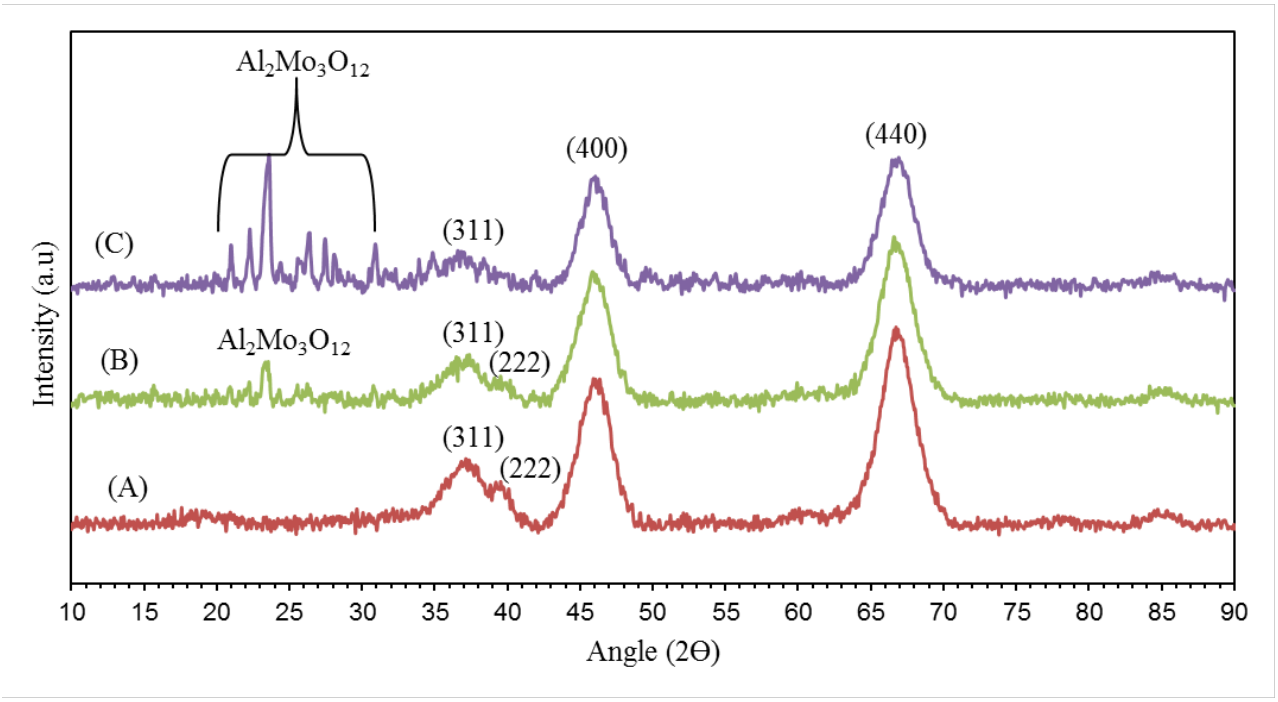

Figure 5.5 X-ray diffraction patterns of (A) 5 wt% MoO_3/Al_2O_3, (B) 10 wt% MoO_3/Al_2O_3, and (C) 15 wt% MoO_3/Al_2O_3.

The Raman spectra of 5 – 15 wt% MoO_3/Al_2O_3 catalysts are shown in Figure 5.6. For all molybdenum oxide loading, the high intensity peak observed at ~ 970 cm^{-1} corresponds to Mo=O stretching and low intensity peak at ~ 350 cm^{-1} is due to Mo=O bending vibrations of surface

molybdate species. The broad band identified at ~ 850 cm^{-1} shows increasing intensity at higher molybdenum oxide loading which is due to Mo-O-Mo asymmetric stretching modes (second surface molybdate species). The low intensity peaks at 110, 220, and 370 cm^{-1} indicate the presence of MoO_3 particles on the dehydrated alumina surface (Vuurmant et al. 1992). Raman spectra also confirm the presence of molybdenum oxide species dispersed on the alumina surface.

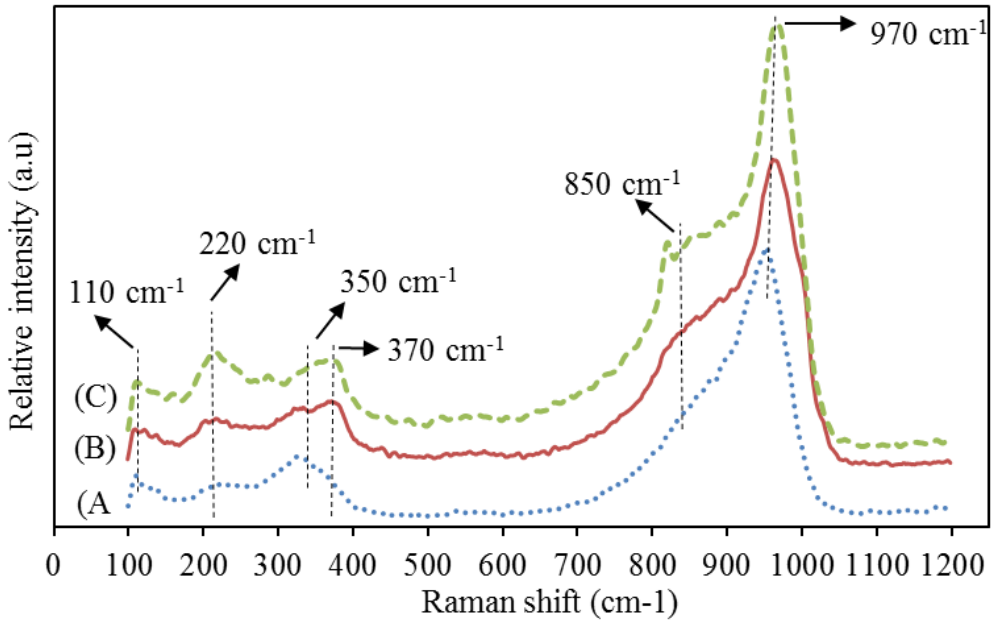

Figure 5.6 Raman spectra of (A) 5 wt% MoO_3/Al_2O_3, (B) 10 wt% MoO_3/Al_2O_3, and (C) 15 wt% MoO_3/Al_2O_3.

The pyridine adsorbed infrared (IR) spectra of the calcined catalysts showed four distinct peaks at 1445, 1490, 1540 and 1630 cm^{-1}, respectively (Figure 5.7). The infrared transmittance bands at 1540 and 1630 cm^{-1} are due to the pyridinium ion (PyH^+) which infer the existence of Bronsted acid type sites on the MoO_3/Al_2O_3 catalyst surface. This Bronsted acidity could be due to the presence of Mo-OH, Mo-OH-Mo, and Mo-OH-Al. Furthermore, the transmittance band at 1445 cm^{-1} corresponds to pyridine coordinated (PyL) to Lewis acid sites in MoO_3/Al_2O_3, and the transmittance band at 1490 cm^{-1} was due to the adsorption of pyridine on both acidic sites on the catalyst surface (Badoga et al. 2014; Kitano et al. 2013). The pyridine IR analysis confirms the presence of Lewis and Bronsted acid sites on the catalyst surface for all the metal loadings which play important role in favoring epoxidation and epoxide ring open by nucleophilic addition of acetate group (di-O-acetylation reaction) (Satyarthi et al. 2011; Somidi et al. 2015).

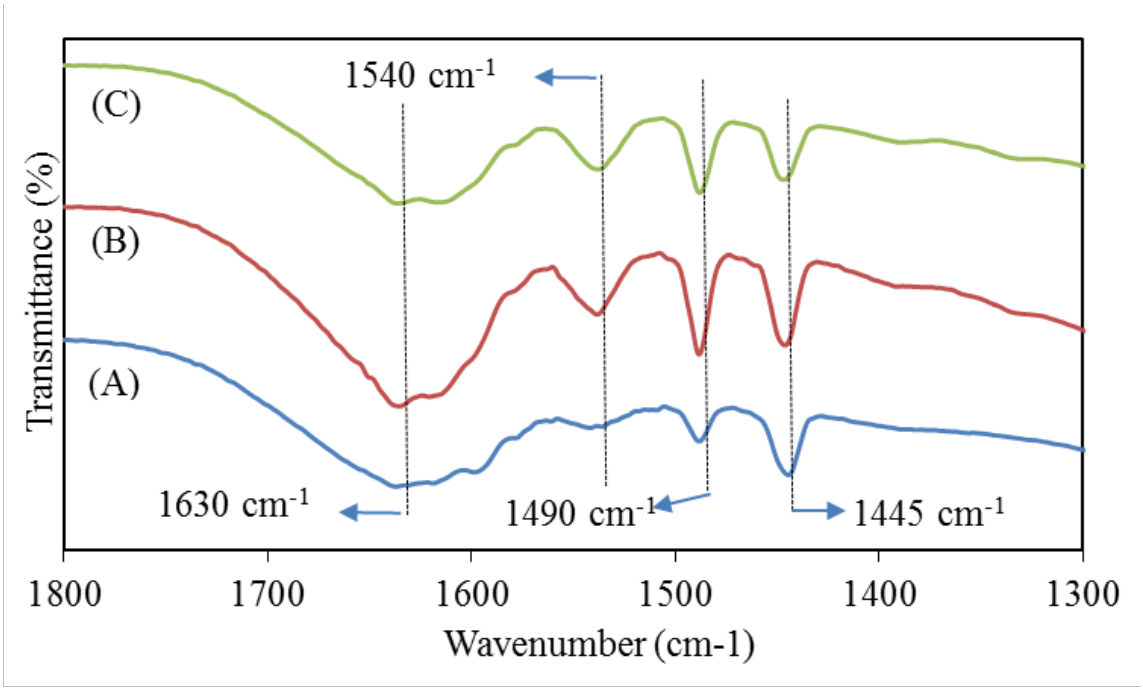

Figure 5.7 Pyridine adsorbed infrared spectra (IR) of (A) 5 wt% MoO_3/Al_2O_3, (B) 10 wt% MoO_3/Al_2O_3, and (C) 15 wt% MoO_3/Al_2O_3.

The distribution of acidic sites among 5, 10 and 15 wt% MoO_3/Al_2O_3 catalyst samples were investigated by ammonia temperature programmed desorption analysis. Figure 5.8 shows distinct ammonia desorption peaks of the catalysts between temperatures 90 - 550 ^oC and Table 5.4 illustrates the amount of ammonia desorbed by each catalyst sample at weak acidic (<300 ^oC), moderately acidic (300 to 450 ^oC) and strong acidic (> 450 ^oC) strength regions. There are no major differences found in the overall surface acidity of all the three catalyst samples. This could be due to very similar metal dispersion that is evident from CO chemisorption analysis (Table 5.3). However, from Table 5.4 it can be observed that the acidic site distributions among the catalysts are different. 5 and 15 wt% MoO_3/Al_2O_3 catalysts exhibited high surface acidity in the weak acidic strength region. Literature report suggests that high surface acidity of MoO_3/Al_2O_3 in weak acid strength region renders high selectivity for epoxidation reactions (Satyarthi et al. 2011). Hence, these catalysts were expected to give higher unsaturation conversions to epoxide derivatives. Furthermore, the metal support interactions in 10 wt% MoO_3/Al_2O_3 catalyst resulted in less surface acidity in weak acid strength region and was found to have high acidity in strong acid strength region which is required for nucleophilic addition reactions.

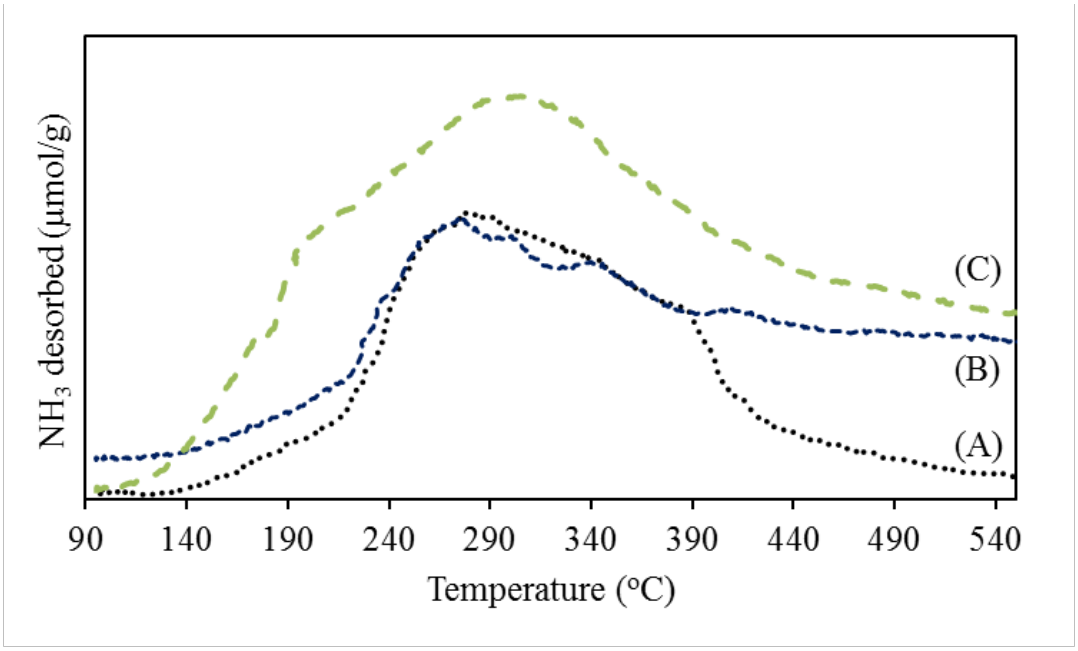

Figure 5.8 NH_3-temperature programmed desorption of (A) 5 wt% MoO_3/Al_2O_3, (B) 10 wt% MoO_3/Al_2O_3, and (C) 15 wt% MoO_3/Al_2O_3.

Table 5.4 NH_3-temperature programmed desorption of MoO_3/Al_2O_3 at different temperatures

Temperature (°C)	NH_3-desorption (µmol/g)		
	5% MoO_3/Al_2O_3	10% MoO_3/Al_2O_3	15% MoO_3/Al_2O_3
< 300	562	294	692
300-450	95	93	-
> 450	-	200	-
Total acidity	657	587	692

5.4.3 RSM optimization of process parameters for the epoxidation of canola oil

The Central Composite Design scheme (Table 5.5) was designed based on four process parameters and each parameter having three levels. As per the CCD scheme, 27 experiments were performed to optimize the process variables for the epoxidation of canola oil. The goal of this study was to maximize the conversion of unsaturated groups in the canola oil to its epoxide derivative. Tables 5.1 and 5.5 illustrate the selected process parameters (chosen symbols in parenthesis) such as: temperature (X_1), metal loading (X_2), unsaturation in the canola oil to tert-

butyl hydroperoxide molar ratio (X_3) and catalyst loading (X_4), coded levels of each factor (lowest, centre and highest), and responses (percentage unsaturation conversion in the canola oil after 4 h). Based on the experimental responses (Table 5.5), a quadratic model for the response surface was developed as shown in equation 5.5.

$$U = -275.5 + 4.29\,X_1 + 11.9\,X_2 + 71.7\,X_3 + 0.96\,X_4 - 0.01X_1^2 - 0.26\,X_2^2 - 11.25\,X_3^2 - 0.10\,X_4^2 - 0.05\,X_1X_2 - 0.08\,X_1X_3 - 0.005\,X_1X_4 - 0.66\,X_2X_3 + 0.03\,X_2X_4 + 0.38\,X_3X_4 \quad (5.5)$$

where U is the percentage unsaturation conversion in the canola oil in 4 h reaction time as calculated from ^{1}H NMR. The analysis of variance of the surface quadratic model was performed as per the equation 5.5 and the individual coefficients were summarized in Table 5.6. The significance or importance of a process variable in the epoxidation reaction was determined based on the magnitude of obtained F and P-values. Greater the magnitude of F-value of a process variable, greater would be its effect on the overall response. Similarly, smaller the P-value ($P < 0.05$), greater would be its importance to the response characteristic (Borugadda et al. 2015). From Table 5.6, based on the F-value (25.37) and the P-value (<0.0001) of the model, it is clear that the aforementioned quadratic model is highly significant. Also, the regression coefficient value (R^2) was found to be 0.97 which reveals that the obtained surface model is successful in interpreting the variance of percentage unsaturation conversion in the canola oil by 97%. Furthermore, the P-values of the process variables shown in Table 5.6 infers that temperature (X_1), metal loading (X_2), tert-butyl hydroperoxide molar ratio (X_3), and quadratic and cross effects of process variables such as X_1^2, X_2^2, X_3^2 and X_1 X_2 are highly significant ($P < 0.05$) for the epoxidation reaction. The catalyst loading (X_4) was found to be insignificant in its linear, quadratic and cross effect forms for the epoxidation reaction.

Table 5.5 Central composite design matrix for epoxidation of canola oil reaction.

Run	Process parameters in coded units				Process parameters in natural units				Unsaturation conversion (mol %)
	X_1	X_2	X_3	X_4	X_1	X_2	X_3	X_4	Reaction time (4h)
1	-1	-1	0	0	60	5	2	8	39.8
2	0	0	0	0	90	10	2	8	100
3	0	0	+1	-1	90	10	3	4	100
4	0	0	0	0	90	10	2	8	100
5	+1	0	0	+1	120	10	2	12	100
6	0	+1	+1	0	90	15	3	8	100
7	+1	0	+1	0	120	10	3	8	100
8	-1	0	0	+1	60	10	2	12	68.5
9	0	-1	+1	0	90	5	3	8	100
10	-1	0	+1	0	60	10	3	8	79.7
11	0	+1	0	-1	90	15	2	4	100
12	+1	0	-1	0	120	10	1	8	73.8
13	0	-1	-1	0	90	5	1	8	58.8
14	-1	0	-1	0	60	10	1	8	43.5
15	+1	0	0	-1	120	10	2	4	100
16	0	0	-1	+1	90	10	1	12	68.8
17	0	+1	-1	0	90	15	1	8	72
18	+1	-1	0	0	120	5	2	8	100
19	0	-1	0	+1	90	5	2	12	83.4
20	-1	0	0	-1	60	10	2	4	66.1
21	+1	+1	0	0	120	15	2	8	100
22	-1	+1	0	0	60	15	2	8	69.3
23	0	-1	0	-1	90	5	2	4	86.01
24	0	0	+1	+1	90	10	3	12	100
25	0	+1	0	+1	90	15	2	12	100
26	0	0	-1	-1	90	10	1	4	74.9
27	0	0	0	0	90	10	2	8	100

Table 5.6 Analysis of Variance for (ANOVA) response surface quadratic model (epoxidation of canola oil reaction)

Source	Degrees of freedom (DF)	Sum of squares	Mean squares	F-values	P-values
Model	14	8864.69	633.19	25.37	0.000
X_1	1	3567.30	3567.30	142.91	0.000
X_2	1	447.62	447.62	17.93	0.001
X_3	1	2942.20	2942.20	117.87	0.000
X_4	1	3.32	3.32	0.13	0.722
X_1^2	1	1216.79	1216.79	48.75	0.000
X_2^2	1	227.30	675.55	27.06	0.011
X_3^2	1	675.55	675.55	27.06	0.000
X_4^2	1	15.93	15.93	0.64	0.44
X_1X_2	1	217.56	217.56	8.72	0.012
X_1X_3	1	25	25	1	0.337
X_1X_4	1	1.44	1.44	0.06	0.814
X_2X_3	1	43.56	43.56	1.75	0.211
X_2X_4	1	1.70	1.70	0.07	0.798
X_3X_4	1	9.30	9.30	0.37	0.553
Error	12	299.55	24.96		
Lack-of-it	10	299.55	29.95		
Pure error	2	0	0		
Total	26	9164.24			

$R^2 = 0.97$; $R_{Adj}^2 = 0.93$.

The main effect plots shown in Figure 5.9 show that the unsaturation conversion in the canola oil increases with an increase in temperature, metal loading, and tert-butyl hydroperoxide molar ratio. The increase in the catalyst loading from 4 to 12 wt% showed insignificant behaviour on the overall response characteristic. Considering the trend in the main effect plots and to locate the optimized process conditions in the conversion of unsaturated groups in the canola oil, a two-dimensional counter plot was generated by keeping temperature at 120 ^oC and metal loading at 15

wt% to optimize two other process parameters with minimum catalyst loading and tert-butyl hydroperoxide molar ratio (Figure 5.10). The important objective behind minimizing the aforementioned process parameters is to make the process economical and environmentally friendly. Also, excess usage of tert-butyl hydroperoxide may result in tedious aqueous work-up procedures to extract the products. The counter plot shown in Figure 5.10 indicates that more than 96% unsaturation conversion is achieved in 4 h reaction time by maintaining the tert-butyl hydroperoxide molar ratio between 2.1 to 2.75, and catalyst loading in the range between 4 to 12 wt%. Based on the above study, the optimum reaction conditions selected for the complete epoxidation of canola oil are as follows: temperature 120 ^{o}C, molybdenum loading 15 wt% on the support, unsaturation in the canola oil to tert-butyl hydroperoxide molar ratio (1:2.25), catalyst loading 5 wt% per gram of canola oil, and a stirring speed of 450 rpm. At optimum reaction conditions, a 100% conversion of unsaturated groups in the canola oil to its epoxide derivative was achieved in 1 h, and the conversion remained constant without any epoxide ring opening until 4 h (observed only up to 4 h). The experiment was repeated five times at the aforementioned optimum conditions and 100% conversion was achieved in each time in 1 h. The mass values of m/z 932.7, 946.73, 960.71, 974.72, and 988.72 were found after complete epoxidation of canola oil which confirm the formation of the desired products.

5.4.4 RSM optimization of process parameters for the preparation of canola oil biolubricant

Similar matrix of CCD scheme (Table 5.7) with 27 experimental runs was chosen to optimize the process parameters for the preparation of biolubricant from canola oil (epoxide ring opening and vicinal di-O-acetylation reaction). The selected process variables (with symbols) and their levels are shown in Table 5.2. The percentage of epoxide conversion obtained in 4 h reaction time at different experimental conditions are measured by ^{1}H NMR and is shown in Table 5.7. Among all the runs, the epoxide conversion obtained at experimental run 5 was found to be the highest (97.2%) in 4 h reaction time (Table 5.7). Since the objective of this study is to achieve maximum epoxide conversion, the process conditions used in the experimental run 5 were considered as optimum. A 100% epoxide conversion to vicinal di-O-acetylation was achieved in 5 h. Hence, the optimum process conditions for the preparation of canola oil biolubricant are as follows: temperature (120 ^{o}C), epoxide to acetic anhydride molar ratio (1:2), Mo loading (10 wt%), catalyst loading of 12 wt% per gram of epoxidized canola oil taken, speed of agitation (450 rpm),

and the reaction time for 5 h. The formation of vicinal di-O-acetylated products was confirmed by ^{1}H NMR and electron spray mass spectroscopy. The mass distributions were found m/z 1238.85, 1252.84, 1266.84, 1354.8, and 1368.86 which support the formation of the desired products.

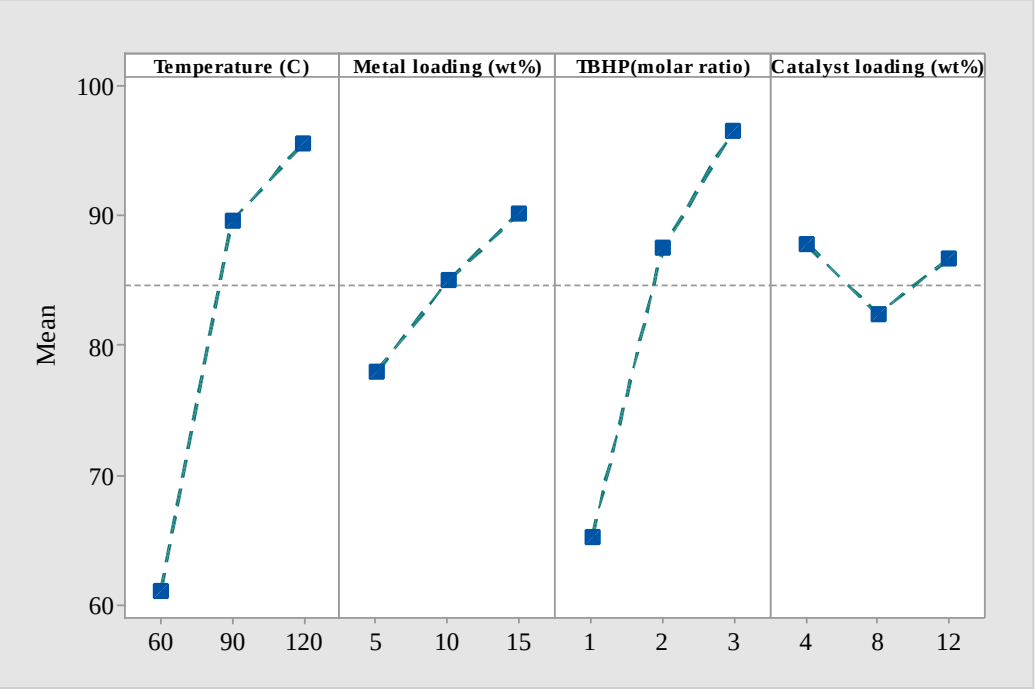

Figure 5.9 Main effect plots for the epoxidation of canola oil**.**

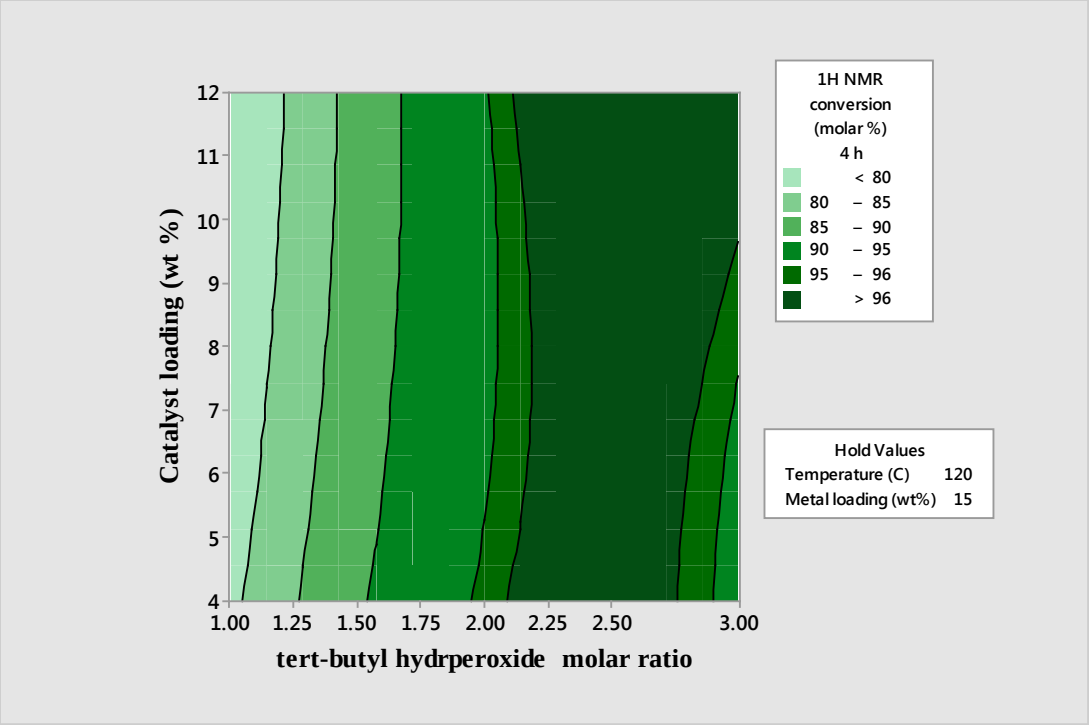

Figure 5.10 Counter plot between tert-butyl hydroperoxide molar ratio and catalyst loading for the epoxidation of canola oil.

Table 5.7 Central composite design matrix for the preparation canola oil biolubricant

Run	Process parameters in coded units				Process parameters in natural units				Epoxide conversion (mol %)
	Y_1	Y_2	Y_3	Y_4	Y_1	Y_2	Y_3	Y_4	After 5 h reaction time
1	-1	-1	0	0	60	5	2	8	0
2	0	0	0	0	90	10	2	8	14.9
3	0	0	+1	-1	90	10	3	4	14.9
4	0	0	0	0	90	10	2	8	20.3
5	+1	0	0	+1	120	10	2	12	97.2
6	0	+1	+1	0	90	15	3	8	30.3
7	+1	0	+1	0	120	10	3	8	88.8
8	-1	0	0	+1	60	10	2	12	0
9	0	-1	+1	0	90	5	3	8	13.9
10	-1	0	+1	0	60	10	3	8	0
11	0	+1	0	-1	90	15	2	4	14.6
12	+1	0	-1	0	120	10	1	8	67.3
13	0	-1	-1	0	90	5	1	8	4.3
14	-1	0	-1	0	60	10	1	8	0
15	+1	0	0	-1	120	10	2	4	74.5
16	0	0	-1	+1	90	10	1	12	12.5
17	0	+1	-1	0	90	15	1	8	7.6
18	+1	-1	0	0	120	5	2	8	87.9
19	0	-1	0	+1	90	5	2	12	26
20	-1	0	0	-1	60	10	2	4	0
21	+1	+1	0	0	120	15	2	8	90.1
22	-1	+1	0	0	60	15	2	8	0
23	0	-1	0	-1	90	5	2	4	6.3
24	0	0	+1	+1	90	10	3	12	52.6
25	0	+1	0	+1	90	15	2	12	30.3
26	0	0	-1	-1	90	10	1	4	9.1
27	0	0	0	0	90	10	2	8	20.6

Furthermore, the statistical analysis was undertaken to develop a model for the response surface, for understanding the effects of process variables on the formation of vicinal di-O-acetylated product and ANOVA analysis. Figure 5.11 shows the main effects of process variables. The temperature effect shows that no epoxide ring opening was observed up to 60 ^{o}C. The rate of epoxide ring opening was found to be very fast with an increase in the reaction temperature above 60 ^{o}C and the maximum conversions (> 75%) are obtained at 120 ^{o}C. The reaction temperature above 130 ^{o}C is not recommended as it was found that epoxidized oil tends to polymerize, and the rate of adsorption of acetic anhydride on the catalyst sites becomes very high leading to lower conversions and the deactivation of active sites (Somidi et al. 2015). Increase in the catalyst loading favoured high epoxide conversions due to the availability of more number of active sites on MoO_3/Al_2O_3. However, the metal loading above 10 wt% shows a decrease in the epoxide conversion. The rate of epoxide conversion increased with an increase in the acetic anhydride molar ratio up to 2 and further the conversion remained constant.

The response surface quadratic model obtained between the process parameters (Table 5.2) in all the forms and the response (E is the epoxide conversion in 4 h) for the epoxide ring opening and vicinal di-O-acetylation of canola oil is presented in equation 5.6. Table 5.8 shows ANOVA analysis of the model and the process parameters in linear, quadratic and cross effect forms. The results of ANOVA analysis show a low P-value (<0.0001), and a regression coefficient of 0.99 which indicate that the fitted model is highly significant. As per the model, temperature, MoO_3/Al_2O_3 catalyst loading, and acetic anhydride molar ratio are most significant parameters to be considered for the epoxide ring opening and vicinal di-O-acetylation reaction.

$$E = 178.1 - 4.085\,Y_1 - 0.08\,Y_2 - 23.6\,Y_3 - 8.59\,Y_4 + 0.026\,Y_1^2 - 0.029\,Y_2^2 - 1.98\,Y_3^2 + 0.16\,Y_4^2 + 0.0037\,Y_1Y_2 + 0.179\,Y_1Y_3 + 0.0473\,Y_1Y_4 + 0.66\,Y_2Y_3 - 0.05\,Y_2Y_4 + 2.14\,Y_3Y_4 \quad (5.6)$$

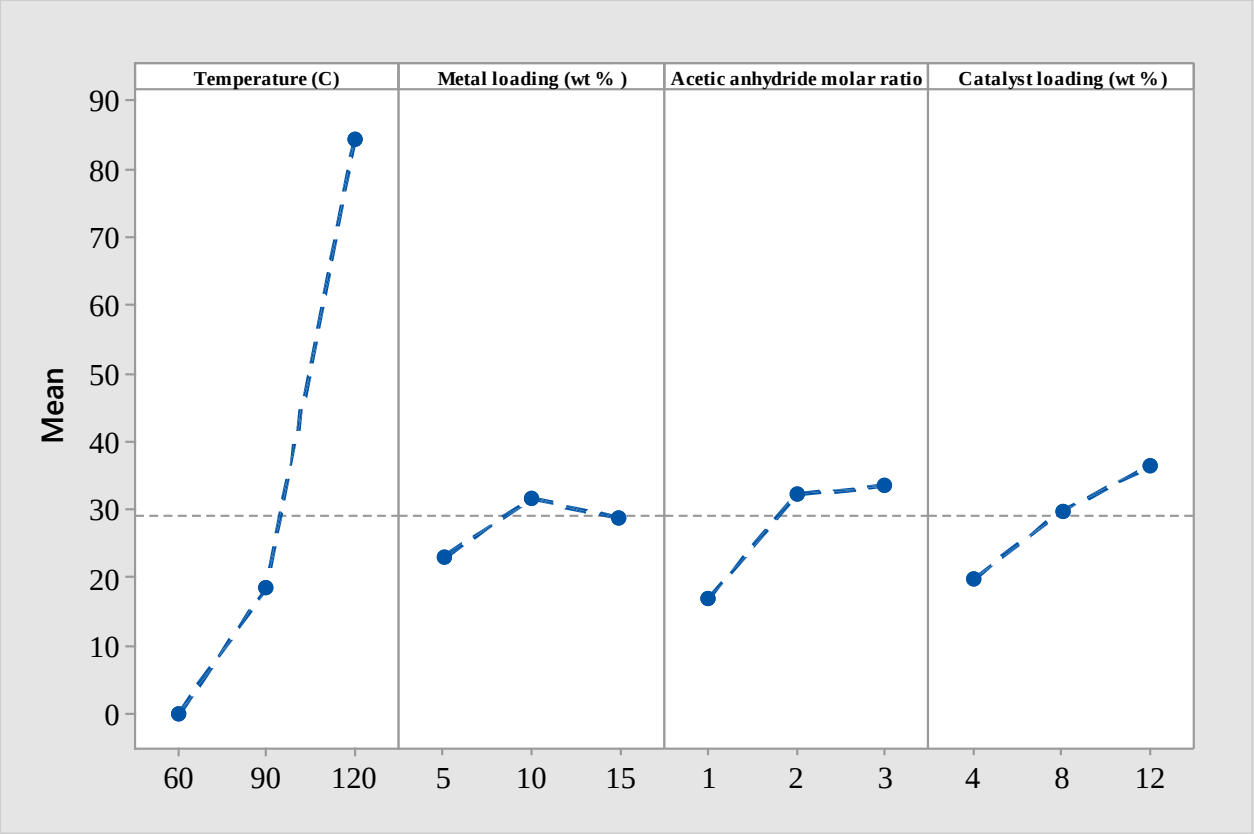

Figure 5.11 Main effect plots for the epoxide ring opening and vicinal di-O-acetylation of canola oil.

Table 5.8 Analysis of Variance for (ANOVA) response surface quadratic model (preparation of canola oil biolubricant)

Source	Degrees of freedom (DF)	Sum of squares	Mean squares	F-values	P-values
Model	14	27457.8	1961.3	66.26	0.000
Y_1	1	21319.5	21319.5	720.3	0.000
Y_2	1	99.2	99.2	3.4	0.092
Y_3	1	828.3	828.3	27.9	0.000
Y_4	1	820.1	820.1	27.7	0.000
Y_1^2	1	2966.3	2966.3	100.2	0.000
Y_2^2	1	2.8	2.8	0.1	0.762
Y_3^2	1	20.9	20.9	0.7	0.417
Y_4^2	1	36.3	36.3	1.2	0.290
Y_1Y_2	1	1.2	1.2	0.1	0.843
Y_1Y_3	1	115.6	115.6	3.9	0.072
Y_1Y_4	1	128.8	128.8	4.4	0.059
Y_2Y_3	1	42.9	42.9	1.5	0.252
Y_2Y_4	1	4.0	4.0	0.2	0.720
Y_3Y_4	1	294.1	294.1	9.9	0.008
Error	12	355.2	29.6		
Lack-of-it	10	334.6	33.5	3.3	0.258
Pure error	2	20.6	10.3		
Total	26	27813			

$R^2 = 0.99$; $R^2_{Adjusted} = 0.98$.

5.4.4.1 Interactions between significant parameters for maximum epoxide conversion

Figure 5.12 demonstrates the interaction between significant parameters such as temperature, acetic anhydride molar ratio and catalyst loading for epoxide conversion using MoO_3/Al_2O_3 catalyst. The results show that epoxide ring opening and vicinal di-O-acetylation reaction cannot be promoted at a temperature < 60 ^oC at any selected acetic anhydride molar ratio and catalyst loadings. From experimental observations, it was found that the reaction temperature

above 70 ^{o}C is favourable for vicinal di-O-acetylation reaction. Increase in the reaction temperature >70 ^{o}C activates epoxide moiety for the oxirane cleavage in the presence of a nucleophile and decreases the viscosity of the epoxidized oils which help in free flowing through the catalyst pores (Borugadda et al. 2015; Somidi et al. 2015). These observations are in accordance with the obtained experimental data which is shown in Table 5.7. The conversion of epoxide into its corresponding di-O-acetylated products was found to increase with an increase in the reaction temperature and the high conversions were noted at an optimum temperature of 120 ^{o}C. The effect of acetic anhydride molar ratio on the epoxide conversion with respect to temperature showed monotonic increment. This may be due to high oxirane cleavage at a higher acetic anhydride loadings. At 120 ^{o}C, the epoxide conversion was found constant using a molar ratio of acetic anhydride above 2. Hence, epoxide to acetic anhydride molar ratio 1: 2 was considered optimum loading. The interaction between the catalyst loading and temperature shows a significant trend. Higher catalyst loading promoted high epoxide conversion due to more availability of active sites. The epoxide conversion was found maximum at 120 ^{o}C with a catalyst loading of 12 wt %. Hence 12 wt% was considered optimum.

5.4.5 One-pot synthesis of canola oil biolubricant

From the process optimization studies, MoO_3/Al_2O_3 was found to be a promising catalyst for both epoxidation as well as vicinal di-O-acetylation reaction of canola oil. After epoxidation of canola oil, the reaction mixture consists of toluene, tert-butyl hydroperoxide, and tert-butyl alcohol. The epoxidized products were isolated from the reaction mixture using tedious solvent extraction process and further removal of solvent under reduced pressure using a rotatory evaporator. This results in the use of additional organic solvents that add to extra operations and cost to the process. Besides that fresh catalyst needs to be added for the conversion of epoxidized material to vicinal di-O-acetylated products. Considering these aspects, a one-pot process technology was developed for the preparation of canola oil biolubricant from canola oil in view of making the process: more economical by using less amount of catalyst loading, ecofriendly by eliminating solvent extractions and extra operations in the intermediate steps and to make the process amenable for easy scale-up for commercialization. The reaction scheme for the conversion of canola oil to canola biolubricant is shown in Figure 5.1. The experimental setup and the procedure employed for one-pot synthesis of canola oil biolubricant is presented in Figure 5.13

which involves epoxidation, distillation of solvents from the reaction mixture followed by addition of acetic anhydride.

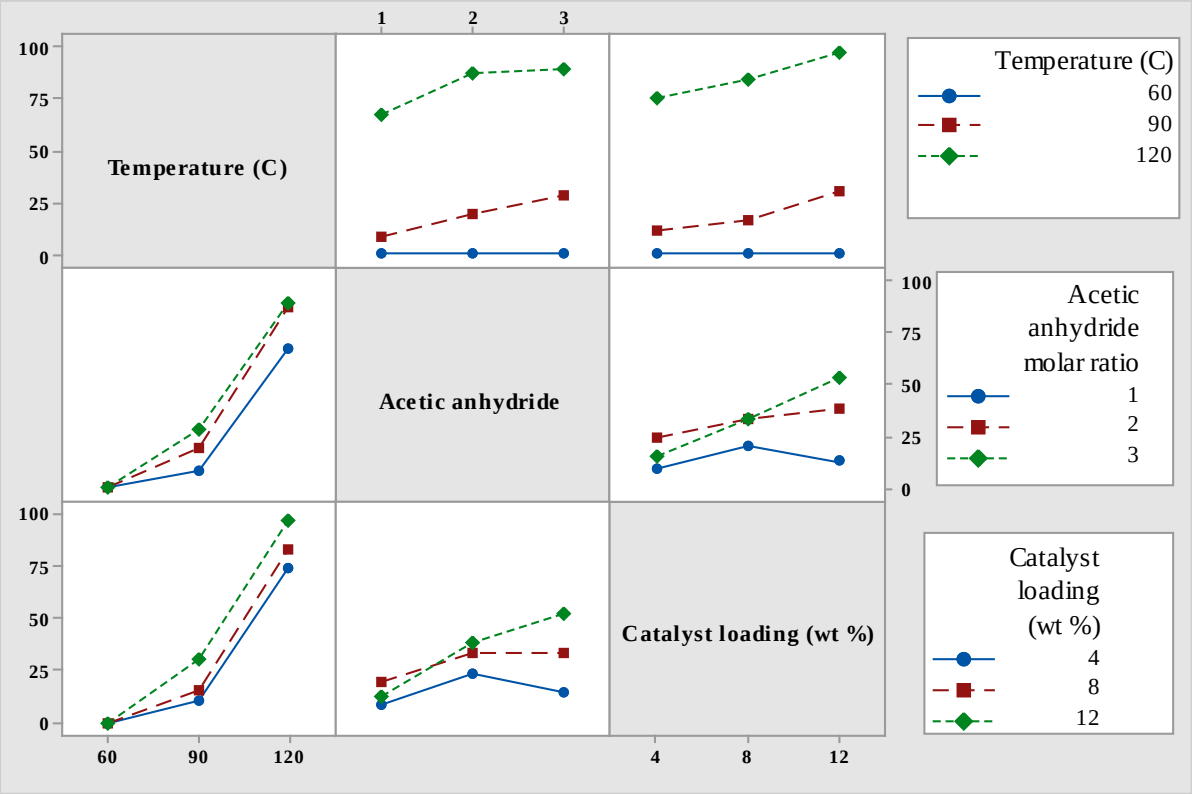

Figure 5.12 Interactions between significant parameters for the epoxide ring opening and vicinal di-O-acetylation reaction. (Temperature in ^{o}C).

For the one-step process, 10 wt% MoO_3/Al_2O_3 was used and the reaction was carried out at 120 ^{o}C which is the most favourable temperature for both epoxidation and vicinal di-O-acetylation reaction steps to achieve high conversions. Other optimum process conditions were chosen as follows: unsaturation in the canola oil to tert-butyl hydroperoxide molar ratio (1: 2.25), speed of agitation 450 rpm, 10 wt% MoO_3/Al_2O_3 as catalyst for both steps, 12 wt% of catalyst loading (per g of canola oil), and epoxide to acetic anhydride molar ratio (1:2). These conditions were selected based on the aforementioned RSM optimization studies performed individually for each reaction step. At these conditions, 100% unsaturation conversion in the canola oil to its epoxide derivative was achieved in 30 min. In the presence of a solvent, further reaction of epoxidized canola oil with acetic anhydride was very sluggish (conversion 72% in 24 h). Therefore the solvent was completely distilled off from the reaction mixture under reduced pressure at 120

^{o}C and acetic anhydride was added. A complete conversion of epoxide to the di-O-acetylated product was achieved in 5 h. The experiment was repeated in triplicate and the results were reproducible. In the presence of a solvent, the conversion of epoxide canola oil to its vicinal di-O-acetylated product was very slow, however, the reaction proceeded to completion in 5 h when the solvent was stripped off after epoxidation reaction.

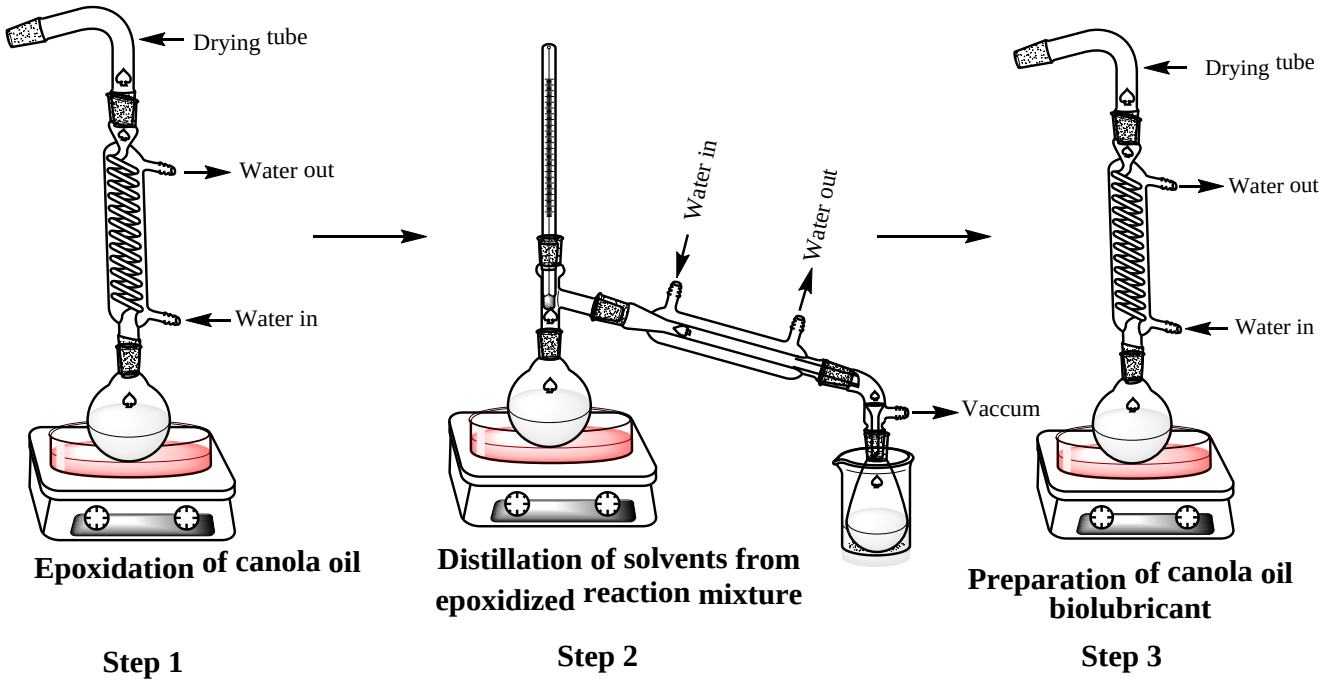

Figure 5.13 One-pot synthesis of canola oil biolubricant using 10 wt% MoO_3/Al_2O_3. **Step 1**: canola oil (0.5 g), TBHP in toluene (0.99 g), temperature (120 ^{o}C), speed of agitation (450 rpm), catalyst loading (0.06 g), reaction time (30 min). **Step 2**: temperature (120 ^{o}C), speed of agitation (450 rpm), and vacuum distillation of solvents. **Step 3**: acetic anhydride (0.44 g), speed of agitation (450 rpm) and reaction time (5 h).

The formation of epoxidized and vicinal di-O-acetylated products were confirmed by ^{1}H NMR and mass spectrometry for each batch. There was no indication of any additional products formed from any side reactions. The mass values were found similar to the products obtained using fresh 10 wt% MoO_3/Al_2O_3. ^{1}H NMR spectra of canola oil, epoxidized canola oil and vicinal di-O-acetylated canola oil (biolubricant) are shown in Figure 5.14. Table 5.9 illustrates the chemical shift of the assigned proton peaks in ^{1}H NMR spectra. A detailed explanation of these chemical shifts has already been illustrated in our published reports (Sharma et al. 2015; Somidi et al. 2014).

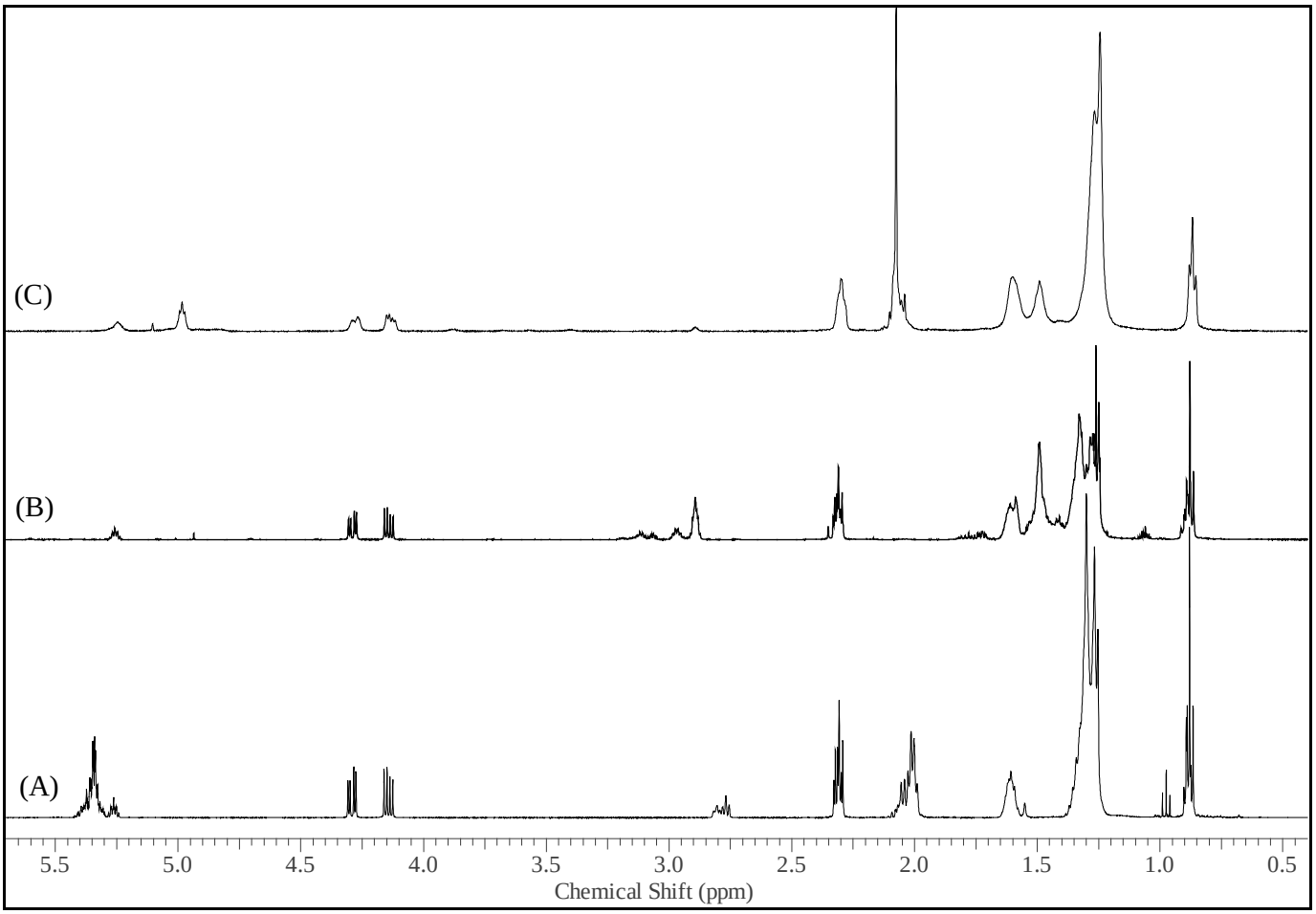

Figure 5.14 ^{1}H NMR spectra of (A) canola oil, (B) epoxidized canola oil, and (C) vicinal di-O-acetylated canola oil (biolubricant).

Table 5.9 Assignment of ^{1}H NMR chemical shifts in canola oil, epoxidized canola oil, and canola oil biolubricant

Type of protons	Chemical shift (δ) for each compound		
	Canola oil	Epoxidized canola oil	Canola oil biolubricant
-C**H₃** attached to terminal carbon	0.84 – 0.92 ppm	0.84 – 0.92 ppm	0.84 – 0.92 ppm
=CH-CH_2-C**H₃**	0.95 – 1.0 ppm	-	-
-CH_2 attached to fatty acid chain	1.2 – 1.4 ppm	1.2 – 1.55 ppm	1.2 – 1.55 ppm
β- C**H₂**	1.6 ppm	1.6 ppm	1.6 ppm
α- C**H₂**	2.3 ppm	2.3 ppm	2.3 ppm
=CH-C**H₂**-CH=	1.95 – 2.15 ppm	-	-
-C**H₂** of glycerol	4.25 – 4.32 ppm	4.25 – 4.32 ppm	4.25 – 4.32 ppm
-C**H** of glycerol	4.1 – 4.2 ppm	4.1 – 4.2 ppm	4.1 – 4.2 ppm
-C**H**=C**H**- unsaturation protons	5.29 – 5.43 ppm	-	-
-CHOCH- , protons attached to epoxide group	-	2.85 – 3.15 ppm	-
-C**H** protons of –$OCOCH_3$ after diacylation	-	-	5 ppm
-C**H₃** protons of –$OCOCH_3$ after diacylation	-	-	2.1 ppm

* $CDCl_3$ was used as solvent and its chemical shift reference taken is 7.26 ppm

5.4.6 MoO_3/Al_2O_3 catalytic activity for the preparation of biodiesel biolubricant

Unsaturated fatty acid methyl esters (canola biodiesel) obtained from the Miligan Biofuels Inc. (without the addition of antioxidants) was used as the starting raw material for the synthesis of biodiesel biolubricant. This material was characterized by ^{1}H NMR and electron spray mass spectrometry. Unsaturated protons in the canola biodiesel appear at a chemical shift δ 5.25 – 5.45 ppm and the mass spectrometry results reveal three major components in the canola biodiesel:

methyl oleate (~ 65%), methyl linoleate (~ 30%), and methyl linolenate (~ 4.8%). The optimum reaction conditions obtained from the conversion of canola oil to canola biolubricant were applied to prepare vicinal di-O-acetylated fatty acid methyl esters (biodiesel biolubricant).

In a two-step reaction process, a complete epoxidation of unsaturated fatty acid methyl esters was achieved in 30 min following the reaction condition as follows: canola biodiesel (0.5 g), tert-butyl hydroperoxide in toluene (4.4 M, 0.99 g) (1:2.25 molar ratio w.r.t canola biodiesel), 15 wt% MoO_3/Al_2O_3 (0.025 g) (5 wt% with respect to canola biodiesel), reaction temperature (120 ^oC) and the speed of agitation 450 rpm. In ^1H NMR spectra of epoxidized biodiesel, the absence of unsaturated protons at δ = 5.25 – 5.45 ppm and appearance of epoxide protons at δ 2.9 – 3.25 ppm reveal a complete conversion of canola oil to epoxide canola oil (Figure 5.15.B). Also, the mass spectrometry analysis showed three compounds: epoxidized methyl oleate (m/z 312.26), epoxidized methyl linoleate (m/z 326.23) and epoxidized methyl linolenate (m/z 340.23). The experiments were repeated in triplicate and were found to be reproducible as found from ^1H NMR and mass spectrometry results.

The catalytic activity of MoO_3/Al_2O_3 was tested for the epoxide ring opening and vicinal di-O-acetylation of epoxidized canola biodiesel. The optimum reaction conditions used are as follows: epoxide biodiesel (0.5 g), acetic anhydride (0.44 g, 1: 2 molar ratio), temperature 120 ^oC, 10 wt% MoO_3/Al_2O_3 catalyst (0.06 g) and speed of agitation 450 rpm. A complete epoxide conversion to vicinal di-O-acetylated product was achieved in 4 h. The absence of epoxide protons at δ 2.9 – 3.25 ppm in the ^1H NMR spectra of biodiesel biolubricant confirms 100% epoxide conversion and the appearance of new peaks at 2.1 ppm (CH_3 protons of –OCO$\underline{CH_3}$ group) and 5.0 ppm (CH proton of –$\underline{CH}$–$OCOCH_3$ group) reveals the formation of di-O-acetylated products (Figure 5.15.C). Also, the mass spectra data did not show any mass values corresponding to epoxidized biodiesel. The mass spectrometry analysis of biodiesel biolubricant at 100% epoxide conversion showed expected mass values m/z 414.28, 530.3, and 763.54.

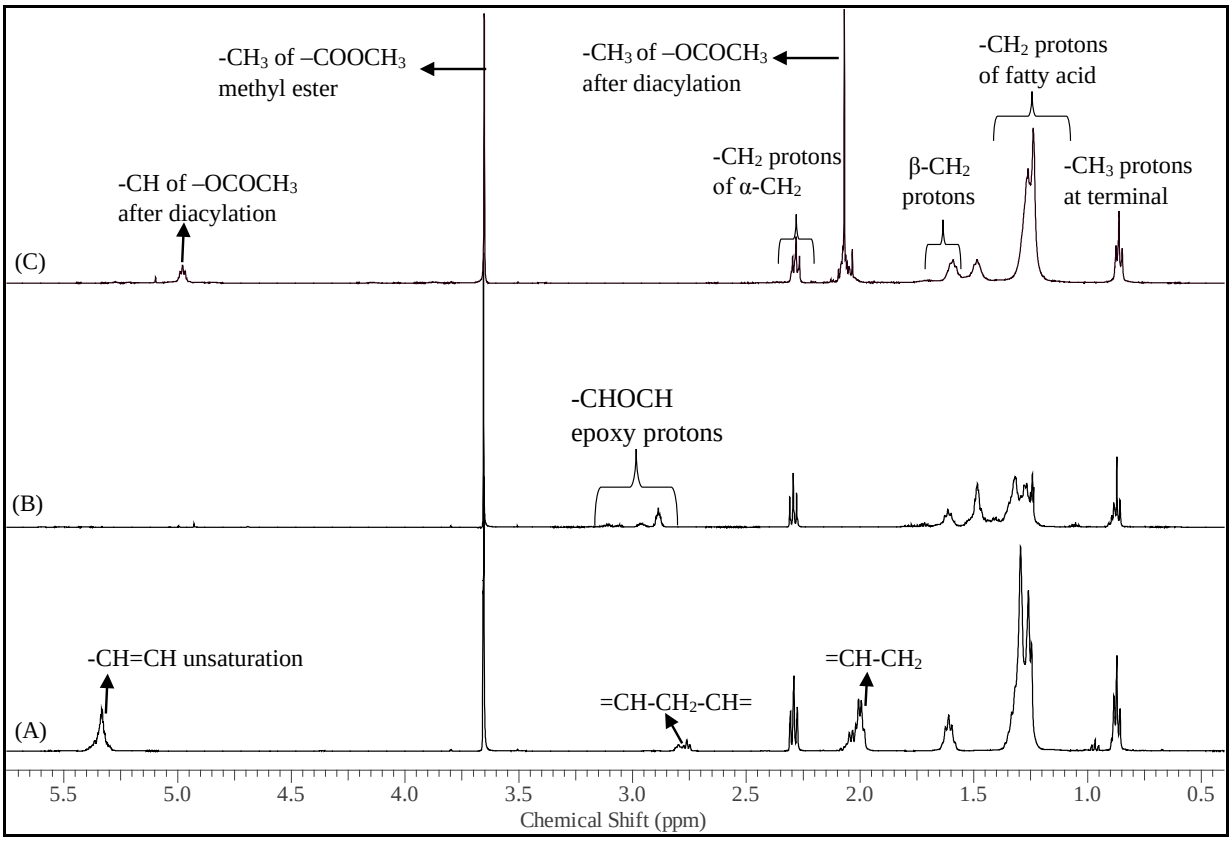

Figure 5.15 ^{1}H NMR spectra of (A) canola biodiesel, (B) epoxidized canola biodiesel, and (C) vicinal di-O-acetylated biodiesel (biodiesel biolubricant).

For one-pot reaction process, the same experimental conditions and reaction setup were used as described in the Figure 5.13. Figure 5.2 shows the reaction scheme involving the synthesis of biodiesel biolubricant from canola biodiesel. A 100% conversion of canola biodiesel to biodiesel biolubricant was obtained in the one-pot synthesis using 10 wt% MoO_3/Al_2O_3 as a catalyst. The reaction time for a complete epoxidation of canola biodiesel was found 15 min and is 4 h for vicinal di-O-acetylation reaction. The formation of vicinal di-O-acetylated product was confirmed by ^{1}H NMR and mass spectrometry. The experiments were repeated in triplicate and were reproducible. Hence, 10 wt% MoO_3/Al_2O_3 was also found to be successful for the one-pot synthesis of biodiesel biolubricant.

5.4.7 Catalyst reusability study

The reusability of 10 wt% MoO_3/Al_2O_3 catalyst was tested for the one-pot synthesis of canola oil biolubricant. After each run, MoO_3/Al_2O_3 catalyst was separated and treated with chloroform and ethyl acetate mixture to take out adsorbed oil in the catalyst pores. The catalyst was then dried for 12 h at 110 ºC for regeneration. The reusability studies were performed up to three runs using the regenerated catalyst. The catalyst exhibited a 100% unsaturation conversion to epoxide each time. For subsequent vicinal di-O-acetylation reaction, the percentage of epoxide conversion was found 98.3% for the first run, 97.1% for the second run, and the activity dropped to 65% in the third run. Strong adsorption of the acetic anhydride on the active sites of MoO_3/Al_2O_3 catalyst could be the primary reason for the subsequent catalyst deactivation (Somidi et al. 2014). Hence, 10 wt% MoO_3/Al_2O_3 can be reused for the preparation of biolubricants up to two times without addition of any fresh catalyst.

5.4.8 Evaluation and comparison of physicochemical properties of vicinal di-O-acetylated canola oil and vicinal di-O-acetylated canola biodiesel

5.4.8.1 Low Temperature Properties

The cold flow temperature properties of the biolubricants from canola oil (vicinal di-O-acetylated canola oil) and canola biodiesel (vicinal di-O-acetylated canola biodiesel) were represented by the cloud point and pour point. These properties of lubricants derived from vegetable oil are poor, hence, make it difficult to use in cold countries. It can be improved by reducing the aliphatic carbon chain length. Table 5.10 represents the low temperature properties of epoxidized canola oil, epoxidized biodiesel, biolubricant from canola oil, and biolubricant from canola biodiesel. The epoxidized canola oil and epoxidized canola biodiesel have the cloud points of 15 and 6 ºC, and the pour points of 9 and 0 ºC, respectively. It was found that cloud and pour point of epoxidized biodiesel are low as compared with epoxidized canola oil, which can be due to the presence of less number of aliphatic carbon atoms present in epoxidized biodiesel. Hence, an increase in the aliphatic carbon chain length reduced the low temperature properties. Also, these low temperature properties can be improved by adding the ester linkage in the epoxidized molecules which promote steric hindrance. The cloud points of biolubricant from canola oil, and biolubricant from canola biodiesel were found to be -3 and -12 ºC; while, pour points were -9 and

-18 ºC, respectively. Hence, it elucidates that biolubricant obtained from biodiesel has better low temperature properties as compared to biolubricant obtained from canola oil which can be due to the less steric hindrance. Hence, biolubricant from canola biodiesel is superior for low temperature applications and has better future prospects for the automotive industry as compared to biolubricant from canola oil.

Table 5.10 Low temperature properties of biolubricants

Entry	Product	Low temperature property	
		Cloud point (°C)	Pour point (°C)
1	Epoxidized canola oil	15	9
2	Epoxidized canola biodiesel	6	0
3	Biolubricant from canola oil	-3	-9
4	Biolubricant from canola biodiesel	-12	-18

5.4.8.2 Viscosity

The viscosity of the fluid defines the effectiveness of the lubricant to lubricate the contact surface of the metals. The kinematic viscosity of canola oil derived biolubricant and biodiesel derived biolubricant were measured at 40 °C and found to be 200 and 116 cSt, whereas, at 100 °C was found to be 80 and 19 cSt. The viscosity index for biolubricant from canola biodiesel was found to be 185 and is 435 for canola oil derived biolubricant. High viscous nature of canola oil biolubricant is because of the addition of ester linkage in the oil at the unsaturation. The increase in the viscosity is also attributed to the intramolecular hydrogen bonding of the ester linkages (Zaher et al. 2012). Canola oil derived biolubricant is highly viscous and can be used as a lubricant for high temperature, high load, and high speed operations like heavy machinery. However, biolubricant from canola biodiesel is less viscous as compared with biolubricant from canola oil. It might be because of less number of aliphatic carbon present in the biolubricant derived from canola biodiesel which creates less steric hindrance and fewer hydrogen bondings as compared with the biolubricant derived from canola oil. Therefore, biolubricant derived from biodiesel can be used as a lubricant for automobiles at low temperature. Hence, it can be anticipated that the biolubricant from biodiesel has better future prospects for the automobile sector.

5.4.8.3 Friction and Anti-Wear Properties

Lubricity testing was performed according to the ASTM D6079 and ASTM D7688 standard test methods. All the samples were tested twice and the average value is reported. The wear scar diameter of standard diesel sample was found to be 600 µm. With the addition of 1 % of canola oil biolubricant to the standard diesel sample, the diameter of the wear scar was found to reduce to 130 µm, while 1% of biolubricant derived from canola biodiesel integrated into the standard diesel sample showed a wear scar diameter of 95 µm. It was noticed that canola oil biolubricant resulted in more wear scar on steel test ball as compared with biolubricant from canola biodiesel. This can be due the presence of more steric hindrance and intramolecular hydrogen bonding present in the canola oil derived biolubricant which increases the viscosity and hence decreases the solubility in the standard diesel sample and resulted in more wear scar diameter (130 µm). Furthermore, a lower number of aliphatic carbon atoms is present in biodiesel derived biolubricant as compared with canola derived biolubricant which makes it less viscous and less non-polar, and hence increases the solubility in diesel fuel and resulted in less wear scar (95 µm). The better lubricity property of biodiesel derived biolubricant can also be explained by the presence of ester oxygen moieties in 1, 9, and 10 positions which are free of hydrogen bonding and help to reduce the friction by developing the anti-frictional film on metal surfaces (Dixit et al. 2012). Table 5.11 indicates that with the increase in lubricant content in pure diesel fuel the wear scar on the steel test ball is decreased.

Table 5.11 Wear scar diameter of biolubricants diluted in low lubricity diesel fuel

Biolubricant in pure diesel fuel (%)	Wear scar length (µm)	
	Biolubricant from canola oil	Biolubricant from biodiesel
1	130	95
2	125	90
5	120	86
10	115	81

5.4.8.4 Thermogravimetric (TGA) Analysis

Thermal stability of canola oil, epoxidized canola oil, canola derived biolubricant, biodiesel, epoxidized biodiesel and biodiesel derived biolubricant was studied by thermo gravimetric differential thermal analyzer (TG/DTA). The graphs of weight loss against temperature are shown in Figure 5.16. It is clear from the graph that canola oil, epoxidized canola oil and canola derived biolubricant are thermally stable below 305 °C. Maximum weight loss (90-95 %wt) was observed in all these three materials at the temperatures 460, 461 and 530 °C, respectively. However, canola biodiesel, epoxidized canola biodiesel, and biodiesel derived biolubricant are found to be thermally stable below the temperatures 305, 160 and 194 °C, respectively, and about 90-95 % weight loss was found for each sample at the temperatures 462, 251, 370 °C, respectively (Table 5.12). Hence, it is conclusive that canola biolubricant is thermally more stable as compared to biolubricant from canola biodiesel which can be due the presence of intra molecular hydrogen bonding. Thermogravimetric analysis (TGA) also confirms that canola biolubricant can be more useful for high temperature applications, whereas biodiesel biolubricant is useful for low temperature applications.

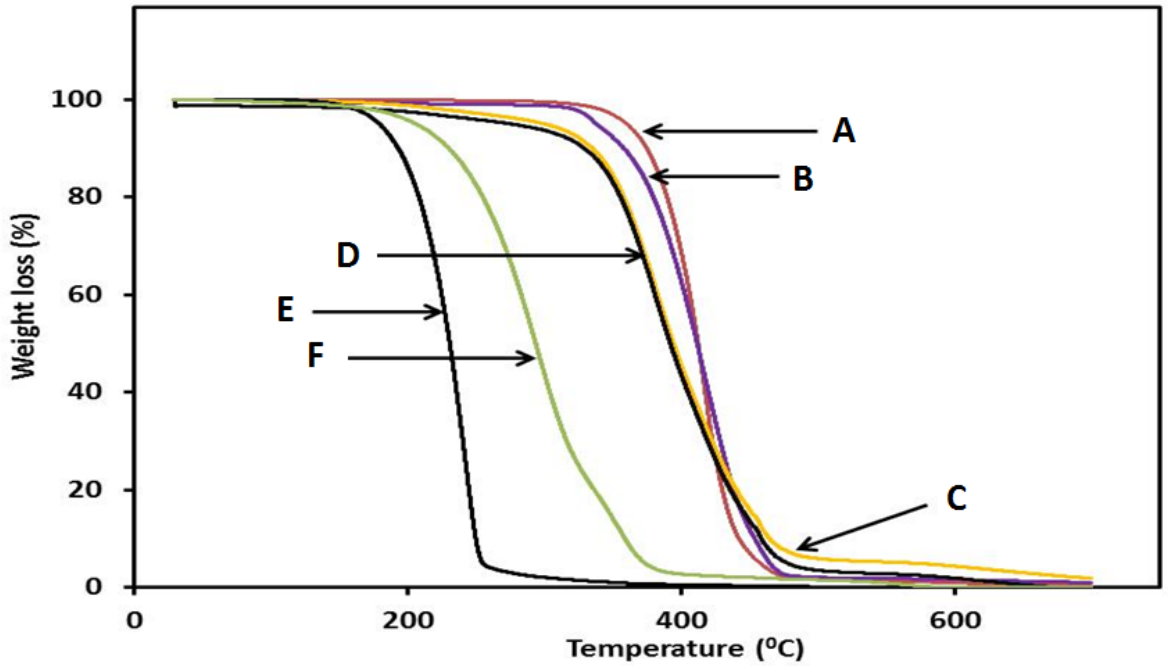

Figure 5.16 TGA thermogram of (A) canola oil, (B) epoxidized canola oil, (C) canola oil derived biolubricant, (D) canola biodiesel, (E) epoxidized biodiesel, and (F) biodiesel biolubricant.

Table 5.12 Thermal stability data of deed and the products.

Product	Temperature (°C)		
	Stability	15-20% wt loss	90-95% wt loss
Canola oil	333	375	460
Epoxidized canola oil	319	370	461
Canola derived biolubricant	309	364	530
Biodiesel	309	360	462
Epoxidized biodiesel	160	204	251
Biodiesel derived biolubricant	194	247	370

5.4.8.5 Oxidation Stability Study

The oxidation stability of biolubricants depends on the degree of unsaturation present in the molecules which are very prone to oxidation. These oxidation processes of lubricants take place during the combustion process of the fuel inside the engine hence it is a critical parameter (Pederson et al. 1999). Canola biolubricant showed a lower value of 56.1 h whereas biodiesel biolubricant gave 76.3 h of oxidative induction time. This increase in the oxidative stability is because of the existence of short chain ester linkage in canola biodiesel biolubricant as compared with canola biolubricant (Dixit et al. 2012). Hence, biodiesel biolubricant is close to 1.5 times more stable when compared with canola biolubricant, under similar oxidative conditions which makes it more suitable for automotive applications.

5.5 Conclusions

Among the selected group VI metal oxides, MoO_3 supported on aluminum oxide was found to be the most promising catalyst for epoxidation as well as for the conversion of epoxides into vicinal di-O-acetylated products. The Central Composite Design (CCD) methodology was used to optimize the process conditions for both epoxidation and vicinal di-O-acetylation steps. Based on the optimized process conditions for both the steps, a one-pot process was developed for the conversion of canola oil into canola biolubricant directly using 10 wt% MoO_3/Al_2O_3 which has advantages over the two-step process: that involves epoxidation and epoxide ring opening by acetic anhydride to produce vicinal di-O-acetylated products. One-step process eliminates unnecessary extra operations and tedious solvent extractions, and is environmentally-friendly. The epoxidized

and di-O-acetylated products were isolated and the structures were confirmed by ^{1}H NMR supported by mass spectrometry. The one-pot procedure was also effective for the preparation of biodiesel biolubricant. The optimum conditions for the one-pot synthesis of biolubricants from canola oil and canola biodiesel are as follows: temperature (120 ^{o}C), molar ratio of unsaturation to tert-butyl hydroperoxide (1:2.25), 12 wt% catalyst loading per gram of feedstock, molar ratio of epoxide to acetic anhydride (1:2), speed of agitation 450 rpm and reaction time 5 h for the canola oil biolubricant synthesis, 4 h for the biodiesel biolubricant. Biolubricant from canola biodiesel has better low temperature properties -12 °C and -18 °C, kinematic viscosity (19 cSt at 100 °C), low friction and anti-wear scar (95 µm), and high oxidative stability (76.3 h). Therefore, biolubricant derived from biodiesel can be used for low temperature and general application like automotive lubricants. However, canola oil derived biolubricant has a cloud point of -3 °C and pour point of -9 °C, the kinematic viscosity measured at 100 ^{o}C is found 670 cSt, friction and anti-wear scar (130 µm), and oxidative stability (56.1 h). As biolubricant from canola oil has high thermal stability (305 °C), and is highly viscous even at high temperature, it can be used at high temperature, heavy load, and high speed operations such as heavy machinery. This study shows that prepared biolubricants are effective, attractive, renewable, and thus have good characteristics as industrial lubricants.

CHAPTER 6

SYNTHESIS OF CANOLA OIL DERIVED BIOLUBRICANTS BY EPOXIDATION, EPOXIDE RING OPENING AND O-PROPYLATION REACTION USING Al-SBA-15 (10) CATALYST

This part of the work has been communicated to a journal as a research article.

Asish K. R. Somidi, and Ajay K. Dalai, "Synthesis of O-propylated canola oil derivatives using Al-SBA-15 (10) catalyst and study on their application as fuel additive," communicated to Catalysis Today Journal (2016).

Contribution of the Ph.D. candidate

All the experimental and characterization work was conducted by Asish Somidi. Manuscript writing and revision work was done by Asish Somidi based on the suggestions from Dr. Ajay K. Dalai.

The contribution of this chapter to the overall Ph. D. work

This research work was focused on the synthesis of biolubricants from canola oil and canola biodiesel by epoxidation, epoxide ring opening and O-propylation reaction.

6.1 Abstract

This research work provides insights on the application of Al-SBA-15 (10) as an efficient catalyst for the epoxide ring opening and O-propylation of epoxidized triglycerides of canola oil, and epoxidized methyl esters of canola biodiesel. The objective of this study was to prepare potential lubricants from canola oil and canola biodiesel. The presence of unsaturation (>95%) in the oils is a limiting factor for lubricant, and hence a two-step chemistry involving epoxidation followed by ring opening and O-alkylation has been employed to enhance the properties and make feedstocks promising as a lubricant. Catalyst screening studies showed that Al-SBA-15 (10) catalyst is highly active in ring opening reactions with 1-propanol as a nucleophile. The physicochemical characterization showed that existence of Al^{+3} ions in Al-SBA-15 (10) promoted the desired transformation. Process optimization and statistical analysis were undertaken using CCD and RSM. Following are the optimal conditions at which 100% conversion of epoxidized oils to O-propylated biolubricants was achieved based on the experimental design: temperature (100 ^{o}C), epoxide to 1-propanol molar ratio (1:6), catalyst loading of 12 % (w/w), and reaction time of 6 h. A detailed investigation was presented in this article to optimize process conditions and to develop a plausible mechanism. The reaction kinetics showed that ring opening and O-propylation reaction followed second-order reaction, and the apparent activation energy was 12 kcal/mol. Evaluation of physicochemical properties of O-propylated canola oil and O-propylated canola biodiesel showed their properties meet the specification of transmission gear oil and anti-wear hydraulic oils.

6.2 Introduction

The present study focuses on the preparation of canola oil derived biolubricants using a heterogeneous catalyst. The chemical composition of canola oil elucidates the presence of significant amount of unsaturation (limitation) which needs to be chemically modified to make the feedstock suitable as a potential lubricant for the industrial or automotive purpose. The two-step chemical modification employed in this work is: (i) synthesis of epoxidized canola oil (biolubricant base oil) by epoxidation of unsaturated fatty acids in the canola oil; and (ii) epoxide ring opening and O-alkylation with 1-propanol (Figure 6.1). The important motivation behind this approach is that, it helps to synthesize biolubricants at moderate process conditions (because of active epoxy moiety) (Somidi et al. 2016), and addition of stable alkoxy functionality at the unsaturation is

anticipated to increase the cold flow temperature properties, oxidative stability and lubricity (antiwear) of the feedstock. Also, literature on the preparation of biolubricants confirms that addition of O-alkyl functionality at the unsaturation produces vegetable oil derivatives suitable for industrial applications such as bioplasticizers, polyols, and lubricants (Sankaranarayanan et al. 2015; Madankar et al. 2013). Commercially available cation exchange resins, montmorillonite (K10), silica supported transition, and rare earth metal complexes were reported to be active in promoting epoxide ring opening and O-alkylation reactions (Das et al. 2011; Zaccheria et al. 2011; Kollbe et al. 2012).

In this study, the novel application of mesoporous Al-SBA-15 as an active catalyst is reported for the epoxide ring opening and O-propylation reaction (EROP reaction). Also, to the best of our knowledge, this is the only report that elucidates the catalytic activity of Al-SBA-15 for the preparation of O-propylated canola oil derived biolubricants. Al-SBA-15 finds its application as versatile catalyst and support for many organic transformations such as transesterification of vegetable oils (Meloni et al. 2016), hydrotreating of gas oils (Badoga et al. 2014). This report shows that it also a promising catalyst for the preparation of vegetable oil derived biolubricants through EROP reaction. Also, the properties of O-propylated canola oil derivatives are nowhere reported. Furthermore, the activity of Al-SBA-15 was tested for the first time for the preparation of O-propylated methyl esters (canola biodiesel derived biolubricant) and its physicochemical properties were reported.

A systematic research approach is implemented to achieve the aforementioned objectives. This study also includes catalyst activity screening tests with different alcohols, detailed catalyst characterization to identify the properties that resulted in effective catalysis, process parameter optimization using central composite design scheme (CCD scheme), statistical analysis to identify the significant parameters that effect the conversion and to build the response model, evaluation of mass transfer and thermodynamic parameters, kinetic studies to develop a kinetic model, spectroscopic characterization for confirming the product formation, and physicochemical characterization of prepared biolubricants to identify their application for industrial and automotive purpose.

6.3 Materials and methods

6.3.1 Chemicals and reagents

Catalyst precursor aluminum isopropoxide (98%) was purchased from Alfa Aesar (Massachusetts, USA), the support SBA-15 was prepared from precursor's tetraethyl orthosilicate (TEOS, 98%) and pluronic P-123 poly (ethylene glycol) block which were purchased from Sigma-Aldrich (St. Louis, USA). The reagent *tert*-Butyl hydroperoxide (70 wt% in water), and solvents such as toluene (ACS grade), ethyl acetate (ACS grade) were obtained from Fisher Chemicals (Edmonton, Canada). Methanol (HPLC grade), ethanol (HPLC grade) and 1-propanol (> 99.5%) are procured from Sigma-Aldrich (St. Louis, USA).

6.3.2 Catalyst preparation method

The procedure for the preparation of Al-SBA-15 catalyst with Si to Al ratio 10 (Al-SBA-15 (10)) is described as follows: Initially 320 ml of 0.1 M HCl solution in distilled water was prepared. About 8 g of polyethylene glycol (Pluronic-123 template) was added to 300 ml 0.1 M HCl solution and the mixture was stirred at 40 ^{o}C to completely dissolve the polymer template (solution A). Then, 1.64 g of aluminum isopropoxide was added to 18 ml of tetraethyl orthosilicate and 20 ml of 0.1 M HCl solution, and the resultant solution is stirred for 15 min (solution B). Solution A and B were mixed and stirred at 40 ^{o}C for 1 h. The mixture was then transferred into PTFE (polytetrafluoroethylene) bottle for hydrothermal treatment (thermal aging) at 100 ^{o}C for 48 h. The resultant solid obtained after hydrothermal treatment was filtered and washed with distilled water to remove excess HCl (pH 7 should be maintained). The white gel obtained after washing is then dried at 110 ^{o}C for 12 h and then calcined at 550 ^{o}C for 6 h. SBA-15 was prepared based on the above-mentioned procedure without the addition of aluminum isopropoxide. Aluminum oxide was prepared using $Al(OH)_3.xH_2O$ and calcined at 550 ^{o}C for 6 h. The above-mentioned procedure for the preparation of SBA-15 support was followed as per the literature (Badoga et al. 2014).

6.3.3 Catalyst characterization methods

The X-ray absorption near edge structure (XANES) K-edge spectra of aluminum oxide impregnated in the hexagonal SBA-15 crystal lattice was obtained using spherical grafting monochromator (SGM) beamline at the Canadian Light Source (Saskatoon, Canada). The energy range was between 250 – 2000 eV and the source is 45 mm planar undulator. The low angle X-ray

diffraction patterns of Al-SBA-15 (10) were obtained on Bruker D8 diffractometer (Cu Kα radiation, λ = 0.154 nm) and the diffraction angle (2ϴ) was maintained between 0.5 – 10˚. The average particle diameter of the catalyst sample was measured on Malvern Mastersizer S long bench particle size analyzer. About 1 g of sample was dispersed in the distilled water and is passed through an optical bench, where the particle size distributions are measured based on the laser beam diffractions. The other catalyst characterization techniques are clearly explained in Chapters 3, 4 and 5.

6.3.4 Response surface methodology (RSM) for process parameter optimization of O-propylated canola oil derived biolubricant preparation

RSM was used to ensure the robustness in optimizing the process conditions and developing a response surface model for the preparation of O-propylated canola oil derived biolubricant. The design of experiments using CCD scheme and the statistical analysis was done with the aid of the Minitab 17 statistical software (Pennsylvania, USA). The design of experiments (DOE) not only minimizes the number of experimental runs in optimization studies but also helps in studying the effect of each parameter and interaction between the parameters on the response statistic (Leticia et al. 2014). Table 6.1 shows the factors and corresponding levels chosen to optimize the process conditions for the EROP reaction of epoxidized canola oil. The CCD scheme consisted of 20 experiments that were performed in this study. These 20 experiments were obtained based on the conventional design formula, N = factorial (2^3) + axial (2×3) + centre point runs (6). From the data obtained from the CCD scheme, a response surface polynomial model was developed followed by ANOVA analysis to measure the significance of the model, process parameters in all forms and regression coefficients based on the F-test statistic and p-values (calculated probability testing against the null hypothesis, H_0: no effect of process parameters on the conversion) (Somidi et al. 2016; Kang et al. 2015).

Table 6.1 Experimental factors and their levels for optimizing EROP reaction

Parameters	Coded levels		
	-1	0	+1
Temperature (^oC)	60	80	100
Catalyst loading (wt %)	4	8	12
Epoxide to 1-propanol (molar ratio)	1:3	1:6	1:9

6.3.5 Analysis methods

For the epoxidation of canola oil, ^1H NMR was used to measure the percentage unsaturation conversion to epoxy groups based on the conventional integration method at the respective chemical shifts. The analysis procedure was explained in detail in Chapter 5 (Somidi et al. 2016). To measure the epoxy conversion to O-propylated groups, AOCS Cd 9-57volumetric titration method was used (Somidi et al. 2014). The percentage change in the epoxy conversion during the course of the reaction is measured as per equation 6.1 (Somidi et al. 2015). Also, the formation of O-propylated canola oil was identified by ^1H NMR and mass spectrometry. The identification of ^1H NMR shifts in the product was made based on the model compound studies and literature reports (Sankaranarayanan et al. 2015).

$$\text{Epoxy conversion (\%)} = \frac{\text{Initial epoxy content } (t_0) - \text{epoxy content at time (t)}}{\text{Initial epoxy content } (t_0)} \times 100 \qquad (6.1)$$

6.3.6 Methods for physicochemical characterization of biolubricants

The detailed procedures on the evaluation of physicochemical properties of biolubricants as per ASTM and AOCS standard methods can be found in Chapters 2 and 4.

6.3.7 Synthesis procedure

Figure 6.1 shows the reaction scheme for the preparation of O-propylated canola oil derived biolubricant through EROP reaction. The base oil for the synthesis of O-propylated canola oil is epoxidized canola oil. The detailed procedure for the synthesis of epoxidized canola oil using

MoO_3/Al_2O_3 catalyst can be found in Chapter 5. The optimum conditions used for the preparation of epoxidized canola oil are: reaction temperature (120 ^oC), molar ratio between per unsaturation in the oil to anhydrous *tert*-Butyl hydroperoxide (1:2.25), catalyst (15 wt% MoO_3/Al_2O_3), catalyst loading (5 wt% per gram of oil taken), and reaction time of 1 h. The complete formation of epoxidized canola oil was confirmed by ^1H NMR and the spectra are shown in the supplementary information (Appendix A). The product was extracted by aqueous work up procedures followed by separation of solvents using rotary evaporator. All the experiments conducted as per DOE for optimizing process conditions for the synthesis of O-propylated canola oil derived biolubricant are performed in batch slurry reactor which is equipped with a reflux condenser, temperature controlled oil bath and magnetic stirrer for uniform mixing. The epoxide conversion during the course of the reaction was monitored using the aforementioned volumetric titration method (equation 6.1). The bulk preparation of O-propylated canola oil used for physicochemical characterization was prepared at the following conditions which were obtained from process parameter optimization: temperature (100 ^oC), epoxide to 1-propanol molar ratio (1:6), catalyst loading (12 wt% per gram of epoxidized oil taken), speed of agitation (400 rpm) and reaction time (6 h).

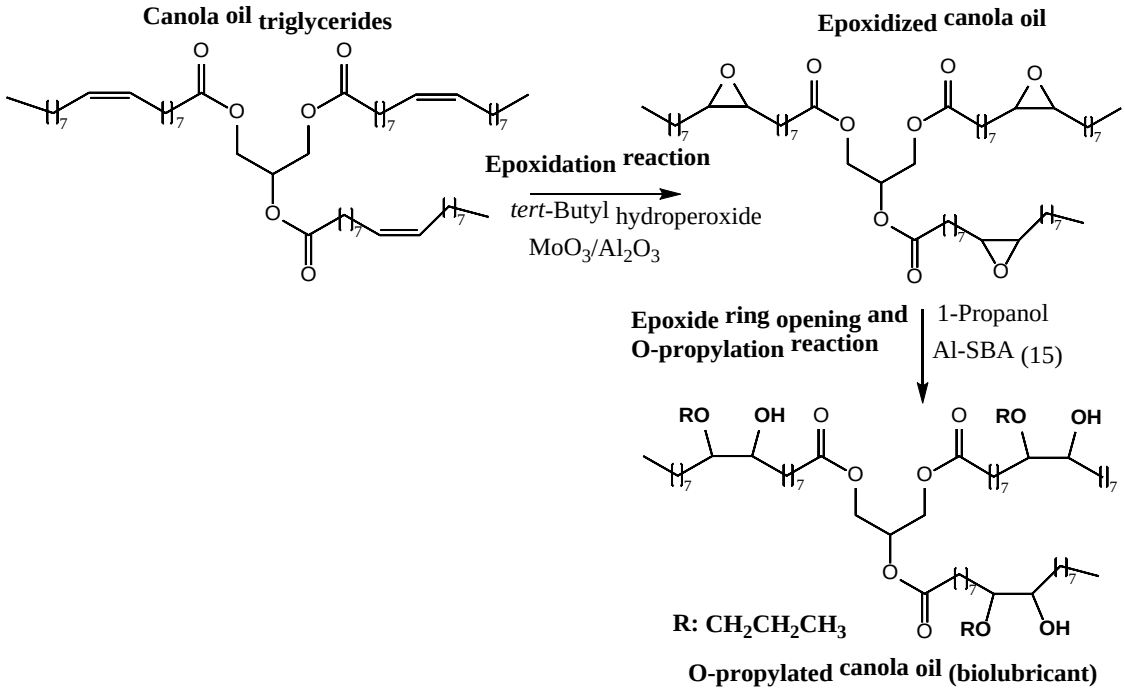

Figure 6.1 Reaction scheme for the synthesis of epoxidized canola oil and O-propylated canola oil.

6.4 Results and discussion

6.4.1 Catalyst screening studies

Before investigating the active catalyst for epoxide ring opening and O-alkylation of epoxidized triglycerides of the canola oil (complex and conjugated molecules) using different alcohols, the screening tests were done on the model compounds such as epoxidized methyl oleate, epoxidized methyl linolenate and epoxidized methyl linoleate. These model compounds constitute major portion (> 95 %) among the epoxidized canola triglycerides. The metals (in the form of metal oxide) that are screened for the above mentioned reaction are Mo, Mn, Sn, Cu, V, Zn, Fe, Ti, Al and Zr. These were impregnated on the supports such as aluminum oxide and aluminosilicates. The important reason behind selecting the supports mentioned above and active metals is based on the literature reports (Das et al. 2011), and also preliminary experimental studies showed aluminum oxide as promising support for nucleophilic substitution reactions. The catalyst screening tests showed that aluminum oxide impregnated in the crystal lattice of hexagonal SBA-15 promoted epoxide ring opening and nucleophilic substitution with alcohols such as methanol, ethanol, 1-propanol and tert-Butyl alcohol. There was no conversion observed using aluminum oxide and SBA-15 as catalysts. The Lewis acidity (Al^{+3}) generated because of the impregnation of aluminum (Al) in the crystal defects of silicon oxide is anticipated to promote the nucleophilic addition reaction (O-propylation). Al was found to be active metal for this reaction. The activity of Al-SBA-15 (10) was found high in O-alkylation reaction with 1-propanol compared to other selected alcohols in terms of minimum reactant loading and reaction time. 100% conversion of epoxidized methyl esters (model compounds) to O-propylated methyl esters was obtained at reaction conditions: temperature (90 ^{o}C), epoxy to alcohol molar ratio (1:6), catalyst loading (10 wt% per g of feed taken), and reaction time (5 h). The complete conversion of epoxidized methyl esters was identified using AOCS volumetric titration method (equation 1) and confirmed with ^{1}H NMR. Based on these preliminary experimental studies Al-SBA-15 (10) was selected as an active catalyst for the optimization of process conditions and preparation of canola oil based biolubricants with O-propyl functionality at the unsaturation.

6.4.2 Catalyst characterization of Al-SBA-15 (10)

The physicochemical characterization of Al-SBA-15 (10) was done to identify and measure the properties that resulted in effective catalysis for EROP reaction. Figure 6.2 shows the N_2 adsorption and desorption isotherm, pore size and pore volume distribution in the catalyst sample Al-SBA-15 (10) after the calcination. The isotherm was found similar to type IV with hysteresis loop (H1), and distinct N_2-capillary condensation between relative pressures 0.5 – 0.9 elucidates the existence of uniform mesoporosity which could be due to ordered pores of the SBA-15 support. The measured BET surface area was 793 m^2/g, with a pore volume of 1.4 cm^3/g and average pore diameter is 5.8 nm.

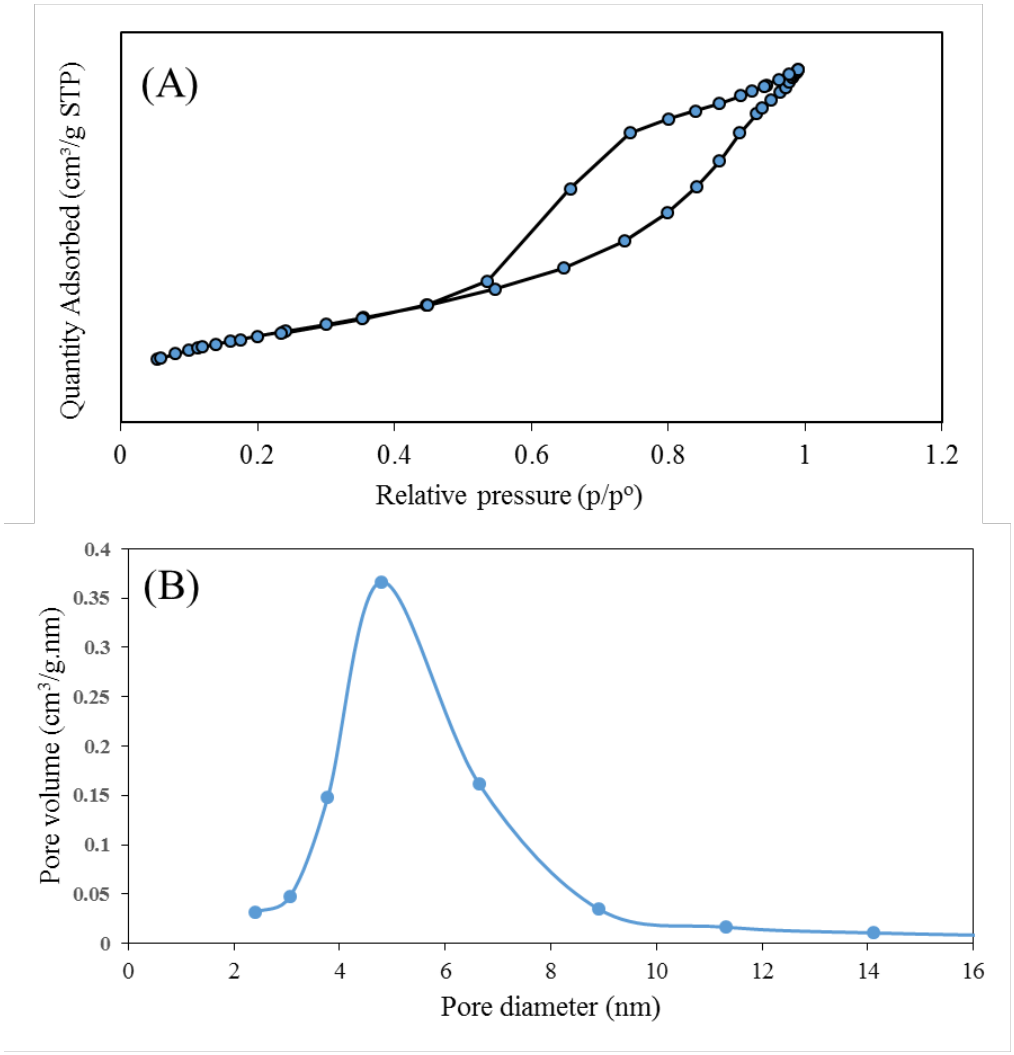

Figure 6.2 N_2– adsorption/desorption isotherms for measuring BET surface area (A), and pore size distributions (B) of Al-SBA-15 (10).

The NH_3–TPD of Al-SBA-15 (10) (Figure 6.3) showed ammonia desorption between temperatures 100 – 350 ^oC indicating the presence of surface acidic sites (moderate strength) on the catalyst surface. This acidity could be due to the substitution of Al^{+3} atoms in the crystal lattice of SBA-15 as SBA-15 was reported to have no surface acidity (Badoga et al. 2014; Zhang et al. 2004).

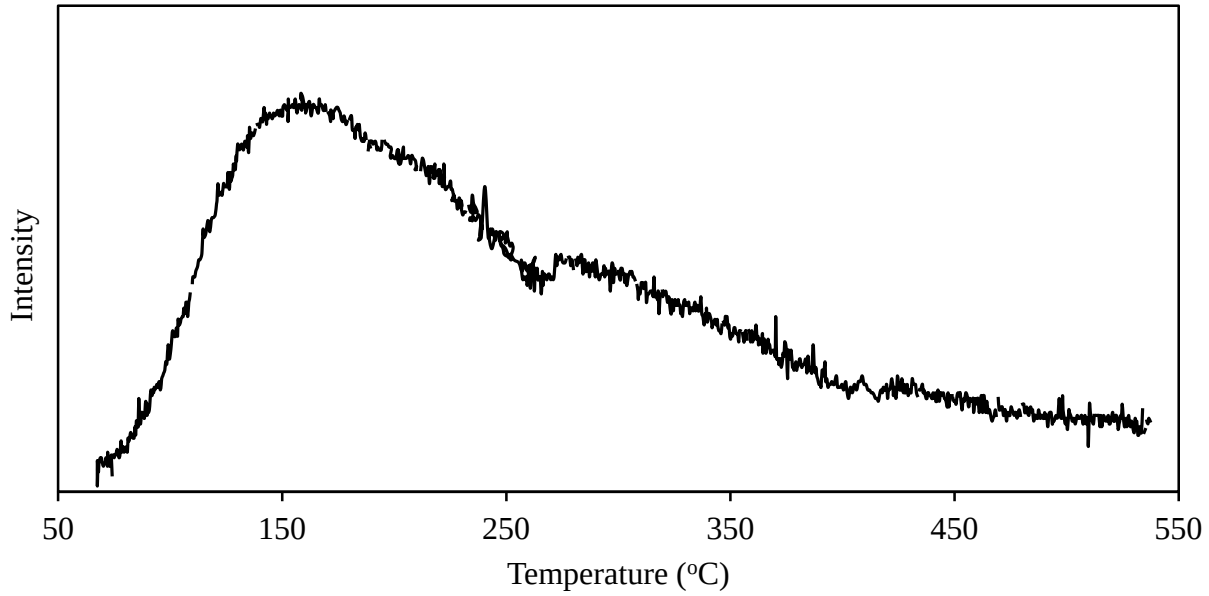

Figure 6.3 NH_3-TPD profile of Al-SBA-15 (10)

The low angle X-ray diffraction patterns of Al-SBA-15 (10) catalyst (Figure 6.4) showed one well-resolved diffraction peak at $2\Theta = 0.9^{\circ}$ which could be attributed to d(100) diffractions from 2D hexagonal silica symmetry (Zhao et al. 1998). There are no diffraction peaks associated with aluminum oxide indicating uniform dispersion. The average crystallite size calculated from Scherrer's equation was found to be 33 nm and atomic spacing ($d_{spacing}$) obtained from Brags equation is 10 nm. The $d_{spacing}$ value also confirms that Al-SBA-15 (10) catalyst has p6mm hexagonal structured SBA-15. From XRD analysis it is clear that the calcination temperature was sufficient to form mesoporous SBA-15.

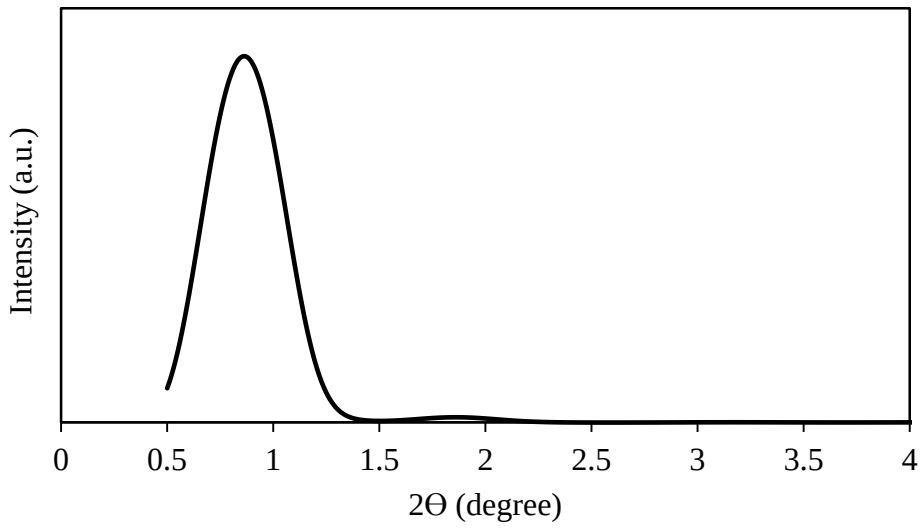

Figure 6.4 X-ray diffraction pattern of Al-SBA-15 (10)

The XANES K-edge spectra of Al in the Al-SBA-15 (10) catalyst in the oxide form was done to get a clear understanding of the structure and coordination of aluminum oxide impregnated in the hexagonal SBA-15 support after the calcination. Figure 6.5 shows the XANES K-edge spectra of Al in the catalyst sample Al-SBA-15 (10) and reference standard $AlPO_4$. From Figure 6.5 it is clearly evident that the K-edge of Al in the catalyst sample and standard $AlPO_4$ is at 1565 eV. Also, the K-edge energy jump looks similar in both catalyst sample and standard elucidating that Al in the framework has +3 oxidation state. The post edge spectra is not exactly similar to $AlPO_4$ which might be due to the interactions of Al with silica.

6.4.3 Process parameter optimization and statistical analysis

The influence of three independent process parameters such as reaction temperature, epoxide to 1-propanol molar ratio and catalyst loading per amount of feed taken are studied to determine the optimal conditions for the maximum conversion of epoxidized canola oil to O-propylated canola oil. Table 6.1 shows the independent parameters and their levels selected respectively, and Table 6.2 shows the CCD experimental scheme executed to optimize the response which is EROP reaction in a selected reaction time of 4 h. The important reason behind optimizing the reaction temperature between 60 to 100 ^oC is that the catalyst exhibited no activity below 60 ^oC and more than 100 ^oC would be above the boiling point of 1-propanol. Preliminary experimental studies conducted with lower concentrations of 1-propanol (< 3 molar ratios) in the

reaction mixture and catalyst loadings (< 4 wt %) exhibited very slow rate of reaction and complete conversion was found difficult to achieve. Hence, aforementioned (Table 6.1) epoxide to 1-propnaol molar ratios and catalyst loadings were selected.

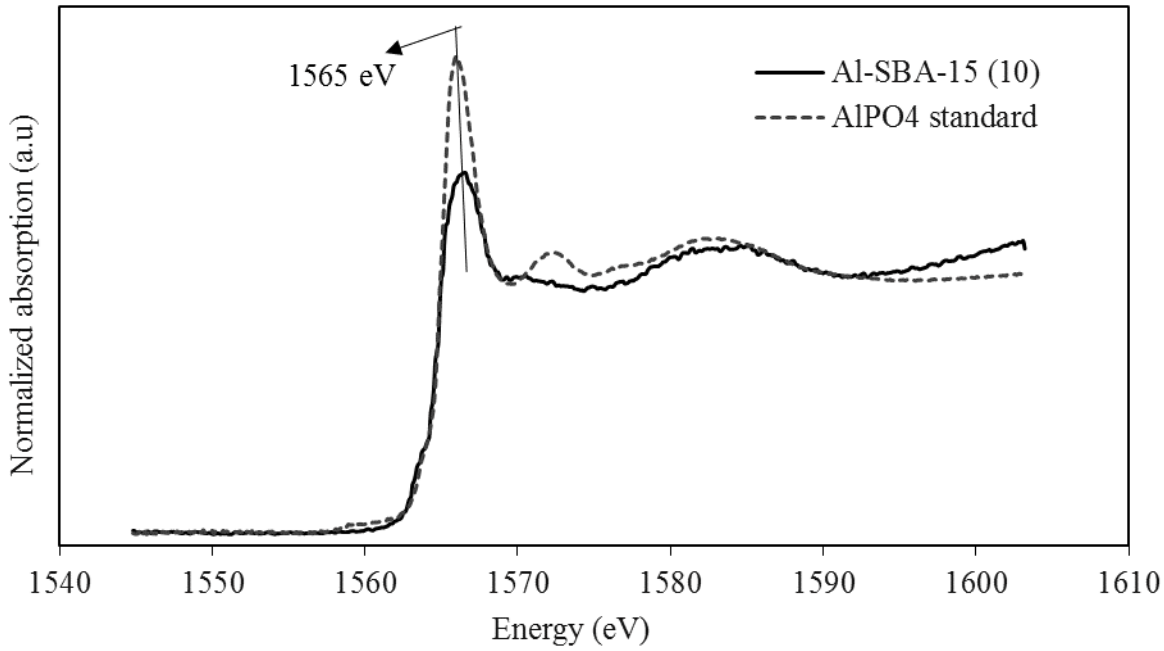

Figure 6.5 XANES K-edge spectra of Al in Al-SBA-15 (10) and $AlPO_4$ standard sample

Also, literature on the preparation of vegetable oil derived biolubricants using alcohols as solvents mostly recommended to use high concentrations because of two prominent reasons: (1) addition of solvent in higher amounts decreases the viscosity of epoxidized oils and promotes reaction by decreasing mass transfer resistances in heterogeneous catalysts; and (2) solvents can be easily recovered and reused after the completion of the reaction. These principles are followed in this work.

Based on the experimental observations obtained from the CCD scheme, the epoxide conversion to O-propylated canola oil (response) was tabulated in Table 6.2. The effect of each parameter and its corresponding level on the overall response was interpreted based on the main effects plot (Figure 6.6). The main effects plot infers that mean epoxide conversion was found to increase with the increase in reaction temperature and catalyst loading. Epoxide to 1-propanol molar ratio showed increment in conversion until the molar ratio of 1: 6 and then mean conversion decreased with higher 1-propanol loading. From main effects plot, it is clearly evident that the

reaction temperature (100 ^{o}C), epoxide to 1-propanol molar ratio (1:6) and catalyst loading of 12 wt% on the basis of the feed taken are promising conditions to maximize EROP formation.

Table 6.2 CCD scheme for optimizing process conditions for the preparation of O-propylated canola oil biolubricant

Run	Temperature (^{o}C)	Molar ratio (Epoxide to 1-propanol)	Catalyst loading (wt% of feed taken)	Experimental response (Reaction time is 4 h) (mol %)	Predicted response as per model (mol %)
1	80	1:6	4	43	36
2	80	1:6	8	50	50
3	100	1:6	8	72	70
4	80	1:9	8	42	43
5	100	1:9	12	97	96
6	60	1:3	12	42	40
7	100	1:3	4	22	25
8	100	1:3	12	75	74
9	60	1:9	12	33	30
10	80	1:6	12	63	70
11	80	1:6	8	49	50
12	80	1:6	8	48	50
13	80	1:6	8	50	50
14	100	1:9	4	50	52
15	60	1:6	8	29	32
16	80	1:6	8	52	50
17	80	1:3	8	36	35
18	80	1:6	8	51	50
19	60	1:9	4	8	9
20	60	1:3	4	15	16

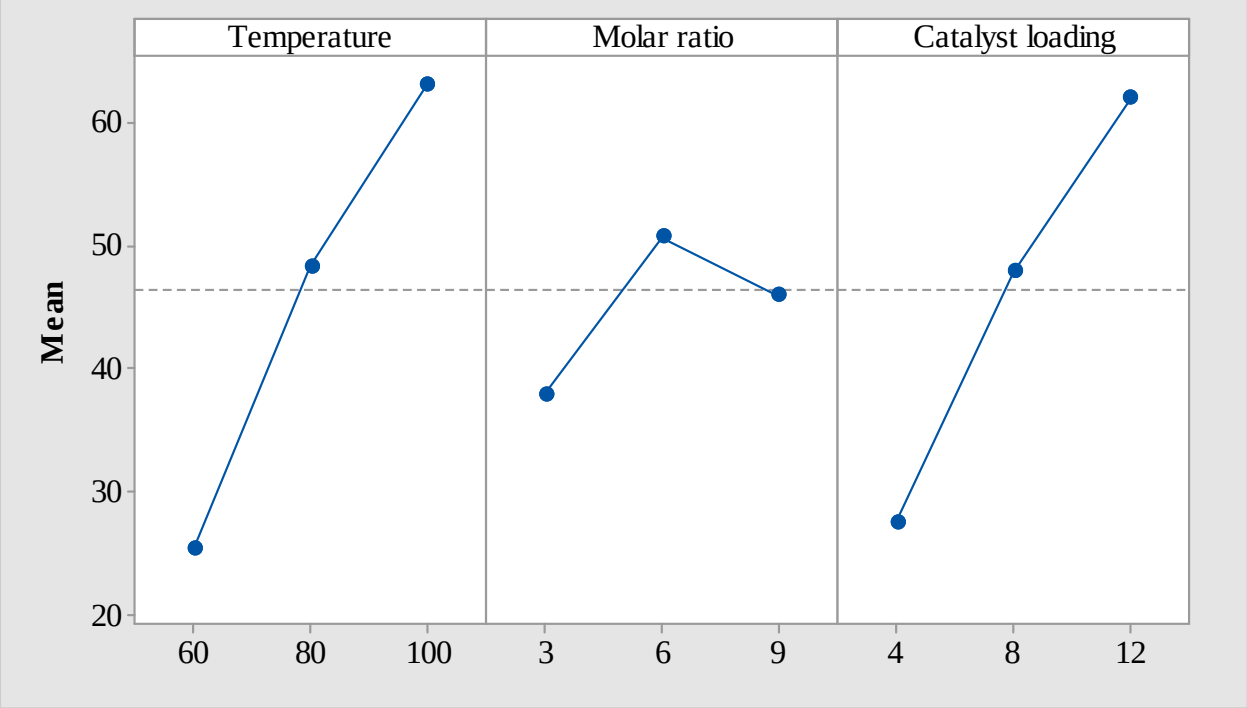

Figure 6.6 Main effects plot for epoxide ring opening and O-propylation reaction based on CCD scheme

Furthermore, at any given condition there was no progress in the EROP reaction without the presence of the catalyst. This refers the importance of the active sites present in the Al-SBA-15 (10) catalyst in promoting EROP reaction at a given condition. The interactions between the catalyst against reaction temperature and 1-propanol molar ratio (Figure 6.7) has been studied for better understanding on the activity of Al-SBA-15 (10) catalyst in promoting EROP reaction. The interaction plot shows a linear relationship between reaction temperature and catalyst loading. This can be explained as follows, an increase in the reaction temperature leads to decrease in the viscosity of the reaction mixture and helps in increasing mass diffusivity through the catalyst pores resulting in high conversions. This is clearly evident from Figure 6.7 which shows high epoxide conversions at all catalyst loadings when the reaction temperature is high. The interaction between catalyst loading to 1-propanol concentration shows that there is no significant increase in the mean epoxide conversions at higher 1-propanol molar ratios. This could be because of the accumulation of 1-propanol in the catalyst pores or on the active sites during the course of the reaction resulting in lower mass diffusivity (hindrance) of epoxidized canola oil. The interaction between reaction temperature and 1-propanol concentration shows increment in epoxide conversion up to 1-

propanol molar ratio of 6 at the selected temperatures. Higher concentration of 1-propanol (> 6 molar ratios) at all the temperatures resulted in a decrement of epoxide conversion which could be because of the strong adsorption onto the active sites.

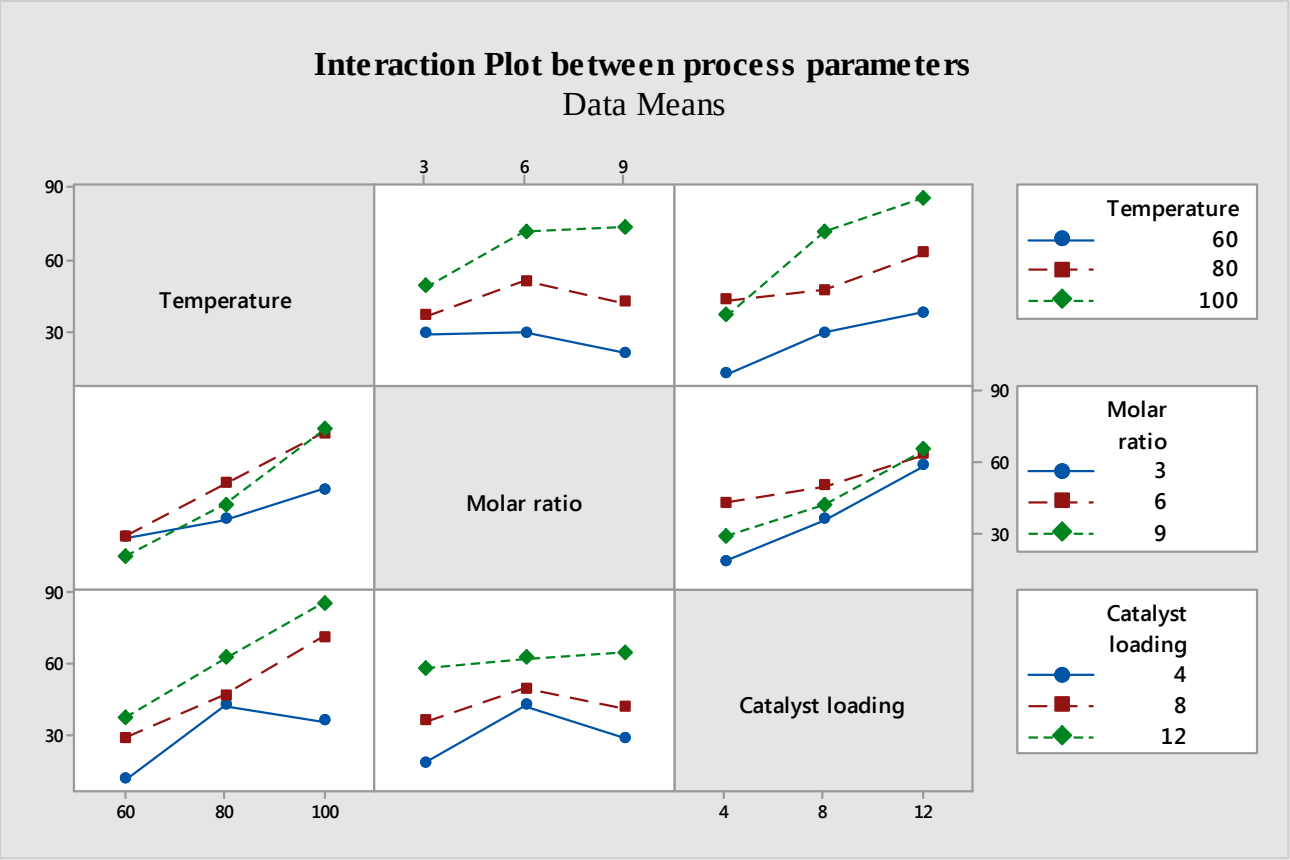

Figure 6.7 Interactions between process parameters on the epoxide conversion to O-propyl canola oil biolubricant.

Further, for EROP reaction to occur, dissociation of 1-propanol to free radicals (carbocation ($CH_3CH_2CH_2O^-$) and carbanion (H^+)) may happen during the course of the reaction to react with epoxide moiety (Das et al. 2011). The increase in the temperature along with the high concentration of 1-propanol not only increases generation of free radicals but also surface chemisorption of free radicals could happen if the availability of reactive epoxidized molecules is limited. Based on the main effects plot and interaction plots, the optimum conditions selected for EROP reaction are as follows: reaction temperature (100 ^oC), epoxide to 1-propanol molar ratio (1:6), and catalyst loading of 12 wt% per gram of epoxy oil taken. The optimum speed of agitation maintained was 400 rpm. Complete formation of O-propylated canola oil biolubricant was

achieved in 6 h reaction time. The reaction was repeated for three times at the aforementioned optimum conditions and found the same epoxide conversion (100 %) each time. The complete epoxide conversion to O-propylation was assessed using AOCS Cd 9-57 volumetric titration method, and confirmed with ^{1}H NMR which is discussed later in this chapter.

The experimental responses obtained are analyzed using response surface design to obtain a mathematical model which is represented in equation 6.2. The predicted epoxide conversions as per the obtained model are shown in Table 6.2. The calculated predicted conversion at the optimum conditions based on the model was found to be 95 % and the experimental observation was 100 % conversion. Also, from Table 6.2 the average deviation between experimental and predicted epoxide conversion values was found to be less than 3 % which validates the proposed model. Furthermore, the acceptability and significance of the proposed model was justified based on the F-test statistic which includes analysis of variance (ANOVA). Table 6.3 shows the ANOVA of the proposed response model for the EROP reaction. The probability value of the model was found to be very low ($p < 0.0001$) elucidating high significance. The variability in the epoxide conversion (R^2) as per the model was found to be 98 % (Table 6.3). This justifies that the model can successfully interpret variation in the response (epoxide conversion) by 98%. The p-values of the selected process parameters were found highly significant to promote EROP reaction.

$$\begin{aligned}\text{Epoxide conversion (mol \%)} &= 20.1 - 0.72\,\text{Temperature} + 5.6\,\text{Molar ratio} - 4.3\,\text{Catalyst loading} \\ &+ 0.001\,\text{Temperature} \times \text{Temperature} - 1.2\,\text{Molar ratio} \times \text{Molar ratio} \\ &+ 0.2\,\text{Catalyst loading} \times \text{Catalyst loading} + 0.13\,\text{Temperature} \times \text{Molar ratio} \\ &+ 0.08\,\text{Temperature} \times \text{Catalyst loading} - 0.08\,\text{Molar ratio} \\ &\times \text{Catalyst loading} \qquad (6.2)\end{aligned}$$

Where temperature (^{o}C) and catalyst loading (wt %).

Table 6.3 Analysis of Variance (ANOVA) for the response quadratic model developed for the EROP reaction

Source	DF	Adjusted Sum of squares	Adjusted Mean squares	F-value	P-value
Model	9	7945.5	882.8	54.8	0.000
Linear	3	6690.5	2230.1	138.5	0.000
Temperature	1	3572.1	3572.1	221.8	0.000
Molar ratio	1	160	160	9.9	0.010
Catalyst loading	1	2958.4	2948.4	183.7	0.000
Square	3	414.5	138.1	8.6	0.004
Temperature × Temperature	1	0.9	0.9	0.1	0.812
Molar ratio × Molar ratio	1	327.2	327.2	20.3	0.001
Catalyst loading × Catalyst loading	1	26.2	26.2	1.6	0.230
2-way interaction	3	840.5	280.1	17.4	0.000
Temperature × Molar ratio	1	544.5	544.5	33.8	0.000
Temperature × Catalyst loading	1	288.0	288.0	17.8	0.002
Molar ratio × Catalyst loading	1	8	8	0.5	0.497
Error	10	161.0	16.1		
Lack-of-it	5	151.0	30.2	15.1	
Pure error	5	10.0	2.0		
Total	19	8106.5			

Model summary: R^2 (98.01 %), R^2 adjusted (96.2 %), R^2 predicted (85.0 %)

6.4.4 Confirmation and characterization of O-propylated canola oil biolubricant using ^{1}H NMR

This section shows the methods employed to extract the products and ^{1}H NMR chemical shifts of products. The solvents (alcohols) present in the reaction mixture after epoxidation or O-propylation reaction are extracted into aqueous phase using brine solution. Ethyl acetate was found to be promising solvent to extract the oil phase. Our observations showed more yield with ethyl acetate as compared to other solvents. The solvent phase was treated with anhydrous sodium sulfate to adsorb traces of moisture, and the oil was then separated under reduced pressure using rotary evaporator. Use of high vacuum is necessary to eliminate the traces of solvents that gets trapped because of the bulkiness of oil. The ^{1}H NMR spectra and chemical shifts of canola oil and epoxidized canola oil are explained in detail in Chapter 5. The ^{1}H NMR spectra of epoxide ring opened and O-propylated canola oil biolubricant are shown in Figure 6.8 and the chemical shifts pertaining to biolubricant molecules are tabulated in Table 6.4. From Figure 6.8, it is clearly evident that the O-propylated canola oil biolubricant has no unsaturation (no chemical shift between δ (5.3 – 5.4 ppm)) and no epoxy functionality (no chemical shift between δ (2.9 – 3.1 ppm)) in the oil confirming 100 % conversion. After epoxide ring opened and O-propylation reaction, five new chemical shifts are found in O-propylated canola oil biolubricant. All the chemical shifts are assigned based on the integration and tabulated in Table 6.4. The triplet between 0.91 – 0.96 ppm is because of the 3-methyl protons of 1-propanol molecules attached at the epoxy moiety. The 2-methylene and 1-methylene protons of 1-propanol after O-propylation reaction at epoxy moiety are found between 3.3 – 3.4 ppm and 3.5 – 3.65 ppm, respectively. The –CH proton of O-propyl and –CH proton of OH groups showed chemical shifts at 3.46 and 3.1 ppm respectively. The ^{1}H NMR chemical shifts confirm the formation of O-propylated biolubricant.

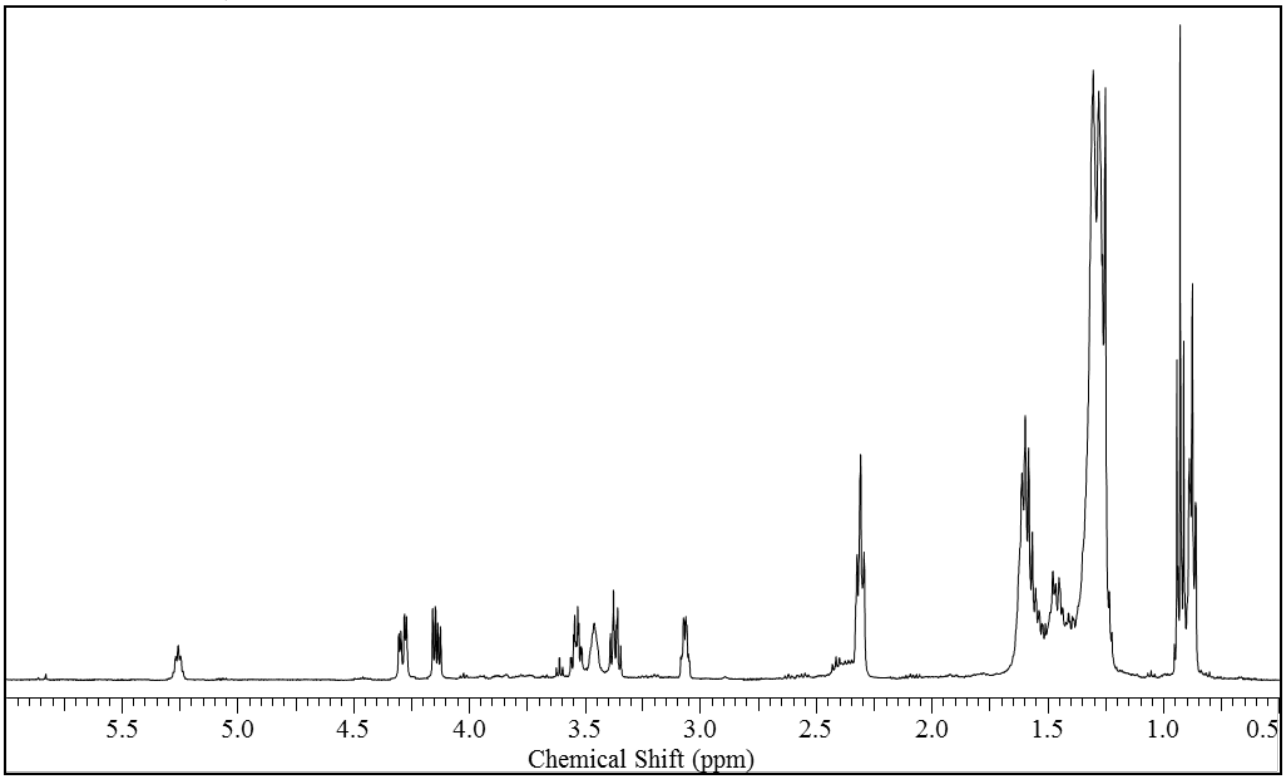

Figure 6.8 ^{1}H NMR spectra of O-propylated canola oil biolubricant.

Table 6.4 ^{1}H NMR chemical shifts of O-propylated canola oil biolubricant and O-propylated canola biodiesel derived biolubricant. (Positioning ^{1}H of 1-propanol: $(CH_3)^{III}$ $(CH_2)^{II}$ $(CH_2)^{I}$ OH; III (3-methyl), II(2-methylene), I (1-methylene))

Type of hydrogen	Chemical shifts (δ, ppm)	
	O-propylated canola oil biolubricant	O-propylated biodiesel biolubricant
Terminal –C**H₃** protons of fatty acids	0.84 – 0.90	0.84 – 0.90
3-methyl protons of 1-propanol after O-propylation	0.91 – 0.96	0.91 – 0.96
–C**H₂** protons of fatty acids	1.2 – 1.52	1.2 – 1.52
α–C**H₂** protons of fatty acids	2.3– 2.48	2.2 – 2.48
β–C**H₂** protons of fatty acids	1.6	1.6
–OC**H₃** of methyl esters in biodiesel	–	3.6
–C**H** protons of $–OCH_2CH_2CH_3$ after O-propylation	3.46	3.46
–C**H** protons of OH after O-propylation	3 – 3.1	3 – 3.1
2-methylene protons of 1-propanol after O-propylation	3.3 – 3.4	3.3 – 3.42
1-methylene protons of 1-propanol after O-propylation	3.5 – 3.65	3.5 – 3.58
–C**H₂** protons of glycerol	4.25 – 4.32	–
–C**H** protons of glycerol	4.1 – 4.2	–

Reference $CDCl_3$, δ: 7.26 ppm.

6.4.5 Evaluation of inter and intra-particle mass diffusion resistances

In this section, theoretical calculations are done to identify the presence of external diffusion (inter-particle) and internal diffusion (intra-particle) mass diffusivity resistances during EROP reaction. Thiele modulus criterion which is the ratio of surface reaction rate to mass diffusion rate was used in this study to verify the absence of interparticle mass diffusion resistance (Fogler et al. 2002; Somidi et al. 2015). The surface reaction rate in terms of initial reaction rate was calculated by measuring the change in the concentration of the epoxidized canola oil with time

per g of catalyst and it was found to be 3.1×10^{-9} mol/m^2.s. The mass diffusion rate of epoxidized canola oil (M_{pco}) which is the product of mass transfer coefficient (k_{pco}) and surface concentration of epoxidized canola oil ($C_{pco,s}$) is measured as follows. The k_{eco} can be determined using Sherwood number ($Sh = k_{eco} \times d_{Al\text{-}SBA\text{-}15\,(10)}/D_{pco,1\text{-}propanol}$). The Wilke-Chang equation for diffusion in liquids was used to calculate the diffusivity of epoxidized canola oil into 1-propanol ($D_{pco,1\text{-}propanol}$) and it was found to be 47.2×10^{-12} m^2/s. The mass transfer coefficient value ($k_{pco)}$ obtained was 1.7×10^{-7} m/s. From the calculated parameters the final value of mass diffusion rate (M_{eco}) was found to be 4.7×10^{-5} mol/m^2.s. If Thiele modulus value is very small, the rate limiting would be surface reaction rate (Fogler et al. 2006). From the above calculation it is clear that mass diffusion rate of epoxidized canola oil is much higher that surface reaction rate elucidating EROP reaction is not inter-particle mass diffusion limited reaction.

To measure the presence of internal pore diffusion resistances for EROP reaction, Weisz-Prater criterion (C_{wp}) was used. This is a prominent criterion which is a function of Thiele modulus and internal effectiveness factor is commonly used for heterogeneous reactions. The criterion and the explanation of the terms included in the equation can be found in our papers (Somidi et al. 2014; Baroi et al. 2014). Calculations showed that C_{wp} value is 201 which is higher than 1 indicating that EROP reaction is internal pore diffusion limited. This is also evident from experimental observations which showed high initial reaction rate (> 40 % conversion in 30 min) and took more than 4 h for complete reaction. This is anticipated because of the internal pore diffusion limitations occurred during the course of the reaction. From the aforementioned calculations, it is clear that Al-SBA-15 (10) could be promising for preparing vegetable oil derived biolubricants with no inter-particle mass diffusivity limitations. Since the triglyceride molecules have long chain fatty acids and conjugated in structure internal pore diffusion usually limits the rate of reaction.

6.4.6 Mechanistic insights on Al-SBA-15 (10) catalyst in promoting EROP reaction

This part of the work is focused on understanding the catalytic activity of Al-SBA-15 (10) catalyst in promoting the EROP reaction, and development of plausible reaction mechanism. Mesoporous silica and aluminum oxide surfaces alone showed no activity for EROP reaction. Their combination resulted in favourable activity indicating the significance of surface acidity (Bronsted and Lewis acidity) generated during the preparation. The selective surface acidity in Al-

SBA-15 (10) catalyst might be because of the substitution of Al^{+3} ions in the silica framework which is clearly evident from aforementioned XANES K-edge spectra. Al could be active metal for promoting EROP reaction of epoxidized canola oil. This is also in support of literature which showed that SBA-15 exhibited no activity for epoxide ring opening reaction with any alcohol as a nucleophile (Das et al. 2011).

Furthermore, the acid catalyzed epoxide ring opening and nucleophilic substitution reactions are anticipated to follow either S_N1 or S_N2 mechanism (Das et al. 2011). The plausible mechanism for the EROP reaction of epoxidized canola oil is developed based on previous investigations (Das et al. 2011; Fasi et al. 2005; Li et al. 2010), and is shown in Figure 6.9. The mechanism shows that Al-SBA-15 (10) catalyst surface could have forwarded EROP reaction through three steps such as: (i) coordination of nucleophilic epoxy moiety on Al^{+3} sites leading to single C–O cleavage, (ii) attack of 1-propanol at the adjacent carbocation of epoxy centre, and (iii) addition of nucleophile ($CH_3CH_2CH_2O^-$) to carbocation centre and transfer of electrophile (H^+) to C–O bond leading to O-propylation reaction.

6.4.7 Kinetic studies of the EROP reaction

The reaction between peroxy groups of epoxidized canola oil (PCO) and 1-propanol (POH) to produce O-propylated canola oil biolubricant (PCB) under the catalysis of Al-SBA-15 (10) catalyst is given as:

$$\mathrm{PCO} + \mathrm{POH} \xrightarrow{k_1} \mathrm{PCB} \qquad (6.3)$$

For the kinetic study of EROP reaction, the experiments were conducted at the aforementioned optimal process conditions obtained from RSM at reaction temperatures 70, 80, 90 and 100 ^oC. Epoxide conversion was assessed at periodic intervals of time to measure the rate of reaction. The kinetic model was developed after considering the following experimental observations: (i) the reaction was not forwarded with the absence of the catalyst; (ii) the reaction was found irreversible; and (iii) the active sites on the Al-SBA-15 (10) catalyst are responsible for promoting the reaction as shown in equation 6.3. The kinetic equation is written based on the power law is given as:

$$-\frac{dC_{PCO}}{dt} = k_1 [C_{PCO}] [C_{POH}] \qquad (6.4)$$

C_{PCO} : Concentration of epoxidized canola oil; C_{POH} : Concentration of 1 − propanol

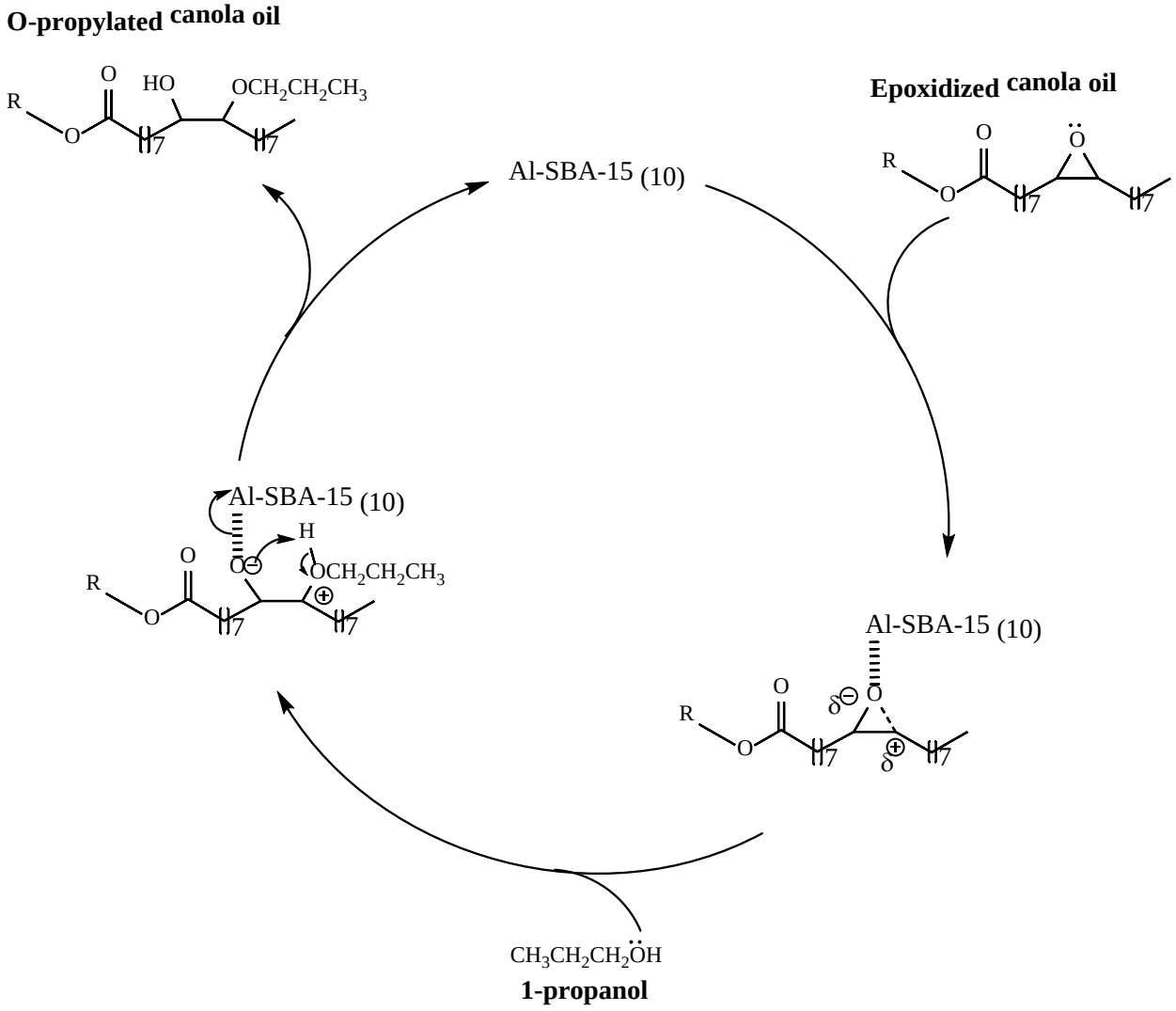

Figure 6.9 Plausible mechanism of epoxide ring opening and O-propylation reaction on Al-SBA-15 surface.

The optimal molar ratio maintained between epoxide and 1-propanol is 1:6, which can be taken as $C_{POH,0} = 6\ C_{PCO,0}$. Where $C_{POH,0}$ and $C_{PCO,0}$ represent initial concentrations of 1-propanol and epoxidized canola oil.

If $C_{POH} = C_{PCO,0}\ (6 - X_{PCO})$, equation 6.4 can be rewritten as:

$$-\frac{dC_{pco}}{dt} = k_1\ [C_{PCO,0}\ (1 - X_{PCO})]\ [C_{PCO,0}\ (6 - X_{PCO})] \quad (6.5)$$

X_{PCO} is epoxide conversion;

$C_{PCO,0}$ is initial concentration of epoxidized canola oil

$$-\frac{d(C_{pco,0}(1 - X_{PCO})}{dt} = k_1\ [C_{PCO,0}\ (1 - X_{PCO})]\ [C_{PCO,0}\ (6 - X_{PCO})] \quad (6.6)$$

$$-\frac{d(1 - X_{PCO})}{dt} = k_1\ C_{PCO,0}(1 - X_{PCO})(6 - X_{PCO}) \quad (6.7)$$

$$\frac{d(X_{PCO})}{(1 - X_{PCO})(6 - X_{PCO})} = k_1\ C_{PCO,0}\ dt \quad (6.8)$$

After integration equation 6.8 is reduced to:

$$\ln(6 - X_{PCO}) - \ln(1 - X_{PCO}) = 5k_1\ C_{PCO,0}\ t + C \quad (6.9)$$

C is a constant.

The graph between $\ln(6–X_{PCO}) – \ln(1– X_{PCO})$ vs. time was made at temperatures 70, 80, 90 and 100 ^oC and is shown in Figure 6.10. Table 6.5 shows the rate expressions and rate constant values obtained at the selected temperatures respectively. The proposed kinetic equations are validated with the experimental observations at the selected reaction times and the difference between conversions is not significant. Hence, from the above kinetic studies, it is clearly evident that EROP reaction followed a second order and the proposed kinetic model is validated. The activation energy of the EROP reaction was calculated from the measured rate constants (Table 6.5). Based on the Arrhenius plot shown in Figure 6.11, the measured apparent activation energy of the EROP reaction was 12 kcal/mol and the pre-exponential factor A was found to be 18.

Table 6.5 Kinetic data for epoxide ring opening and O-propylation reaction carried out at various temperatures

Reaction temperature (°C)	Rate equation in terms of conversion	Rate constant (cc. mol^{-1} min^{-1})	R^2
70	$\ln(6 - X_{PCO}) - \ln(1 - X_{PCO}) = 3 \times 10^{-3}\,t + 1.9$	2	0.96
80	$\ln(6 - X_{PCO}) - \ln(1 - X_{PCO}) = 4 \times 10^{-3}\,t + 2$	3	0.98
90	$\ln(6 - X_{PCO}) - \ln(1 - X_{PCO}) = 7 \times 10^{-3}\,t + 2$	5	0.96
100	$\ln(6 - X_{PCO}) - \ln(1 - X_{PCO}) = 10 \times 10^{-3}\,t + 2.1$	7	0.99

*These equations are validated with experimental observations between 30 min to 6 h.

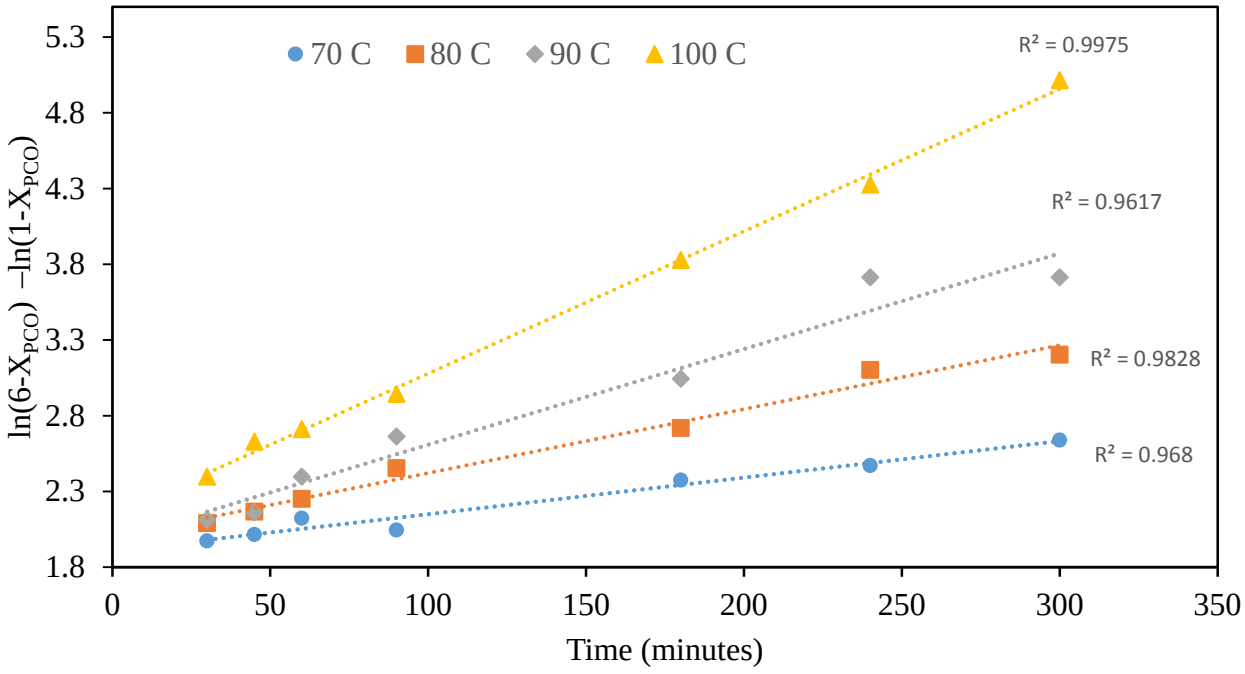

Figure 6.10 Kinetic plot epoxide ring opening and O-propylation reaction at different temperatures.

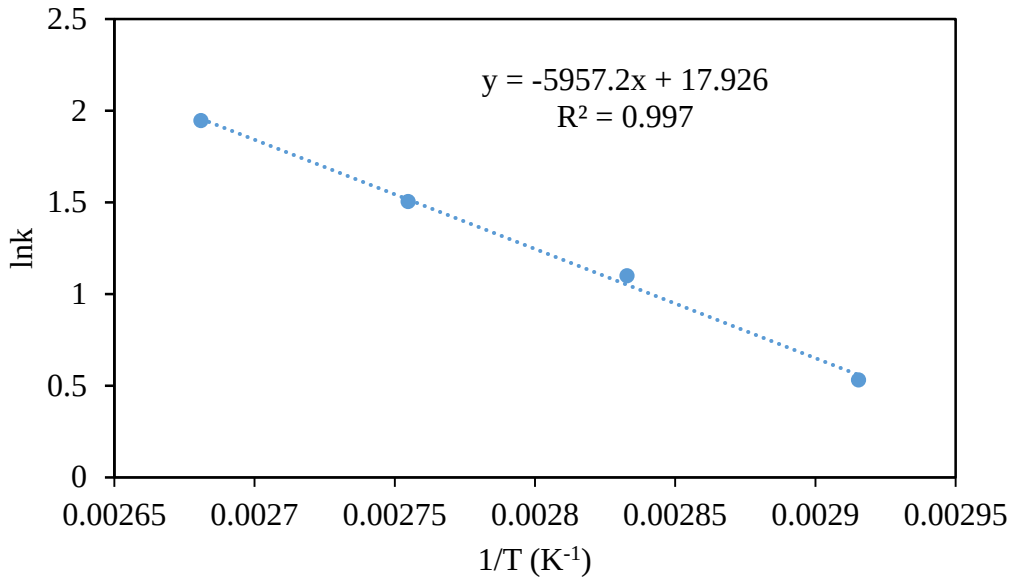

Figure 6.11 Arrhenius plot (lnk vs 1/T) for epoxide ring opening and O-propylation reaction

6.4.8 Physicochemical characterization and prospects of O-propylated canola oil as biolubricant

O-propylated canola oil is an ester with considerably stable alkoxy functionality at the unsaturation. Esters are prominently used for lubricity purpose. Hence, evaluating the properties of the O-propylated canola oil helps in identifying the suitability of the oil as a fuel additive. The cold flow properties which include cloud point and pour point of O-propylated canola oil are measured to ensure the mobility of the oil at low temperatures. The cloud point and pour point of O-propylated canola oil biolubricant are observed to be -15 ^{o}C and -24 ^{o}C, respectively. The pour point of epoxidized canola oil (feedstock) was observed to be 9 ^{o}C. This indicates that addition of O-propyl functionality at the unsaturation of canola oil promoted resistance to self-stacking of triglycerides at low temperatures and resulted in higher liquid mobility up to -24 ^{o}C (Salih et al. 2011). Thermogravimetric analysis (TGA) of O-propylated canola oil was made to identify the flash point and fire point of the prepared oil. From our observations, it is strongly recommended to do TGA analysis of vegetable oils in a closed pan with a perforation to get accurate results. Doing TGA in the open pan gives an error in the analysis because of the ignition of vegetable oils at a certain temperature. Figure 6.12 shows the TGA analysis of O-propylated canola oil biolubricant. The ASTM D92-16 method was used as a reference. O-propylated canola oil showed

thermal stability up to 225 ^{o}C, and the weight loss observed because of the thermal decomposition beyond this temperature was found to be high (5 – 95 %). Flash point of oil is considered to be at the lowest temperature where the oil starts generating vapors which lead to ignition, and fire point (ignition) happens due to combustion of the oil. Maximum weight loss could happen because of the ignition of the oil (Wang et al. 2015). As per the aforementioned analysis, the flash point of the O-propylated canola oil was considered to be 225 ^{o}C.

The kinematic viscosity and viscosity index of a lubricant show the suitability of oil for industrial and automobile purpose. The dynamic viscosity of the O-propylated canola oil at 40 and 100 ^{o}C are measured using viscometer to determine the above-mentioned parameters. The kinematic viscosity of the O-propylated canola oil at 40 ^{o}C was calculated to be 462 cSt and was 33 cSt at 100 ^{o}C. Canola oil was found to have kinematic viscosity 28 cSt at 40 ^{o}C and 0.1 cSt at 100 ^{o}C (Somidi et al. 2014). The viscosity of the oil increased largely after O-propylation because of the increase in the aliphatic carbon chain length. The viscosity index of O-propylated canola oil calculated as per ASTM D2270 method was found to be 105.

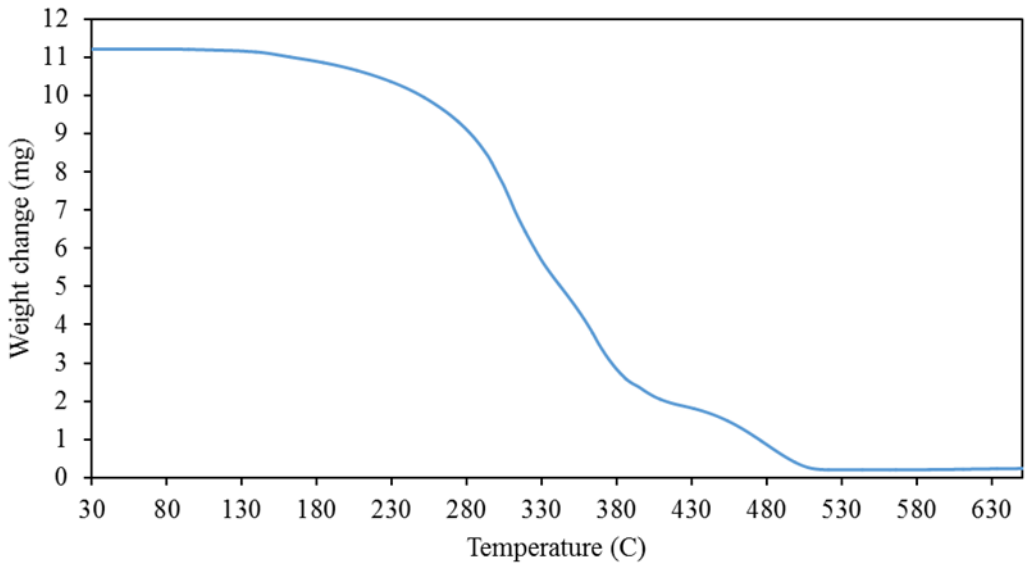

Figure 6.12 Thermogravimetric analysis of O-propylated canola oil biolubricant.

The oxidative stability of O-propylated canola oil was measured to confirm the significance of two-step method involved in this research. AOCS Cd 12-57 test method is used as a reference. The oxidative stability of canola oil was 3.8 h and was 188 h for the O-propylated canola oil. The

oxidative rancidity happens because of the homolysis of the oil in the presence of air. The oxidative induction times of canola oil (3.8 h), epoxidized canola oil (60 h) and O-propylated canola oil (188 h) provide a more perspicuous explanation that addition of stable functionality at the unsaturation reduces homolytic reactions and enhances oxidative stability to a great extent. Furthermore, the lubricity characteristic of O-propylated canola oil was measured in terms of wear scar diameter to confirm the capability of prepared biolubricant in minimizing friction, wear and tear. High frequency reciprocating rig apparatus was used to carry out lubricity test, and optical microscope for the wear scar measurement. Initially, the wear scar diameter of the mineral oil, which has no additives, was tested and it was found to be 2852 µm. The mineral oil was then blended with 2 %, 5 % and 10 % vol/vol of O-propylated canola oil and tested for the lubricity. The wear scar diameter obtained with 2 % blend was 2695 µm, 2430 µm with 5 % blend and no wear scar obtained with 10 % blend. These values showed that addition of O-propylated canola oil provided lubricity between contacted surfaces which resulted in decrease in wear scar diameter.

The physicochemical properties of O-propylated canola oil are compared with International Organization for Standardization (ISO) and Society of Automotive Engineers (SAE) lubricant specifications to identify the suitability of the oil for various purpose. The properties of the O-propylated canola oil are found close to the specifications of 80W-140 and ISO VG 460 lubricant grades (Table 6.6) (McNutt et al. 2016). This indicates that O-propylated canola oil can be used as gear transmission lubricant especially when high viscosity, heavy load, and extreme pressure are to be handled.

Table 6.6 Physicochemical properties of O-propylated canola oil biolubricant

Lubricant requirement	Viscosity at 40 ^{o}C (cSt)	Viscosity at 100 ^{o}C (cSt)	Viscosity index	Pour point (^{o}C)	Flash point (^{o}C)	Oxidative stability (h)
O-propylated canola oil	462	33	105	-24	225	188
80W-140	310	31.2	139	-36	210	-
ISO VG 460	461	31	97	-43	260	-

6.4.9 An application study of Al-SBA-15 (10) catalyst

In this section, the application of Al-SBA-15 (10) catalyst was extended for the epoxide ring opening and O-propylation of methyl esters in the canola biodiesel. The aim behind this study is to prepare potential biolubricant from canola biodiesel, evaluate the properties of the oil and find its suitability as a lubricant. Canola biodiesel is a mixture of methyl esters of oleic, linoleic and linolenic fatty acids as major composition (>95 %). The optimum conditions that were obtained from the RSM optimization of EROP reaction of epoxidized canola oil are applied for the O-propylation of epoxidized canola biodiesel. Epoxidized canola biodiesel was prepared as per our previous report (Somidi et al. 2016). Following are the conditions at which 100 % conversion of epoxidized canola biodiesel to O-propylated canola biodiesel occurred: reaction time of 6 h, reaction temperature (100 ^{o}C), epoxide to 1-propanol molar ratio (1:6), catalyst loading (12 wt%) and speed of agitation (400 rpm). The complete conversion was assessed with volumetric titration method as shown in equation 1 and confirmed with ^{1}H NMR. Figure 6.13 shows the ^{1}H NMR of O-propylated canola biodiesel, and Table 6.4 details about the chemical shifts associated with the molecule after O-propylation. The physiochemical properties of the O-propylated canola oil are shown in Table 6.7. The properties are found close to ISO VG 22 and VG 32 antiwear hydraulic oils used in high pressure output pumps.

Table 6.7 Physicochemical properties of O-propylated canola biodiesel

Lubricant requirement	Viscosity at 40 ^{o}C (cSt)	Viscosity at 100 ^{o}C (cSt)	Viscosity index	Pour point (^{o}C)	Flash point (^{o}C)	Oxidative stability (h)
O-propylated canola biodiesel	23	5	149	-12	230	1.2
ISO VG 22	21	4.5	>90	-30	200	-
ISO VG 32	Minimum 28	>4.1	>90	-6	206	-

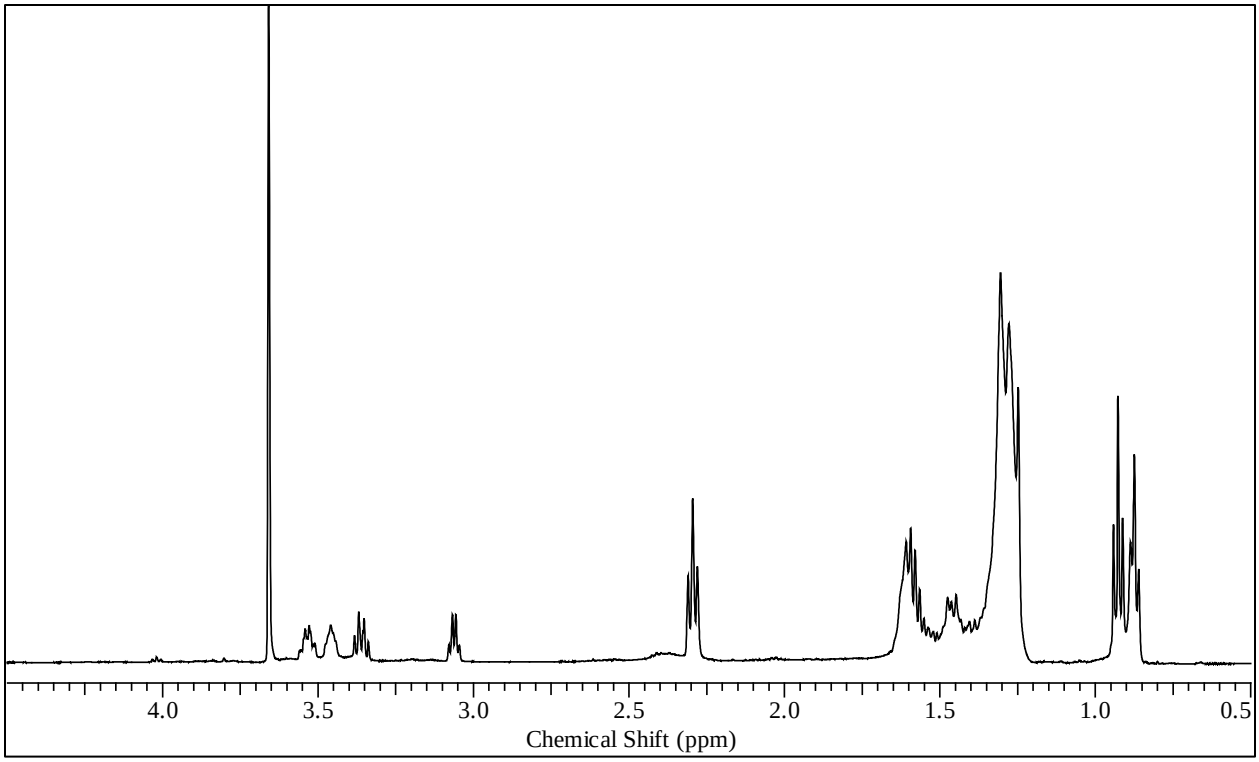

Figure 6.13 ^{1}H NMR spectra of O-propylated biodiesel biolubricant

6.5 Conclusions

This work described the synthesis and novel application of Al-SBA-15 (10) as an active catalyst for the ring opening and O-propylation of epoxidized triglycerides of canola oil and epoxidized methyl esters of canola biodiesel. The catalyst demonstrated 100 % conversion at the optimum conditions: reaction temperature (100 ^{o}C), epoxide to 1-propanol molar ratio (1:6), catalyst loading (12 % w/w), and reaction time of 6 h. ^{1}H NMR characterization confirmed the product formation. EROP reaction was found to follow a second order reaction and the developed kinetic model is validated with the experimental observations. Theoretical calculations showed that EROP reaction of canola oil is internal pore diffusion limited, endothermic, and reactant favored reaction. A plausible reaction mechanism was proposed which is in accordance with the literature and experimental investigations. The addition of O-propyl functionality at the unsaturation enhanced physicochemical properties of the feedstocks and made them suitable as transmission gear oil and antiwear hydraulic oil. The properties of O-propylated canola oil were found close to 80W-140 and ISO VG 460 specifications, and the properties of O-propylated canola biodiesel were found close to ISO VG 22 and ISO VG 32 specifications.

CHAPTER 7

RESEARCH SUMMARY, CONCLUSIONS AND RECOMMENDATIONS

7.1 Research summary

This section summarizes the research work done in this thesis along with the implications and limitations associated in each phase of work.

The first phase (Chapter 3) involved with the preparation of epoxidized canola oil. The ability of metal oxide catalyst for the epoxidation of unsaturated fatty acids in the triglycerides of canola oil is identified. The catalyst screening tests showed the existence of sulfate ions on the surface of tin oxide promoted epoxidation reaction and favored 100% conversion at the optimum reaction conditions (reaction temperature (70 ^{o}C), catalyst loading of 10 wt% with respect to amount of canola oil taken, ethylenic unsaturation to 30 wt% H_2O_2 molar ratio (1:3), and ethylenic unsaturation to acetic acid molar ratio (1:2) and reaction time of 6 h). Preparation of epoxidized canola oil at the aforementioned optimum conditions is important to prevent side reactions (mono acetylation and hydroxylation) and to achieve maximum yield and selectivity. Also, acetic acid loading should be maintained minimum. Determination of product selectivity and occurrence of side reactions were found challenging with the volumetric titration methods. Hence, ^{1}H NMR and FT-IR spectroscopic methods are employed for product formation confirmation. Catalyst deactivation studies showed that existence of oil in the catalyst pores resulted in less activity after each reusability. The solvent work-up procedures employed showed unpromising results. Hence, detailed investigations should be carried out to investigate deactivation studies. From literature and experimental observations, catalyst deactivation could occur because of four reasons: (i) leaching of sulfate species in the presence of moisture, (ii) loose of surface acidity by the catalyst during the course of reaction because of the interaction between water and Lewis acid sites, (iii) accumulation of oil inside the catalyst pores and (iv) exchange of protons by the acetate ions during the course of the reaction. Physicochemical characterization of epoxidized canola oil showed that the properties meet the specifications of ISO VG 46 gear oil and SAE 20W40 engine oil. However, pour point of the oil makes it unsuitable for use at extreme cold weather conditions. This could be solved by adding pour point depressants.

The second phase (Chapter 4) involved with the preparation of canola oil derived biolubricant with ester functionality at the unsaturation. This preparation involved epoxidation, epoxide ring opening and vicinal di-O-acetylation. The potential of metal oxide catalysts for the preparation of vicinal di-O-acetylated canola oil was investigated in this phase. Catalyst screening tests showed that catalysts such as sulfated-ZrO_2, TiO_2-SBA-15, TPA-TiO_2-SBA-15, Amberlyst-15, Amberlite IR 400 and sulfated-TiO_2-SBA-15 are also found to be active for epoxide ring opening and vicinal di-O-acetylation of epoxidized canola oil. However, the Bronsted or Lewis acidity of sulfated-ZrO_2 was found to be more active and promoted high conversions. The optimum conditions at which 100% epoxide conversion to vicinal di-O-acetylation formation occurred are: reaction temperature (130 ^oC), epoxy to acetic anhydride molar ratio (1: 1.25), 16 wt% of catalyst loading with respect to grams of epoxy oil taken, and a reaction time of 1 h 15 min. The complete formation of vicinal di-O-acetylated fatty acids was confirmed with ^1H NMR and mass spectrometry. Sodium spray mass spectrometry showed more promising results (mass values) compared to GCMS (gas chromatography and mass spectrometry) and MS (mass spectrometry). This is because of the capability of sodium ions in minimizing the fragmentation of oil which resulted in precise measurements. Furthermore, use of high concentrations of acetic anhydride resulted in lower epoxide conversions as well as side reactions. Hence, for epoxide ring opening and vicinal di-O-acetylation of epoxidized canola oil acetic anhydride molar ratio should be maintained minimum (1:1.25). Evaluation of physicochemical properties of di-O-acetylated canola oil showed that removal of unsaturation in the canola oil enhanced kinematic viscosity, oxidative stability and lubricity properties. Also, the properties of vicinal di-O-acetylated canola oil meet the specifications of ISO VG 220 vacuum pump oil and SAE 90 gear oil. Hence, the oil finds its potential application as vacuum pump oil and gear oil.

The third phase of the work was focused on the development of metal oxide catalysts which can promote epoxidation, epoxide ring opening and vicinal di-O-acetylation reactions in a one-pot. Catalyst screening tests showed that Group VI metal oxides (MoO_3, WO_3 and Cr_2O_3) impregnated on aluminium oxide are found to be active for both epoxidation, epoxide ring opening and vicinal di-O-acetylation of unsaturated triglycerides in canola oil. The catalytic activity of MoO_3/Al_2O_3 was found to be superior when compared to Cr_2O_3/Al_2O_3 and WO_3/Al_2O_3. Process parameter optimization was carried out using response surface methodology to optimize process conditions for epoxidation, epoxide ring opening and vicinal di-O-acetylation reactions separately.

Based on the optimum conditions derived from individual analysis, one-pot synthesis was executed. The optimum conditions for the one-pot synthesis of biolubricants from canola oil are as follows: temperature (120 ^{o}C), molar ratio of unsaturation to tert-butyl hydroperoxide (1:2.25), 12 wt% catalyst loading per gram of feedstock taken, molar ratio of epoxide to acetic anhydride (1:2), speed of agitation 450 rpm and reaction time of 5 h. The one-pot synthesis included three steps: (i) epoxidation of canola oil using 10 wt% MoO_3/Al_2O_3, (ii) separation of solvents from reaction mixture at the reaction temperature, and (iii) addition of acetic anhydride to epoxidized canola oil and 10 wt% MoO_3/Al_2O_3 for epoxide ring opening and vicinal di-acetylation reaction. The one-pot synthesis procedure showed that MoO_3/Al_2O_3 catalyst is efficient to catalyze both reactions in one-pot, and the synthesis procedure minimized work-up procedures for product extraction, minimized catalyst usage and reaction. Furthermore, the optimum conditions are also applied for the preparation of biolubricant from canola biodiesel. Also, the one-pot synthesis procedure was found effective for both epoxidation, epoxide ring opening and vicinal di-O-acetylation of methyl esters of canola biodiesel. Evaluation of physicochemical properties of biodiesel derived biolubricant showed that the properties of the oil are found close to the specifications of SAE 20W40 engine oil and SAE 75W-90 gear oil.

The fourth phase of the work is on the synthesis of biolubricants from canola oil and canola biodiesel by epoxidation, epoxide ring opening and O-propylation reaction. The main objectives are to develop catalyst for the abovementioned reaction and to evaluate the physicochemical properties of prepared biolubricants. Catalyst screening tests showed that Al-SBA-15 with Si to Al ratio 10 was found to be efficient catalyst. The catalyst was more active with 1-propanol as nucleophile when compared to methanol, ethanol and tert-butanol. Catalyst characterization showed that Al is the active metal for this reaction and existence of Al^{+3} in the crystal walls of SBA-15 promoted the reaction. Response surface methodology was used to optimize the process conditions. The optimum conditions at which 100% formation of O-propylated canola oil biolubricant and O-propylated canola biodiesel biolubricant happened are: reaction temperature (100 ^{o}C), epoxide to 1-propanol molar ratio (1:6), catalyst loading 12 wt% per mass of epoxidized oil taken, and reaction time of 6 h. O-propylated canola oil meets the specifications of SAE 80W-140 gear oil.

Biolubricants prepared in this research are eco-friendly because, the qualitative analysis showed the absence of aromatics, sulfur and nitrogen compounds in the feedstocks. Also, the

boiling points of biolubricants are found much higher when compared to mineral oil based lubricants. This could result in no emissions when used as lubricants in engines and gears. However, biodegradability studies should be carried out in future to measure the time frame of degradation of prepared biolubricants.

7.2 Conclusions

1. Sulfated-SnO_2 was found to be highly active for the preparation of epoxidized canola oil (biolubricant base oil). 100 % unsaturation conversion to epoxide was obtained in 6 h at the optimum conditions: temperature (70 ^oC), catalyst loading of 10 wt% with respect to amount of canola oil taken, ethylenic unsaturation to 30 wt% H_2O_2 molar ratio (1:3), and ethylenic unsaturation to acetic acid molar ratio (1:2). The final product formation was also confirmed with ^1H NMR, ^{13}C NMR and FTIR. The reaction followed pseudo first order. The calculated energy of activation was found to be 18 kcal/mol. Evaluation of physicochemical properties of epoxidized canola oil showed that removal of unsaturation in the canola oil enhanced kinematic viscosity, oxidative stability and lubricity properties.
2. Heterogeneous sulfated-ZrO_2 was found to be highly active and selective catalyst for the preparation of vicinal di-O-acetylated canola oil (biolubricant type 1). The optimum conditions obtained from the Taguchi experimental design for 100% formation of canola oil derived biolubricant achieved are: reaction temperature (130 ^oC), epoxy to acetic anhydride molar ratio (1: 1.25), 16 wt% of catalyst loading with respect to grams of epoxy oil taken, and reaction time of 1 h 15 min. The complete formation of the di-O-acetylated canola oil was confirmed with ^1H NMR spectroscopy and electron spray mass spectrometry. The LHHW dual site (similar in nature) model was tested to generate rate expression for the epoxide ring opening and vicinal di-O-acetylation reaction. The reaction was found to follow overall the second-order and calculated apparent activation energy was 23 kcal/mol.
3. MoO_3/Al_2O_3 was found to be the promising catalyst for both epoxidation of canola oil and its further conversion to vicinal di-O-acetylated product. One-pot procedure eliminates tedious work-up procedures for product extraction, minimizes catalyst usage, reaction time and is an eco-friendly process. The optimum conditions for the one-pot synthesis of biolubricants from canola oil and canola biodiesel are as follows: temperature (120 ^oC), molar ratio of unsaturation to tert-butyl hydroperoxide (1:2.25), 12 wt% catalyst loading per gram of feedstock, molar

ratio of epoxide to acetic anhydride (1:2), speed of agitation 450 rpm and reaction time of 4-5 (5 h for the canola oil biolubricant synthesis, and 4 h for the biodiesel biolubricant).

4. Al-SBA-15 (10) finds its novel application as a promising catalyst for the epoxide ring opening and O-propylation reaction, and also as an active catalyst for the preparation of biolubricants from canola oil and canola biodiesel. The existence of Al^{+3} ions in Al-SBA-15 (10) catalyst promoted the reaction. 100 % conversion of epoxidized canola oil/canola biodiesel to O-propylated biolubricants was achieved at the optimum conditions. The product formation was also confirmed with ^{1}H NMR. Power law model was developed and the reaction followed second-order reaction, and the apparent activation energy was 12 kcal/mol.

7.3 Recommendations

1. Preparation of biolubricants from canola oil and canola biodiesel through epoxidation, epoxide ring opening and etherification reaction should be carried out and their physicochemical properties should be evaluated. This could be a novel study and helps to synthesize biolubricants with stable ether functionality at the unsaturation of the feedstocks.
2. There is no metal oxide catalyst reported in the literature that is active for above-mentioned epoxide ring opening and etherification reaction. Hence, development of catalyst would be a novel contribution.
3. Research on the insitu synthesis of canola oil derived biolubricants should be carried out. This involves simultaneous epoxidation and epoxide ring opening reactions in a single pot using a single heterogeneous catalyst.
4. Synthesis of canola oil derived biolubricants by epoxide ring opening and O-acetylation reaction using carboxylic acids should be conducted and their physicochemical properties need to be evaluated. This helps to synthesize biolubricants with mono-acetyl functionality at the unsaturation.
5. Metal oxide catalysts for the one-pot synthesis of epoxide ring opened and O-propylated canola oil /canola biodiesel is nowhere reported. Hence, this work should be carried out.
6. Vegetable oil derived biolubricants are found to exhibit loss in lubricity property with repeated use. Hence, long term lubricity studies of prepared biolubricants (vicinal di-O-acetylated canola oil, vicinal di-O-acetylated canola biodiesel, O-propylated canola oil and O-propylated canola biodiesel) should be evaluated.

7. Studies on the preparation of canola oil derived biolubricants using continuous fixed bed reactors should be carried out to check the efficiency of the prepared catalysts in this research and also to develop insights on the continuous biolubricant production.
8. Also, catalyst development studies for continuous biolubricant production could be novel and promising.
9. Studies on the biodegradability of canola oil derived biolubricants should be made to determine their potential application for industrial and automobile applications and safe disposal to environment.
10. Studies on the long storage stability of prepared biolubricants is not investigated. Hence, this could be a promising work.

REFERENCES

Adhvaryu, A., and S.Z. Erhan, "Epoxidized soybean oil as a potential source of high-temperature lubricants," Industrial Crops and Products, 15, 247–254 (2002).

Adhvaryu, A., S. Z. Erhan, "Synthesis of novel alkoxylated triacylglycerols and their lubricant base oil properties," Industrial Crops and Products, 21, 113-119 (2005).

Ahulwalia, V., and K. R. K. Parashar., "Text book on: Organic Reaction Mechanisms," Narosa Publishing House (2002).

Akintayo, E. T., T. Ziegler, and A. Onipede, "Gas chromatographic and spectroscopic analsysis of epoxidised canola oil," Bulletin of the Chemical Society of Ethiopia, 20(1), 5-81 (2006).

Ali, A., and D. Kumar, "Ti/SiO_2 as a nanosized solid catalyst for the epoxidation of fatty acid methyl esters and triglycerides," Energy and Fuels, 26, 2953-2961 (2012).

Ali-Darbi, M. M., N. O. Saeed, M. R. Islam, "Biodegradation of natural oils in seawater," Energy Sources, 27, 19-34 (2005).

Asthana, S. N., and G. D. Yadav, "Selective decomposition of cumene hydroperoxide into phenol and acetone by a novel cesium substituted heteropolyacid on clay," Applied Catalysis A: General, 244, 341-357 (2003).

ASTM International United States. Standard Test Method for Flash and Fire Points by Cleveland Open Cup Tester. Annu B ASTM Stand 2007;i: 1–10.

Badoga, S., R. V. Sharma, A.K. Dalai, and J. Adjaye, "Hydrotreating of heavy gas oil on mesoporous zirconia supported NiMo catalyst with EDTA," Fuel, 128, 30–38 (2014).

Baroi, C., and A. K. Dalai, "Esterification of free fatty acids (FFA) of green seed canola (GSC) oil using H-Y zeolite supported 12-tungstophosphoric acid (TPA)," Applied Catalysis A: General, 485, 99–107 (2014).

Baroi, C., and A. K. Dalai, "Simultaneous esterification, transesterification and chlorophyll removal from green seed canola oil using solid acid catalysts," Catalysis Today, 207, 74-85 (2013).

Bart, J. C. J., E. Gucciardi, and S. Cavallaro, Biolubricants: Science and Technology, Woodhead Publishing Limited, Ist Edition, UK, Date accessed (09-01-2016).

Becker, R., and A. Knorr, “An evaluation of antioxidants for vegetable oils at elevated temperatures,” Lubrication Science, 8, 95–117 (1996).

Bella, F., A. Chiappone, J.R. Nair, G. Meligrana, and C. Gerbaldi, “Effect of different green cellulosic matrices on the performance of polymeric dye-sensitized solar cells,” Chemical Engineering Transactions, 41, 211–216 (2014).

Bella, F., F. Colò, J.R. Nair, and C. Gerbaldi, “Photopolymer electrolytes for sustainable, upscalable, safe, and ambient-temperature sodium-ion secondary batteries,” Chemistry and Sustainability Energy and Materials (ChemSusChem), 8, 3668–3676 (2015).

Berlini, C., G. Ferraris, and M. Guidotti, “A comparison between [Ti]-MCM-41 and amorphous mesoporous silica-titania as catalysts for the epoxidation of bulky unsaturated alcohols,” Microporous and Mesoporous Materials, 44-45, 595-602 (2001).

Biresaw, G., G. B. Bantchev, and S. C. Cermak, “Tribological properties of vegetable oils modified by reaction with butanethiol,” Tribology Letters, 43(1), 17-32 (2011).

Blayo, A., A. Gandini, and Nest J. F. Le, “Chemical and rheological characterizations of some vegetable oils derivatives commonly used in printing inks,” Industrial Crops and Products, 14, 155-167 (2001).

Borugadda, V. B., and V. V. Goud, “Response surface methodology for optimization of bio-lubricant basestock synthesis from high free fatty acids castor oil,” Energy Science and Engineering, 3, 371–383 (2015).

Broekhuizen, P., D. Theodori, L. Blanch, and S. Ulmer, “Lubrication in inland and coastal water activities,” A. A. Balkema Publishers, Tokyo (2003).

Cai, C., H. Dai, R. Chen, C. Su, X. Xu, S. Zhang and L. Yang, “Studies on the kinetics of insitu epoxidation of vegetable oil,” European Journal of Lipid Science and Technology, 110 (4), 341-346 (2008).

Campanella, A., E. Rustoy, A. Baldessari, M. A. Baltanas, “Lubricants from chemically modified vegetable oils,” Bioresource Technology, 101, 245-254 (2010).

Campanella, A., M. A. Baltanas, M. C. Capel-Sanchew, J. M. Campos-Martin, and J. L. G. Fierro, "Soybean oil epoxidation with hydrogen peroxide using an amorphous Ti.SiO_2 catalyst," Green Chemistry, 6, 330-334 (2004).

Campo, P. Z. Y., M. T. Suidan, A. D. Venosa, G. A. Sorial, "Biodegradation kinetics and toxicity of vegetable oil triacylglycerols under aerobic conditions," Chemosphere, 68 (11), 2054-2062 (2007).

Castro, R.H.R., and D. V Quach, "Analysis of anhydrous and hydrated surface energies of gamma-al_2o_3 by water adsorption microcalorimetry," Journal of Physical Chemistry C, 116, 24726–24733 (2012).

Cermak, S. C., T. A. Isbell, "Synthesis of estolides from oleic and saturated fatty acids," Journal of American Oil Chemists Society, 78(6), 557-565 (2001).

Cermak, S. C., K. B. Brandon, and T. A. Isbell, "Synthesis and physical properties of estolides from lesquerella and castor fatty acid esters," Industrial Crops and Products, 23(1), 54-64 (2006).

Cermak, S. C., J. W. Bredsguard, B. L. John, J. S. McCalvin, T. T. Thompson, K. N. Isbell, K. A. Feken, T. A. Isbell, and R. E. Murray, "Synthesis and physical properties of new estolide esters," Industrial Crops and Products, 46, 386-391 (2013).

Cermak, S. C., A. L. Durhan, T. A. Isbell, R. L. Evangelista, and R. E. Murray, "Synthesis and physical properties of pennycress estolides and esters," Industrial Crops and Products, 67, 179-184 (2015).

Cermak, S. C., T. A. Isbell, R. L. Evangelista, and B. L. Johnson, "Synthesis and physical properties of petroselinic based estolide esters," Industrial Crops and Products, 33(1), 132-139 (2011).

Chen, S., Y. Yin, D. Wang, Y. Liu, and X. Wang, "Structures, growth modes and spectroscopic properties of small zirconia clusters," Journal of Crystal Growth, 282,498–505 (2005).

Choo, H. P., K. Y. Liew, H. F. Liu, and C. E. Seng, "Hydrogenation of palm olein catalyzed by polymer stabilized Pt colloids," Journal of Molecular Catalysis A: Chemical, 165 (1-2), 127-134 (2001).

Choo, H. P., K. Y. Liew, H. F. Liu, C. E. Seng, W. A. K. Mahmood and M. Bettahar, "Activity and selectivity of noble metal colloids for the hydrogenation of polyunsaturated soybean oil," Journal of Molecular Catalysis A: Chemical, 191 (1), 113-121 (2003).

Chowdhury, A., R. Chakraborty, D. Mitra, and D Biswas, "Optimization of the production parameters of octyl ester biolubricant using Taguchi's design method and physico-chemical characterization of the product," Industrial Crops and Products, 52, 783-789 (2014).

Das, S., and T. Asefa, "Epoxide ring-opening reactions with mesoporous silica-supported Fe (III) catalysts," ACS Catalysis, 1, 502–510, 2011.

Dejaegere, E. A., J. W. Thybaut, G. B. Marin, G. V. Baron, and J. F. M. Denayer, "Modeling of toluene acetylation with acetic anhydride on H-USY zeolite," Industrial and Engineering Chemistry Research, 50, 11822–11832 (2011).

Dellamorte, J. C., J. Lauterbach, and M. A. Barteau, "Palladium–silver bimetallic catalysts with improved activity and selectivity for ethylene epoxidation," Applied Catalysis A: General, 391(1–2), 281-288 (2011).

Demirba, A., "Biodegradability of biodiesel and petrodiesel fuel energy sources," Part A: Recovery, Utilization and Environmental Effects, 31 (2), 169-174 (2009).

Deshmane, G. V., and G. Y. Adewuyi, "Mesoporous nanocrystalline sulfated zirconia synthesis and its application for FFA esterification in oils," Applied Catalysis A: General, 462-463, 196-206 (2013).

Deutsch, J., H. A. Prescott, D. Muller, E. Kemnitz, and H. Lieske, "Acylation of naphthalenes and anthracenes on sulfated zirconia," Journal of Catalysis, 231, 269-278 (2005).

Deutsch, J., V. Quaschning, E. Kemnitz, H. Lieske, and H. Ehwald, "Catalytic acylation of aromatics with carboxylic anhydrides over sulfated zirconia," Topics in Catalysis, 13, 281-285 (2000).

Dinda, S., A. V. Patwardhan, V. V. Goud, and N. C. Pradhan, "Epoxidation of cottonseed oil by aqueous hydrogen peroxide catalysed by liquid inorganic acids," Bioresource Technology, 99 (9), 3737-3744 (2008).

Dinda, S., V. V. Goud, A. V. Patwardhan, and N. C. Pradhan, “Selective epoxidation of natural triglycerides using acidic ion exchange resin as catalyst,” Asia-Pacific Journal of Chemical Engineering, 6 (6), 870-878 (2011).

Dixit, S., Kanakraj, S., Rehman, A., “Linseed oil as a potential resource for bio-diesel: A review,” Renewable and Sustainable Energy Reviews, 16, 4415-4421 (2012).

Fadhel, A. Z., P. Pollet, C. L. Liotta, and C. A. Eckert, “Combining the benefits of homogeneous and heterogeneous catalysis with tunable solvents and nearcritical water molecules,” 15, 8400–8424 (2010).

Fan, R., and Hou, X., “Tributylphosphine-catalyzed ring-opening reaction of epoxides and aziridines with acetic anhydride,” Tetrahedron Letters, 44, 4411-4412 (2003).

Fasi, A., I. Palinko, A. Gomory, I. Kiricsi, “The ring opening and oligomerisation reactions of an epoxide and an episulfide on aluminosilicates in the liquid phase,” Central European Journal of Chemistry, 3, 230–244 (2005).

Fogler, H. S., “Elements of Chemical Reaction Engineering,” 3rd Edition, Prentice Hall, Massachussetts, USA , 618-619 (2002).

Fogler, H.S., “Elements of Chemical Reaction Engineering,” 3rd edition, Prentice Hall, Massachussetts, USA, 741–760 (2002).

Fox, N. J., and G. W. Stachowiak, “Vegetable oil-based lubricants–A review of oxidation,” Tribology International, 40, 1035-1047 (2007).

Frenkel, P., and C. T. Danbury, “Bio-based Plasticizer,” (19) United States, 1-21 (2012), US 2012/0214920 A1.

Gamage, K. P., O. M. Brien, and L. Karunanayake, “Epoxidation of some vegetable oils and their hydrolysed products with peroxyformic acid- optimized to industrial scale,” Journal of National Science Foundation, 37(4), 229-240 (2009).

Garcia-Zapaterio, L. A., J. M. Franco, C. Valencia, M. A. Delgado, and C. Gallegos, “Viscous, thermal and tribological characterization of oleic and ricinoleic acids-derived estolides and their blends with vegetable oils,” Journal of Industrial and Engineering Chemistry, 19(4), 1289-1298 (2013).

Garcia-Zapaterio, L. A., J. M. Franco, C. Valencia, M. A. Delgado, M. V. Rulz-Mendez, R. Garces and C. Gallegos, " Oleins as a source of estolides for biolubricant applications," Grasas Y Aceities, 61(2), 171-174 (2010).

Gawade, B., and G. D. Yadav, "Novelties of combustion synthesized and functionalized solid superacid catalysts in selective isomerization of styrene oxide to 2-phenyl acetaldehyde," Catalysis Today, 207, 145-152 (2013).

Gawrilow, I., "Vegetable oil usage in lubricants," Inform: International News Fats Oils Related Material, 15 (11), 1-4 (2004).

Goering, C. E., A. W. Schwab, M. J. Daugherty, E. H. Pryde, and A. J. Heakin, "Fuel properties of eleven vegetable oils," Transactions of American Society of Agricultural Engineers, 25, 1472-1483 (1982).

Gorla, G., S. M. Kour, K. V. Padmaja, M. S. L. Karuna, and R. B. N. Prasad, "Novel acyl derivative from karanja oil: alternative renewable lubricant base stocks," Industrial and Engineering Chemistry Research, 53, 8685-8693 (2014).

Goud, V. V., A. V. Patwardhan, and N. C. Pradhan, "Studies on the epoxidation of mahua oil (Madhumica Indica) by hydrogen peroxide, Bioresource Technology, 97, 1365-1371 (2006).

Gryglewicz, S., M. Stankiewicz, F. A. Oko, and I. Surawska, "Esters of dicarboxylic acids as additives for lubricating oils," Tribology International, 39, 560-564 (2006).

Gryglewicz, S., M. Muszynski, and J. Nowicki, "Enzymatic synthesis of rapeseed oil-based lubricants," Industrial Crops and Products, 45, 25-29 (2013).

Guo-dong, F., H. Yun, X. Bin, and Z. Yong-Hong, "Synthesis and characterization plasticizer epoxy acetyl polyglycerol ester," Journal of Forest Products and Industries, 3(2), 100-105 (2014).

Hamid, H.A., R. Yunus, U. Rashid, T.S.Y. Choong, and A.H. Al-Muhtaseb, "Synthesis of palm oil-based trimethylolpropane ester as potential biolubricant: Chemical kinetics modeling," Chemical Engineering Journal, 200-202, 532–540 (2012).

Hashem, A. I., W. S. I. A. Elmagd, A. E. Salem, M. El-Kasaby and A. M. El-Nahas, "Conversion of some vegetable oils into synthetic lubricants," Energy Sources, Part A: Recovery, Utilization, and Environmental Effects, 35, 397-400 (2013).

Heshmatpour, F., and R. B. Aghakhanpour, "Synthesis and characterization of superfine pure tetragonal nanocrystalline sulfated zirconia powder by a non-alkoxide sol-gel route," Advanced Powder Technology, 23, 80-87 (2012).

Hill, G. J., B.E. Rossiter, and B. Sharpless, "Anhydrous tert-butyl hydroperoxide in toluene: the preferred reagent for applications requiring dry TBHP," Journal of Organic Chemistry, 48, 3607–3608 (1983).

Hofland, A., "Alkyd resins: from down and out to alive and kicking," Progress in Organic Coating, 73 (4), 274-282 (2012).

Hwang, H. S., A. Adhvaryu, and S. Z. Erhan, "Preparation and properties of lubricant basestocks from epoxidized soybean oil and 2-ethylhexanol," Journal of American Oil Chemists Society, 80 (8), 811-815 (2003).

Hwang, H. S., Z. S. Erhan, "Modification of epoxidized soybean oil for lubricant formulations with improved oxidative stability and low pour point," Journal of American Oil Chemists Society, 78, 1179-1184 (2001).

Hwang, H. S., and S. Z. Erhan, "Synthetic lubricant basestocks from epoxidized soybean oil and Guerbet alcohols," Industrial Crops and Products, 23 (3), 311-317 (2006).

Isbell, T. A., "Chemistry and Phyical Properties of Estolides," Grasas Y Aceites, 62(1), 8-20 (2011).

Issariyakul, T., M.G. Kulkarni, L.C. Meher, A.K. Dalai, and N.N. Bakhshi, "Biodiesel production from mixtures of canola oil and used cooking oil," Chemical Engineering Journal, 140, 77–85 (2008).

Jain, A. K., and A. Suhane, "Research approach & prospects of non edible vegetable oil as a potential resource for biolubricant – A review," Advanced Engineering and Applied Sciences: An International Journal, 1(1), 23-32 (2012).

Jia, B. B., T. Li, X. Liu, and P. H. Cong, “Tribological behaviours of several polymer-polymer sliding combinations under dry friction and oil-lubricated conditions,” Wear, 262 (11-12), 1353-1359 (2007).

Ji, H., B. Wang, X. Zhang, and T. Tan, “Synthesis of levulinic acid-based polyol ester and its influence on tribological behaviour as a potential lubricant,” RSC Advances, 5, 100443–100451 (2015).

Jogalekar, A. Y., R. G. Jaiswal, and R. V. J. Jayaram, “Activity of modified SnO_2 catalysts for acid-catalyzed reactions,” Chemical Technology Biotechnology, 71, 234-240 (1998).

Johansson, L.E., “Copper catalysts in the selective hydrogenation of soybean and rapeseed oils: IV. Copper on silica gel, phase composition and preparation,” Journal of American Oil Chemists Society, 56, 974–980 (1979).

Jovanovica, D., R. Radovic, L. Mares, M. Stankovica, B. Markovic, “Nickel hydrogenation catalyst for tallow hydrogenation and for the selective hydrogenation of sunflower seed oil and soybean oil,” Catalysis Today, 43 (1-2), 21-28 (1998).

Kamalakar, K., A. K. Rajak, R. B. N. Prasad, and M.S.L. Karuna, “Rubber seed oil-based biolubricant base stocks: A potential source of hydraulic oils,” Industrial Crops and Products, 51, 249–257 (2013).

Kang, K., R. Azargohar, A. K. Dalai, and H. Wang, “Noncatalytic gasification of lignin in supercritical water using a batch reactor for hydrogen production: An experimental and modeling study,” Energy and Fuels, 29, 1776–84 (2015).

Kang, K., R. Azargohar, A.K. Dalai, and H. Wang, “Systematic screening and modification of Ni based catalysts for hydrogen generation from supercritical water gasification of lignin,” Chemical Engineering Journal, 283, 1019–1032 (2016).

Khalaf, H. A., S. E. Mansour, and E. A. El-Madani, “The influence of sulfate contents on the surface properties of sulfate-modified tin (IV) oxide catalysts,” Journal of Association of Arab Universities Basic Applied Sciences, 10, 15-20 (2011).

Khder, A. S., E. A. El-Sharkawy, S. A. El-Halam, and A. I. Ahmed, “Surface characterization and catalytic activity of sulfated tin oxide catalyst,” Catalysis Communications, 9, 769-777 (2008).

Kitano, T., S. Okazaki, T. Shishido, K. Teramura, and T. Tanaka, “Brønsted acid generation of alumina-supported molybdenum oxide calcined at high temperatures: Characterization by acid-catalyzed reactions and spectroscopic methods,” Journal of Molecular Catalysis A: Chemical, 371, 21–28 (2013).

Kollbe Ahn, B., H. Wang, S. Robinson, T. B. Shrestha, D. L. Troyer, and S. H. Bossmann, “Ring opening of epoxidized methyl oleate using a novel acid-functionalized iron nanoparticle catalyst,” Green Chemistry, 14, 136–42 (2012).

Koh, M. Y., T. I. M. Ghazi, and A. Idris, “Synthesis of palm based biolubricant in an oscillatory flow reactor,” Industrial Crops and Products, 52, 567-574 (2014).

Koo, D. H., M. Kim, and S. Chang, “WO_3 Nanoparticles on MCM-48 as a high selective and versatile heterogeneous catalyst for the oxidation of olefins, sulfides, and cyclic ketones,” Organic Letters, 7 (22), 5015-5018 (2005).

Krishnakumar T., R. Jayaprakash, V. N. Singh, B. R Mehta, and A. R. Phani, “Synthesis and characterization of tin oxide nanoparticle for humidity sensor application,” Journal of Nano Research, 4, 91-101 (2008).

Kritchevsky D., The Effects of Dietary Trans Fatty Acids. Chemistry & Industry, 15, 565–567 (1996).

Krzan, B., J. Vizintin, “Ester based lubricants derived from renewable,” Tribology in Industry, 26, 58-62 (2004).

Kulkarni, R. D., P. S. Deshpande, S. U. Mahajan, and P. P. Mahulikar, “Epoxidation of mustard oil and ring opening with 2-ethylhexanol for biolubricants with enhances thermo-oxidative and cold flow characteristics,” Industrial Crops and Products, 49, 586-592 (2013).

Lathi, P. S., and B. Mattiasson, “Green approach for the preparation of biodegradable lubricant base stock from epoxidized vegetable oil,” Applied Catalysis B: Environmental, 69, 207-212 (2007).

Laubli, M. W., and P. A. Bruttel, “Determination of the oxidation stability of fats and oils: Comparison between the active oxygen method (AOCS Cd 12-57) and the rancimat,” Journal of American Oil Chemical Society, 63(6), 792-795 (1986).

Leticia, A., Ray, L. P. Ortega, J. Moreno-dorado, F. J. Guerra, G. M. Massanet, “Optimization by response surface methodology (RSM) of the Kharasch − Sosnovsky oxidation of valencene,” Organic Process Research and Development, 1662–1666 (2014).

Levizzari, A., M. Voglino, P. Volpi, “Environmental and Economic Impact of re-refined products: A Life Cycle Analysis,” Proceedings of the 6th International LFE congress, Brussels (1999).

Li, Y., W. Zhang, L. Zhang, Q. Yang, Z. Wei, and Z. Feng, “Direct Synthesis of Al−SBA-15 mesoporous materials via hydrolysis-controlled approach,” Journal of Physical Chemistry B, 108, 9739–9744 (2004).

Li, Y., Y. Tan, E. Herdtweck, M. Cokoja, F. E. Kühn, “Synthesis of nitrile coordinated Lewis acids $Al(OC(CF_3)_2R)_3$ and their application in catalytic epoxide ring-opening reactions,” Applied Catalysis A: General, 384 (1-2), 171–176 (2010).

Liang, C., M.C. Wei, H.H. Tseng, and E.C. Shu, “Synthesis and characterization of the acidic properties and pore texture of Al-SBA-15 supports for the canola oil transesterification,” Chemical Engineering Journal, 223, 785–794 (2013).

Lian-Kun, J., L. Xiang, J. W. Jiao, and K. C. You, “Synthesis of vegetable oil based polyols with cottonseed oil and sorbitol derived from natural source,” Chinese Chemical Letters, 22(11), 1289-1292 (2011).

Lligadas, G., J. C. Ronda, M. Galià., and V. Cádiz., “Renewable polymeric materials from vegetable oils: A perspective,” Materials Today, 16, 337–343 (2013).

Lozada, Z., G. J. Suppes, Y-Ch. Tu, and F. H. Hsieh, “Soy-based Polyols from oxirane-ring opening by alcoholysis reaction,” Journal of Applied Polymer Science, 113, 2552-2560 (2009).

Madankar, C. S., A. K. Dalai, and S. N. Naik, “Green synthesis of biolubricant base stock from canola oil,” Industrial Crops and Products, 44, 139–144 (2013).

McNutt, J., and Q. S. He, “Development of biolubricants from vegetable oils via chemical modification,” Journal of Industrial and Engineering Chemistry, 36, 1–12 (2016).

Meloni, D., D. Perra, R. Monaci, M. G. Cutrufello, E. Rombi, and I. Ferino, “Transesterification of *Jatropha curcas* oil and soybean oil on Al-SBA-15 catalysts,” Applied Catalysis B: Environmental, 184,163–173 (2016).

Meyer, P. P., N. Techaphattana, S. Manundawee, S. Sangkeaw, W. Junlakan, and C. Tongurai, “Epoxidation of soybean oil and jatropha oil,” International Journal of Science and Technology, 13, 1-5 (2008).

Mizuno, N., K. Yamaguchi, and K. Kamata, “Innovative catalysis in organic synthesis,” Chemical Reviews, 249, 1944-1956 (2005).

Mobarak, H. M., E. N. Mohamad, H. H. Masjuki, and M. A. Kalam, “The prospects of biolubricants as alternatives in automotive applications,” Renewable and Sustainable Energy Reviews, 33, 34-43 (2014).

Mohamed, T. B., B. B. Naima, and G. Gelbard, “Kinetics of tungsten-catalysed sunflower oil epoxidation catalyzed by ^{1}H NMR,” European Journal of Lipid Science and Technology, 109, 1186-1193 (2007).

Muhammad, F. M. G. R., T. I. M. Ghazi, and A. Idris, “Temperature dependence on the synthesis of jatropha biolubricant,” Material Science and Engineering, 17, 12-32 (2011).

Mungroo, R., N. C. Pradhan, V. V. Goud and A. K. Dalai, “Epoxidation of canola oil with hydrogen peroxide catalysed by acidic ion exchange resin,” Journal of the American Oil Chemists Society, 85 (9), 887-896 (2008).

Mungroo, R., V. V. Goud, N. C. Pradhan, and A. K. Dalai, “Modification of epoxidized canola oil,” Asia-Pacific Journal of Chemical Engineering, 6, 14-22 (2011).

Nagendramma, P., and S. Kaul, “Development of ecofriendly/biodegradable lubricants: An overview,” Renewable and Sustainable Energy Reviews, 16, 764–774 (2012).

Oh, J., S. Yang, C. Kim, I. Choi, J. H. Kim, and H. Lee, “Synthesis of biolubricants using sulfated zirconia catalysts,” 455, 164-171 (2013).

Ozbek, M. O., I. Onal, and R. A. Santen, “Why silver is the unique catalyst for ethylene epoxidation,” Journal of Catalysis, 284 (2), 230-235 (2011).

Pagliaro, M., R. Ciriminna, H. Kimura, M. Rossi, and C. D. Pina, “From glycerol to value-added products,” Angewandte Chemie International Edition, 46, 4434–4440 (2007).

Park, S. J., F. L. Jin, J. R. Lee, and J. S. Shin, “Cationic polymerization and physicochemical properties of a biobased epoxy resin initiated by thermally latent catalysts,” European Polymer Journal, 41, 231-237 (2005).

Patchara K, T. Supawan, “Preparation of cold flow improver property from epoxidized palm oil and 2-ethylhexanol,” PACCON, Pure and applied chemistry international conference (2011).

Pedersen, J.R., Ingemarsson, A., Olsson, J.O., “Oxidation of rapeseed oil, rapeseed methyl ester (RME) and diesel fuel studied with GS/MS,” Chemosphere, 38, 2467-2474 (1999).

Petrovic, Z. S., A. Zlatanic, and S. Sinadinovic-Fiser, “Epoxidation of soya bean oil in toluene with peroxoacetic acid and peroxoformic acid- kinetics and side reactions,” European Journal of Lipid Science and Technology, 104 (5), 293-299 (2002).

Poli, E., J.M. Clacens, J. Barrault, and Y. Pouilloux, “Solvent-free selective epoxidation of fatty esters over a tungsten-based catalyst,” Catalysis Today, 140, 19–22 (2009).

Przybylski, R., “Canola oil: physical and chemical properties,” Canola Council of Canada, 1–6 (2011).

Raji, V., M. Chakraborty, and P. A. Parikh, “Catalytic performance of silica-supported silver nanoparticles for liquid-phase oxidation of ethylbenzene,” Industrial and Engineering Chemistry Research, 51, 5691-5698 (2012).

Ratnam, K. J., S. R. Reddy, N. S. Sekhar, L. M. Kantam, and F. Figueras, “Sulphated zirconia catalyzed acylation of phenols, alcohols and amines under solvent free conditions,” Journal of Molecular Catalysis A: Chemical, 276, 230-234 (2007).

Ravasio, N., F. Zaccheria, M. Gargano, S. Recchia, and S. Fusi, “Environmentally friendly lubricants through selective hydrogenation of rapeseed oil over supported copper catalysts,” Appled Catalysis A: General, 233 (1-2), 1-6 (2002).

Roy, R. K., “Design of Experiments Using the Taguchi Approach: 16 Steps to Product and Process Improvement,” John Wiley & Sons Inc. United States (2001).

Salih, N., J. Salimon, and E. Yousif, “The physicochemical and tribological properties of oleic acid based triester biolubricants,” Industrial Crops and Products, 34, 1089–1096 (2011).

Salimon, J., N. Sali, and E. Yousif, “Synthesis, characterization and physicochemical properties of oleic acid ether derivatives as biolubricant basestocks,” Journal of Oleo Science, 60(12), 613-618 (2011).

Salimon, J., B.M. Abdullah, and N. Salih, “Optimization of the oxirane ring opening reaction in biolubricant base oil production,” Arabian Journal of Chemistry, 1–6 (2011).

Salimon, J., N. Salih, and E. Yousif, “Synthetic biolubricant basestocks from epoxidized ricinoleic acid: improved low temperature properties,” Journal of Chemists Chemical Engineers, 60, 127-134 (2011).

Sammaiah, A., K. V. Padmaja, and R. B. N. Prasad, “Synthesis and evaluation of novel acyl derivatives from jatropha oil as potential lubricant basestocks,” Journal of Agriculture and Food Chemistry, 62, 4652–4660 (2014).

Sankaranarayanan, S., and K. Srinivasan, “Preparation of functionalized castor oil derivatives with tunable physical properties using heterogeneous acid and base catalysts,” RSC Advances, 5, 50289–50297 (2015).

Satyarthi, J.K., and D. Srinivas, “Selective epoxidation of methyl soyate over alumina-supported group VI metal oxide catalysts,” Applied Catalysis A: General, 401, 189–198 (2011).

Saurabh, T., M. Patnaik, S. Bhagt, and L. Renge, “Epoxidation of vegetable oils: A review,” International Journal of Advanced Engineering Technology, 2, 491-501 (2011).

Saurabh, T., M. Patnaik, S. L. Bhagat, and V.C. Renge, “Studies on synthesis of biobased epoxide using cottonseed oil,” International Journal of Advanced Engineering Research and Studies, 12, 79–84 (2012).

Schneider, M., “Plant-oil based lubricants and hydraulic fluids,” Journal of the Science of Food and Agriculture, 86, 1769-1780 (2006).

Shangde, S., K. Xiaoqiao, C. Longlong, Y. Guolong, B. Yanlan, S. Fanfan and X. Xiadi, "Enzymatic epoxidation of Sapindus mukorossi seed oil by perstearic acid optimized using response surface methodology," Industrial Crops and Products, 33, 676-682 (2011)

Sharma, B. K., A. Adhvaryu, and S. Z. Erhan, "Synthesis of hydroxy thio-ether derivatives of vegetable oil," Journal of Agriculture and Food Chemistry, 54, 9866-9872 (2006).

Sharma, B. K., A. Adhvaryu, Z. Liu, and S. Erhan, "Chemical modification of vegetable oils for lubricant applications," Journal of American Oil Chemists Society, 83, 129-136 (2006).

Sharma, R. V., A.K.R. Somidi, and A.K. Dalai, "Preparation and properties evaluation of biolubricants derived from canola oil and canola biodiesel," Journal of Agriculture and Food Chemistry, 63, 3235–3242 (2015).

Sharma, R. V., and A. K. Dalai, "Synthesis of bio-lubricant from epoxy canola oil using sulfated Ti-SBA-15 catalyst," Applied Catalysis B: Environmental, 142-143, 604–614 (2013).

Sharma, Y. C., B. Singh, and S. N. Upadhyay, "Advancements in development and characterization of biodiesel: A review," Fuel, 87, 2355-2373 (2008).

Sheldon, R. A., and J. K. Kochi, "Metal-catalyzed oxidation of organic compounds," Academia Press, New York, 43-45 (1981).

Silva, M. S., E. L. Foletto, S. M. Alves, T. N. C. Dantas, and A. A. D. Neto, "New hydraulic biolubricants based on passion fruit and moringa oils and their epoxy," Industrial Crops and Products, 69, 362-370 (2015).

Silva, J. A. C., and A. C. Habert, "A potential biodegradable lubricant from castor biodiesel esters," Lubrication Science, 25 (1), 53-61 (2013).

Sinadinovic-Fiser, M. Jankovic, and Z. S. Petrovic, "Kinetics of insitu epoxidation of soya bean oil in bulk catalysed by ion exchange resin," Journal of American Oil Chemists Society, 85, 887-896 (2008).

Somidi, A. K. R., R. V. Sharma, and A.K. Dalai, "Catalytic vicinal diacylation of epoxidized triglycerides in canola oil," Journal of American Oil Chemists Society, 92 (9), 1365-1378 (2015).

Somidi, A. K. R., U. Das, and A. K. Dalai, “One-pot synthesis of canola oil based biolubricants catalyzed by MoO_3/Al_2O_3 and process optimization study,” Chemical Engineering Journal, 293, 259–272 (2016).

Somidi, K. R. A., R. V. Sharma, and A. K. Dalai, “Synthesis of epoxidized canola oil using sulfated-sno_2 catalyst,” Industrial and Engineering Chemistry Research, 53, 18668-18677 (2014).

Soni, S., and M. Agarwal, “Lubricants from renewable energy sources – a review,” Green Chemistry Letters and Reviews, 7 (4), 359-382 (2014).

Sripada, P. K., R. V. Sharma, and A. K. Dalai, “Comparative study of tribological properties of trimethylolpropane-based biolubricants derived from methyl oleate and canola biodiesel," Industrial Crops and Products,” 50, 95-103 (2013).

Sun, S., X. Ke, L. Cui, G. Y. Bi, F. Song, and X. Xu, “Enzymatic epoxidation of Sapindus mukorossi seed oil by perstearic acid optimized using response surface methodology,” Industrial Crops and Products, 33, 676-682 (2011).

Sun, Y., S. Ma, Y. Du, L. Yuan, S. Wang, J. Yang, F. Deng, and F. Xia, “Solvent-free preparation of nanosized sulfated zirconia with brønsted acidic sites from a simple calcination,” Journal of Physical Chemistry B, 109, 2567-2572 (2005).

Tan, S. G., and Chow, W. S., “Biobased epoxidized vegetable oils and its greener epoxy blends: a review,” Polymer-Plastics Technology and Engineering, 49 (15), 1581-1590 (2010).

Tilay, A., M. Bule, and U. Annapure, “Production of biovanillin by one-step biotransformation using fungus *Pycnoporous cinnabarinus*,” Journal of Agricultural and Food Chemistry, 58, 4401-4405 (2010).

Tornvall, U., C. Orellana-Coca, R. Hatti-kaul, and D. Adlecreutz, “Stability of immobilized Candida antartica lipase B during chemo-enzymatic epoxidation of fatty acids,” Enzyme Microbial Technology, 40, 447-451 (2007).

Tse-Lok, H., M. Fieser, and L. Fieser, ‘Fieser and Fieser's Reagents for Organic Synthesis,” 1, 459-460 (2006).

Veldsink, J. W., “Selective hydrogenation of sunflower seed oil in a three-phase catalytic membrane reactor,” Journal of American Oil Chemists Society, 78, 443-446 (2001).

Vlcek, T., and Z. S. Petrovic, “Optimization of chemo enzymatic epoxidation of soybean oil,” Journal of American Oil Chemists Society, 83, 247-252 (2006).

Vuurmant, M. A., I. E. Wachs, “In-situ Raman spectroscopy of alumina-supported metal oxide catalysts,” 96, 5008–5016 (1992).

Wang, X. and W. Li, “Bio-lubricants derived from waste cooking oil with improved oxidation stability and low temperature properties,” Journal of Oleo Science, 64 (4), 367-374 (2015).

Wu, X., X. Zhanga, S. Yang, H. Chen, and, D. Wang, “The study of epoxidized rapeseed oil used as a potential biodegradable lubricant,” Journal of the American Oil Chemists Society, 77(5), 561-563 (2000).

Xie, S., S. Huang, W. Wei, X. Yang, Y. Liu, and X. Lu, “Chitosan waste-derived Co and N Co-doped carbon electrocatalyst for efficient oxygen reduction reaction,” ChemElectroChem, 2, 1806–1812 (2015).

Yadav, G. D., P. A. Chandan, and N. Gopalaswami, “Green etherification of bioglycerol with 1-phenyl ethanol over supported heteropolyacid,” Clean Technologies and Environmental Policy, 14, 85–95 (2012).

Yin, G., M. Buchalova, A. Danby, M. Perkins, M. Kitko, D. Carter, J. Scheper, M. Busch, “Olefin oxygenation by the hydroperoxide adduct of a nonheme Manganese (IV) Complex: Epoxidations by a metallo-peracid produces gentle selective oxidations,” Journal of American Oil Chemists Society, 127(49), 17170-17171 (2005).

Zaccheria, F., F. Santoro, R. Psaro, and N. Ravasio, “CuO/SiO2: a simple and efficient solid acid catalyst for epoxide ring opening,” Green Chemistry, 13, 545-548 (2011).

Zaher, F. A., El-Kinawy, O. S., and Abdullah, R., “The esterification of Jatropha oil using different short chain alcohols to produce esters to be used as biodiesel fuel,” Energy Sources, 34, 2214-2219 (2012).

Zhao, D., Q. Huo, J. Feng, B. F. Chmelka, and G. D. Stucky, “Tri-, tetra-, and octablock copolymer and nonionic surfactant syntheses of highly ordered, hydrothermally stable,” Mesoporous Silica Structures, Journal of American Chemical Society, 120, 6024–6036 (1998).

Zhao, J., Y. Yue, D. C. Zhai, J. Miao, and H. Shen, Characterization and catalytic activities of Al_2O_3-promoted sulfated tin oxides,” Catalysis Letters, 133, 119-124 (2009).

APPENDIX A

^{1}H NMR SPECTRA OF MODEL COMPOUNDS

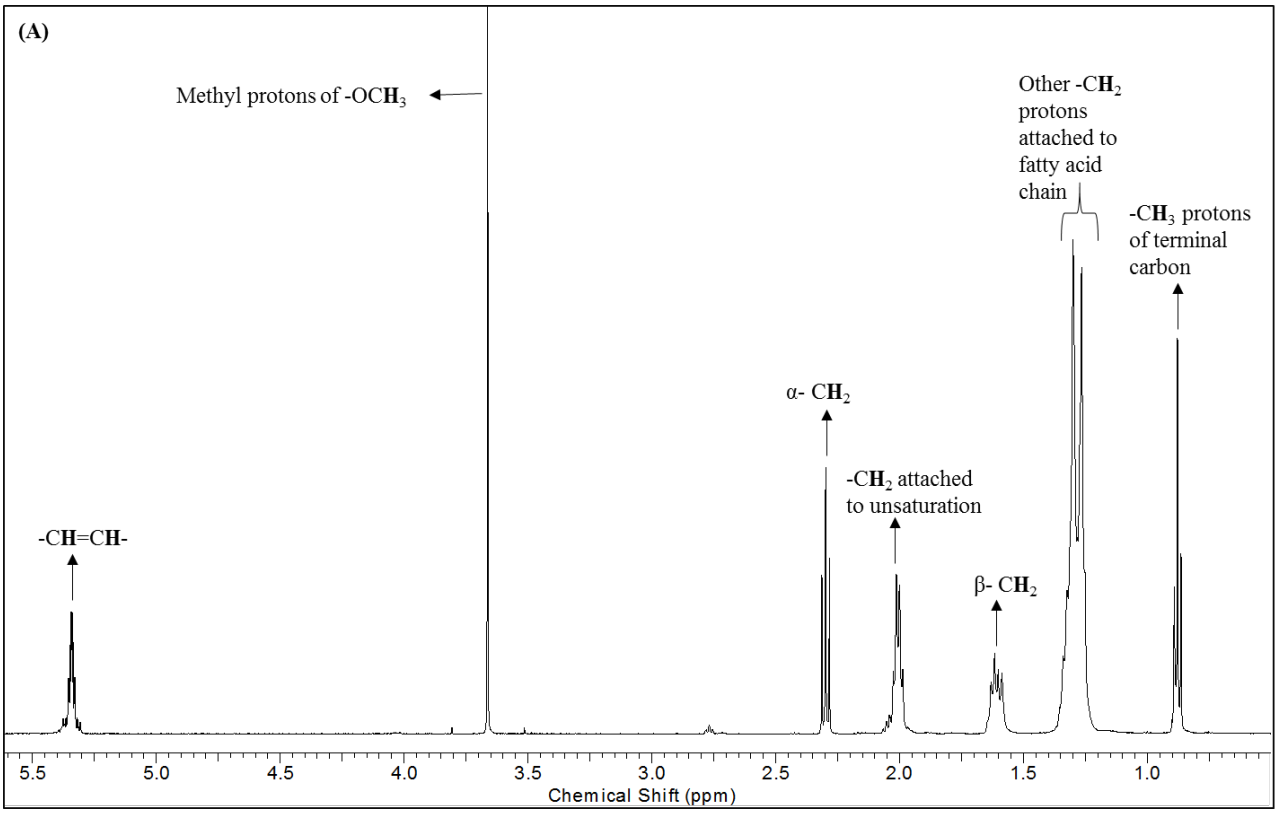

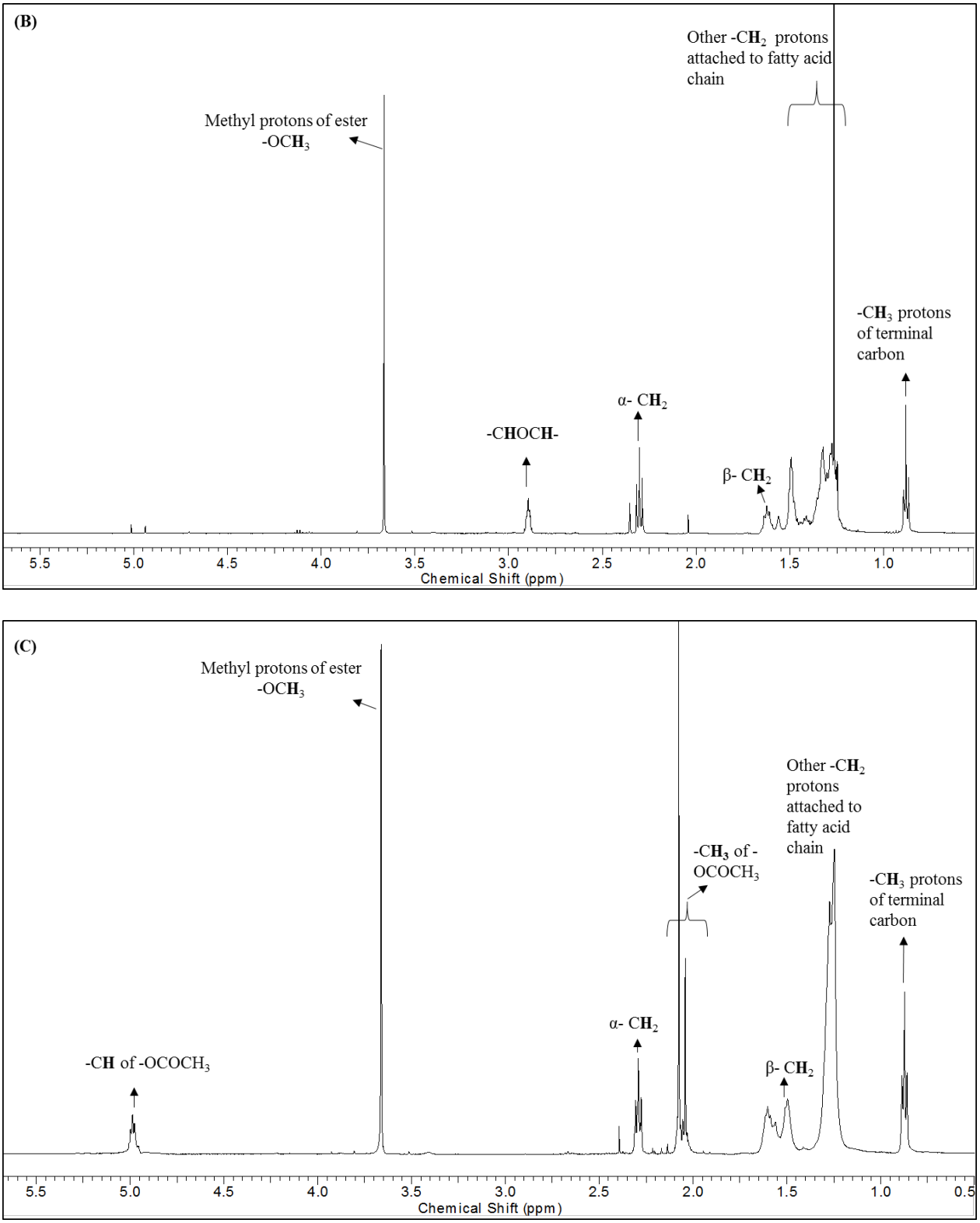

Figure A1 ^{1}H NMR spectra of (A) Methyl oleate, (B) Epoxidized methyl oleate, and (C) Vicinal di-O-acetylated methyl oleate.

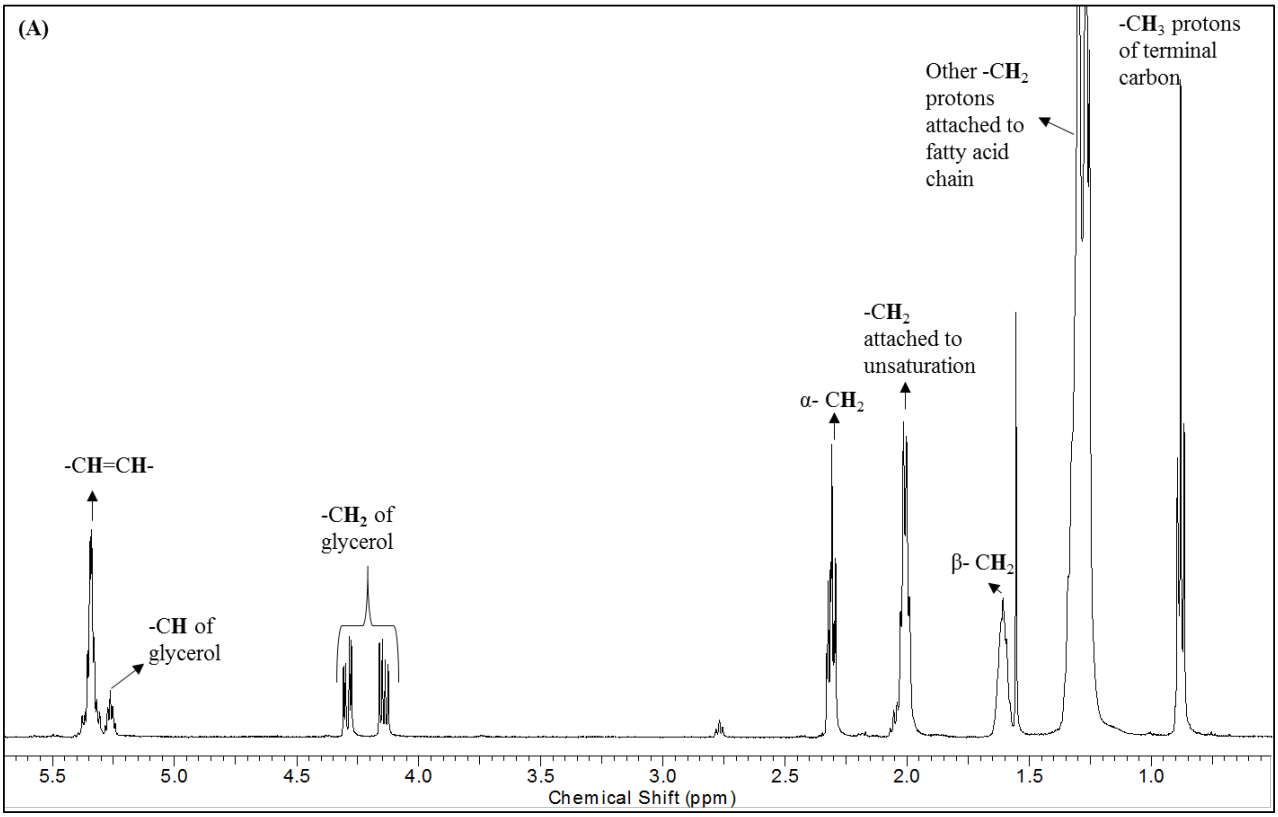
(A)
-CH=CH-
-CH of glycerol
-CH2 of glycerol
α- CH2
-CH2 attached to unsaturation
β- CH2
Other -CH2 protons attached to fatty acid chain
-CH3 protons of terminal carbon
5.5
5.0
4.5
4.0
3.5
3.0
2.5
2.0
1.5
1.0
Chemical Shift (ppm)

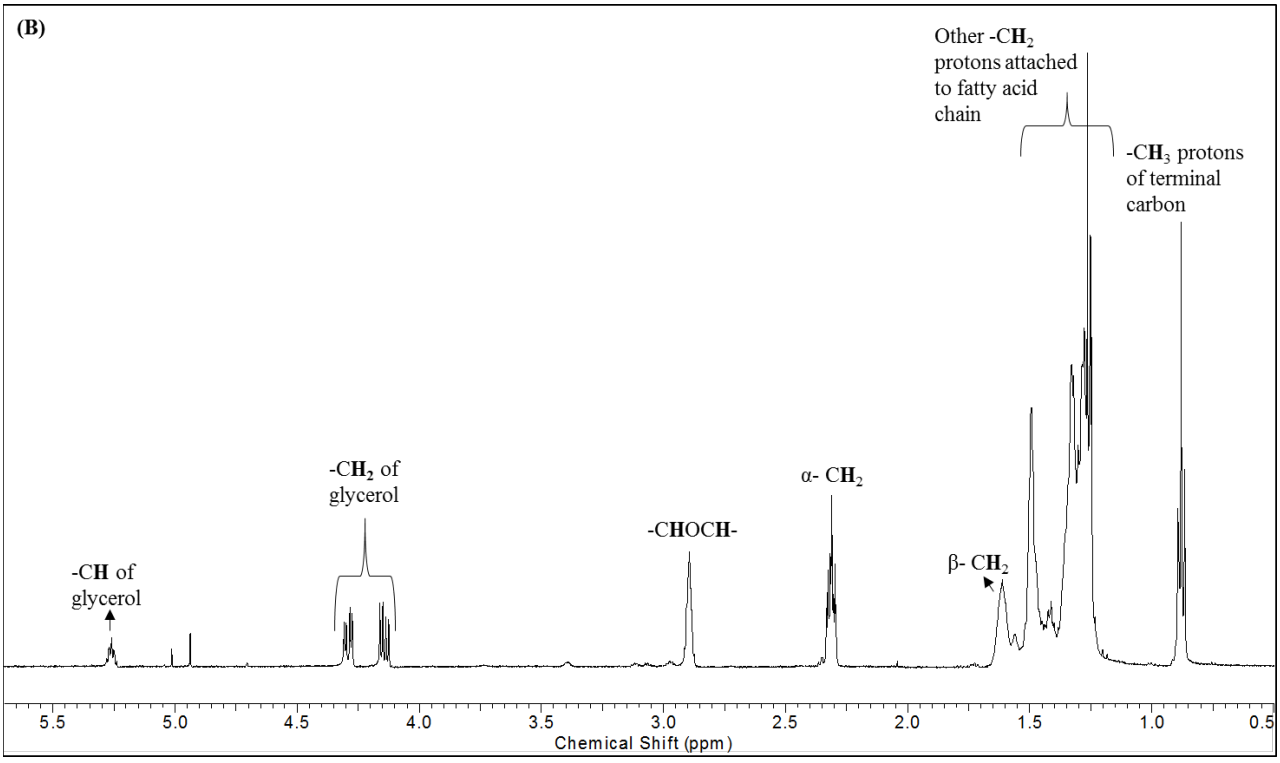
(B)
-CH of glycerol
-CH2 of glycerol
-CHOCH-
α- CH2
β- CH2
Other -CH2 protons attached to fatty acid chain
-CH3 protons of terminal carbon
5.5
5.0
4.5
4.0
3.5
3.0
2.5
2.0
1.5
1.0
0.5
Chemical Shift (ppm)

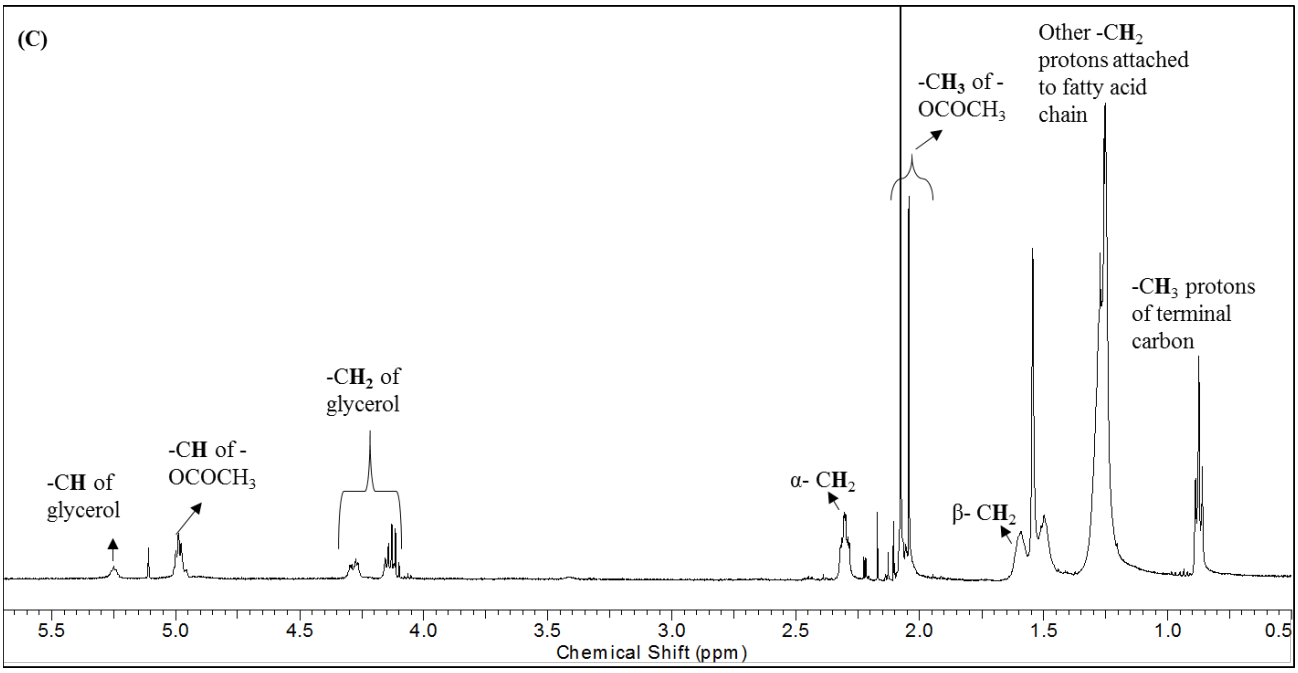

Figure A2 ^{1}H NMR spectra of (A) Glyceryl trioleate, (B) Epoxidized glyceryl trioleate, and (C) vicinal di-O-acetylated glyceryl trioleate.

APPENDIX B

COPYRIGHTS AND PERMISSION TO USE OF PUBLISHED ARTICLES IN THE THESIS

CHAPTER 3

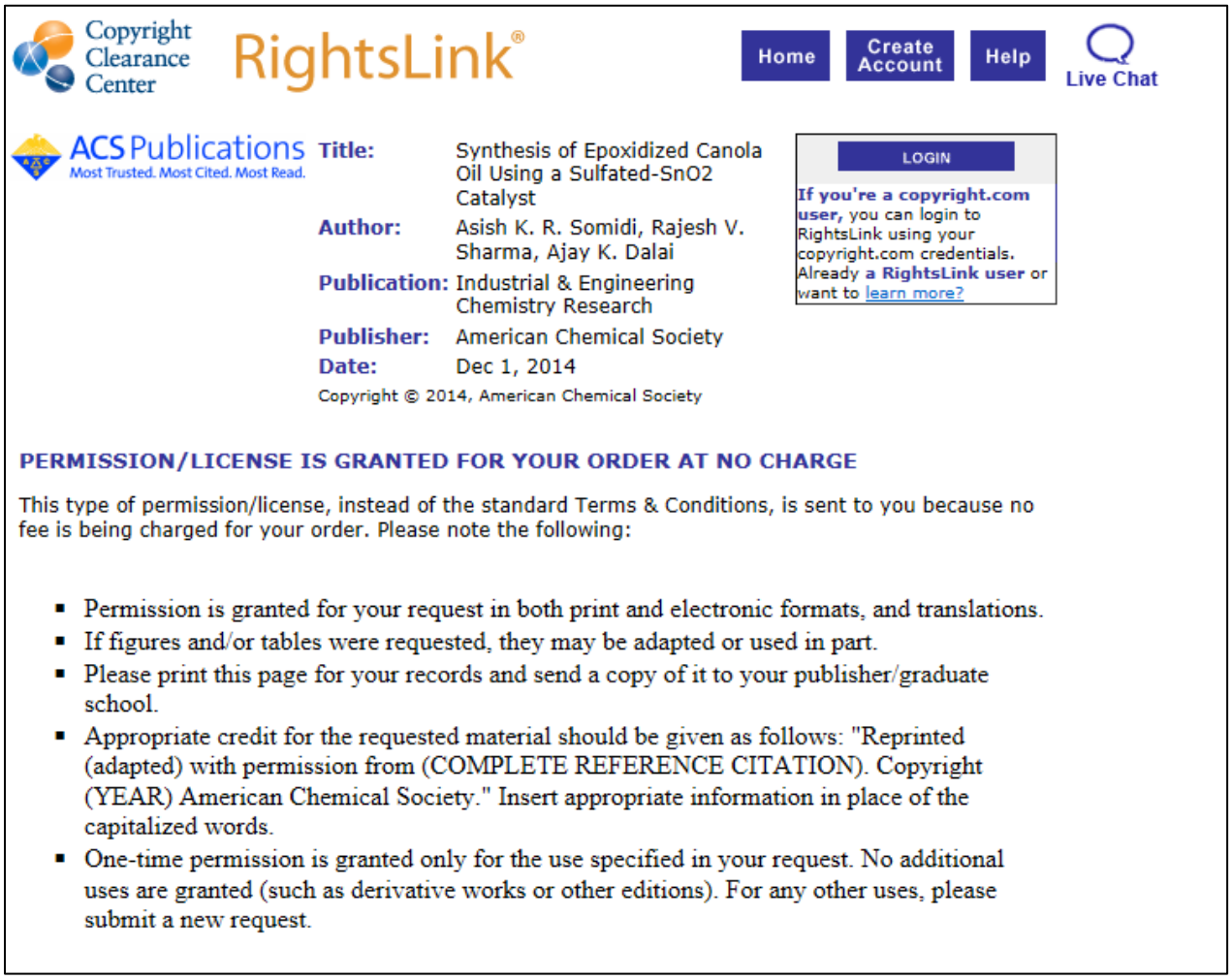

Copyright Clearance Center RightsLink®

Home | Create Account | Help | Live Chat

ACS Publications
Most Trusted. Most Cited. Most Read.

Title: Synthesis of Epoxidized Canola Oil Using a Sulfated-SnO2 Catalyst

Author: Asish K. R. Somidi, Rajesh V. Sharma, Ajay K. Dalai

Publication: Industrial & Engineering Chemistry Research

Publisher: American Chemical Society

Date: Dec 1, 2014

Copyright © 2014, American Chemical Society

LOGIN

If you're a copyright.com user, you can login to RightsLink using your copyright.com credentials. Already a RightsLink user or want to learn more?

PERMISSION/LICENSE IS GRANTED FOR YOUR ORDER AT NO CHARGE

This type of permission/license, instead of the standard Terms & Conditions, is sent to you because no fee is being charged for your order. Please note the following:

- Permission is granted for your request in both print and electronic formats, and translations.
- If figures and/or tables were requested, they may be adapted or used in part.
- Please print this page for your records and send a copy of it to your publisher/graduate school.
- Appropriate credit for the requested material should be given as follows: "Reprinted (adapted) with permission from (COMPLETE REFERENCE CITATION). Copyright (YEAR) American Chemical Society." Insert appropriate information in place of the capitalized words.
- One-time permission is granted only for the use specified in your request. No additional uses are granted (such as derivative works or other editions). For any other uses, please submit a new request.

CHAPTER 4

SPRINGER LICENSE
TERMS AND CONDITIONS

Aug 22, 2016

This Agreement between ASISH SOMIDI ("You") and Springer ("Springer") consists of your license details and the terms and conditions provided by Springer and Copyright Clearance Center.

License Number	3934340207473
License date	Aug 22, 2016
Licensed Content Publisher	Springer
Licensed Content Publication	Journal of the American Oil Chemists' Society
Licensed Content Title	Catalytic Vicinal Diacylation of Epoxidized Triglycerides in Canola Oil
Licensed Content Author	Asish K. R. Somidi
Licensed Content Date	Jan 1, 2015
Licensed Content Volume Number	92
Licensed Content Issue Number	9
Type of Use	Thesis/Dissertation
Portion	Full text
Number of copies	1
Author of this Springer article	Yes and you are a contributor of the new work
Order reference number	
Title of your thesis / dissertation	Synthesis of Canola Oil Based Biolubricants Using Heterogeneous Catalysts and Evaluation of Physico-Chemical Properties
Expected completion date	Dec 2016
Estimated size(pages)	200
Requestor Location	ASISH SOMIDI 202 101 CUMBERLAND AVE S SASKATOON SASKATOON, SK S7N1L5

CHAPTER 5 (First manuscript)

ELSEVIER LICENSE
TERMS AND CONDITIONS

Aug 22, 2016

This Agreement between ASISH SOMIDI ("You") and Elsevier ("Elsevier") consists of your license details and the terms and conditions provided by Elsevier and Copyright Clearance Center.

License Number	3934340454825
License date	Aug 22, 2016
Licensed Content Publisher	Elsevier
Licensed Content Publication	Chemical Engineering Journal
Licensed Content Title	One-pot synthesis of canola oil based biolubricants catalyzed by MoO3/Al2O3 and process optimization study
Licensed Content Author	Asish K.R. Somidi,Umashankar Das,Ajay K. Dalai
Licensed Content Date	1 June 2016
Licensed Content Volume Number	293
Licensed Content Issue Number	n/a
Licensed Content Pages	14
Start Page	259
End Page	272
Type of Use	reuse in a thesis/dissertation
Intended publisher of new work	other
Portion	full article
Format	both print and electronic
Are you the author of this Elsevier article?	Yes
Will you be translating?	No
Order reference number	

CHAPTER 5 (Second manuscript, Asish Somidi being Second author)

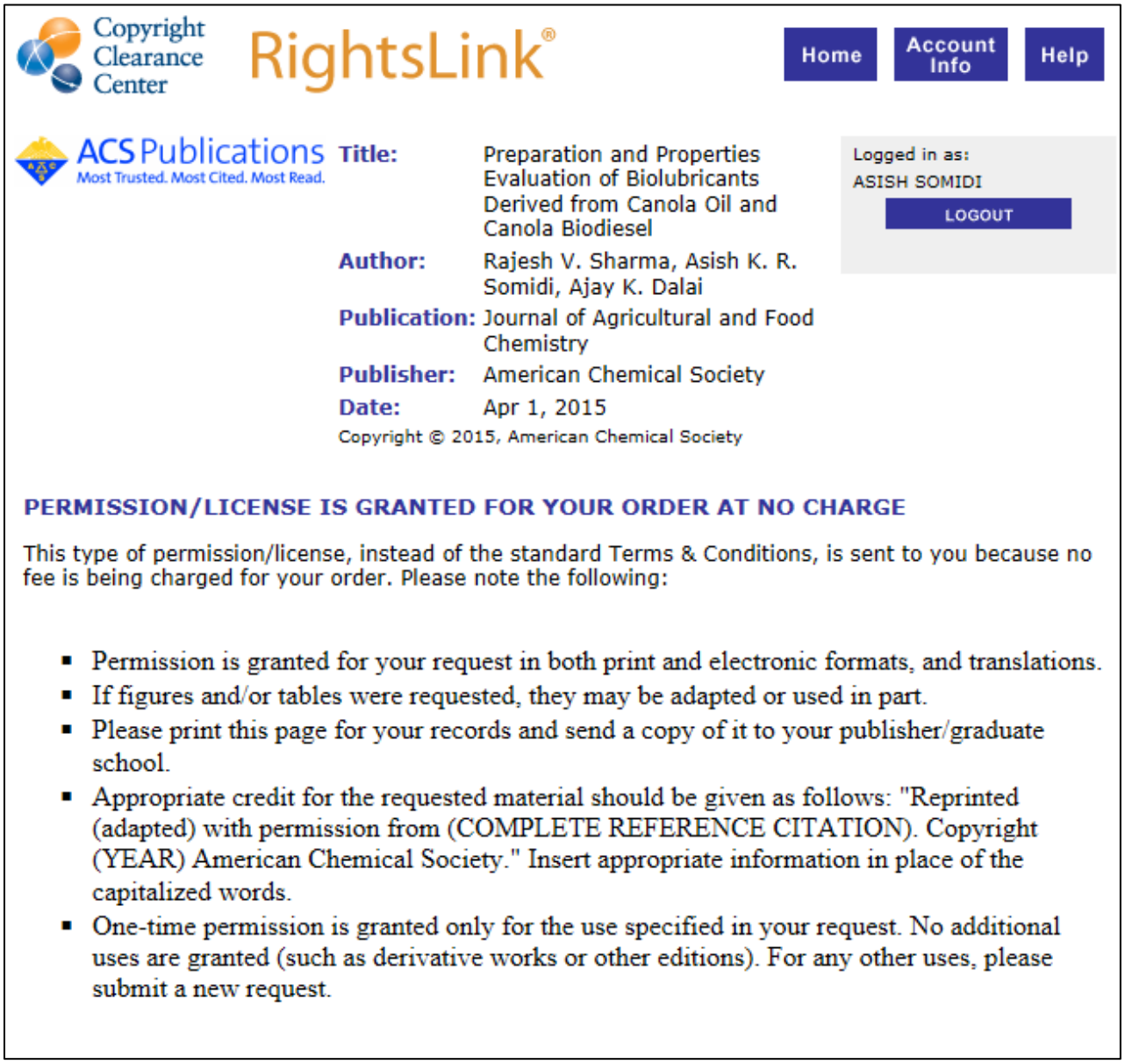

Copyright Clearance Center RightsLink®

Home | Account Info | Help

ACS Publications
Most Trusted. Most Cited. Most Read.

Logged in as:
ASISH SOMIDI
LOGOUT

Title: Preparation and Properties Evaluation of Biolubricants Derived from Canola Oil and Canola Biodiesel

Author: Rajesh V. Sharma, Asish K. R. Somidi, Ajay K. Dalai

Publication: Journal of Agricultural and Food Chemistry

Publisher: American Chemical Society

Date: Apr 1, 2015

Copyright © 2015, American Chemical Society

PERMISSION/LICENSE IS GRANTED FOR YOUR ORDER AT NO CHARGE

This type of permission/license, instead of the standard Terms & Conditions, is sent to you because no fee is being charged for your order. Please note the following:

- Permission is granted for your request in both print and electronic formats, and translations.
- If figures and/or tables were requested, they may be adapted or used in part.
- Please print this page for your records and send a copy of it to your publisher/graduate school.
- Appropriate credit for the requested material should be given as follows: "Reprinted (adapted) with permission from (COMPLETE REFERENCE CITATION). Copyright (YEAR) American Chemical Society." Insert appropriate information in place of the capitalized words.
- One-time permission is granted only for the use specified in your request. No additional uses are granted (such as derivative works or other editions). For any other uses, please submit a new request.